EWG-RPT-0013 Rev. 0.0
PNNL-27138

Pacific Northwest
NATIONAL LABORATORY

Proudly Operated by **Battelle** *Since 1965*

Glass Compositions and Properties of Enhanced Waste Glass with High Alumina Content for High-Level Waste

January 2018

RL Russell
YS Chou
BP McCarthy
LP Darnell
V Gervasio
JL Mayer
JB Lang
SK Cooley
JD Vienna
GF Piepel
MJ Schweiger

U.S. DEPARTMENT OF ENERGY

Prepared for the U.S. Department of Energy
under Contract DE-AC05-76RL01830

PACIFIC NORTHWEST NATIONAL LABORATORY
operated by
BATTELLE
for the
UNITED STATES DEPARTMENT OF ENERGY
under Contract DE-AC05-76RL01830

Printed in the United States of America

Available to DOE and DOE contractors from the
Office of Scientific and Technical Information,
P.O. Box 62, Oak Ridge, TN 37831-0062;
ph: (865) 576-8401
fax: (865) 576-5728
email: reports@adonis.osti.gov

Available to the public from the National Technical Information Service
5301 Shawnee Rd., Alexandria, VA 22312
ph: (800) 553-NTIS (6847)
email: orders@ntis.gov <http://www.ntis.gov/about/form.aspx>
Online ordering: http://www.ntis.gov

This document was printed on recycled paper.
(8/2010)

EWG-RPT-0013, Rev. 0.0
PNNL-27138

Glass Compositions and Properties of Enhanced Waste Glass with High Alumina Content for High-Level Waste

RL Russell
YS Chou
BP McCarthy
LP Darnell
V Gervasio
JL Mayer
JB Lang
SK Cooley
JD Vienna
GF Piepel
MJ Schweiger

January 2018

Prepared for
the U.S. Department of Energy
under Contract DE-AC05-76RL01830

Pacific Northwest National Laboratory
Richland, Washington 99352

Summary

This report documents the work performed to collect critical property data on high-level waste (HLW) glasses with high alumina content. This report covers the experimental results of thermal, physical, chemical, and electrical properties of 46 high alumina (15 to 30 wt%) borosilicate waste-glass compositions with one duplicate for a total of 47 glasses. These experimental results are essential for developing property-composition models for the future operation of the Hanford Tank Waste Treatment and Immobilization Plant (WTP) currently under construction at the Hanford Site in Richland, Washington. Pacific Northwest National Laboratory (PNNL) was requested by the U.S. Department of Energy's Office of River Protection to provide expert evaluation and experimental work in support of the vitrification technology development program.

The 47 borosilicate HLW glasses with high alumina content were statistically designed to cover a HLW experimental glass composition region (EGCR). The EGCR was specified by constraints on 1) individual glass components and 2) mathematical expressions involving multiple glass components. The test matrix of 47 glasses consists of 45 extreme vertices of the EGCR and two replicates of a center glass. This test matrix is the first phase of work to investigate the high alumina EGCR. A subsequent phase is envisioned to explore the interior of the high alumina EGCR.

These 47 test-matrix glasses were batched and melted in Pt-alloy crucibles. No problem was encountered when making glasses with maximum alumina content of 30 wt%, although the melting temperatures of these glasses were all over 1200 ºC. The 47 glasses were chemically analyzed to check for batching errors and volatility issues. Results showed that analyzed compositions were very consistent with targeted compositions, with the sum of all analyzed components ranging from 96.9 wt% to 103.5 wt%. These results indicate the analyzed compositions had good accuracy and precision. Detailed comparisons of analyzed and targeted component values were performed to assess possible batching errors and volatility.

Glasses cooled in two ways were investigated: 1) quenched (Q) and 2) canister centerline cooled (CCC). The Q glass samples were first subjected to chemical analysis. Both Q and CCC samples were tested for toxicity and chemical durability using the Toxicity Characteristic Leaching Procedure (TCLP) and the Product Consistency Test (PCT). TCLP normalized releases ranged from below detection limits to 5.93 mg/L. The PCT normalized B, Na, and Li values ranged from 0.097 to 45.505, 0.077 to 21.78, and below detection limits to 23.995 g/m^2, respectively. After CCC treatment, the microstructures of many glasses changed and various crystalline phases formed, primarily nepheline and spinel. In general, the presence of crystalline phases led to poorer performance in both the TCLP and PCT. For the liquidus temperature test, 24 glasses showed spinel as a primary phase while four glasses were found to contain nepheline, eskolaite, or baddeleyite as a primary phase. Measured T_L, $T_{1\%}$, and $T_{2\%}$ values ranged from <850 to 2095 ºC, 914 to 1802 °C, and 798 to 1693 °C, respectively.

Property data for the 47 HLW glasses with high alumina were compared with predictions from existing property-composition models developed from older WTP-baseline data. The existing models generally provided poor predictions, indicating that new models are needed for HLW glasses containing high alumina content.

Acknowledgments

The authors gratefully acknowledge the financial support provided by the U.S. Department of Energy Office of River Protection Waste Treatment and Immobilization Plant Project managed by Albert Kruger.

The authors thank Kevin Fox and Thomas Edwards of Savannah River National Laboratory for their help in the analysis and testing of the glasses. We also thank Cary Counts and Matthew Wilburn (PNNL) for their editorial review of this report, and Kirsten Meier, Hans Brandal, and Veronica Perez (all PNNL) for programmatic support during the conduct of this work.

Acronyms and Abbreviations

ACED	Algorithms for the Construction of Experimental Designs
AD	acid dissolution
ARM	Approved Reference Material
BNI	Bechtel National, Inc.
CCC	canister centerline cooled
DOE	U.S. Department of Energy
DWPF	Defense Waste Processing Facility
EA	Environmental Assessment
EC	electrical conductivity
EGCR	experimental glass composition region
EPA	U.S. Environmental Protection Agency
EWG	enhanced waste glass
HDI	"How Do I…?" (web-based standards system at PNNL)
HLW	high-level waste
IC	ion chromatography
ICP-OES	inductively coupled plasma-optical emission spectroscopy
LRM	low-activity waste reference material
MCC	multiple-component constraints
ORP	Office of River Protection
PCT	Product Consistency Test
PF	peroxide fusion
PNNL	Pacific Northwest National Laboratory
PSAL	Process Science Analytical Laboratory
PUREX	plutonium uranium reduction extraction
QA	quality assurance
QGCR	qualified glass composition region
RCRA	Resource Conservation and Recovery Act
REDOX	reduction-oxidation
SCC	single-component constraints
SRNL	Savannah River National Laboratory
S/V	surface to volume ratio
SwRI	Southwest Research Institute
TCLP	Toxicity Leaching Characteristic Procedure
T_L	liquidus temperature
UTS	Universal Treatment Standards
VFT	Vogel- Fulcher-Tammann

WTP	Hanford Tank Waste Treatment and Immobilization Plant
WWFTP	Washington River Protection Solutions Waste Form Testing Program
XRD	x-ray diffraction

Contents

Figures

Tables

1.0 Introduction

The U.S. Department of Energy's (DOE) Office of River Protection (ORP) requested Pacific Northwest National Laboratory (PNNL) to provide expert evaluation and experimental work in support of the River Protection Project vitrification technology development (DOE 2012). This work was performed under the PNNL project titled "ORP Glass Support Work." The long-term objective of this work is to expand the Hanford Site high-level waste (HLW) and low-activity waste glass database and property-composition models to cover the post-commissioning portion of the Hanford Site tank waste treatment and immobilization mission.

This report presents the glass compositions and glass property data developed to explore an alumina-rich composition region of enhanced Hanford HLW glasses. When the data-development effort for Hanford HLW glasses with high alumina content is complete, enhanced HLW glass property-composition models will be developed. Section 1.1 summarizes the status of the HLW glass composition regions and waste loading constraints prior to the data-development effort documented in this report. Section 1.2 summarizes the HLW glass with high alumina content composition region and test matrix. Section 1.3 documents the Quality Assurance (QA) program used in performing the work discussed in this report.

1.1 Status of HLW Experimental Glass Composition Regions and Waste Loading Constraints

In this document, the term *experimental glass composition region* (EGCR) is used to refer to a composition region of glasses that has been (or will be) experimentally explored through fabricating glasses and testing their properties. An EGCR should include glass compositions that span the range of compositions and property responses beyond those expected to be produced in the plant (e.g., including glasses that do not satisfy property constraints). Experimental data collected on glass compositions covering the EGCR then provide information for developing property-composition models that can 1) discriminate between glass compositions that satisfy and fail the requirements and 2) adequately predict glass properties of compositions that satisfy all requirements. The term *qualified glass composition region* (QGCR) then refers to the subset of the EGCR for which all processing and product-quality constraints are satisfied with sufficient confidence, after accounting for applicable uncertainties.

The Hanford Tank Waste Treatment and Immobilization Plant (WTP) project has developed HLW glass property-composition models (Piepel et al. 2008) and algorithms (Vienna and Kim 2014) to formulate compositions and qualify HLW glasses for disposal. These models are based on data from crucible-scale tests with simulants, crucible-scale tests with actual waste, and scaled-melter tests with simulants collected under the Bechtel National, Inc. (BNI) contract to design, construct, and commission the WTP (DOE 2000). Because the scope of the BNI contract is limited to operating the plant for only 20 days with a limited amount of waste, the data and resulting glass property-composition models only cover a fraction of the HLW glass compositions needed for the entire Hanford Site mission. In addition, the data and models developed by BNI are targeted at glasses that only modestly exceed contract minimum waste loadings rather than maximum achievable waste loadings.

EGCRs are specified using processing and product-quality constraints, with two main kinds of constraints. Single-component constraints (SCC) involve lower and upper limits on individual HLW glass components. Multiple-component constraints (MCC) involve lower and/or upper limits on linear combinations of HLW glass components. For some MCCs, the linear combinations of components are existing property-composition models for HLW glasses. In other cases, the linear combinations are stand-in expressions for properties that have not yet been modeled, or are not easily measured or predicted.

As one example of a stand-in constraint, currently the weight percent (wt%) SO_3 targeted in glass is limited because the salt accumulation in the melter has not yet been modeled for WTP HLW glasses. As a second example, the equilibrium fraction of crystals at 950°C is limited to 1 volume percent (vol%) because crystal blockage of the melter pour-spout has not yet been modeled. To determine the ultimate waste loadings and formulations of HLW glasses, these stand-in constraints must be replaced with constraints based on true operating and product performance property limits. Therefore, we seek to develop 1) glass property data across broader glass composition regions and 2) methods to measure (directly or indirectly) and model the properties that fundamentally limit the melter operating limits or the performance property limits of the glass.

The baseline WTP HLW EGCR focuses on glasses for waste from the plutonium uranium reduction extraction (PUREX) process known as neutralized current acid waste, which is relatively high in iron and lower in aluminum compared to other HLW. Figure 1.1 conceptually shows the full Hanford HLW EGCR and how it compares to the baseline WTP HLW EGCR. The full Hanford EGCR is sufficiently large to warrant division into composition subregions as shown in Figure 1.2. The subregions can be specified in a number of different ways as described below:

- Major processes that generated the waste, including bismuth-phosphate carrier precipitation, reduction oxidation (REDOX), PUREX, uranium-recovery, Plutonium Finishing Plant, etc.
- Composition of the waste (e.g., high iron, high alumina, or high sulfate).
- A number of other grouping schemes; examples are provided in Agnew et al. (1997), Higley et al. (2004), Sasaki (2001), and Hill and Simpson (1994).

For the purposes of this study, HLW waste glasses were grouped into subregions based on glass composition limitations, as shown in Figure 1.3.

Figure 1.1. Two-Dimensional Conceptual Representation of the Full Hanford HLW EGCR

Figure 1.2. Conceptual Representation of the Full Hanford HLW EGCR Divided into Subregions of Similar Glass Compositions (as gray ovals)

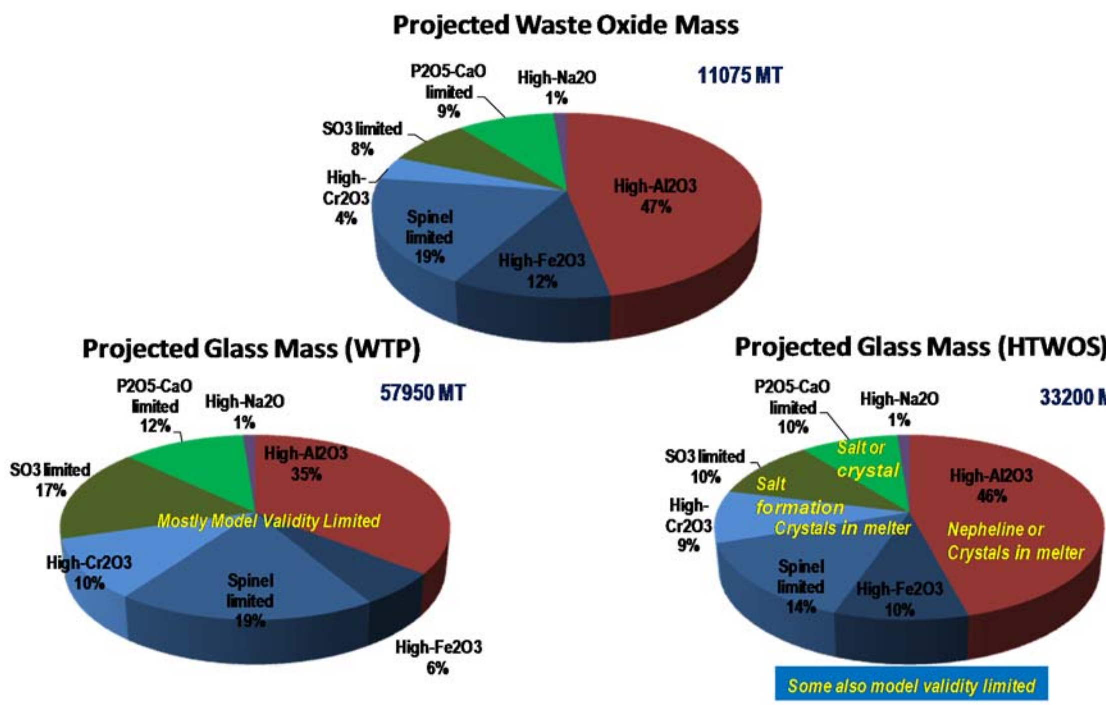

Figure 1.3. Pie Chart of All Hanford HLW Grouped by Limits on Waste Loading in Glass (Kim et al. 2011)

Over the last 12 years, new HLW glass formulations with high waste loadings have been developed by The Catholic University of America in support of ORP (Matlack et al. 2005a, 2007a, 2008, 2009a, 2010a, 2010b, 2011, 2012a, 2012b; Kot et al. 2011; Gan et al. 2009) and by PNNL in support of ORP (Kim et al. 2008, 2011; Rodriguez et al. 2011; McCloy et al. 2010). The resulting data are summarized in Muller et al. (2012) and Vienna et al. (2016), with some newer data not yet reported. The basic conclusions of these studies are that loadings for specific HLWs in glass can be increased significantly over the loadings allowed by the WTP baseline constraints. Examples of the gains made in these studies include the following:

- HLW glasses with 26 wt% Al_2O_3, which is double the 13 wt% maximum value allowed by the baseline WTP HLW EGCR.
- HLW glasses with 4 wt% Bi_2O_3, which is roughly 13 times the maximum value of 0.3 wt% in the baseline WTP HLW EGCR. There is no specific limit for Bi_2O_3 in the WTP baseline constraints, because it is lumped into minor components.
- HLW glasses with CaO concentrations of 7 wt%, compared to the 1 wt% limit in the WTP baseline constraints.

Although there is more than one glass for each type of waste represented in the available data, the coverage of the full Hanford HLW EGCR is sparse and is focused either on the high waste loading boundaries or in the low waste loading WTP EGCR. Figure 1.4 conceptually illustrates how the currently available data are distributed over the full Hanford HLW glass composition region. The detailed distribution of data can most easily be visualized in a scatterplot matrix—a matrix of plots in which each glass oxide is compared to each other oxide. The scatterplot matrix of available Hanford HLW glass data, including WTP baseline data and newer enhanced waste glass (EWG) data, is shown in Figure 1.5.

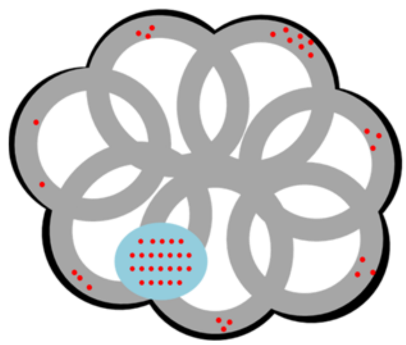

Figure 1.4. Distribution of HLW Glass Property-Composition Data Shown Conceptually on the Full Hanford HLW EGCR (each red dot represents test compositions and the blue region is the current WTP EGCR)

To address the above listed issues and revise the WTP baseline constraints to allow for HLW glasses with higher waste loadings, the following activities need to be completed:

- Fill the gaps in the full Hanford HLW EGCR. A sufficient number of glasses need to be tested within each EGCR subregion to accurately model composition properties of interest within each subregion.
- Effective glass processing must be demonstrated for HLW glass compositions across the QGCR for each region within the full Hanford HLW EGCR. A subset of compositions tested at crucible scale will need to be tested at small scale melter. Still fewer compositions will need to be tested at pilot scale melter.
- The glass property-composition models for the WTP baseline situation (Piepel et al. 2008) will need to be updated and revised to incorporate the new glass property-composition data for HLW glasses with higher waste loadings. If possible, global models, applicable to the entire composition region, will be developed to help guide formulation work and estimate waste loadings in system planning efforts. It is further anticipated that sets of local property-composition models will need to be developed and used to operate the WTP within some of the EGCR subregions. The local models

will likely have significantly lower uncertainty and will allow the plant to operate closer to constraint boundaries. A series of models for several properties applicable to one or two of the subregions may allow for sufficiently low model prediction uncertainties to support significantly higher waste loadings.

- Update the HLW glass formulation algorithm (Vienna 2014) with the new HLW glass property-composition models, constraints, and relevant composition and model uncertainties.

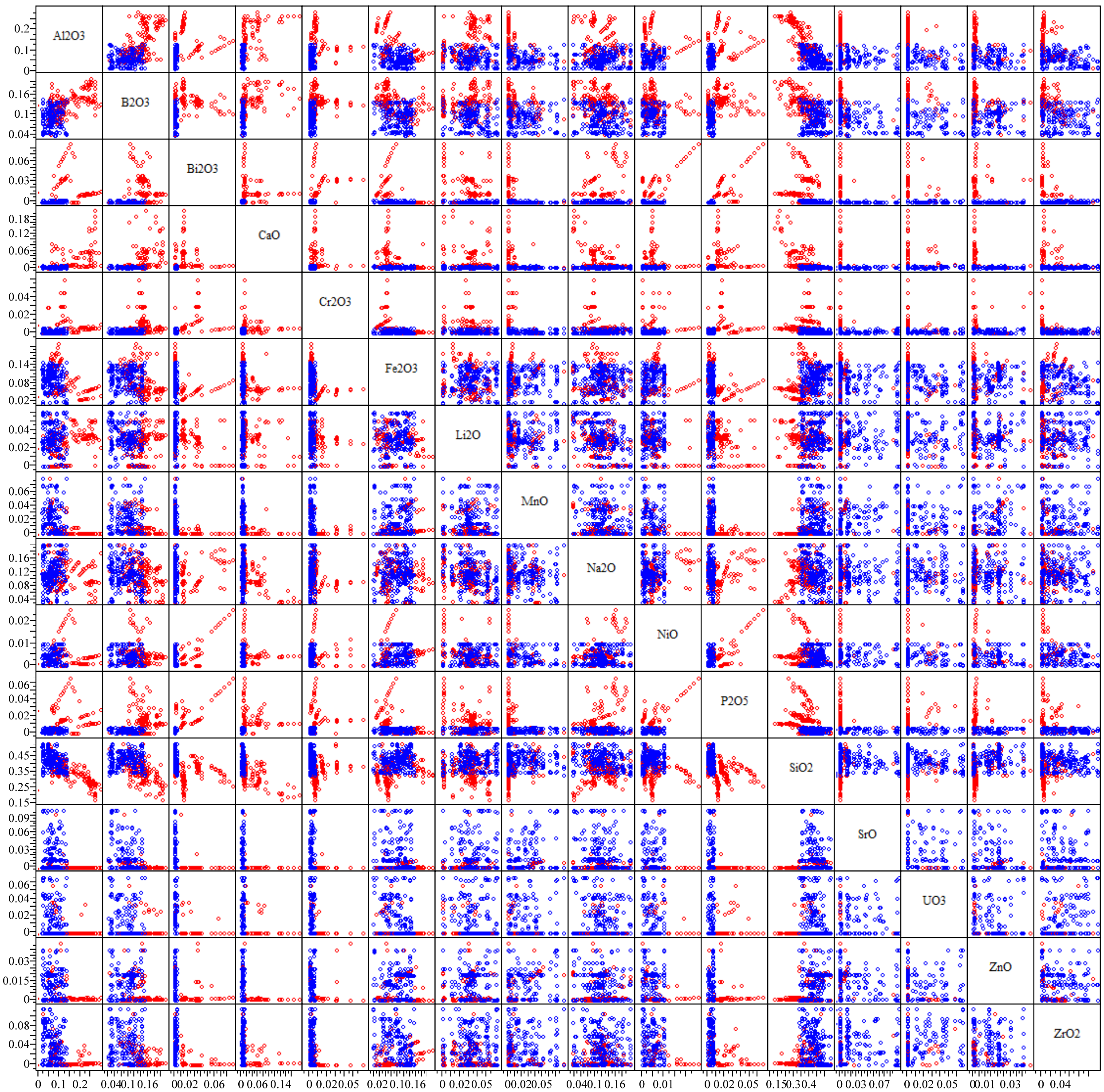

Figure 1.5. Scatterplot Matrix of Available Hanford HLW Test Glass Compositions with Blue Points for WTP Data and Red Points for Newer "ORP Data" (a.k.a., EWG data) (Plot for information only)

The development of new HLW property-composition models applicable to subregions or the full Hanford HLW EGCR is expected to be a multi-year effort. Rather than attempting to fill the EGCRs of multiple subregions in one step, the subregions were prioritized based on the estimated impacts on total HLW glass volume likely to result from immobilizing each subregion of wastes. The two with the highest potential impacts are the "high alumina" and the "chromium and sulfur" subregions. The high alumina (Al_2O_3) subregion was selected for initial study because it makes up roughly 50% of the waste (see Figure 1.3), and it is expected to be the first subregion to be processed by WTP after treatment of the commissioning tank. In addition, the chromium and sulfur subregion will likely require extensive melter testing to evaluate composition effects on salt accumulation in the melter.

Schematically, a composition subregion will be filled by HLW glass compositions as shown in Figure 1.6. Methods for selecting glass compositions to cover a specific EGCR are discussed in Section 1.2.

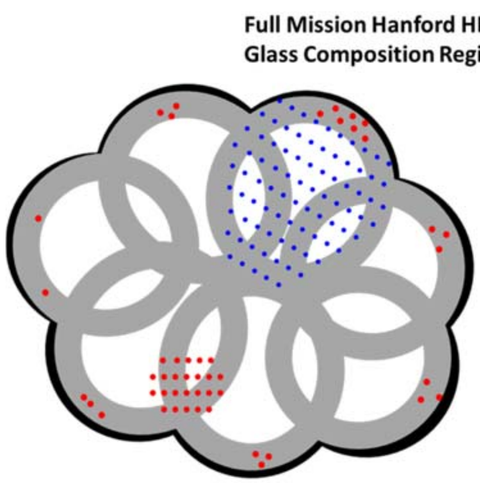

Figure 1.6. Glass Composition Data Shown Conceptually on the Full Hanford HLW EGCR (each red dot representing an existing test glass composition) with New Composition Data Required to Fill a Single Subregion (shown in blue dots)

1.2 Enhanced HLW Experimental Glass Composition Region and Test Matrix

This section discusses the development of the EGCR and test matrix for HLW glasses within the high alumina subregion of enhanced HLW glasses. Table 1.1 lists the 15 HLW glass components selected for study in the experimental work, including an "Others" component mix discussed subsequently. Also listed in Table 1.1 are the component lower and upper bounds (SCC) chosen to partially specify the enhanced high alumina glass EGCR subregion. Note that the "others" component was chosen to have a constant value (0.01545 mf), and hence it was not varied in the study. The remaining 14 components summed to 0.98455 in the matrix. However, it was decided to round the values in the matrix to four decimal places instead of five and four decimal places were used for the rest of the study. These 15 HLW glass components and the SCCs were chosen based on waste-glass knowledge, preliminary waste composition estimates, and experience from previous HLW glass testing.

The high alumina EGCR for enhanced HLW glasses was also partially specified by three MCCs, which also are listed in Table 1.1.

Table 1.1. Single-Component Constraints, Multiple-Component Constraints, and Center Point[(a)] of the 15-Component Enhanced High-Alumina Experimental Glass Composition Region

Single-Component Constraints			
Component	**Lower Bound**	**Upper Bound**	**Center Point**
Al_2O_3	0.1500	0.3000	0.2200
B_2O_3	0.0800	0.2200	0.1550
Bi_2O_3	0.0000	0.0300	0.0100
CaO	0.0000	0.1000	0.0350
Cr_2O_3	0.0000	0.0160	0.0075
Fe_2O_3	0.0000	0.1000	0.0550
K_2O	0.0000	0.0300	0.0070
Li_2O	0.0000	0.0600	0.0300
MgO	0.0000	0.0400	0.0050
MnO	0.0000	0.0300	0.0100
Na_2O	0.0500	0.1800	0.1150
P_2O_5	0.0000	0.0300	0.0100
SiO_2	0.2000	0.4300	0.3150
ZrO_2	0.0000	0.0400	0.0100
Others[(b)]	0.0155	0.0155	0.0155
Multiple-Component Constraints			
Expression			
$Al_2O_3 + Fe_2O_3$	0	0.30	
$Al_2O_3+ZrO_2$	0	0.30	
η_{1150} (Pa-s)[(c)]	0.5	20	

(a) The lower and upper bounds of the single-component constraints are in terms of mass fractions of the components.
(b) The Others component was composed of the following mixture of the following minor components (expressed as mass fractions): Cd = 0.0645, NiO = 0.2581, F = 0.1936, PbO = 0.1936, SO_3 = 0.1936 SrO = 0.0774, RuO_2 = 0.0064, and Ag_2O = 0.0129.
(c) The η_{1150} constraints were implemented using a property-composition model for ln(η_{1150}), given in Equation (1.1).

Two of the MCCs were stand-in constraints, $Al_2O_3 + Fe_2O_3 \leq 0.30$ (mf) and $Al_2O_3+ZrO_2 \leq 0.30$ (mf). These MCCs were intended to focus on glasses that did not have excessive refractory component concentrations (Al_2O_3, Fe_2O_3, and ZrO_2) while still covering the anticipated glass composition region. Glass compositions generated using the River Protection Project System Plan (Rev. 7) with advanced glass models include glasses that are high in only one of Al_2O_3, Fe_2O_3, or ZrO_2. Hence, these two MCCs were specified to restrict Al_2O_3, Fe_2O_3, or ZrO_2 from being high at the same time. The third MCC specified lower and upper bounds on glass viscosity at 1150ºC, namely $0.5 \leq \eta_{1150} \leq 20$ Pa-s. During operation of the WTP HLW vitrification facility, a narrower range for η_{1150} will be used, but for the purposes of specifying the high alumina HLW EGCR, a wider range was chosen so as to provide data both inside and outside the viscosity range of interest for operating the WTP HLW vitrification facility. The model described by Equation 1.1 was used to implement the η_{1150} constraints.

Statistical mixture experimental design methods (Cornell 2002) were used to generate the test matrix for the high alumina HLW EGCR. Specifically, statistical optimal experimental design methods (Atkinson et al. 2007) and software (discussed subsequently) were used to augment existing HLW glass compositions with new HLW glass compositions to adequately explore the high alumina HLW EGCR of interest. The following steps were used.

1. The MIXSOFT (Piepel 2003) software was used to generate the set of 39,197 extreme vertices of the high alumina HLW EGCR specified by the SCCs and MCCs in Table 1.1.
2. A set of 22 existing HLW glass compositions were collected that are within the high alumina HLW EGCR and have experimental values for all properties of interest.
3. It was determined that a total of 47 HLW glasses would be fabricated and tested in this phase of the high alumina HLW glass study. It was decided that 45 of the glasses would be extreme vertices, and the other two would be two replicates of a center point of the EGCR (listed in Table 1.1).
4. The Algorithms for the Construction of Experimental Designs (ACED) software (Welch 1987) was used to augment the set of 22 existing glass compositions (from Step 2) and the center point (from Table 1.1) with 45 of the EGCR vertices (from Step 1) using three optimality criteria based on a linear mixture model (i.e., $\sum_{i=1}^{14} \beta_i g_i$). Three experimental design optimality criteria were considered, which involved minimizing the uncertainty in 1) model coefficients fitted to the existing plus new test-matrix glasses, 2) the maximum prediction uncertainty over the EGCR, and 3) the average prediction uncertainty over the vertices of the EGCR. Because the ACED software uses an optimization algorithm that does not guarantee obtaining the optimal design for a given criterion on a given try, 20 tries with each of the three optimality criteria were performed. Hence, a total of 60 sets of 45 vertices from Step 1 were chosen to optimally augment the 22 existing HLW glass compositions (from Step 2) plus the center point (from Table 1.1). Not all of the 60 sets were necessarily unique, since a given "try" may produce the same set of vertices as some other "try."
5. Statisticians used various numerical and graphical approaches to assess the unique (out of 60) sets of 45 extreme vertices, and narrow the number down to three sets for consideration by glass scientists. Glass scientists then chose one of the sets of 45 extreme vertices.
6. After the set of 45 extreme vertices was selected, the test matrix was completed by adding two replicates of the center point. One of the center point replicates had been accounted for in selecting the sets of 45 extreme vertices. The second replicate of the center point was added after the selected set of 45 outer-layer vertices was determined.

The 47 high alumina HLW glasses making up the test matrix, including the chosen set of 45 extreme vertices and two replicates of the center point, are listed in Table 1.2. However, ultimately 12 of the 47 glasses required some modifications to their compositions for them to melt and form macroscopically homogenous glasses. This is understandable because the new test-matrix glasses were selected from the extreme vertices of the EGCR, which was chosen to investigate HLW glasses with significantly higher waste loadings. The 12 modified target glass compositions are listed in Table 1.3 with the extension "Mod" added to the glass identification. A description of how these modified compositions were obtained is discussed in Kroll et al. (2015). Note that glass property data were generated only for the "Mod" glasses and not their original "as-designed" counterparts.

This report summarizes the experimental methods to fabricate, heat treat, and test the 47-glass test matrix prepared at PNNL. The center glass was prepared and measured in duplicate resulting in a total of 47 glasses prepared and properties measured with 46 distinct target compositions. However, as noted in a footnote on Table 1.2, the first replicate of the center glass was mis-batched, with P_2O_5 = 0.005 instead of 0.01 mf. Measured properties relating to glass performance and processing are described in this report and are provided in appendices.

Table 1.2. Targeted Compositions (mass fractions) for the HLW Glasses in the High Alumina Study

	Glass ID[(a)]											
Component	**EWG-HAI-Centroid-1[(b)]**	**EWG-HAI-Centroid-2[(b)]**	**EWG-OL-801**	**EWG-OL-1369**	**EWG-OL-1580**	**EWG-OL-1672**	**EWG-OL-1755**	**EWG-OL-2463**	**EWG-OL-2619**	**EWG-OL-3063**	**EWG-OL-3122**	**EWG-OL-3208**
Al_2O_3	0.22111	0.22000	0.30000	0.15000	0.15000	0.30000	0.15000	0.19460	0.18460	0.15000	0.30000	0.15000
B_2O_3	0.15578	0.15500	0.21455	0.08000	0.08000	0.22000	0.08000	0.08000	0.22000	0.22000	0.08000	0.08000
Bi_2O_3	0.01005	0.01000	0.03000	0.03000	0.00000	0.03000	0.03000	0.00000	0.03000	0.03000	0.00000	0.00000
CaO	0.03518	0.03500	0.00000	0.10000	0.10000	0.10000	0.00000	0.10000	0.10000	0.00000	0.10000	0.00000
Cr_2O_3	0.00754	0.00750	0.00000	0.01600	0.01600	0.01600	0.01600	0.00000	0.00000	0.01600	0.01600	0.01600
Fe_2O_3	0.05528	0.05500	0.00000	0.00000	0.00000	0.00000	0.10000	0.10000	0.10000	0.10000	0.00000	0.00000
K_2O	0.00704	0.00700	0.00000	0.00000	0.00000	0.00000	0.00000	0.03000	0.03000	0.03000	0.03000	0.03000
Li_2O	0.03015	0.03000	0.00000	0.06000	0.06000	0.00000	0.06000	0.00000	0.00000	0.00000	0.00000	0.06000
MgO	0.00503	0.00500	0.00000	0.00000	0.00000	0.00000	0.00000	0.00000	0.00000	0.00000	0.00000	0.00000
MnO	0.01005	0.01000	0.03000	0.00000	0.03000	0.03000	0.03000	0.03000	0.03000	0.00000	0.03000	0.03000
Na_2O	0.11558	0.11500	0.18000	0.05000	0.05000	0.05000	0.05000	0.18000	0.05000	0.05000	0.18000	0.18000
P_2O_5	0.00503	0.01000	0.03000	0.03000	0.03000	0.03000	0.00000	0.03000	0.00000	0.03000	0.00000	0.03000
SiO_2	0.31658	0.31500	0.20000	0.42855	0.42855	0.20855	0.42855	0.20000	0.20000	0.31855	0.24855	0.40855
ZrO_2	0.01005	0.01000	0.00000	0.04000	0.04000	0.00000	0.04000	0.04000	0.04000	0.04000	0.00000	0.00000
CdO	0.00101	0.00100	0.00100	0.00100	0.00100	0.00100	0.00100	0.00100	0.00100	0.001000	0.00100	0.00100
NiO	0.00402	0.00400	0.00400	0.00400	0.00400	0.00400	0.00400	0.00400	0.00400	0.00400	0.00400	0.00400
F	0.00302	0.00300	0.00300	0.00300	0.00300	0.00300	0.00300	0.00300	0.00300	0.00300	0.00300	0.00300
PbO	0.00302	0.00300	0.00300	0.00300	0.00300	0.00300	0.00300	0.00300	0.00300	0.00300	0.00300	0.00300
SO_3	0.00302	0.00300	0.00300	0.00300	0.00300	0.00300	0.00300	0.00300	0.00300	0.00300	0.00300	0.00300
SrO	0.00121	0.00120	0.00120	0.00120	0.00120	0.00120	0.00120	0.00120	0.00120	0.00120	0.00120	0.00120
RuO_2	0.00005	0.00005	0.00005	0.00005	0.00005	0.00005	0.00005	0.00005	0.00005	0.00005	0.00005	0.00005
Ag_2O	0.00020	0.00020	0.00020	0.00020	0.00020	0.00020	0.00020	0.00020	0.00020	0.00020	0.00020	0.00020
Total	1.00000	1.00000	1.00000	1.00000	1.00000	1.00000	1.00000	1.00000	1.00000	1.00000	1.00000	1.00000

Table 1.2. Targeted Compositions (mass fractions) for the HLW Glasses in the High Alumina Study (continued)

	Glass ID[(a)]											
Component	**EWG-OL-3231**	**EWG-OL-3388**	**EWG-OL-3872**	**EWG-OL-4099**	**EWG-OL-4744**	**EWG-OL-5155**	**EWG-OL-5385**	**EWG-OL-5549**	**EWG-OL-5801**	**EWG-OL-6080**	**EWG-OL-6198**	**EWG-OL-6257**
Al_2O_3	0.15000	0.15000	0.15000	0.15000	0.19855	0.19855	0.25455	0.15000	0.18455	0.30000	0.15000	0.30000
B_2O_3	0.22000	0.22000	0.08000	0.22000	0.08000	0.22000	0.08000	0.22000	0.22000	0.21855	0.22000	0.08000
Bi_2O_3	0.00000	0.03000	0.03000	0.00000	0.03000	0.03000	0.00000	0.03000	0.00000	0.00000	0.00000	0.03000
CaO	0.10000	0.00000	0.10000	0.10000	0.10000	0.00000	0.10000	0.09455	0.00000	0.10000	0.00000	0.10000
Cr_2O_3	0.01600	0.01600	0.00000	0.00000	0.01600	0.01600	0.00000	0.00000	0.00000	0.01600	0.01600	0.01600
Fe_2O_3	0.00000	0.09855	0.00000	0.00000	0.10000	0.10000	0.00000	0.00000	0.10000	0.00000	0.10000	0.00000
K_2O	0.03000	0.03000	0.00000	0.00000	0.00000	0.00000	0.03000	0.03000	0.03000	0.03000	0.03000	0.03000
Li_2O	0.06000	0.00000	0.06000	0.06000	0.00000	0.06000	0.06000	0.00000	0.06000	0.00000	0.06000	0.06000
MgO	0.00000	0.00000	0.04000	0.04000	0.04000	0.04000	0.04000	0.04000	0.04000	0.04000	0.04000	0.04000
MnO	0.03000	0.03000	0.00000	0.03000	0.00000	0.03000	0.00000	0.00000	0.03000	0.00000	0.00000	0.00000
Na_2O	0.05000	0.18000	0.18000	0.05000	0.18000	0.05000	0.18000	0.18000	0.05000	0.05000	0.05000	0.05000
P_2O_5	0.03000	0.03000	0.03000	0.03000	0.00000	0.00000	0.00000	0.00000	0.03000	0.03000	0.03000	0.00000
SiO_2	0.29855	0.20000	0.31455	0.30455	0.20000	0.20000	0.20000	0.20000	0.20000	0.20000	0.24855	0.27855
ZrO_2	0.00000	0.00000	0.00000	0.00000	0.04000	0.04000	0.04000	0.04000	0.04000	0.00000	0.04000	0.00000
CdO	0.00100	0.00100	0.00100	0.00100	0.00100	0.00100	0.00100	0.00100	0.00100	0.00100	0.00100	0.00100
NiO	0.00400	0.00400	0.00400	0.00400	0.00400	0.00400	0.00400	0.00400	0.00400	0.00400	0.00400	0.00400
F	0.00300	0.00300	0.00300	0.00300	0.00300	0.00300	0.00300	0.00300	0.00300	0.00300	0.00300	0.00300
PbO	0.00300	0.00300	0.00300	0.00300	0.00300	0.00300	0.00300	0.00300	0.00300	0.00300	0.00300	0.00300
SO_3	0.00300	0.00300	0.00300	0.00300	0.00300	0.00300	0.00300	0.00300	0.00300	0.00300	0.00300	0.00300
SrO	0.00120	0.00120	0.00120	0.00120	0.00120	0.00120	0.00120	0.00120	0.00120	0.00120	0.00120	0.00120
RuO_2	0.00005	0.00005	0.00005	0.00005	0.00005	0.00005	0.00005	0.00005	0.00005	0.00005	0.00005	0.00005
Ag_2O	0.00020	0.00020	0.00020	0.00020	0.00020	0.00020	0.00020	0.00020	0.00020	0.00020	0.00020	0.00020
Total	1.00000	1.00000	1.00000	1.00000	1.00000	1.00000	1.00000	1.00000	1.00000	1.00000	1.00000	1.00000

Table 1.2. Targeted Compositions (mass fractions) for the HLW Glasses in the High Alumina Study (continued)

	Glass ID[a]											
Component	**EWG-OL-6311**	**EWG-OL-6489**	**EWG-OL-8548**	**EWG-OL-10278**	**EWG-OL-11318**	**EWG-OL-12707**	**EWG-OL-14547**	**EWG-OL-14827**	**EWG-OL-15698**	**EWG-OL-15968**	**EWG-OL-16450**	**EWG-OL-23401**
Al_2O_3	0.15000	0.30000	0.20000	0.26000	0.26000	0.15000	0.18153	0.15000	0.15000	0.15000	0.15000	0.15000
B_2O_3	0.08000	0.08000	0.08000	0.08000	0.22000	0.22000	0.08000	0.22000	0.08000	0.22000	0.22000	0.08000
Bi_2O_3	0.03000	0.00000	0.00000	0.00000	0.00000	0.03000	0.03000	0.03000	0.03000	0.00000	0.03000	0.00000
CaO	0.00000	0.00000	0.00000	0.10000	0.00000	0.10000	0.10000	0.10000	0.10000	0.00000	0.10000	0.10000
Cr_2O_3	0.01600	0.01600	0.01600	0.00000	0.01600	0.00000	0.01600	0.01600	0.00000	0.01600	0.01600	0.01600
Fe_2O_3	0.10000	0.00000	0.10000	0.00000	0.00000	0.00000	0.10000	0.00000	0.10000	0.00000	0.00000	0.00000
K_2O	0.03000	0.03000	0.00000	0.03000	0.00000	0.00000	0.03000	0.03000	0.00000	0.00000	0.00000	0.00000
Li_2O	0.06000	0.06000	0.00000	0.06000	0.00000	0.00440	0.06000	0.05899	0.02903	0.05149	0.00000	0.00000
MgO	0.04000	0.04000	0.04000	0.00000	0.04000	0.00000	0.00000	0.00000	0.04000	0.04000	0.04000	0.00000
MnO	0.00000	0.03000	0.03000	0.03000	0.03000	0.03000	0.00000	0.03000	0.03000	0.00000	0.03000	0.00000
Na_2O	0.18000	0.18000	0.18000	0.18000	0.17855	0.18000	0.14702	0.05000	0.18000	0.18000	0.17775	0.17539
P_2O_5	0.03000	0.03000	0.03000	0.00000	0.00000	0.03000	0.00000	0.00000	0.03000	0.00000	0.00000	0.00000
SiO_2	0.26855	0.21855	0.26855	0.20455	0.20000	0.20015	0.20000	0.29956	0.21552	0.28706	0.22080	0.42317
ZrO_2	0.00000	0.00000	0.04000	0.04000	0.04000	0.04000	0.04000	0.00000	0.00000	0.04000	0.00000	0.04000
CdO	0.00100	0.00100	0.00100	0.00100	0.00100	0.00100	0.00100	0.00100	0.00100	0.00100	0.00100	0.00100
NiO	0.00400	0.00400	0.00400	0.00400	0.00400	0.00400	0.00400	0.00400	0.00400	0.00400	0.00400	0.00400
F	0.00300	0.00300	0.00300	0.00300	0.00300	0.00300	0.00300	0.00300	0.00300	0.00300	0.00300	0.00300
PbO	0.00300	0.00300	0.00300	0.00300	0.00300	0.00300	0.00300	0.00300	0.00300	0.00300	0.00300	0.00300
SO_3	0.00300	0.00300	0.00300	0.00300	0.00300	0.00300	0.00300	0.00300	0.00300	0.00300	0.00300	0.00300
SrO	0.00120	0.00120	0.00120	0.00120	0.00120	0.00120	0.00120	0.00120	0.00120	0.00120	0.00120	0.00120
RuO_2	0.00005	0.00005	0.00005	0.00005	0.00005	0.00005	0.00005	0.00005	0.00005	0.00005	0.00005	0.00005
Ag_2O	0.00020	0.00020	0.00020	0.00020	0.00020	0.00020	0.00020	0.00020	0.00020	0.00020	0.00020	0.00020
Total	1.00000	1.00000	1.00000	1.00000	1.00000	1.00000	1.00000	1.00000	1.00000	1.00000	1.00000	1.00001

Table 1.2. Targeted Compositions (mass fractions) for the HLW Glasses in the High Alumina Study (continued)

	Glass ID[(a)]										
Component	**EWG-OL-26012**	**EWG-OL-29285**	**EWG-OL-31644**	**EWG-OL-32706**	**EWG-OL-33115**	**EWG-OL-33558**	**EWG-OL-33694**	**EWG-OL-33858**	**EWG-OL-35387**	**EWG-OL-38081**	**EWG-OL-38552**
Al_2O_3	0.15000	0.15000	0.15000	0.15000	0.15000	0.15000	0.15000	0.30000	0.15000	0.26000	0.26000
B_2O_3	0.08000	0.18576	0.08000	0.22000	0.08000	0.08000	0.22000	0.09910	0.08000	0.08000	0.08000
Bi_2O_3	0.03000	0.00000	0.00000	0.00000	0.03000	0.00000	0.03000	0.03000	0.03000	0.03000	0.03000
CaO	0.00000	0.10000	0.10000	0.00000	0.10000	0.10000	0.00000	0.00000	0.00000	0.00000	0.00000
Cr_2O_3	0.00000	0.00000	0.01600	0.00000	0.00000	0.00000	0.00000	0.00000	0.01600	0.00000	0.00000
Fe_2O_3	0.00000	0.00000	0.10000	0.00000	0.10000	0.10000	0.00000	0.00000	0.00000	0.00000	0.03617
K_2O	0.03000	0.00000	0.00000	0.03000	0.03000	0.03000	0.03000	0.03000	0.03000	0.03000	0.00000
Li_2O	0.01680	0.00000	0.01376	0.01229	0.00000	0.00261	0.00018	0.06000	0.00023	0.06000	0.06000
MgO	0.00000	0.04000	0.04000	0.04000	0.04000	0.04000	0.04000	0.04000	0.04000	0.00000	0.04000
MnO	0.00000	0.00000	0.03000	0.00000	0.00000	0.03000	0.03000	0.03000	0.03000	0.03000	0.03000
Na_2O	0.18000	0.05000	0.05000	0.06227	0.06559	0.05000	0.05437	0.05000	0.18000	0.07962	0.05000
P_2O_5	0.03000	0.03000	0.00000	0.00000	0.03000	0.03000	0.00000	0.00000	0.00000	0.00000	0.03000
SiO_2	0.42775	0.38879	0.40479	0.43000	0.35896	0.37194	0.43000	0.34546	0.42832	0.37493	0.32838
ZrO_2	0.04000	0.04000	0.00000	0.04000	0.00000	0.00000	0.00000	0.00000	0.00000	0.04000	0.04000
CdO	0.00100	0.00100	0.00100	0.00100	0.00100	0.00100	0.00100	0.00100	0.00100	0.00100	0.00100
NiO	0.00400	0.00400	0.00400	0.00400	0.00400	0.00400	0.00400	0.00400	0.00400	0.00400	0.00400
F	0.00300	0.00300	0.00300	0.00300	0.00300	0.00300	0.00300	0.00300	0.00300	0.00300	0.00300
PbO	0.00300	0.00300	0.00300	0.00300	0.00300	0.00300	0.00300	0.00300	0.00300	0.00300	0.00300
SO_3	0.00300	0.00300	0.00300	0.00300	0.00300	0.00300	0.00300	0.00300	0.00300	0.00300	0.00300
SrO	0.00120	0.00120	0.00120	0.00120	0.00120	0.00120	0.00120	0.00120	0.00120	0.00120	0.00120
RuO_2	0.00005	0.00005	0.00005	0.00005	0.00005	0.00005	0.00005	0.00005	0.00005	0.00005	0.00005
Ag_2O	0.00020	0.00020	0.00020	0.00020	0.00020	0.00020	0.00020	0.00020	0.00020	0.00020	0.00020
Total	1.00000	1.00000	1.00000	1.00001	1.00000	1.00000	1.00000	1.00001	1.00000	1.00000	1.00000

(a) The number following "OL-" is the number of an outer-layer vertex selected to be in the test matrix.

(b) EWG-HAI-Centroid-1 was mis-batched with P_2O_5 = 0.005, while EWG-HAI-Centroid-2 was correctly batched with P_2O_5 = 0.01. The composition of EWG-HAI-Centroid-1 was changed to reflect this.

Table 1.3. Targeted Compositions (mass fractions) for the HLW Glasses in the High Alumina Study

	Glass ID [(a)]											
Component	**EWG-OL-1755 Mod**	**EWG-OL-3063 Mod**	**EWG-OL-4744 Mod**	**EWG-OL-5385 Mod**	**EWG-OL-6257 Mod**	**EWG-OL-6311 Mod**	**EWG-OL-6489 Mod**	**EWG-OL-8548 Mod**	**EWG-OL-10278 Mod**	**EWG-OL-11318 Mod**	**EWG-OL-14547 Mod**	**EWG-OL-15698 Mod**
Al_2O_3	0.15000	0.15000	0.19855	0.25455	0.30000	0.17000	0.30000	0.21500	0.26000	0.26000	0.18153	0.15000
B_2O_3	0.10000	0.22000	0.10500	0.12000	0.12000	0.12000	0.11000	0.08000	0.15000	0.22000	0.12500	0.11000
Bi_2O_3	0.03000	0.03000	0.03000	0.00000	0.03000	0.03000	0.00000	0.00000	0.00000	0.00000	0.03000	0.03000
CaO	0.00000	0.00000	0.10000	0.10000	0.08000	0.00000	0.00000	0.00000	0.10000	0.00000	0.10000	0.10000
Cr_2O_3	0.01600	0.01600	0.01600	0.00000	0.01600	0.01600	0.01600	0.01600	0.00000	0.01600	0.01600	0.00000
Fe_2O_3	0.08000	0.10000	0.07500	0.00000	0.00000	0.10000	0.00000	0.10000	0.00000	0.00000	0.10000	0.10000
K_2O	0.03000	0.03000	0.00000	0.03000	0.03000	0.00000	0.03000	0.00000	0.03000	0.00000	0.01500	0.00000
Li_2O	0.06000	0.03000	0.00000	0.04000	0.06000	0.06000	0.04000	0.00000	0.05000	0.00000	0.04000	0.02903
MgO	0.00000	0.00000	0.04000	0.01000	0.01000	0.04000	0.04000	0.04000	0.00000	0.02000	0.00000	0.04000
MnO	0.03000	0.00000	0.00000	0.00000	0.00000	0.00000	0.03000	0.03000	0.01500	0.03000	0.00000	0.03000
Na_2O	0.05000	0.05000	0.18000	0.17000	0.05000	0.15000	0.15000	0.18000	0.15000	0.17855	0.13702	0.15000
P_2O_5	0.00000	0.03000	0.00000	0.00000	0.00000	0.03000	0.03000	0.03000	0.00000	0.00000	0.00000	0.03000
SiO_2	0.42855	0.31855	0.23000	0.24000	0.28855	0.26855	0.23855	0.28355	0.21955	0.25000	0.23000	0.21552
ZrO_2	0.01000	0.01000	0.01000	0.02000	0.00000	0.00000	0.00000	0.01000	0.01000	0.01000	0.01000	0.00000
CdO	0.00100	0.00100	0.00100	0.00100	0.00100	0.00100	0.00100	0.00100	0.00100	0.00100	0.00100	0.00100
NiO	0.00400	0.00400	0.00400	0.00400	0.00400	0.00400	0.00400	0.00400	0.00400	0.00400	0.00400	0.00400
F	0.00300	0.00300	0.00300	0.00300	0.00300	0.00300	0.00300	0.00300	0.00300	0.00300	0.00300	0.00300
PbO	0.00300	0.00300	0.00300	0.00300	0.00300	0.00300	0.00300	0.00300	0.00300	0.00300	0.00300	0.00300
SO_3	0.00300	0.00300	0.00300	0.00300	0.00300	0.00300	0.00300	0.00300	0.00300	0.00300	0.00300	0.00300
SrO	0.00120	0.00120	0.00120	0.00120	0.00120	0.00120	0.00120	0.00120	0.00120	0.00120	0.00120	0.00120
RuO_2	0.00005	0.00005	0.00005	0.00005	0.00005	0.00005	0.00005	0.00005	0.00005	0.00005	0.00005	0.00005
Ag_2O	0.00020	0.00020	0.00020	0.00020	0.00020	0.00020	0.00020	0.00020	0.00020	0.00020	0.00020	0.00020
Total	1.00000	1.00000	1.00000	1.00000	1.00000	1.00000	1.00000	1.00000	1.00000	1.00000	1.00000	1.00000

(a) The number following "OL-" is the number of an outer-layer vertex selected to be in the test matrix.

1.3 Quality Assurance

1.3.1 PNNL QA Program

The PNNL QA Program is based on the requirements specified in DOE Order 414.1D, *Quality Assurance*, and 10 CFR 830, *Energy/Nuclear Safety Management*, Subpart A, *Quality Assurance Requirements* (a.k.a., the Quality Rule). PNNL has chosen to implement the following consensus standards in a graded approach:

- American Society of Mechanical Engineers (ASME) NQA-1-2000, Quality Assurance Requirements for Nuclear Facility Applications, Part I, "Requirements for Quality Assurance Programs for Nuclear Facilities"
- ASME-NQA-1-2000, Part II, Subpart 2.7, "Quality Assurance Requirements for Computer Software for Nuclear Facility Applications," including problem reporting and corrective action
- ASME-NQA-1-2000, Part IV, Subpart 4.2, "Guidance on Graded Application of Quality Assurance (QA) for Nuclear-Related Research and Development."

The PNNL *Quality Assurance Program Description/Quality Management M&O Program Description* describes the PNNL-level QA program that applies to all work performed by PNNL. Laboratory-level procedures for implementing the QA requirements described in the standards identified above are deployed through PNNL's web-based "How Do I…?" (HDI) system, a standards-based system for managing and deploying requirements and procedures to PNNL staff. The HDI procedures (called Workflows and Work Controls) provide detailed guidance for performing some types of tasks, such as protecting classified information and procuring items and services, as well as general guidelines for performing research-related tasks, such as preparing and reviewing calculations and calibrating and controlling measuring and test equipment.

1.3.2 EWG QA Program

Until May 31, 2016, the Enhanced Waste Glass Project used the Washington River Protection Solutions Waste Form Testing Program (WWFTP) QA program as the basis for performing work. The WWFTP QA program implements the requirements of

- NQA-1-2008, Quality Assurance Requirements for Nuclear Facility Applications, and
- NQA-1a-2009, Addenda to ASME-NQA-1-2008, Quality Assurance Requirements for Nuclear Facility Applications

graded on the approach presented in NQA-1-2008, Part IV, Subpart 4.2.

On June 1, 2016, the Enhanced Waste Glass Project transferred to the PNNL Nuclear Quality Assurance Program. This QA program is compliant with ASME-NQA-1-2012, 10 CFR 830, Subpart A DOE Order (O) 414.1D for use by research and development projects and programs that are compatible with the editions of ASME-NQA-1 2000 through 2012.

All of the work reported in this document was performed to the QA level of Applied Research, which is described as follows.

Applied research work activities (or deliverables) apply to nuclear and non-nuclear research and development (work activities or deliverables) that are processes initiated with the intent of solving a specific problem or meeting a practical need. For applied research activities, grading is minimal and largely contingent upon the complexity of the research and the ability to duplicate the research if data were lost. The elements of QA grading, including the level of documentation, were applied to the program, project, and task levels.

The analytical results from work performed according to test instructions TI-EWG-0004[1] and TI-EWG-0014[2] were obtained prior to May 31, 2016. Hence, those analytical results were originally obtained under the WWFTP QA Program. Those analytical results were subsequently qualified as acceptable under the Nuclear Quality Assurance Program (QA) Program through the "Qualifying Existing Data" process documented in EWG-DQP-0012,[3] EWG-DQP-0002,[4] EWG-DQR-0011,[5] and EWG-DQR-0007.[6]

---

[1] Pires, RP. 2013. *EWG-High Alumina Outer Layer Matrix (OL) for High Level Waste Glass Studies*. TI-EWG-0004, Rev. 0, Pacific Northwest National Laboratory, Richland, WA.

[2] Russell, RL. 2014. *EWG-Modified Compositions of 12 High Alumina Outer Layer Matrix (OL) for High Level Waste Glass Studies*. TI-EWG-0014, Rev. 0, Pacific Northwest National Laboratory, Richland, WA.

[3] Meier, KM. 2016. *Data Qualification Plan for Test Instruction EWG-004*. EWG-DQP-0012, Rev. 0, Pacific Northwest National Laboratory, Richland, WA.

[4] Meier, KM. 2016. *Data Qualification Plan for Test Instruction EWG-014*. EWG-DQP-0002, Rev. 0, Pacific Northwest National Laboratory, Richland, WA.

[5] Meier, KM. 2016. *Data Qualification Report for Test Instruction EWG-004*. EWG-DQR-0011, Rev. 0, Pacific Northwest National Laboratory, Richland, WA.

[6] Meier, KM. 2016. *Data Qualification Report for Test Instruction EWG-014*. EWG-DQR-0007, Rev. 0, Pacific Northwest National Laboratory, Richland, WA.

2.0 Test Methods

This section describes how data were obtained for the 47 high alumina HLW test-matrix glasses described in Section 1.0. The descriptions include the methods for 1) glass fabrication, 2) chemical composition analysis, 3) density determination, 4) viscosity measurement, 5) electrical conductivity (EC) measurement, 6) crystal fraction from isothermal heat treatments, 7) secondary phase identification from centerline canister cooling (CCC) treatment, 8) Product Consistency Test (PCT) measurement, and 9) Toxic Leaching Characteristic Procedure (TCLP) measurement of the test glasses.

2.1 Glass Fabrication

Glass fabrication was performed according to the PNNL procedure Glass Development Laboratory Procedure: Glass Batching and Melting (GDL-GBM-1).[7] Single metal oxides, single metal carbonates, and sodium salts were mixed in the appropriate masses to form the target composition for each glass. Ruthenium was prepared separately from a nitrate solution to distribute the metal uniformly. The Ru solution was evenly dripped onto SiO_2 powders and then dried at 85°C to 100°C for at least 1 h. The Ru-containing SiO_2 powders were then added to the remaining powders in a plastic bag. After thoroughly mixing in the plastic bag for at least 30 s until uniform color developed, the powders were transferred to an agate milling chamber and milled for 4 min in an Angstrom milling machine. The powders were then transferred to a clean Pt-10%Rh crucible for melting at elevated temperatures. Each glass was melted in a Pt-alloy crucible using a two-step melt process. For glasses having a high iron oxide concentration, the temperature was kept as low as possible to avoid the rapid re-boil caused by the reduction of Fe^{3+} to Fe^{2+} and the release of oxygen around 1250°C. Initial melting was performed at temperatures ranging from 980°C to 1450°C for 0.67 h to 1.3 h in order for the compositions to melt and form macroscopically homogenous glasses. A second melt of the glass was accomplished after the first melt was quenched and the glass ground to a fine powder in a tungsten carbide vibratory mill. Generally, the second melt was at the same temperature or 25°C to 50°C higher than the initial melt and 0.75 h to 1.2 h in duration. Table 2.1 shows specific melt times and temperatures for each glass.

A few of the matrix glasses required melting temperatures up to 1450°C to fully dissolve all the starting materials. Using higher melting temperature is deemed to be an acceptable method of fabricating challenging glass compositions. Laboratory crucible-scale fabrication of glasses is not intended to mimic the actual melter process or feed processability. Rather it is intended to fabricate a glass sample with controlled composition for property testing. Composition is the primary variable in determine glass properties. The other primary impact of temperature history of glass melts is the impact on phase assemblage. Both liquid and crystalline phase separation may occur in some glasses. The impacts of thermal history on phase assemblage is measured for test glasses by systematic isothermal heat treatments at a range of temperatures and the CCC heat treatments, bounding the anticipated behavior in the plant.

The morphology and color of each quenched glass is shown in Appendix A.

[7] Schweiger, MJ. 2014. *Glass Development Lab Procedure: Glass Batching and Melting.* GDL-GBM-1, Pacific Northwest National Laboratory, Richland, WA.

Table 2.1. Melting Temperatures and Times Used in Fabricating the 47 HLW Glasses in the High Alumina Study

	First Melt			Second Melt		
Glass ID	Date	Temp. (°C)	Time (h)	Date	Temp. (°C)	Time (h)
EWG-OL-801	7/18/13	1250	0.9	7/18/13	1250	0.9
EWG-OL-1369	8/12/13	1250	0.9	8/12/13	1250	0.75
EWG.OL-1580	6/22/15	1250	1	6/23/15	1250	1
EWG.OL-1672	6/6/13	1350	0.67	6/6/13	1300	0.83
EWG.OL-2463	8/3/15	1200	NR	8/3/15	1200	0.83
EWG.OL-2619	6/12/13	1150	0.67	6/14/13	NR	NR
EWG-OL-3122	7/8/15	1450	1.2	7/9/15	1450	1
EWG.OL-3208	7/26/13	1100	0.83	7/26/13	1100	0.9
EWG-OL-3231	7/10/15	1100	1	7/13/15	1100	1.1
EWG.OL-3388	7/16/15	1027	1	7/16/15	1027	1
EWG.OL-3872	6/19/13	1050	1	6/19/13	1050	0.9
EWG.OL-4099	7/24/15	1000	NR	7/24/15	1000	1
EWG.OL-5155	7/16/13	1200	0.5	7/16/13	1225	0.83
EWG-OL-5549	7/23/15	1050	NR	7/23/15	1050	NR
EWG.OL-5801	8/16/13	1100	0.5	8/16/13	1050	NR
EWG.OL-6080	6/25/13	1450	1	6/26/13	1450	1
EWG.OL-6198	7/27/15	1100	1	7/27/15	1150	1
EWG-OL-12707	7/30/15	1050	0.75	7/31/15	1050	0.75
EWG-OL-14827	7/20/15	980	1	7/21/15	980	1.1
EWG-OL-15968	6/13/13	1150	0.83	6/13/13	1150	NR
EWG-OL-16450	11/6/13	1025	0.75	11/6/13	1025	NR
EWG-OL-23401	6/15/15	1400	1	6/17/15	1400	1
EWG-OL-26012	7/25/13	1250	1	7/25/13	1225	NR
EWG-OL-29285	7/22/13	1360	1	7/23/13	1360	1
EWG-OL-31644	8/6/13	1400	0.75	8/6/13	1350	1
EWG-OL-32706	9/9/13	1410	0.75	9/10/13	1400	1.4
EWG-OL-33115	6/11/13	1300	0.9	6/12/13	1300	NR
EWG-OL-33558	11/8/13	1350	0.83	11/9/13	1350	1
EWG-OL-33694	9/24/13	1450	0.83	9/25/13	1450	NR
EWG-OL-33858	7/22/15	1300	1.1	7/22/15	1300	1
EWG-OL-35387	6/9/15	1350	1	6/10/15	1350	1
EWG-OL-38081	9/23/13	1350	1	9/23/13	1350	NR
EWG-OL-38552	6/17/13	1250	0.9	6/17/13	1250	NR
EWG-OL-1755 Mod 8% Fe 10% B	5/27/14	1250	0.75	5/28/14	1275	1
EWG-OL-3063 Mod 1% Zr 3% Li	6/3/14	1400	0.83	6/3/14	1400	0.9
EWG-OL-4744 Mod 7.5% Fe 1% Zr	6/4/14	1250	0.83	6/6/14	1250	0.83
EWG-OL-5385 Mod 12% B 17% Na	6/2/14	1225	0.83	6/2/14	1225	0.75
EWG-OL-6257 Mod 12% B 8% Ca	6/3/14	1225	0.83	6/4/14	1225	0.83
EWG-OL-6311 Mod Reduced Na&K	12/2/14	1125	0.9	12/3/14	1125	1
EWG-OL-6489 Mod 11% B 15% Na	11/19/14	1150	1.1	11/20/14	1200	NR
EWG-OL-8548 Mod 1% Zr	12/4/14	1300	1.1	12/10/14	1300	1.2
EWG-OL-10278 Mod 15% B 1% Zr	12/11/14	1025	1	12/16/14	1025	1.1
EWG-OL-11318 Mod 1% Zr	11/6/14	1250	1.1	11/18/14	1250	0.9
EWG-OL-14547 Mod Reduced Alkali & 1% Zr	11/25/14	1100	1.2	11/26/14	1125	1.1
EWG-OL-15698 Mod Low Na	11/7/14	1050	1	11/10/14	1050	1
EWG-HAI-Centroid-1	4/12/13	1150	0.9	4/23/13	1150	0.4
EWG-HAI-Centroid-2 R-1	11/13/13	1150	1.3	11/13/13	1150	NR

NR = not recorded

2.2 Chemical Analysis of Glass Composition

To confirm that the "as-fabricated" glasses corresponded to the specified target compositions, a representative sample of each glass was chemically analyzed at the Savannah River National Laboratory (SRNL) Process Science Analytical Laboratory (PSAL). Two preparation techniques, including sodium peroxide fusion (PF) and acid dissolution (AD) were used to prepare glass samples, in duplicate, for analysis.

Each of the four preparations (two each for the two preparation techniques) was analyzed, twice for each element of interest, by inductively coupled plasma-optical emission spectroscopy (ICP-OES). Glass composition standards also were intermittently prepared and analyzed to assess the performance of the analyses over the course of these analyses. Specifically, several samples of the low-activity waste reference material (LRM) were included as part of the SRNL-PSAL analytical plan. The preparation and measurement methods used for each of the reported glass analytes are listed in Table 2.2.

Table 2.2. Preparation and Measurement Methods Used in Reporting the Measured Analyte Concentrations for Each of the High Alumina Study Glasses

Analyte	Preparation Method	Measurement Method
Ag	Not analyzed	Not analyzed
Al	PF	ICP-OES
B	PF	ICP-OES
Bi	PF	ICP-OES
Ca	PF	ICP-OES
Cd	AD	ICP-OES
Cr	PF	ICP-OES
F	Not analyzed	Not analyzed
Fe	PF	ICP-OES
K	AD	ICP-OES
Li	AD	ICP-OES
Mg	PF	ICP-OES
Mn	PF	ICP-OES
Na	AD	ICP-OES
Ni	PF	ICP-OES
P	AD	ICP-OES
Pb	AD	ICP-OES
Ru	AD	ICP-OES
S	AD	ICP-OES
Si	PF	ICP-OES
Sr	AD	ICP-OES
Zr	AD	ICP-OES

PF = peroxide fusion
AD = acid dissolution
ICP-OES = inductively coupled plasma-optical emission spectrometry

Two components of the study glasses, F and Ag, were not measured because an additional preparation method would have been required and these elements were present at very low concentrations. For example, the F concentration is 0.3 wt% (0.003 mf) and the Ag_2O concentration is 0.02 wt% (0.0002 mf) in all the study glasses. Their targeted concentrations were so low that they were likely to be near or below analytical detection limits.

A detailed analysis of the chemical composition measurements is published elsewhere (Fox et al. 2014, 2015a, 2015b). A short summary of these analyses is included in Section 3.1.

2.3 Glass Density

The room temperature density of each glass was measured according to PNNL procedure *Density Using a Gas Pycnometer* (OP-WTPSP-008)[8] using a AccuPyc II 1340 gas pycnometer (MicroMeritics, Norcross, GA) with approximately 0.1 mg of glass pieces. The glass was loaded into a vial and placed within the instrument. The instrument then determined the density by the difference in amount of helium gas needed to fill the vial. After five runs for each glass, the average glass densities were calculated. The pycnometer was calibrated before and after measurements for that day using a National Institute of Standards and Technology traceable standard tungsten carbide ball. These results are discussed in Section 3.2.

2.4 Canister Centerline Cooling and Crystal Identification

A portion (~150 g) of each test glass was subjected to the simulated CCC temperature profile shown in Table 2.3 and Figure 2.1.

Table 2.3. Temperature Schedule during CCC Treatment of Hanford HLW Glasses

Canister Centerline Cooling Treatment Schedule		
Segment	**Start-Stop Temp. (°C)**	**Rate (°C/min)**
1	1050–980	−1.556
2	980–930	−0.807
3	930–875	−0.591
4	875–825	−0.388
5	825–775	−0.253
6	775–725	−0.278
7	725–400	−0.303

[8] Rinehart DE. 2011. *Density Using a Gas Pycnometer*. OP-WTPSP-008, Rev. 1, Pacific Northwest National Laboratory, Richland, Washington.

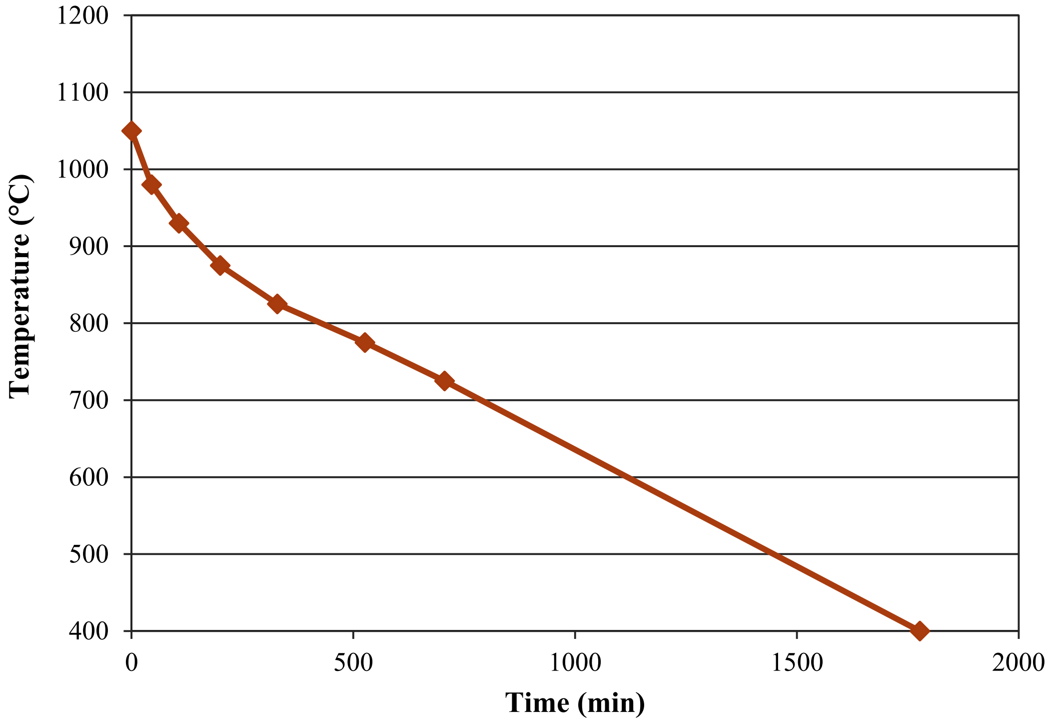

Figure 2.1. Plot of Temperature Schedule during CCC Treatment of Hanford HLW Glasses Viscosity

This profile is the temperature schedule of CCC treatment for Hanford HLW glasses planned for use at WTP.[9] Pieces of quenched glass >3 cm in diameter, were placed in a Pt-alloy crucible and covered with a Pt-alloy lid. The glass samples in simulated CCC treatment were brought to a target temperature of the glass melting temperature and held for 30 min. Then they were quickly cooled to 1050°C. The cooling profile was then started at 1050°C and progressed down to about 400°C based on seven cooling segments shown in Table 2.3. The starting temperature for the seven segments of cooling are 1050°C, 980°C, 930°C, 875°C, 825°C, 775°C, and 725°C.

The amount and type of crystalline phases that formed during CCC treatment were analyzed by X-ray diffraction (XRD) according to Section 12.4.4 of the standard ASTM International procedure *Standard Test Method for Determining Liquidus Temperature of Immobilized Waste Glasses and Simulated Waste Glasses* (ASTM C1720). Powdered glass samples were prepared using roughly 5 wt% CaF_2 as an internal standard phase with between 1.5 g and 2.5 g of powdered glass. Glass and CaF_2 were milled together for 2 min in a 10 cm^3 tungsten carbide disc mill. The powdered glass samples were loaded into XRD sample holders and scanned at a 0.04° 2θ step size, 4 second dwell time, from 10° to 70° 2θ scan range. XRD spectra were analyzed with TOPAZ software for phase identification. Full-pattern Rietveld refinement was performed to quantify the amounts of crystal phases on some samples with high crystalline content. Optical microscopy-image analysis and scanning electron microscopy were also used to examine the crystalline phases found in some CCC glass samples. These results are discussed in Section 3.3.

[9] Petkus LL. 2003. "Canister Centerline Cooling Data, Revision 1," to C.A. Musick, CCN: 074851, October 29, 2003, River Protection Project, Hanford Tank Waste Treatment and Immobilization Plant, Richland, Washington.

2.5 Viscosity

The viscosities (η) of the glass melts were measured as a function of temperature with a fully automated Anton Parr FRS 1600 Furnace Rheometer System according to the PNNL procedure *High-Temperature Viscosity Measurement Using Anton Paar FRS1600* (EWG-OP-0046).[10] Approximately 200 g of each quenched glass was first crushed in a tungsten carbide mill and 25 to 30 mL or ~70 g of glass was placed into a Pt-alloy cylindrical cup. It was then heated to ~1150°C and maintained at that temperature until thermal equilibrium was reached. A Pt-alloy bob (spindle) was then lowered into the cup of molten glass. An initial torque reading (at a constant spindle speed) was taken at ~1150°C with subsequent measurements at targets of 1050°C, 950°C, 1150°C, 1250°C, and then 1150°C in that order to evaluate hysteresis. Some glasses required adjustment of the target temperatures due to melting temperature and volatility and therefore higher and lower temperatures ranging from 850°C to 1390°C were tested. The hysteresis approach allows for the potential impacts of crystallization (at lower temperatures) to be assessed (via reproducibility) with duplicate measurements being taken at approximately T_M. Also volatilization (at higher temperatures) is minimized by measuring viscosity at temperatures above T_M near the end of the viscosity measurement sequence. The soak time was 30 min at each temperature. Prior to viscosity measurements, the test instrumentation was calibrated using a standard glass (Defense Waste Processing Facility [DWPF] Startup Frit) as discussed in the literature (Crum et al. 2015). These results are discussed in Section 3.4.

2.6 Electrical Conductivity

The ECs of glass melts were determined with an Anton Parr FRS 1600 Furnace Rheometer System high-temperature furnace and a Solartron impedance analyzer according to PNNL procedure *High-Temperature Electrical Conductivity Measurement* (EWG-OP-0047),[11] Platinum plates (1.3 in. long by 0.28 in. wide) were placed parallel to each other with a separation of 0.367 in. A 50-mL glass sample was used for conductivity measurement in a Pt-alloy crucible. Before measuring ECs of the test-matrix glass melts, calibration was conducted at room temperature with reference solutions of KCl (0.1 M and 1 M) by measuring the resistance values at three frequencies (1, 10, and 100 kHz). Four readings were taken at each frequency over a period of 2 to 5 min. For high temperatures, verification was conducted with DWPF startup frit. The averaged values of the four readings were then used to calculate the cell constant. For glass measurement, the sample was first heated to melting temperature and the probe was slowly lowered into the molten glass to a depth of 12.7 mm. After the temperature was stabilized, a scan from 1 MHz to 0.1 Hz in 3 min was conducted and resistance at 1 kHz was used to calculate the EC. Two scans were made for each temperature after the glass was held 10 min at each temperature before measurement for temperature stabilization. The EC was measured at four different temperatures in a range around the melting temperature of the glass. These results are discussed in Section 3.5.

[10] McCarthy, BP. 2017. *High-Temperature Viscosity Measurement Using Anton Paar FRS1600*. EWG-OP-0046, Rev. 0, Pacific Northwest National Laboratory, Richland, WA.
[11] McCarthy, BP. 2017. *High-Temperature Electrical Conductivity Measurement*. EWG-OP-0047, Rev. 0, Pacific Northwest National Laboratory, Richland, WA.

2.7 Crystal Fraction from Isothermal Heat Treatments

The equilibrium crystal fraction as a function of temperature was measured in Pt-alloy crucibles and boats with tight fitting lids (to minimize volatility) according to the standard ASTM International procedure *Standard Test Method for Determining Liquidus Temperature of Immobilized Waste Glasses and Simulated Waste Glasses* (ASTM C1720). The heat treatment times and temperatures were 24 ±2 h at 820°C to 1250°C to ensure equilibrium was achieved without excessive volatility. The samples were then quenched and analyzed by XRD according to Section 12.4.4 of the standard ASTM International procedure *Standard Test Method for Determining Liquidus Temperature of Immobilized Waste Glasses and Simulated Waste Glasses* (ASTM C1720). Crystal fraction data were extrapolated to obtain T_L and was interpolated or extrapolated to obtain $T_{1\%}$ and $T_{2\%}$ values.

Prior to measuring the crystal fraction of test-matrix glasses, the test instrumentation was calibrated. A standard glass with a known T_L traceable to a round robin study was used to determine the accuracy of each furnace at the start of this testing. Data measured and captured for the standard glass check was stored and maintained with the batch glass data. Data is reported in Section 3.6.

2.8 Product Consistency Test

PCT responses were measured in triplicate at SRNL for quenched and CCC samples of each glass using Method A of the standard ASTM International procedure *Standard Test Methods for Determining Chemical Durability of Nuclear, Hazardous, and Mixed Waste Glasses and Multiphase Glass Ceramics: The Product Consistency Test (PCT)* (ASTM C1285). Also included in the PCT experimental test matrix and tested in triplicate were the Environmental Assessment (EA) glass (Jantzen et al. 1993), the Approved Reference Material (ARM) glass (Mellinger and Daniel 1984), and blanks. Glass samples were ground, sieved to −100 +200 mesh, washed, and prepared according to the standard ASTM C1285 procedure. The prepared glass was added to water in a 1.5 g to 15 mL ratio, resulting in a glass surface area-to-solution-to-volume (S/V) ratio of approximately 2000 m^{-1}. The vessels used were desensitized Type 304L stainless steel. The vessels were closed, sealed, and placed into an oven at 90 ±2°C for 7 days ±3 h.

After 7 days at 90°C, the vessels were removed from the oven and allowed to cool to room temperature. The final mass of the vessel and the solution pH were recorded on a data sheet. Each test solution was then filtered through a 0.45-µm-size filter and acidified with concentrated, high-purity HNO_3 to 1 vol% to assure that the analytes remained in solution. The resulting solutions were analyzed by PSAL for Si, Na, B, and Li. Samples of a multi-element, standard solution also were analyzed as a check on the accuracy of the ICP-OES. Normalized releases (g/L) were calculated based on target, measured, and bias-corrected compositions using the average of the logarithms of the leachate concentrations. Results from the PCT work are published elsewhere (Fox et al. 2014, 2015a, 2015b), and a short summary of these results is included in Section 3.7.

2.9 Toxicity Characteristic Leaching Procedure

The TCLP analyses were conducted at Southwest Research Institute (SwRI) on Q and CCC samples of all HLW glasses. Crushed glass samples were extracted using Environmental Protection Agency (EPA) procedure EPA SW-846 Method 1311 (EPA 1997). For the majority of glasses, 100 g were used for extraction according to the method. However, for some glasses, Method 1311 was “modified” because reduced sample masses (<100 g) were extracted due to limited sample availability. For example, sample masses of 99.22 g to 99.96 g were used for glasses EWG-OL-10278 Mod (Q and CCC) and EWG-OL-14547 Mod (Q). For samples less than 100 g, the ratio of extraction fluid volume to sample weight remained the same as required in the EPA method. Most of the samples were extracted with Fluid #1 (pH = 4.93). However, glasses EWG-OL-4744 Mod (CCC), EWG-OL-5385 Mod (CCC), EWG-OL-6311 Mod (CCC), EWG-OL-6489 Mod (CCC), EWG-OL-10278 Mod (CCC), EWG-OL-14547 Mod (CCC), and EWG-OL-15698 Mod (CCC) were extracted with Fluid #2 (pH = 2.88) based on pH results from preliminary evaluations where the solution of water and small amount of sample showed pH > 5.0 according to Method 1311. Particle size reduction was required for all samples. The extracts were digested according to SW-846 Method 3010A (SwRI TAP01-0406-113, Rev. 4) for the remaining metals and were analyzed by ICP-AES SW-846 Method 6010B (SwRI TAP01-0406-130, Rev. 10) for all of the TCLP metals (As, Ag, Ba, Cd, Cr, Hg, Pb, Se) as well as B. All holding times were met. These results are discussed in Section 3.8.

3.0 Results and Discussion

This section describes the test results for the chemical composition, density, viscosity, EC, crystal fraction from isothermal and CCC heat treatments, PCT, and TCLP. Glass composition modifications for these HLW glasses studied are discussed in Kroll et al. (2015).

3.1 Chemical Analysis of Glass Composition

The targeted and average measured component concentrations (wt%) in the quenched glasses are presented in Appendix B along with the percent differences. The composition analyses of the glass samples were performed as described in Section 2.2.

Plots of the measured oxide values and measured versus targeted compositions are presented in Exhibit A-2 and Exhibit A-4 of Fox et al. (2014; 2015a, 2015b). Rigorous statistical analyses of the data were not performed.

The 47 HLW glasses with high alumina content study analyzed in three separate batches: a first batch of 19 glasses, a second batch of 16 glasses, and a third batch of 14 glasses during a time frame of 8 months. The analyzed glass composition data provided by SRNL were used to assess whether the glasses were mis-batched or were subject to excessive volatility. Overall, the ICP-OES and ion chromatography (IC) compositional analyses resulted in sums of oxides that ranged from about 98 wt% to 101.5 wt%, 99.5 wt% to 103.5 wt%, and 96.9 wt% to 100.8 wt% for the first, second, and third batches of study glasses, respectively, based on the initial concentration of each element compared to amounts measured by ICP-OES, respectively. The close range in sums of measured components indicates very good recovery of all the components, and consistency in analytical capability over eight months.

Most components showed consistent results between the analyzed and targeted values for concentrations >0.5 wt% (see Appendix B). However, exceptions for Cr_2O_3, MgO, and P_2O_5 were observed in the first batch of glasses. The analyzed values for Cr_2O_3 were somewhat low when compared to the targeted values for all of the study glasses targeting Cr_2O_3 concentrations >0.5 wt%. Many of the analyzed MgO and P_2O_5 values were below the targeted values for glasses that contained these components. Other exceptions occurred in the first batch for EWG-OL-1672. This glass had analyzed values for Al_2O_3 and SiO_2 that were lower than the targeted values, and measured value for B_2O_3 that was higher than the targeted values. The Al_2O_3 was low by 12.9%, the SiO_2 was low by 12.1% and the B_2O_3 was high by 41.2%. For the second and third batches of glasses, comparisons of the targeted and analyzed chemical compositions showed that the analyzed concentrations were within 10% of the targeted concentrations for those components present at more than 5 wt%. Only one glass (EWG-OL-33558) showed a larger difference (12.3%) between analyzed Na_2O value (5.61 wt%) and the targeted value (5.0 wt%).

The P_2O_5 concentration of glass EWG-HAI-Centroid-1 was about 53% lower than the targeted value. Upon further inspection, it was determined that the incorrect phosphorus source had been batched into the glass giving it a different composition than what was targeted. This glass composition was modified from the original targeted composition to the targeted composition that was actually batched. Therefore, based on the compositional analysis of these glasses (and comparisons of analyzed and targeted compositions in previous studies over many years), we concluded that the targeted compositions are better representations of the compositions of glasses tested. Hence, target compositions were used in future work to develop property-composition models except for the EWG-HAI-Centroid-1.

The plots of measured oxide concentrations and measured versus targeted oxide concentrations in Exhibit A-1 and Exhibit A-4 of the Fox et al. (2014a, 2015a, 2015b) reports were considered to assess whether any components volatilized. In these plots, the data points associated with the measured F and SO_3 concentrations were observed to be somewhat scattered. Some F and SO_3 volatilization is likely, but the scatter in the measured values makes it difficult to quantify. Other than this observation, there was no indication of significant volatilization.

3.2 Density

This section presents and discusses the results of the glass density measurements obtained using the methods discussed in Section 2.3. The results of the glass density measurements ranged from approximately 2.4 g/cm^3 to 2.8 g/cm^3 and are shown in Table 3.1. Figure 3.1 compares these measured density values to those predicted using the density model

$$\rho = \frac{\sum_{i=1}^{N} M_i x_i}{V} \tag{3.1}$$

where M_i is the molecular mass of the i-th component, x_i is the mole fraction of the i-th component, and V is molar volume (Vienna, Kim, and Hrma 2003). Figure 3.1 shows that the model over-predicts the lowest density values, and tends to under-predict the remaining density values. The biases in prediction are small to moderate, so the existing model could be used for some purposes. However, it would be best in the future to develop a new model that accounts for additional data from high alumina glasses.

Table 3.1. Measured Densities of HLW Glasses in the High Alumina Study

Glass ID	Measured Density (g/cm^3)	Glass ID	Measured Density (g/cm^3)
EWG-OL-801	2.493	EWG-OL-31644	2.785
EWG-OL-1369	2.694	EWG-OL-32706	2.408
EWG-OL-1580	2.647	EWG-OL-33115	2.750
EWG-OL-1672	2.518	EWG-OL-33558	2.731
EWG-OL-2463	2.792	EWG-OL-33694	2.440
EWG-OL-2619	2.793	EWG-OL-33858	2.562
EWG-OL-3122	2.644	EWG-OL-35387	2.623
EWG-OL-3208	2.553	EWG-OL-38081	2.600
EWG-OL-3231	2.589	EWG-OL-38552	2.692
EWG-OL-3388	2.653	EWG-OL-1755 Mod 8% Fe, 10% B	2.658
EWG-OL-3872	2.659	EWG-OL-3063 Mod 1% Zr 3% Li	2.561
EWG-OL-4099	2.599	EWG-OL-4744 Mod 7.5% Fe 1% Zr	2.788
EWG-OL-5155	2.747	EWG-OL-5385 Mod 12% B 17% Na	2.600
EWG-OL-5549	2.663	EWG-OL-6257 Mod 12% B 8% Ca	2.609
EWG-OL-5801	2.658	EWG-OL-6311 Mod Reduced Na & K	2.700
EWG-OL-6198	2.626	EWG-OL-6489 Mod 11% B 15% Na	2.581
EWG-OL-12707	2.697	EWG-OL-8548 Mod 1% Zr	2.694
EWG-OL-14827	2.661	EWG-OL-10278 Mod 15% B 1% Zr	2.581
EWG-OL-15968	2.546	EWG-OL-11318 Mod 1% Zr	2.494
EWG-OL-16450	2.676	EWG-OL-14547 Mod Reduced Alkali 1% Zr	2.770
EWG-OL-23401	2.656	EWG-OL-15698 Mod Low Na	2.812
EWG-OL-26012	2.622	EWG-Centroid-2	2.599
EWG-OL-29285	2.559		

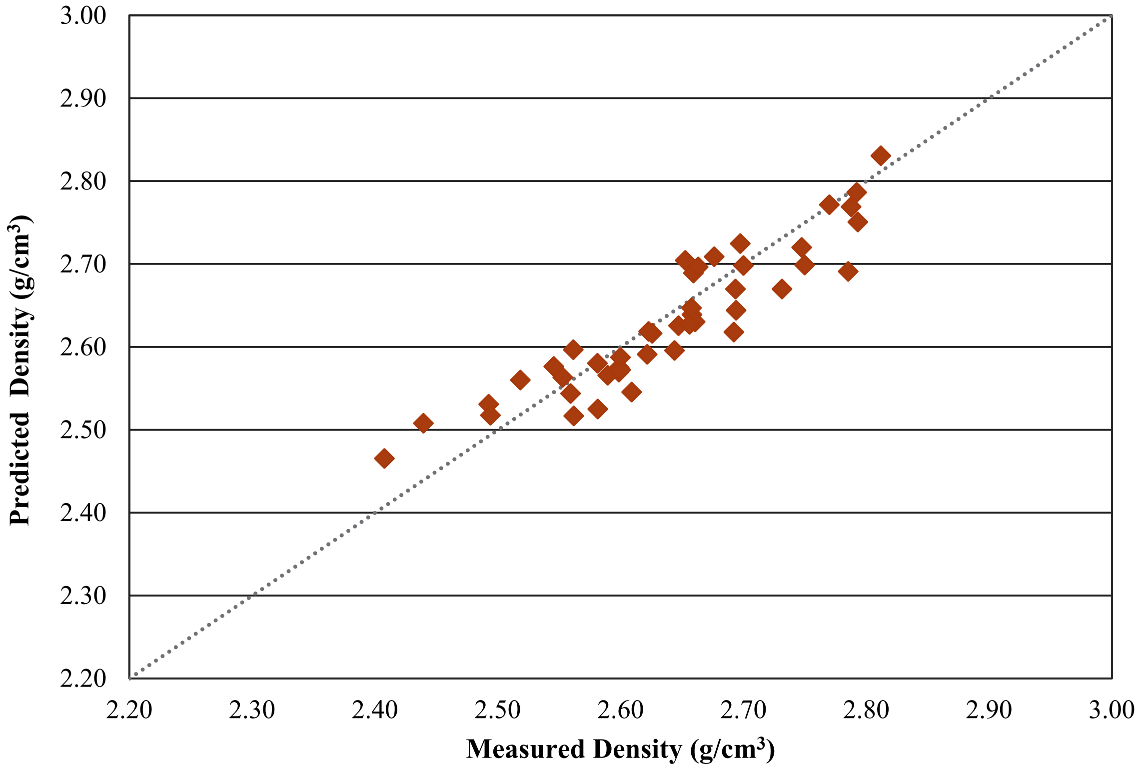

Figure 3.1. Plot of Predicted versus Measured Densities for HLW Glasses in the High Alumina Study, Using the Prediction Model in Equation (3.1)

3.3 Crystal Identification in Canister Centerline Cooling (CCC) Glasses

This section presents and discusses the crystal fraction results from the CCC glasses obtained using the methods discussed in Section 2.4. XRD scans of CCC glass samples identified various crystal types. The crystal types and wt% crystallinity results are summarized in Table 3.2. Fourteen glasses had crystal content of less than 5 mass% while seventeen glasses had crystal content greater than 20 mass%. Some of these glasses had greater than 50 wt% nepheline such as EWG-OL-3122 (55.3 wt%), EWG-OL-6489 Mod 11% B 15% Na (56.2 wt%), and EWG-OL-8548 Mod 1% Zr (51.3 wt%). The other crystalline group that occurred frequently was spinel, which has the generic formula AB_2O_4 where A and B are cations in different site of the structure with different valence of +2 and +3, respectively. There were 20 glasses that showed the presence of spinel, but in relatively low weight percents (<10 wt%). Many spinel types were identified with different chemical compositions; for example, $MnFe_2O_4$, $MgCr_2O_4$, $MnCr_2O_4$, $NiFe_2O_4$, and others (see Table 3.2). Alkali-transition metal oxide and alkaline earth-transition metal oxide phases also occurred frequently (i.e., in 20 glasses). See Appendix C for photos and Appendix D for XRD spectra of the CCC-treated glasses.

Table 3.2. Weight Percent Crystallinity and Identification of Crystals by XRD in CCC-Treated

Glass ID	Starting CCC Temp (°C)	Wt% Crystallinity	Crystal Phase Identification
EWG-HAI-Centroid-1	1150	5.4	$(Li_{0.29}Fe_{1.7})(Li_{0.71}Fe_{1.8}Mn_{1.5})O_8$
EWG-HAI-Centroid-2	1150	4.0	$Li_{0.5}Fe_{2.5}SO_4$
EWG-OL-801	1250	0	No crystals found
EWG-OL-1369	1250	1.4	Eskolite (Cr_2O_3)
		2.6	Apatite-(CaF)
		1.9	$Li_6(Si_2O_7)$
EWG-OL-1580	1250	3.2	Apatite-(CaF)
		1.3	$Li_6(Si_2O_7)$
		1.5	Eskolaite (Cr_2O_3)
EWG-OL-1672	1300	0.41	Eskolaite (Cr_2O_3)
		0.70	Brownmillerite
EWG-OL-2463	1200	45.3	Nepheline, sodian
		4.3	$Ca_{0.82}Fe_{0.18}SiO_3$
		10.3	$MnFe_2O_4$
EWG-OL-2619	1150	37.6	Augite
		9.0	Magnetite
EWG-OL-3122	1450	55.3	Nepheline, sodian
		4.4	Haueyne
EWG-OL-3208	1100	39.9	Nepheline, sodian
		10.3	Li_2SiO_3
		2.1	$MnCr_2O_4$
EWG-OL-3231	1100	4.5	Oxyapatite
		2.1	$Mn(CrMn)O_4$
EWG-OL-3388	1027	6.8	$(Zn,Mn,Fe)(FeMn)_2O_4$
EWG-OL-3872	1050	19.6	Nepheline
		7.0	Potassium Sodium Aluminum Silicate
		5.3	Sanidine low
		1.3	Cristobalite
		1.1	$Al(PO_4)$
		4.0	Megakalsilite
		5.9	Brownmillerite (Mg,Si-exchanged)
		5.8	$K_2Mg(SiO_4)$
		0.50	Zirconia
		0.91	Mn_2O_3
		0.55	Fe_2O_3
		1.8	Haumannite
EWG-OL-4099	1000	0.83	Braunite (Mn_7AlO_{12})
		2.0	Apatite-(CaF)
		0.25	SiO_2
EWG-OL-5155	1225	3.3	$Fe_3Mn_3O_8$
		0.52	ZrO_2
		4.0	Spessartine
		3.6	$Li_{0.5}Fe_{2.5}O_4$
		2.6	Baddeleyite (ZrO_2)
		4.1	$Na_{1.55}Al_{1.55}Si_xO_x$
EWG-OL-5549	1050	0	No crystals found
EWG-OL-5801	1050	2.5	Baddeleyite (ZrO_2)
		8.1	$Li_{0.5}Fe_{2.5}O_4$

Glass ID	Starting CCC Temp (°C)	Wt% Crystallinity	Crystal Phase Identification
EWG-OL-6080	1450	0.43	Cadmium Nickel Aluminum Oxide
		5.9	Spinel (Magnesium Aluminum Chromium Oxide)
		0.31	SiO_2
		1.3	Fluorapatite
		3.4	Magnesium Silicate
		0.05	Ruthenium Oxide
EWG-OL-6198	1150	2.3	Baddeleyite (ZrO_2)
		9.1	$Li_{0.5}Fe_{2.5}O_4$
EWG-OL-12707	1050	5.7	Oxyapatite
		0.66	Brownmillerite
EWG-OL-14827	980	2.6	$MgCr_2O_4$
EWG-OL-15968	1150	1.4	$MgCr_2O_4$
EWG-OL-16450	1025	4.7	Nepheline
		2.7	$Mg_{0.3125}Mn_{2.0625}Al_{0.625}O_4$
		1.2	Sodalite (permanganate)
		0.56	$Na_6(AlSiO_4)_6$
		2.5	Soda-melilite
EWG-OL-23401	1400	26.9	Nepheline, sodian
EWG-OL-26012	1225	0	No crystals found
EWG-OL-29285	1360	1.8	Apatite-(CaF)
		0.33	Braunite (Mn_7AlO_{12})
EWG-OL-31644	1350	1.7	Braunite (Mn_7AlO_{12})
		4.3	Hematite (Fe_2O_3)
		1.1	Gehlenite ($Ca_2Al_2SiO_7$)
EWG-OL-32706	1400	1.9	Baddeleyite (Zr_2O_2)
EWG-OL-33115	1300	9.2	$MgFeO_4$ (Magnesioferrite)
		26.1	Augite (MgFeAlCaSiO)
		3.4	Apatite-(CaF)
		0.21	$KFeO_2$
EWG-OL-33558	1350	5.7	Buckwaldite
EWG-OL-33694	1450	0	No crystals found
EWG-OL-33858	1300	1.9	Pseudo-eucryptite
		5.8	$MgAl_2O_4$
EWG-OL-35387	1350	4.3	$MgAl_2O_4$
		0.04	Pseudo-eucryptite
EWG-OL-38081	1350	18.5	Pseudo-eucryptite
		12.9	$K_{0.25}Na_{6.24}Si_{9.76}O_{32}$
EWG-OL-38552	1250	44.0	Pseudo-eucryptite
		1.9	Baddeleyite (Zr_2O_2)
		5.4	$Li_{0.5}Fe_{2.5}O_4$
		5.2	Spinel (MgFeAlO)
EWG-OL-1755 Mod 8% Fe, 10% B	1275	4.1	Chromite (Iron Chromium Oxide)
		0.65	Nickel Chromium Manganese(III) Oxide
		1.5	Magnetite (Fe_2O_3)
		0.05	Iron Nickel Manganese Oxide
EWG-OL-3063 Mod 1% Zr 3% Li	1400	0.31	Iron Silicon Oxide
		1.9	Hematite (Iron Oxide)
		0.40	Magnetite (Fe_2O_3)
		0.77	Chromite (Iron Chromium Oxide)
		1.9	Lithium Iron Oxide
		1.3	Chromium Iron Oxide

Glass ID	Starting CCC Temp (°C)	Wt% Crystallinity	Crystal Phase Identification
EWG-OL-4744 Mod 7.5% Fe 1% Zr	1250	6.9	Takedaite (Calcium Borate)
		15.2	Nepheline
		9.1	Nepheline, sodian
		0.92	Iron Oxide
		2.0	Iron Silicon Oxide
		1.4	Nosean (Sodium Aluminum Silicate Sulfate)
		0.60	Lazurite
		2.3	Maghemite
		0.26	Massicot (Lead Oxide)
		1.7	Calcium Iron Oxide
		0.08	Strontium Lead Oxide
EWG-OL-5385 Mod 12% B 17% Na	1225	38.0	Nepheline, sodian
		7.6	Takedaite (Calcium Borate)
		0.23	Calcium Aluminum Oxide Sulfate
		1.8	Strontium Aluminum Oxide
		1.7	Corundum (Aluminum Oxide)
		0.45	Lithium Nickel Magnesium Oxide
EWG-OL-6257 Mod 12% B 8% Ca	1225	6.9	Nepheline, sodian
		1.6	Lithium Nickel Oxide
		0.27	Eucryptite
		1.4	Cadmium Nickel Aluminum Oxide
		0.60	SiO_2
EWG-OL-6311 Mod Reduced Na & K	1125	2.6	Magnesium Aluminum Iron Oxide
		8.4	Spinel (Magnesium Aluminum Iron Oxide)
		6.7	Nepheline
		37.4	Nepheline, sodian
		1.8	Nosean (Sodium Aluminum Silicate Sulfate)
		0.93	Cristobalite
		9.0	Lithium Silicate
		0.78	Strontium Chromium Oxide
		0.91	Hematite (Iron Oxide)
		0.50	Iron Magnesium Oxide
EWG-OL-6489 Mod 11% B 15% Na	1200	56.2	Nepheline, sodian
		3.2	Lithium Magnesium Manganese (IV) Oxide
		3.5	Potassium Sodium Manganese Oxide
		2.6	Silicon Oxide
		5.2	Cadmium Nickel Aluminum Oxide
		0.97	Lithium Fluoride Sulfate
EWG-OL-8548 Mod 1% Zr	1300	51.4	Nepheline, sodian
		8.1	Magnesium Aluminum Iron Oxide
		5.4	Trevorite
EWG-OL-10278 Mod 15% B 1% Zr	1150	14.5	Nepheline, sodian
		4.6	Takedaite (Calcium Borate)
		0.81	Lithium Nickel Oxide
		0.30	Lithium Fluoride Sulfate
		6.1	Nepheline
		0.18	Neltnerite (Calcium Manganese Silicon Oxide)
EWG-OL-11318 Mod 1% Zr	1250	1.9	Magnesium Manganese Aluminum Oxide
		1.0	Magnesiochromite
EWG-OL-14547 Mod Reduced Alkali 1% Zr	1125	28.6	Nepheline, sodian
		6.4	Lithium Iron Oxide

Glass ID	Starting CCC Temp (°C)	Wt% Crystallinity	Crystal Phase Identification
		3.3	Lazurite
		4.4	Nosean (Sodium Aluminum Silicate Sulfate)
		11.4	Boron Calcium Oxide
		1.0	Silicon Oxide
		0.20	Lithium Fluoride Sulfate
EWG-OL-15698 Mod Low Na	1050	7.2	Nepheline, sodian
		17.8	Nepheline
		2.5	Iron Nickel Manganese Oxide
		0.81	Magnetite (Fe_2O_3)
		0.22	Iron Silicon Oxide
		0.23	Lazurite
		2.0	Nosean (Sodium Aluminum Silicate Sulfate)
		0.66	Silver Oxide
		5.0	Sodium Aluminum Silicate
		0.30	Massicot (Lead Oxide)
		0.13	Aluminum Phosphate
		0.29	Lithium Aluminum Oxide Silicate
		7.9	Magnesioferrite

3.4 Viscosity (η)

This section presents and discusses the viscosity results obtained using the methods discussed in Section 2.5. The results of the viscosity measurements are listed in Appendix E and summarized in Table 3.3.

Two equations are widely used to fit viscosity-temperature data for each waste glass. The first equation is the Arrhenius equation

$$\ln(\eta) = A + \frac{B}{T_K} \tag{3.2}$$

where *A* and *B* are temperature independent and composition dependent coefficients, and temperature (T_K) is in K [T(°C) + 273.15]. The values for the A and B coefficients obtained by fitting the equation to the viscosity-temperature data for each glass (using least squares regression) are shown in Table 3.4 for each glass. The second equation is the Vogel- Fulcher-Tammann (VFT) equation

$$\ln(\eta) = E + \frac{F}{T_k - T_0} \tag{3.3}$$

where E, F, and T_0 are temperature independent and composition dependent coefficients and T_K is the temperature in K [T(°C) + 273.15]. This equation can be used to estimate the effect of temperature on viscosity over a wide range of temperatures for silicate-based glasses. Therefore, this equation was fit to the data for each glass (using least squares regression) and the resulting A, B, E, F, and T_0 coefficients for each glass are also shown in Table 3.4. Furthermore, Table 3.4 summarizes the viscosity results at 1150°C (η_{1150}) calculated using Equation (3.2) or (3.3) fit to each glass measured data.

Table 3.3. Measured Viscosity (Pa·s) Values Versus Temperature (in the sequence of measurement) for the HLW Test Glass Melts

Glass ID	Date Measured	Measured Temp. (°C)	Measured η (Pa·s)	Measured Temp. (°C)	Measured η (Pa·s)	Measured Temp. (°C)	Measured η (Pa·s)	Measured Temp. (°C)	Measured η (Pa·s)	Measured Temp. (°C)	Measured η (Pa·s)	Measured Temp. (°C)	Measured η (Pa·s)
EWG-OL-801	5/12/15	1250	4.04	1150	10.60	1050	33.01	1250	4.08	1300	2.67	1250	4.16
EWG-OL-1369	6/16/15	1250	5.29	1150	8.66	1050	23.92	1250	4.22	1300	2.54	1250	3.73
EWG-OL-1580	7/15/15	1240	3.20	1140	7.20	1040	19.70	1240	3.25	1340	1.50	1240	3.26
EWG-OL-1672	7/27/15	1300	3.51	1200	5.18	1100	11.32	1300	3.64	1390	3.40	1300	3.77
EWG-OL-2463	8/22/15	1200	1.75	1100	4.84	1000	57.52	1200	1.71	--[a]	--[a]	--[a]	--[a]
EWG-OL-2619	4/23/15	1150	1.43	1050	4.12	950	28.86	1150	1.44	1250	0.62	1150	1.45
EWG-OL-3122	7/20/15	1390	1.58	1300	3.78	1200	9.75	1100	75.41	1390	1.60	--[a]	--[a]
EWG-OL-3208	6/1/15	1100	5.34	1000	12.00	900	32.25	1100	5.38	1200	2.66	1100	5.30
EWG-OL-3231	7/23/15	1100	1.42	1000	3.23	900	24.01	1100	1.44	1200	1.22	1100	2.09
EWG-OL-3388	7/21/15	1025	4.50	950	8.54	850	27.16	1025	4.60	1125	2.24	1025	4.53
EWG-OL-3872	5/14/15	1050	2.31	950	6.02	900	10.70	1050	2.33	1150	1.06	1050	2.32
EWG-OL-4099	8/18/15	1000	2.74	950	4.72	850	34.43	1000	2.74	1100	1.16	1000	2.80
EWG-OL-5155	5/5/15	1225	0.79	1125	3.11	1025	7.01	925	43.20	1225	0.98	1025	6.30
EWG-OL-5549	7/29/15	1050	4.67	950	5.97	900	8.78	1050	4.13	1150	4.51	1050	4.33
EWG-OL-5801	4/29/15	1050	1.33	950	4.47	900	25.08	1050	1.31	1100	0.85	1050	1.28
EWG-OL-6080	5/11/15	1390	1.54	1300	3.16	1200	7.64	1100	24.15	1390	1.45	--[a]	--[a]
EWG-OL-6198	8/21/15	1100	4.77	1000	12.23	900	31.26	1100	4.92	--[a]	--[a]	--[a]	--[a]
EWG-OL-6311	5/6/15	1050	7.76	950	15.51	900	18.58	1050	8.23	1075	6.69	1050	7.59
EWG-OL-12707	8/20/15	1050	1.55	950	6.94	900	14.66	1050	1.49	1150	0.69	1050	1.49
EWG-OL-14827	7/28/15	980	3.02	900	7.34	850	15.00	975	3.18	1025	2.08	980	3.14
EWG-OL-15968	5/13/15	1150	1.03	1050	1.90	950	4.32	1150	0.95	1250	0.51	1150	0.91
EWG-OL-16450	5/18/15	975	3.67	900	9.48	850	24.65	975	3.80	1025	2.39	975	3.98
EWG-OL-23401	7/7/15	1390	2.11	1300	4.34	1200	10.70	1100	31.61	1390	2.07	--[a]	--[a]
EWG-OL-26012	6/18/15	1250	9.03	1150	21.08	1050	57.47	1250	9.14	1300	6.23	1250	9.17
EWG-OL-29285	7/1/15	1360	4.85	1260	8.05	1160	23.90	1360	3.20	1390	2.48	1360	3.15
EWG-OL-31644	7/9/15	1375	3.29	1275	7.98	1175	17.84	1375	4.00	--[a]	--[a]	--[a]	--[a]
EWG-OL-32706	7/8/15	1390	4.61	1300	9.41	1200	23.07	1100	76.05	1390	4.61	--[a]	--[a]
EWG-OL-33115	6/23/15	1300	3.22	1200	8.35	1100	32.89	1300	3.17	--[a]	--[a]	--[a]	--[a]
EWG-OL-33558	6/29/15	1350	1.92	1250	4.70	1150	13.80	1350	1.93	--[a]	--[a]	--[a]	--[a]
EWG-OL-33694	7/16/15	1390	6.70	1300	14.41	1200	38.05	1100	115.00	1390	6.71	--[a]	--[a]
EWG-OL-33858	8/17/15	1300	3.28	1200	7.75	1100	21.50	1300	3.30	1390	1.59	1300	3.27
EWG-OL-35387	6/30/15	1350	4.38	1250	9.36	1150	21.98	1350	4.42	1390	3.25	1350	4.48
EWG-OL-38081	8/14/15	1350	8.24	1250	7.24	1150	20.83	1350	4.43	1390	3.66	1350	3.45
EWG-OL-38552	6/22/15	1250	3.72	1150	11.38	1050	41.41	1250	3.77	--[a]	--[a]	--[a]	--[a]
EWG-OL-1755 Mod 8% Fe, 10% B	7/2/15	1275	4.19	1175	10.19	1075	24.10	1275	4.28	--[a]	--[a]	--[a]	--[a]
EWG-OL-3063 Mod 1% Zr 3% Li	7/6/15	1375	2.02	1275	3.91	1175	8.30	1375	1.83	--[a]	--[a]	--[a]	--[a]
EWG-OL-4744 Mod 7.5% Fe 1% Zr	6/23/15	1250	2.08	1150	4.60	1050	13.10	1250	1.98	--[a]	--[a]	--[a]	--[a]
EWG-OL-5385 Mod 12% B 17% Na	5/26/15	1225	1.88	1125	2.77	1025	6.76	1225	1.66	1325	1.43	1225	1.86

Glass ID	Date Measured	Measured Temp. (°C)	Measured η (Pa·s)	Measured Temp. (°C)	Measured η (Pa·s)	Measured Temp. (°C)	Measured η (Pa·s)	Measured Temp. (°C)	Measured η (Pa·s)	Measured Temp. (°C)	Measured η (Pa·s)	Measured Temp. (°C)	Measured η (Pa·s)
EWG-OL-6257 Mod 12% B 8% Ca	6/9/15	1225	4.98	1125	11.01	1025	27.94	1225	5.38	--[(a)]	--[(a)]	--[(a)]	--[(a)]
EWG-OL-6311 Mod Reduced Na & K	6/8/15	1125	3.39	1025	8.22	925	18.60	1125	3.67	1225	1.73	1125	4.15
EWG-OL-6489 Mod 11% B 15% Na	6/15/15	1200	10.79	1100	24.34	1000	56.82	1200	14.16	1300	8.06	1200	15.60
EWG-OL-8548 Mod 1% Zr	6/25/15	1300	13.16	1200	40.02	1100	117.00	1300	10.93	--[(a)]	--[(a)]	--[(a)]	--[(a)]
EWG-OL-10278 Mod 15% B 1% Zr	5/27/15	1025	3.86	950	8.32	850	29.33	1025	3.85	1125	1.67	1025	3.88
EWG-OL-11318 Mod 1% Zr	6/17/15	1250	5.57	1150	12.25	1050	32.01	1250	5.50	1300	3.86	1250	5.57
EWG-OL-14547 Mod Reduced Alkali 1% Zr	6/10/15	1125	1.53	1025	3.73	925	15.07	1125	1.63	--[(a)]	--[(a)]	--[(a)]	--[(a)]
EWG-OL-15698 Mod Low Na	6/4/15	1050	4.14	950	13.30	900	24.25	1050	3.41	--[(a)]	--[(a)]	--[(a)]	--[(a)]
EWG-Centroid-1	7/30/15	1150	6.32	1050	17.30	950	55.68	1150	6.10	1250	2.49	1150	5.97
EWG-Centroid-2	5/4/15	1050	22.26	950	75.75	900	156.18	1050	22.52	1150	8.01	1050	22.81

(a) "-" denotes that the glass viscosity was too high to measure at the target temperature.

Table 3.4. Fitted Coefficients of Arrhenius and VFT Models for Viscosity of HLW Glasses with High Alumina Content Study

Glass ID	Arrhenius Coefficients		VFT Coefficients			η_{1150} (Pa·s) [(a)]
	A, ln[Pa·s]	B, ln[Pa·s-K]	E, ln[Pa·s]	F, ln[Pa·s-K]	T_0, K	
EWG-OL-801	-12.336	20934	-9.778	14218	252.1	10.62
EWG-OL-1369	-10.165	17637	-15.233	35232	-592.7	9.43
EWG-OL-1580	-10.755	18028	-11.596	20544	-97.1	6.80
EWG-OL-1672	-4.9707	9958.5	0.691	195.6	1260.6	6.65
EWG-OL-2463	-21.326	32047	-1.939	850.6	1131.2	2.65
EWG-OL-2619	-16.34	23843	-4.329	2374	914.1	1.40
EWG-OL-3122	-17.197	29222	-3.326	2222	1082.2	24.27
EWG-OL-3208	-8.7876	14369	-7.172	10457	190.8	3.72
EWG-OL-3231	-12.162	17543	-0.785	379.6	1077.4	1.37
EWG-OL-3388	-9.4799	14293	-4.340	4361	552.3	1.95
EWG-OL-3872	-10.838	15466	-7.505	8090	353.8	1.06
EWG-OL-4099	-15.571	21220	-3.088	1599	881.7	0.87
EWG-OL-5155	-13.302	19800	-5.822	4374	739.5	1.78
EWG-OL-5549	-2.0062	4725.1	1.269	49.55	1119	4.19
EWG-OL-5801	-19.588	26338	-1.647	460.0	1079	0.73
EWG-OL-6080	-12.673	21734	-8.860	11686	402.5	13.32
EWG-OL-6198	-9.3974	15088	-23.637	73129	-1526.4	3.18
EWG-OL-6311	-5.1365	9521.8	-24.641	121275	-3218.3	4.43
EWG-OL-12707	-15.639	21404	-4.961	2746	816.8	0.65
EWG-OL-14827	-12.077	16556	-3.962	2774	707.4	0.92
EWG-OL-15968	-9.3317	13210	-11.670	20326	-325.2	0.96
EWG-OL-16450	-14.21	19442	-2.470	1440	869.1	1.14
EWG-OL-23401	-12.091	21327	-10.027	15514	222.2	18.02
EWG-OL-26012	-9.9258	18482	-7.842	12968	232.7	21.14
EWG-OL-29285	-12.432	22342	-10.166	15893	240.9	26.51
EWG-OL-31644	-10.28	19079	-22.387	75022	-1520.1	22.25
EWG-OL-32706	-11.641	21867	-5.908	7903	601.1	40.65
EWG-OL-33115	-14.739	24974	-4.290	3641	905.4	15.51
EWG-OL-33558	-13.334	22696	-8.725	10808	470.9	13.81
EWG-OL-33694	-11.555	22379	-10.437	19110	114.81	64.66
EWG-OL-33858	-11.789	20399	-12.126	21424	-37.0	12.76
EWG-OL-35387	-10.022	18666	-10.319	19590	-37.3	22.08
EWG-OL-38081	-8.2281	15887	0.172	534.5	1236.1	20.69
EWG-OL-38552	-14.572	24203	-12.004	17436	214.7	11.30
EWG-OL-1755 Mod 8% Fe, 10% B	-10.333	18251	-18.716	50622	-961.9	12.29
EWG-OL-3063 Mod 1% Zr 3% Li	-9.9455	17477	-17.011	46223	-968.2	10.16
EWG-OL-4744 Mod 7.5% Fe 1% Zr	-11.592	18717	-5.907	6015	613.8	4.59
EWG-OL-5385 Mod 12% B 17% Na	-6.6785	10968	-0.548	425.4	1125.2	2.41
EWG-OL-6257 Mod 12% B 8% Ca	-9.2807	16356	-5.366	7230	466.9	8.97
EWG-OL-6311 Mod Reduced Na and K	-8.7791	14076	-25.446	93391	-2092.6	3.06
EWG-OL-6489 Mod 11% B 15% Na	-6.2518	13044	-1.903	3674	654.5	17.75
EWG-OL-8548 Mod 1% Zr	-13.271	24828	-44.764	204229	-2747.7	66.77
EWG-OL-10278 Mod 15% B 1% Zr	-11.305	16452	-7.039	7545	399.0	1.39
EWG-OL-11318 Mod 1% Zr	-9.825	17571	-7.067	10528	323.6	12.28
EWG-OL-14547 Mod Reduced Alkali 1% Zr	-12.935	18671	-3.146	1872	878.6	1.34
EWG-OL-15698 Mod Low Na	-13.434	19534	-47.721	199545	-2745.2	1.16
EWG-HAI-Centroid-1	-11.851	19806	-13.187	23386	-135.7	6.14
EWG-HAI-Centroid-2	-11.756	19307	-9.553	14347	190.3	8.04

(a) VFT model was used to calculate η_{1150}.

Figure 3.2 displays a plot of the ln (predicted η_{1150}) values versus the ln (measured η_{1150}) values based on the latest HLW viscosity model developed prior to this study. This HLW viscosity model is from Piepel et al. (2008) and is shown in Equation (3.4), where g_i denotes the mass fraction of the i^{th} glass component.

$$\ln(\eta_{1150}) = 12.5333(g_{Al2O3}) - 3.1161(g_{B2O3}) - 3.7004(g_{CaO}) - 6.769(g_{Fe2O3}) - 13.409(g_{Li2O}) - 6.8977(g_{MgO}) - 2.8771(g_{MnO}) - 4.6897(g_{Na2O}) + 1.3479(g_{SiO2}) - 14.0315(g_{SrO}) - 15.223(g_{ZrO2}) + 2.3371(g_{Others}) + 127.09(g_{Li2O})^2 - 21.8792(g_{Na2O}g_{B2O3}) - 30.4134(g_{SiO2}g_{Al2O3}) + 30.5925\left(\frac{g_{Al2O3}}{\frac{T}{1000}}\right) + 14.5535\left(\frac{g_{Fe2O3}}{\frac{T}{1000}}\right) - 70.0777\left(\frac{g_{Li2O}}{\frac{T}{1000}}\right) - 8.951\left(\frac{g_{Na2O}}{\frac{T}{1000}}\right) + 23.1245\left(\frac{g_{SiO2}}{\frac{T}{1000}}\right) + 19.1357\left(\frac{g_{SrO}}{\frac{T}{1000}}\right) + 48.4524\left(\frac{g_{ZrO2}}{\frac{T}{1000}}\right) \quad (3.4)$$

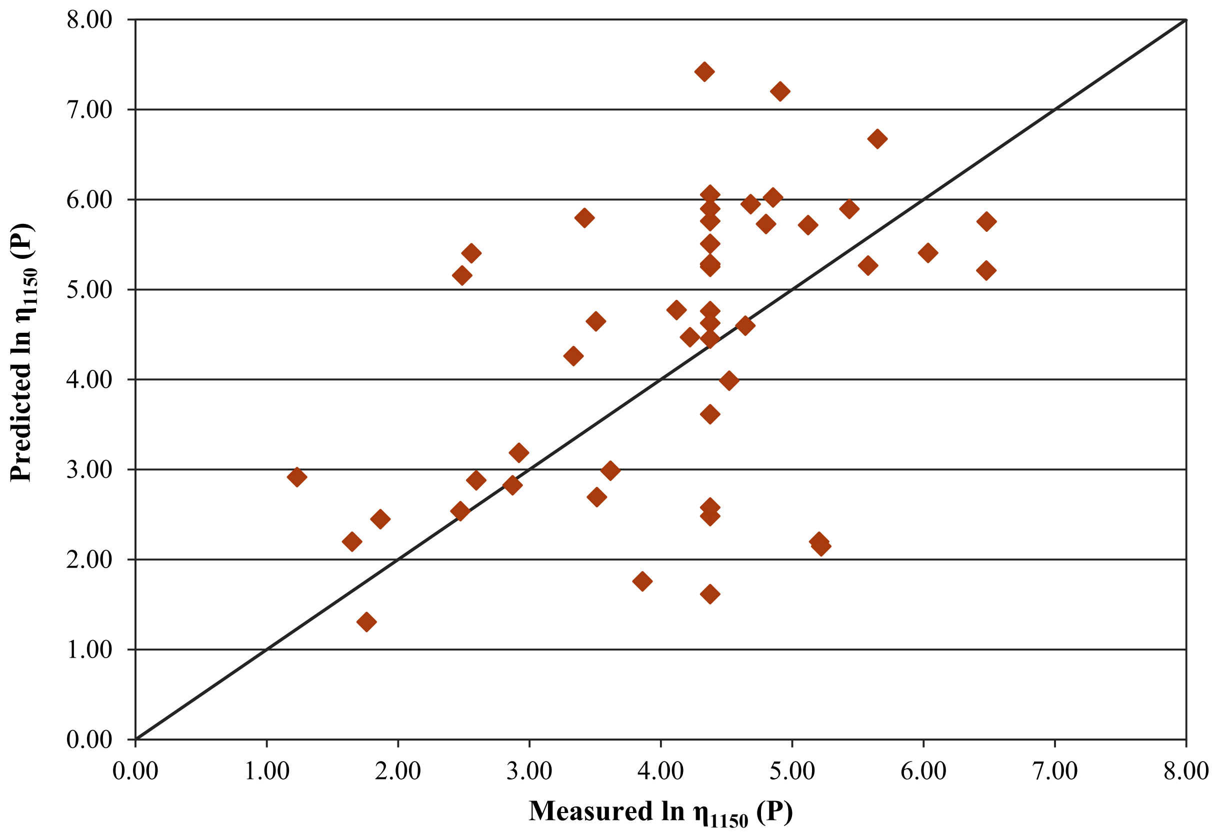

Figure 3.2. Predicted Versus Measured Values of Viscosity at 1150°C, Using a Previous Model in Equation (3.4)

Figure 3.2 shows that this model does not accurately predict the glass melt viscosity of these high alumina glasses. The composition range used to develop this model contained far less alumina than these glasses which may have some effect on this scatter. Therefore, it would be useful to fit a new viscosity model to account for this new data with higher alumina content.

3.5 Electrical Conductivity

This section presents and discusses the EC results obtained using the methods discussed in Section 2.6. Table 3.5 lists the EC versus temperature data for each of the glasses and Appendix F shows the plots for the EC versus temperature data obtained from the EC experiments.

The Arrhenius equation shown below was used to fit EC-temperature data for each waste glass.

$$\ln(\varepsilon) = A + \frac{B}{T_K} \tag{3.5}$$

where *A* and *B* are temperature independent and composition dependent coefficients, and temperature (T_K) is in K [T(°C) + 273.15]. The values for the A and B coefficients obtained by fitting the equation to the EC-temperature data for each glass (using least squares regression) are shown in Table 3.6 for each glass along with the EC results at 1150°C (ε_{1150}) calculated using Equation (3.5) fit to each glass measured data.

Figure 3.3 shows the ln (EC) plot for predicted versus measured EC, where the predicted values were produced by the modified Arrhenius equation parameters expanded as linear mixture models plus one alkali cross-product term (Piepel et al. 2008) shown below:

$$\ln(EC_{1150}) = -4.3754(g_{Al2O3}) + 0.7852(g_{B2O3}) - 2.9876(g_{Fe2O3}) + 32.2034(g_{Li2O}) + 16.344(g_{MgO}) + 1.5985(g_{MnO}) + 11.3872(g_{Na2O}) + 5.7863(g_{SrO}) - 0.3215(g_{SiO2}) + 0.2269(g_{ZrO2}) - 7.1088(g_{Others}) - 113.73(g_{Li2O}\, g_{Na2O}) - 7.7965\left(\frac{g_{B2O3}}{\frac{T}{1000}}\right) - 7.3668\left(\frac{g_{MnO}}{\frac{T}{1000}}\right) - 7.28\left(\frac{g_{SiO2}}{\frac{T}{1000}}\right) - 16.0518\left(\frac{g_{SiO2}}{\frac{T}{1000}}\right) - 7.2539\left(\frac{g_{ZrO2}}{\frac{T}{1000}}\right) \tag{3.6}$$

The model in Equation (3.6) tended to over predict this data. This could be because of the different glass composition region that this study explored versus the composition region explored for the EC models in Piepel et al. (2008). Therefore, a new model exploring a wider composition region should be developed to account for this new data.

Table 3.5. Measured EC (S/m) Values Versus Temperature (in the sequence of measurement)

Glass ID	Date Measured	Measured Temp. (°C)	EC (S/m)	Measured Temp. (°C)	EC (S/m)	Measured Temp. (°C)	EC (S/m)	Measured Temp. (°C)	EC (S/m)	Measured Temp. (°C)	EC (S/m)	Measured Temp. (°C)	EC (S/m)	Measured Temp. (°C)	EC (S/m)	Measured Temp. (°C)	EC (S/m)
EWG-HAI-Centroid-1	8/12/15	850	6.23	850	6.28	1150	27.60	--	--	1050	19.33	1050	19.38	950	11.91	950	11.97
EWG-HAI-Centroid-2	5/5/15	866	6.21	867	6.29	1153	27.34	1152	27.13	1059	19.08	1060	19.19	962	11.71	963	11.81
EWG-OL-801	5/13/15	950	15.36	950	15.51	1250	41.55	--	--	1150	32.36	1150	32.43	1050	23.37	1050	23.46
EWG-OL-1369	6/17/15	1250	40.16	1250	39.96	1150	29.45	1150	29.50	1050	19.61	1050	19.66	950	11.59	950	11.65
EWG-OL-1580	7/16/15	1240	42.24	1240	42.03	1140	30.85	1140	30.91	1040	20.45	1040	20.52	940	11.94	940	12.02
EWG-OL-1672	7/27/15	1000	0.84	1000	0.84	1300	7.70	1200	4.37	1100	2.08	1100	2.09	--	--	--	--
EWG-OL-2463	8/24/15	900	10.98	900	11.10	1200	41.56	1200	41.32	1100	30.69	1100	30.75	1000	19.77	1000	19.84
EWG-OL-2619	4/24/15	1150	5.54	1150	5.58	1250	9.95	1250	9.88	1050	2.55	1050	2.58	950	0.92	950	0.94
EWG-OL-3122	7/21/15	1390	55.36	1390	55.31	1300	44.11	--	--	1200	32.51	1200	32.60	1100	22.41	1100	22.49
EWG-OL-3208	6/2/15	800	22.30	800	22.54	1100	64.92	1100	64.47	1000	55.66	1000	55.79	900	38.01	900	38.34
EWG-OL-3231	7/24/15	800	4.87	800	4.96	1100	32.05	1100	31.86	1000	20.76	1000	20.83	900	11.25	900	11.35
EWG-OL-3388	7/22/15	875	18.74	875	18.80	1027	35.96	1027	35.74	975	30.13	975	30.16	925	24.23	925	24.28
EWG-OL-3872	5/15/15	850	23.30	850	23.49	1050	59.12	1050	58.65	950	40.86	950	41.29	900	31.51	900	31.70
EWG-OL-4099	1/19/17	850	5.73	850	5.79	900	8.75	900	8.67	950	12.38	950	12.30	1000	16.13	1000	16.20
EWG-OL-5155	5/6/15	850	6.77	850	6.91	1150	34.63	1150	34.42	1050	23.36	1050	23.50	950	13.77	950	13.89
EWG-OL-5549	9/22/15	850	8.52	850	8.54	1050	27.58	1050	27.54	950	17.04	950	17.11	900	12.35	900	12.38
EWG-OL-5801	4/30/15	800	4.19	800	4.11	900	9.42	900	9.28	1100	26.36	1100	26.27	1000	16.97	1000	17.08
EWG-OL-6080	5/12/15	1390	12.96	1390	12.91	1300	8.01	1300	8.03	1100	1.88	1100	1.86	1200	4.16	1200	4.14
EWG-OL-6198	8/22/15	800	6.31	800	6.41	900	12.94	900	13.07	1100	32.80	1100	32.69	1000	22.06	1000	22.19
EWG-OL-12707	8/21/15	850	4.57	850	4.57	900	6.64	900	6.66	950	9.36	950	9.41	1050	15.49	1050	15.40
EWG-OL-14827	7/29/15	850	7.95	850	8.00	980	19.18	980	18.93	950	16.68	950	16.69	900	11.95	900	11.99
EWG-OL-15968	5/14/15	850	23.15	850	23.48	950	38.06	950	38.33	1050	54.96	1050	54.82	1150	71.83	1150	71.45
EWG-OL-16450	5/1915	950	8.05	950	8.09	1050	9.98	950	10.07	1150	14.11	1150	14.04	1250	17.85	1250	17.56
EWG-OL-23401	7/8/15	1100	21.85	1100	21.91	1390	51.86	--	--	1300	41.63	1300	41.63	1200	31.21	1200	31.25
EWG-OL-26012	6/19/15	950	19.97	950	20.07	1050	30.05	1050	30.14	1150	40.98	1150	40.86	1250	44.17	1250	47.88
EWG-OL-29285	7/2/15	1050	1.20	1050	1.21	1150	2.53	--	--	1250	4.64	1250	4.63	1350	7.45	1350	7.65
EWG-OL-31644	7/10/15	1075	5.14	1075	5.14	1175	9.28	--	--	1275	15.60	1275	15.56	1375	24.12	--	--
EWG-OL-32706	7/9/15	1100	6.95	1100	6.96	1200	10.44	1200	10.42	1300	14.25	1390	18.66	1390	18.72	--	--
EWG-OL-33115	6/24/15	1000	1.46	1000	1.47	1100	3.21	1100	3.22	1200	6.11	1300	10.31	1300	10.35	--	--
EWG-OL-33558	7/1/15	1050	1.95	1050	1.94	1150	4.22	1150	4.21	1250	7.97	1250	7.94	1350	13.18	--	--
EWG-OL-33694	7/17/15	1100	3.23	1100	3.23	1200	5.11	--	--	1300	7.56	1300	7.55	1390	10.05	1390	10.12
EWG-OL-33858	8/18/15	1000	14.12	1000	14.18	1100	22.23	1100	22.27	1200	31.72	1200	31.68	1300	41.88	--	--
EWG-OL-35387	7/1/15	1050	22.00	1050	21.96	1250	39.40	--	--	1150	30.52	1150	30.45	1350	48.65	--	--
EWG-OL-38081	8/15/15	1050	23.57	1050	23.59	1350	53.35	--	--	1150	33.42	1150	33.40	1250	43.82	--	--
EWG-OL-38552	6/23/15	950	15.24	950	15.17	1050	24.16	1050	24.10	1150	34.62	1150	34.59	1250	45.71	1250	45.87
EWG-OL-1755 Mod 8% Fe, 10% B	7/3/15	950	14.20	950	14.12	1050	22.27	1050	22.21	1150	31.72	1150	31.66	1275	44.37	1275	44.50
EWG-OL-3063 Mod 1% Zr 3% Li	7/7/15	1100	14.95	1100	14.86	1200	20.69	1200	20.64	1300	28.01	1300	27.97	1390	35.64	1390	35.57
EWG-OL-4744 Mod 7.5% Fe 1% Zr	6/25/15	950	13.90	950	14.59	1050	23.88	1050	23.75	1150	35.21	1150	35.13	1250	47.97	1250	47.61
EWG-OL-5385 Mod 12% B 17% Na	5/27/15	925	19.81	925	19.79	1025	32.65	1025	32.58	1125	47.33	1125	47.34	1225	62.18	--	--

Glass ID	Date Measured	Measured Temp. (°C)	EC (S/m)	Measured Temp. (°C)	EC (S/m)	Measured Temp. (°C)	EC (S/m)	Measured Temp. (°C)	EC (S/m)	Measured Temp. (°C)	EC (S/m)	Measured Temp. (°C)	EC (S/m)	Measured Temp. (°C)	EC (S/m)	Measured Temp. (°C)	EC (S/m)
EWG-OL-6257 Mod 12% B 8% Ca	6/10/15	925	8.66	925	8.72	1025	15.53	1025	15.47	1125	24.28	1125	24.22	1225	33.94	1225	34.06
EWG-OL-6311 Mod Reduced Na & K	6/9/15	825	16.68	825	16.39	925	30.77	925	30.53	1025	48.99	1025	48.66	1125	67.12	1125	67.32
EWG-OL-6489 Mod 11% B 15% Na	6/16/15	900	21.95	900	22.04	1000	35.00	1000	34.56	1100	49.53	1100	49.20	1200	53.30	1200	53.18
EWG-OL-8548 Mod 1% Zr	6/26/15	1000	22.96	1000	22.89	1100	31.79	1100	31.74	1200	41.35	1200	41.34	1300	51.59	1300	51.74
EWG-OL-10278 Mod 15% B 1% Zr	5/28/15	875	16.54	875	16.52	925	22.36	925	22.39	975	29.10	975	29.11	1027	35.32	1027	35.79
EWG-OL-11318 Mod 1% Zr	6/18/15	950	15.35	950	15.23	1050	23.48	1050	23.39	1150	32.33	1150	32.28	1250	41.16	1250	41.28
EWG-OL-14547 Mod Reduced Alkali 1% Zr	6/11/15	825	10.06	825	9.77	925	21.62	925	21.15	1025	35.51	1025	35.44	1125	50.37	1125	50.77
EWG-OL-15698 Mod Low Na	1/24/17	859	11.50	860	11.60	907	17.09	908	17.20	958	22.88	960	22.98	1047	34.41	1049	34.77

"—" = not measured

Table 3.6. Fitted Coefficients of Arrhenius Model for EC Study

Glass ID	Arrhenius Coefficients A, ln[S/m]	Arrhenius Coefficients B, ln[S/m-K]	ε_{1150} (S/m)
EWG-OL-801	7.8518	-6239.1	32.07
EWG-OL-1369	8.7778	-7708.2	28.83
EWG-OL-1580	8.8672	-7714.8	31.38
EWG-OL-1672	11.596	-14956	2.97
EWG-OL-2463	8.9692	-7664.4	36.01
EWG-OL-2619	12.025	-14736	5.31
EWG-OL-3122	8.2895	-7097.6	27.17
EWG-OL-3208	8.1153	-5311.4	80.09
EWG-OL-3231	10.242	-9232.9	42.71
EWG-OL-3388	8.5005	-6377.8	55.65
EWG-OL-3872	9.2664	-6835.2	86.79
EWG-OL-4099	10.565	-9877.1	37.51
EWG-OL-5155	9.662	-8653.5	35.93
EWG-OL-5549	9.9032	-8683.8	44.76
EWG-OL-5801	9.9441	-9099.3	34.82
EWG-OL-6080	11.761	-15260	2.82
EWG-OL-6198	9.4065	-8072.4	41.86
EWG-OL-12707	9.5951	-9042.5	25.57
EWG-OL-14827	10.581	-9528.2	48.71
EWG-OL-15968	8.5146	-5996.6	73.77
EWG-OL-16450	6.1445	-5000.6	13.88
EWG-OL-23401	8.0718	-6836.2	26.26
EWG-OL-26012	7.3576	-5281.3	38.34
EWG-OL-29285	10.17	-13190	2.46
EWG-OL-31644	10.166	-11495	8.08
EWG-OL-32706	7.5859	-7741.5	8.55
EWG-OL-33115	10.624	-13013	4.39
EWG-OL-33558	11.156	-13858	4.13
EWG-OL-33694	7.73	-8995.7	4.09
EWG-OL-33858	8.4266	-7335.8	26.36
EWG-OL-35387	7.4267	-5724.9	30.08
EWG-OL-38081	7.6577	-5931	32.79
EWG-OL-38552	8.3491	-6861.4	34.05
EWG-OL-1755 Mod 8% Fe, 10% B	8.1227	-6669	31.08
EWG-OL-3063 Mod 1% Zr 3% Li	7.6993	-6868.8	17.69
EWG-OL-4744 Mod 7.5% Fe 1% Zr	8.8307	-7524.8	34.58
EWG-OL-5385 Mod 12% B 17% Na	8.8349	-6981.2	50.88
EWG-OL-6257 Mod 12% B 8% Ca	9.0187	-8185.2	26.24
EWG-OL-6311 Mod Reduced Na & K	9.4119	-7218.1	76.71
EWG-OL-6489 Mod 11% B 15% Na	7.6392	-5368.1	47.81
EWG-OL-8548 Mod 1% Zr	7.398	-5421.5	36.18
EWG-OL-10278 Mod 15% B 1% Zr	9.412	-7567.3	60.02
EWG-OL-11318 Mod 1% Zr	7.792	-6169	31.73
EWG-OL-14547 Mod Reduced Alkali 1% Zr	9.9577	-8350.5	59.74
EWG-OL-15698 Mod Low Na	10.076	-8590.9	56.80
EWG-HAI-Centroid-1	9.0325	-8055.3	29.15
EWG-HAI-Centroid-2	9.2044	-8367.5	27.79

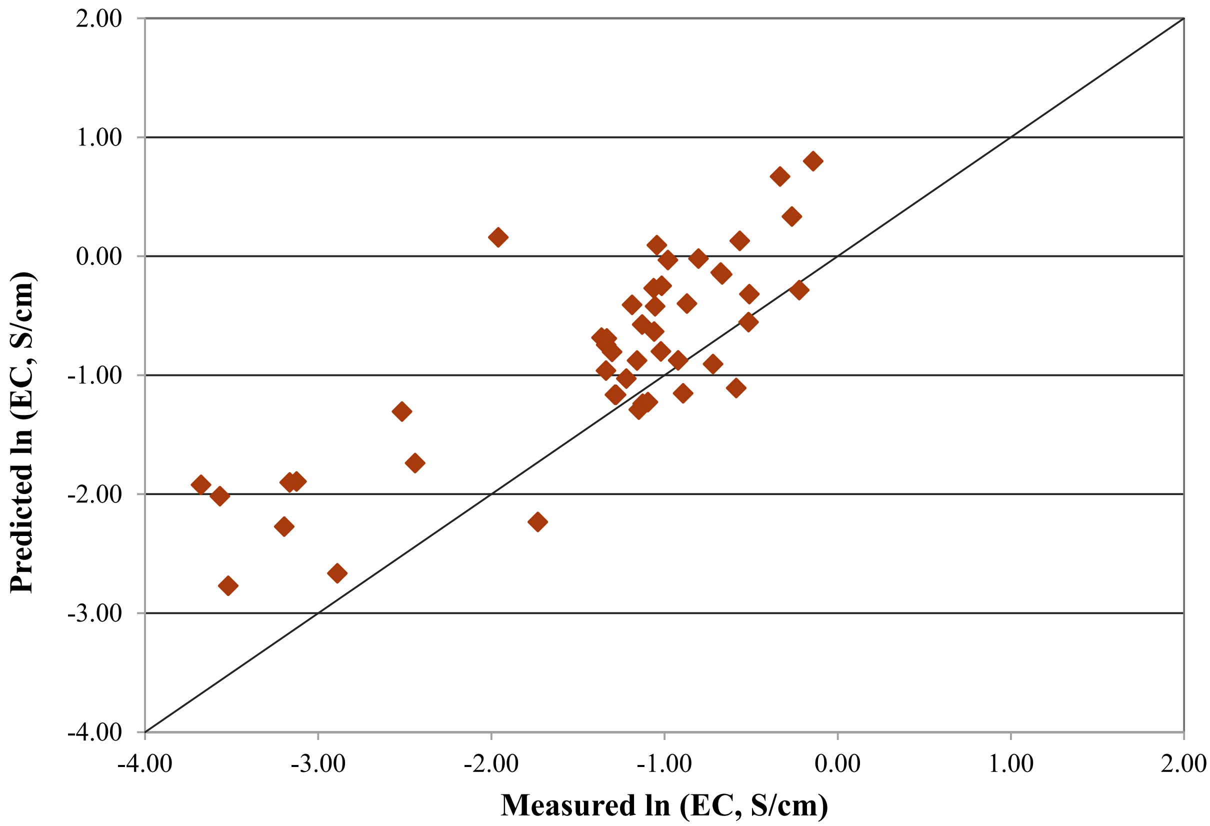

Figure 3.3. Predicted versus Measured Electrical Conductivity at 1150^{0}C for Enhanced HLW Glasses in the High Alumina Study, Using a Previous Model in Equation (3.6)

3.6 Crystal Fraction from Isothermal Heat-Treatments

This section presents and discusses crystal fraction results obtained using isothermal heat treatment methods discussed in Section 2.7. For each glass, the fraction of each crystalline phase was determined over a range of temperatures. T_Ls, $T_{1\%}$, and $T_{2\%}$ values associated crystalline phases were determined and listed in Table 3.7. Individual crystalline phases and their mass fractions at various temperatures of each glass are listed in Appendix G.

Table 3.7. Liquidus Temperature and Primary Crystalline Phase for the HLW Glasses in the High Alumina Study

Glass ID	Liquidus Temp. (°C)	$T_{1\%}$ (°C)	$T_{2\%}$ (°C)	Crystal Phase Identification
EWG-HAI-Centroid-1	1408	1238	1067	Spinel $((Li_{0.29}Fe_{1.7})(Li_{0.71}Fe_{1.8}Mn_{1.5})O_8)$
EWG-HAI-Centroid-2	1495	1210	926	Spinel $((Li_{0.29}Fe_{1.7})(Li_{0.71}Fe_{1.8}Mn_{1.5})O_8)$
EWG-OL-801	<1050	NA	NA	Al_2O_3
EWG-OL-1369	1324	1155	986	Cr-phases
EWG-OL-1580	1266	1130	993	Eskolaite (Cr_2O_3)
EWG-OL-1672	1116, 1114	947, 1062	779, 1010	Cr-phases, Spinel
EWG-OL-2463	1183	1145	1106	Spinel
EWG-OL-2619	1140, 1261	1101, 1150	1062, 1040	Fe Phases, Baddeleyite
EWG-OL-3122	1196, 1357	1156, 1171	1115, 985	Nepheline (Sodalite), Spinel (Magnetite)
EWG-OL-3208	>1000[(a)]	NA	NA	Spinel ($MnCr_2O_4$)
EWG-OL-3231	1227	1050	873	Cr-phases
EWG-OL-3388	1342	1234	1126	Spinel ($MnCr_2O_4$)
EWG-OL-3872	<950	NA	NA	Nepheline ($Na(AlSiO_4)$)
EWG-OL-4099	952	914	876	Oxyapatite
EWG-OL-5155	1202, 1326	1120, 1294	1038, 1262	Baddeleyite, Spinel
EWG-OL-5549	883	880	877	Nepheline
EWG-OL-5801	1170, 1222	1146, 1125	1122, 1028	Spinel, Baddeleyite
EWG-OL-6080	1449	1398	1348	Spinel
EWG-OL-6198	1533	1449	1366	Chromite
EWG-OL-12707	990	981	972	Nepheline
EWG-OL-14827	1225	1037	893	Cr-phases
EWG-OL-15968	1043	920	798	Spinel ($MgCr_2O_4$)
EWG-OL-16450	1125	1026	927	Spinel ($MgCr_2O_4$)
EWG-OL-23401	1208	1065	922	Eskolaite (Cr_2O_3)
EWG-OL-26012	<851	NA	NA	Nepheline
EWG-OL-29285	1174	1121	1067	Apatite
EWG-OL-31644	1383	1331	1279	Chromite
EWG-OL-32706	1272	1193	1114	Zr-phases
EWG-OL-33115	1178, 1182	1149, 1143	1121, 1103	Spinel, Oxyapatite
EWG-OL-33558	1190	1158	1126	Spinel (Magnetite)
EWG-OL-33694	1031	1008	986	$MnMg(B_2O_5)$
EWG-OL-33858	1301	1262	1222	Spinel $((Mg_{0.80}Al_{0.18})(Al_{1.86}Mg_{0.14})O_4)$
EWG-OL-35387	2315	1648	961	Spinel ($MgMn_{1.75}Al_{0.25}O_4$)
EWG-OL-38081	1474	1299	1123	Baddeleyite (ZrO_2)
EWG-OL-38552	1280, 1453	1245, 1301	1211, 1148	Spinel, Zr-phases
EWG-OL-1755 Mod 8% Fe, 10% B	1396	1310	1224	$(Li_{0.64}Fe_{5.36})O_8$
EWG-OL-3063 Mod 1% Zr 3% Li	1101, 1320	963, 1254	825, 1187	Cr_2O_3, Spinel
EWG-OL-4744 Mod 7.5% Fe 1% Zr	1389	1320	1250	Chromite
EWG-OL-5385 Mod 12% B 17% Na	950	946	941	Nepheline
EWG-OL-6257 Mod 12% B 8% Ca	1639	1538	1437	Spinel
EWG-OL-6311 Mod Reduced Na & K	1318	1270	1223	Spinel
EWG-OL-6489 Mod 11% B 15% Na	1827	1760	1693	Spinel
EWG-OL-8548 Mod 1% Zr	1655	1606	1557	Spinel
EWG-OL-10278 Mod 15% B 1% Zr	923	919	916	Nepheline
EWG-OL-11318 Mod 1% Zr	2095	1802	1508	Spinel (MgMnAlO)

EWG-OL-14547 Mod Reduced Alkali 1% Zr	1092	1051	1009	Spinel $((Li_2O)(Fe_2O_3)_{4.0}(Cr_2O_3))$
EWG-OL-15698 Mod Low Na	1162	1130	1099	Spinel (Magnetite)
(a) No crystals seen until 1100°C and then several crystals seen.				
NA = not applicable				

One glass (EWG-OL-6257 Mod 12% B 8% Ca) had a T_L, $T_{1\%}$, and $T_{2\%}$ that could not be determined because the data were scattered and no reliable line could be fit to the data. There were also four glasses for which precise T_L, $T_{1\%}$, and $T_{2\%}$ could not be determined (EWG-OL-801, EWG-OL-3208, EWG-OL-3872, and EWG-OL-26012), but upper or lower limits could be set as <1050°C, >1000°C, <950°C, and <851°C, respectively for the T_L. This is because a crystalline phase was obtained for only one temperature, while the glass was 100% amorphous for all other temperatures. The phases identified in these four glasses were Al_2O_3, $MnCr_2O_4$ (spinel), nepheline, and nepheline, respectively. There were four glasses where T_L, $T_{1\%}$, and $T_{2\%}$ were determined based on a combination of multiple phases of similar chemical compositions because no clear line fitting could be obtained for any single phase. For example, glass EWG-OL-5549 used the total amount of nepheline and $Na_6(AlSiO_4)_6$. The total amount of Fe_2O_3 and Fe_3O_4 was used for glass EWG-OL-2619. Glass EWG-OL-3231 used the total amount of $MnCr_2O_4$ plus Cr_2O_3, while glass EWG-OL-32706 used the total amount of ZrO_2 plus $ZrSi_{0.993}O_4$.

Spinel (generic form of AB_2O_4) was found in 36 glasses, eskolaite (Cr_2O_3) in six glasses, baddeleyite (ZrO_2) in eight glasses, and nepheline ($(Na,K)AlSiO_4$) in 22 glasses. The $T_{1\%}$ ranged from 880°C with alkali-Al-silicate to 1802°C with spinel (MgMnAlO). Twenty-three of the glasses had a $T_{1\%}$ above 1150°C and thirteen of the glasses had a $T_{2\%}$ above 1150°C, which is the target melting temperature.

The model for $T_{1\%}$ of HLW glasses was developed by Piepel et al. (2008) using data for glasses with much lower values of alumina and assuming all crystals were spinels. That model is given by:

$$T_{1\%} = 4301.9031(g_{Al2O3}) + 962.6031(g_{B2O3}) + 8936.8818(g_{Cr2O3}) + 4144.6963(g_{Fe2O3}) - 1947.5122(g_{Li2O}) - 163.7335(g_{MnO}) - 1146.098(g_{Na2O}) + 21966.7988(g_{NiO}) - 2566.0459(g_{SiO2}) + 1474.0702(g_{SrO}) + 466.9017(g_{ZrO2}) + 2842.9261(g_{Others}) + 14871.5(g_{ZrO2}\, g_{ZrO2}) + 29256.3805(g_{MnO} g_{Na2O}) + 47617.3683(g_{Li2O}\, g_{MnO}) - 216741.7305(g_{MnO} g_{NiO}) + 4736.9006(g_{SiO2}\, g_{SiO2}) \quad (3.7)$$

This model was used to predict $T_{1\%}$ values for the HLW glasses. Figure 3.4 shows the plot for predicted versus measured values of $T_{1\%}$, which indicates that this model didn't predict the data from HLW glasses in the high alumina study very well with quite a bit of scatter. This could be because of the different glass composition region explored in this study versus the composition region explored for the $T_{1\%}$ model and/or the assuming of all spinel crystals when several different types of crystals were observed in these glasses. Therefore, a new $T_{1\%}$ model exploring a wider composition region and different crystal structures should be developed to account for the data from the HLW glasses in the high alumina study.

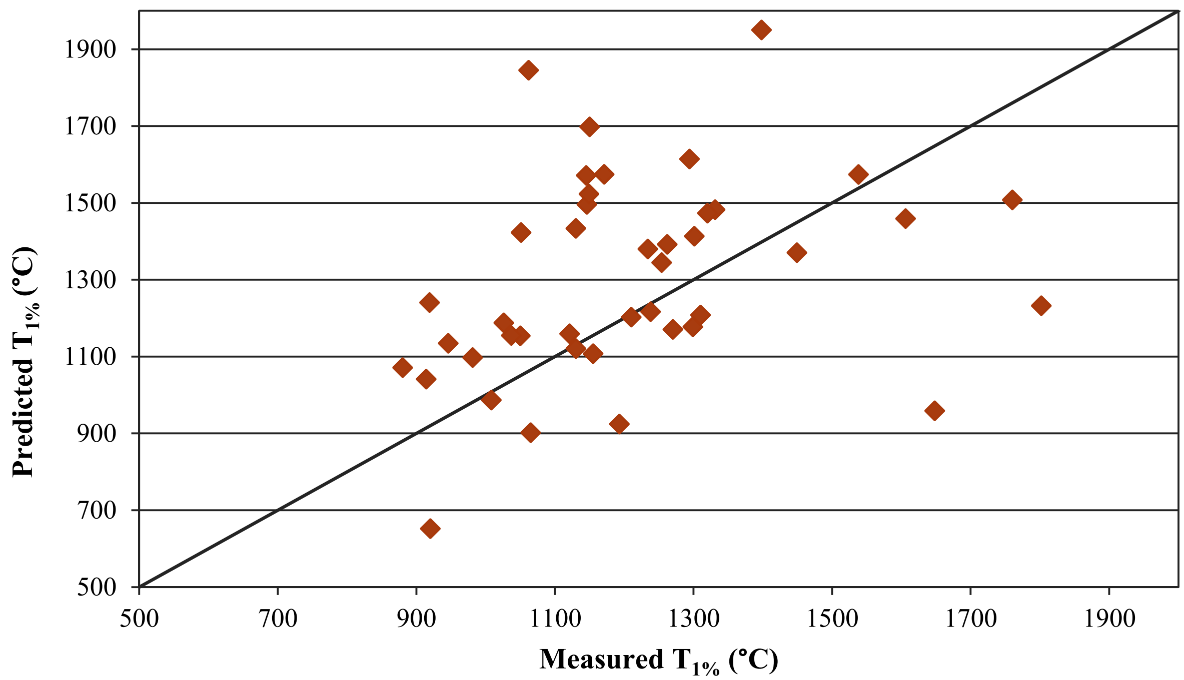

Figure 3.4. Predicted versus Measured $T_{1\%}$ for HLW Glasses in the High Alumina Study, Using a Previous Model in Equation (3.7)

3.7 Product Consistency Test

This section presents and discusses the PCT results obtained using the methods discussed in Section 2.8. The PCT results are published elsewhere (Fox et al. 2014, 2015a and 2015b), but are summarized here in Table 3.8 based on the glass target compositions except for the mis-batched glass (EWG-HAI-Centroid-1). The mis-batched glass was based on the analytical composition.

The PCT normalized B, Na, and Li values ranged from 0.097 to 45.505, 0.077 to 21.78, and below detection limits to 23.995, respectively. The CCC treatment of several test-matrix glasses significantly increased PCT responses.

Table 3.8. HLW Glass PCT Normalized[(a)] Concentration Release Results on the HLW Glasses in the High Alumina Study from Fox et al. (2014, 2015a, and 2015b)

Glass ID	Type	B (g/m²)	Li (g/m²)	Na (g/m²)	Si (g/m²)
EWG-HAI-Centroid-1	Quenched	0.199	0.254	0.194	0.101
	CCC	0.175	0.199	0.148	0.070
EWG-HAI-Centroid-2	Quenched	1.881	1.097	0.812	0.110
	CCC	2.129	1.202	0.896	0.125
EWG-HAI-Centroid-2-R1	Quenched	0.260	0.250	0.185	0.090
	CCC	--[(c)]	--[(c)]	--[(c)]	--[(c)]
EWG-OL-801	Quenched	2.789	---[(b)]	2.328	0.112
	CCC	3.221	---[(b)]	2.578	0.116

Glass ID	Type	B (g/m^2)	Li (g/m^2)	Na (g/m^2)	Si (g/m^2)
EWG-OL-1369	Quenched	0.097	0.161	0.077	0.048
	CCC	0.141	0.162	0.078	0.048
EWG-OL-1580	Quenched	0.116	0.155	0.090	0.049
	CCC	0.134	0.152	0.083	0.049
EWG-OL-1672	Quenched	0.706	---[b]	0.497	0.024
	CCC	0.764	---[b]	0.528	0.027
EWG-OL-2463	Quenched	7.464	---[b]	6.924	0.124
	CCC	16.545	---[b]	15.436	0.091
EWG-OL-2619	Quenched	0.319	---[b]	0.350	0.020
	CCC	0.363	---[b]	0.402	0.020
EWG-OL-3122	Quenched	0.123	---[b]	0.221	0.061
	CCC	10.051	---[b]	6.001	0.013
EWG-OL-3208	Quenched	1.692	1.257	1.483	0.429
	CCC	46.507	8.073	21.780	0.826
EWG-OL-3231	Quenched	0.924	0.955	0.857	0.116
	CCC	0.805	0.841	0.750	0.133
EWG-OL-3388	Quenched	9.444	---[b]	7.923	0.083
	CCC	10.667	---[b]	8.903	0.093
EWG-OL-3872	Quenched	0.712	0.849	1.059	0.256
	CCC	19.670	7.863	13.520	0.680
EWG-OL-4099	Quenched	0.616	0.627	0.598	0.079
	CCC	0.670	0.681	0.641	0.085
EWG-OL-5155	Quenched	1.030	1.001	0.849	0.250
	CCC	3.429	3.279	2.352	0.009
EWG-OL-5549	Quenched	1.955	---[b]	2.167	0.091
	CCC	2.448	---[b]	2.642	0.043
EWG-OL-5801	Quenched	1.205	1.156	1.059	0.216
	CCC	2.752	2.197	2.284	0.009
EWG-OL-6080	Quenched	0.195	---[b]	0.195	0.020
	CCC	0.155	---[b]	0.160	0.035
EWG-OL-6198	Quenched	1.079	1.026	0.817	0.126
	CCC	3.159	2.355	1.877	0.145
EWG-OL-12707	Quenched	3.865	3.583	3.728	0.043
	CCC	3.078	2.934	3.001	0.039
EWG-OL-14827	Quenched	0.355	0.412	0.387	0.068
	CCC	0.313	0.372	0.345	0.064
EWG-OL-15968	Quenched	3.467	3.421	2.613	0.208
	CCC	5.617	5.224	3.652	0.138
EWG-OL-16450	Quenched	2.228	---[b]	2.626	0.050
	CCC	3.104	---[b]	2.676	<0.05
EWG-OL-23401	Quenched	0.098	---[b]	0.198	0.051
	CCC	0.188	---[b]	0.194	0.046
EWG-OL-26012	Quenched	0.225	0.107	0.273	0.262
	CCC	0.268	2.758	0.864	0.173
EWG-OL-29285	Quenched	0.109	---[b]	0.108	0.058
	CCC	0.092	---[b]	0.123	0.031

Glass ID	Type	B (g/m²)	Li (g/m²)	Na (g/m²)	Si (g/m²)
EWG-OL-31644	Quenched	0.166	0.131	0.120	0.038
	CCC	0.136	0.258	0.078	0.041
EWG-OL-32706	Quenched	0.195	0.301	0.171	0.069
	CCC	0.205	0.313	0.170	0.081
EWG-OL-33115	Quenched	0.160	---(b)	0.198	0.048
	CCC	0.165	---(b)	0.180	0.062
EWG-OL-33558	Quenched	0.147	<0.690	0.256	0.052
	CCC	0.167	<0.690	0.167	0.055
EWG-OL-33694	Quenched	0.545	<8.971	0.476	0.071
	CCC	0.258	<8.971	0.225	0.080
EWG-OL-33858	Quenched	0.232	0.254	0.195	0.121
	CCC	1.723	0.684	0.578	0.106
EWG-OL-35387	Quenched	0.811	<8.971	0.602	0.156
	CCC	0.780	<8.971	0.542	0.153
EWG-OL-38081	Quenched	0.281	0.309	0.183	0.168
	CCC	40.235	21.079	4.572	0.124
EWG-OL-38552	Quenched	0.331	0.382	0.195	0.112
	CCC	8.182	1.342	4.890	0.014
EWG-OL-1755 Mod 8% Fe, 10% B	Quenched	0.210	0.250	0.125	0.155
	CCC	0.205	0.245	0.145	0.165
EWG-OL-3063 Mod 1% Zr 3% Li	Quenched	6.705	4.335	1.935	0.110
	CCC	7.100	4.695	2.060	0.120
EWG-OL-4744 Mod 7.5% Fe 1% Zr	Quenched	2.860	---(b)	3.060	0.105
	CCC	--(c)	--(c)	--(c)	--(c)
EWG-OL-5385 Mod 12% B 17% Na	Quenched	0.965	1.140	1.275	0.130
	CCC	18.110	14.435	13.790	0.225
EWG-OL-6257 Mod 12% B 8% Ca	Quenched	0.125	0.130	0.110	0.040
	CCC	2.575	1.645	0.285	<0.01
EWG-OL-6311 Mod Reduced Na & K	Quenched	2.250	1.725	1.695	0.305
	CCC	39.105	21.965	14.900	0.265
EWG-OL-6489 Mod 11% B 15% Na	Quenched	4.100	2.550	2.865	0.015
	CCC	24.210	7.265	14.155	<0.01
EWG-OL-8548 Mod 1% Zr	Quenched	0.455	---(b)	0.425	0.190
	CCC	45.505	---(b)	12.355	0.040
EWG-OL-10278 Mod 15% B 1% Zr	Quenched	0.705	0.790	0.850	0.130
	CCC	4.265	4.835	3.590	0.135
EWG-OL-11318 Mod 1% Zr	Quenched	1.790	---(b)	1.485	0.115
	CCC	1.745	---(b)	1.295	0.115
EWG-OL-14547 Mod Reduced Alkali 1% Zr	Quenched	1.130	1.245	1.360	0.140
	CCC	18.520	23.995	8.645	0.410
EWG-OL-15698 Mod Low Na	Quenched	5.560	5.135	4.545	0.210
	CCC	7.110	9.290	4.905	0.045

(a) Normalized using targeted glass compositions, except for EWG-HAI-Centroid-1, which was normalized using an adjusted targeted composition to account for misbatching.
(b) No Li in the glass composition.
(c) No analysis performed.

Figure 3.5 compares the PCT normalized releases of Na and Li with the normalized release of B for the Q glass samples. The line in the figure corresponds to Na and Li releases being equal to B releases. Figure 3.5 shows that Na and Li leaching tend to be highly linearly correlated with B leaching with only a few outliers. Also, Na and Li releases are roughly equal to B releases for the lower portion of the plot, but then Na and Li releases tend to be slightly less than B releases for the upper portion of the plot. Figure 3.6 compares the PCT normalized releases of Na and Li with the normalized release of B for the CCC glass samples. The data points in Figure 3.6 are more scattered with more outliers than in Figure 3.5. Also, Figure 3.6 shows that Na and Li releases tend to be substantially lower than B releases at the higher end of the scale, more so than in Figure 3.5. The release rates form a fairly straight line in Figure 3.6, but with substantial scatter and a different slope compared to Figure 3.5. This may be due to crystallization in the samples during the CCC process.

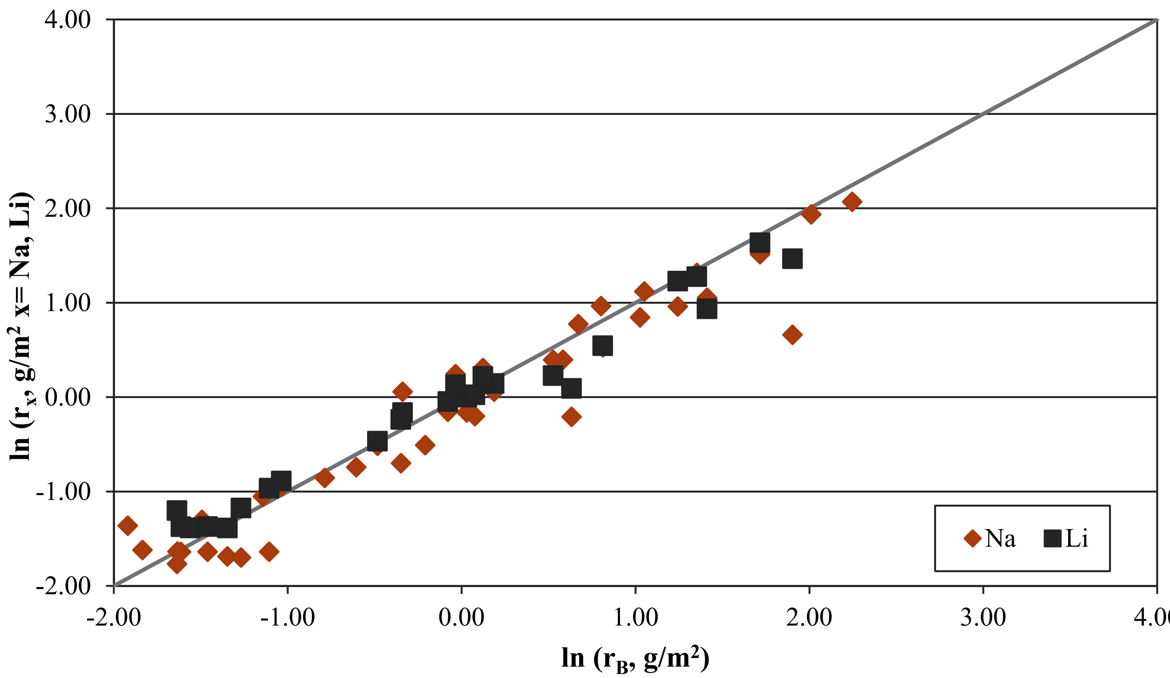

Figure 3.5. Comparison of Natural Logarithm PCT Normalized Release (g/m^2) of Na and Li with B for Quenched Samples of Enhanced HLW Glasses in the High Alumina Study

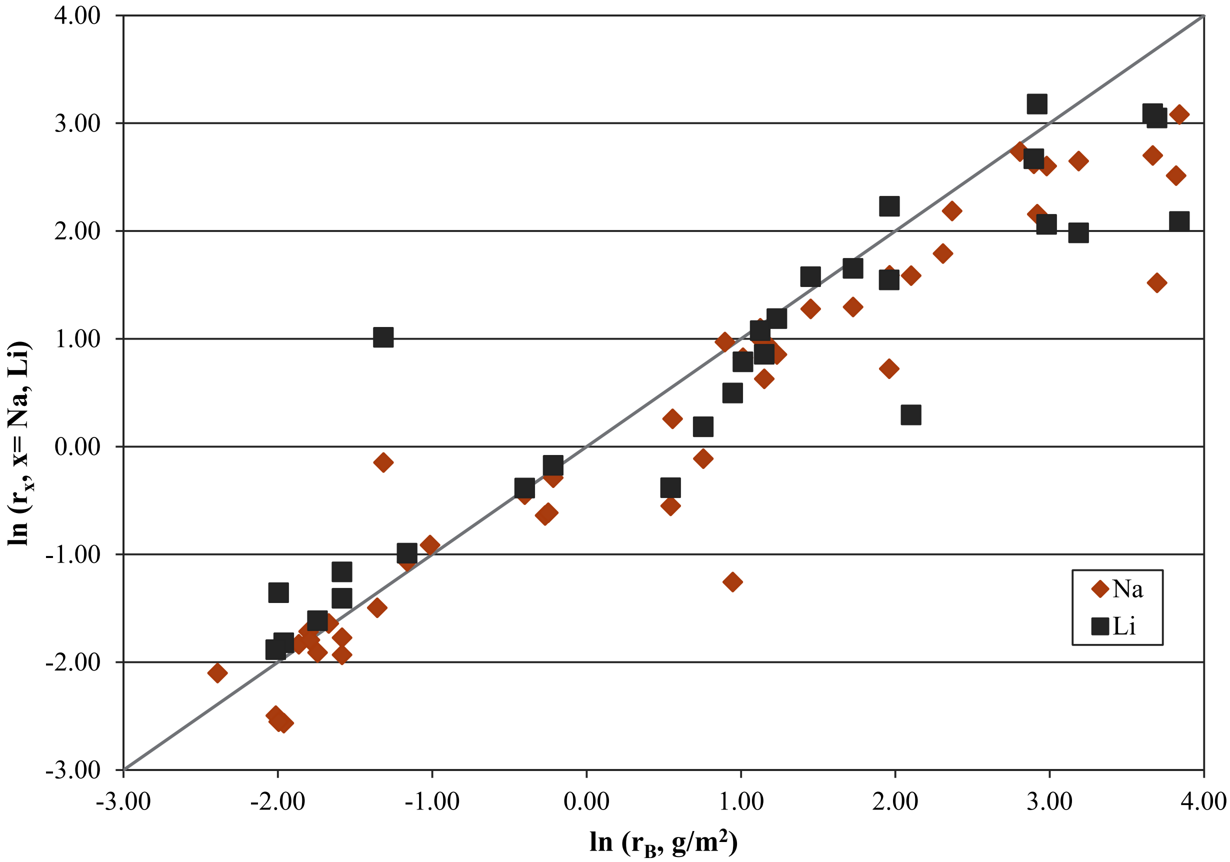

Figure 3.6. Comparison of Natural Logarithm PCT Normalized Release (g/m^2) of Na and Li with B for CCC Samples of Enhanced HLW Glasses in the High Alumina Study

Figure 3.7 compares the logarithms of normalized PCT releases of the quenched and CCC glasses. Normalized PCT releases from CCC glasses are higher than from quenched glasses, sometimes substantially so, for many glasses. Figure 3.8 shows that when significant crystals containing Al and Si (>5 wt%) are present in the glass, CCC-treated samples can have notably higher PCT release rates than quenched samples. This may be because the crystals remove the glass formers (Si and Al) from the bulk glass structure and composition, making it less durable (Kim et al. 1995).

When the natural logarithm of PCT releases for quenched glasses were compared to predictions from a previously developed model (Piepel et al. 2008), the results showed poor prediction with the results scattered as seen in Figure 3.9 and mainly over predicted. Again this appears be due to the composition difference in these glasses versus the glasses the model was developed for as is shown in Figure 3.10. Figure 3.10 shows that as the aluminum concentration increases the amount of over prediction increases. This indicates that a model with an expanded composition region should be developed to account for the data in the HLW high alumina study.

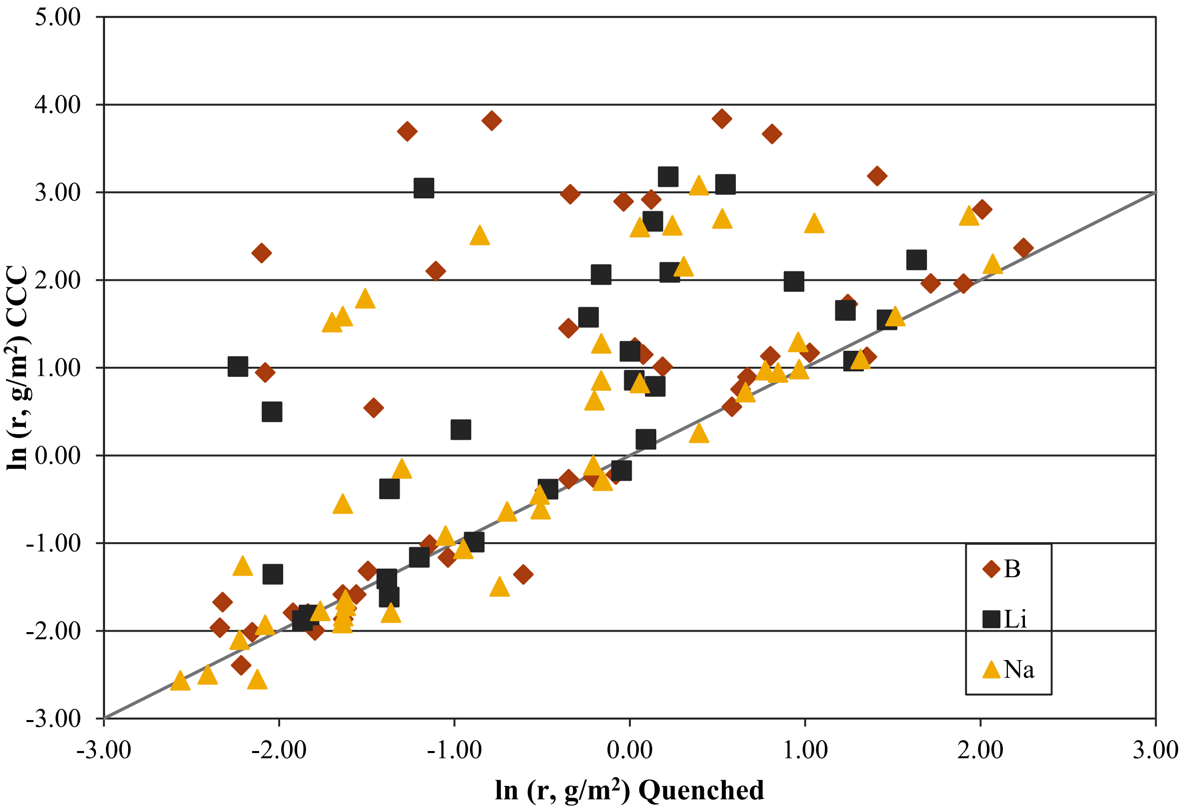

Figure 3.7. Comparison of Natural Logarithm of PCT Normalized Release (g/m^2) of B, Li, and Na for Quenched and CCC-Treated Samples of Enhanced HLW Glasses in the High Alumina Study

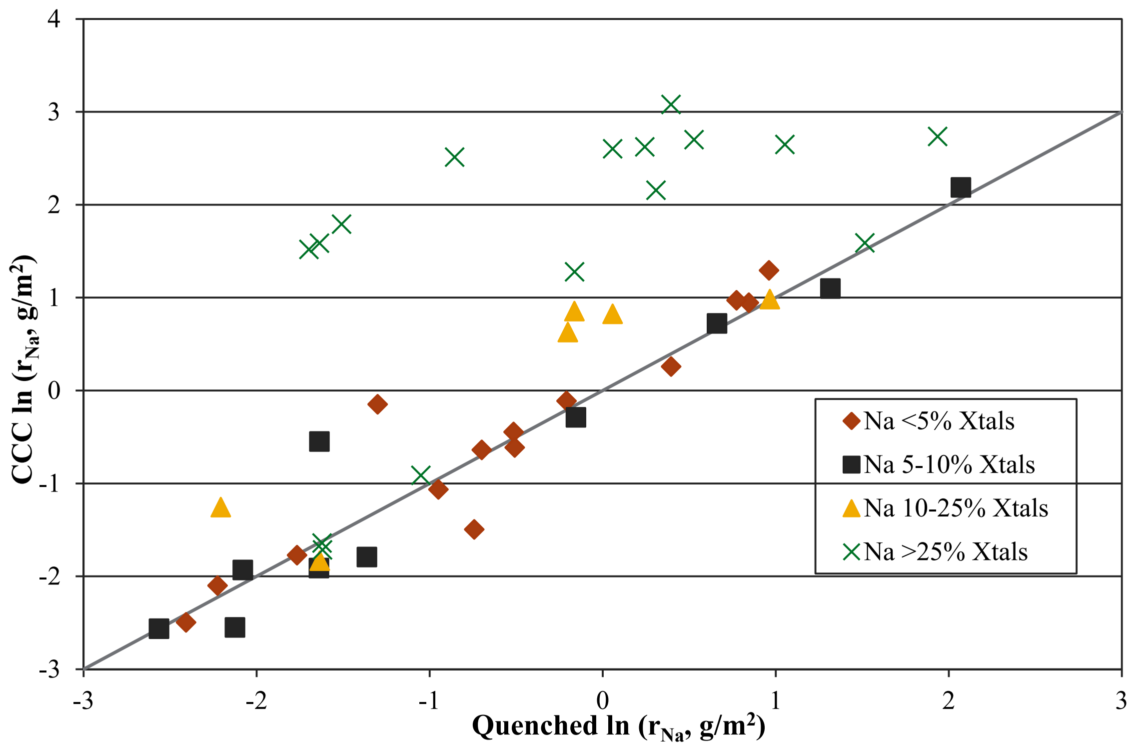

Figure 3.8. Comparison of Natural Logarithm of PCT Normalized Release (g/m^2) of Na for Quenched and CCC-Treated Samples

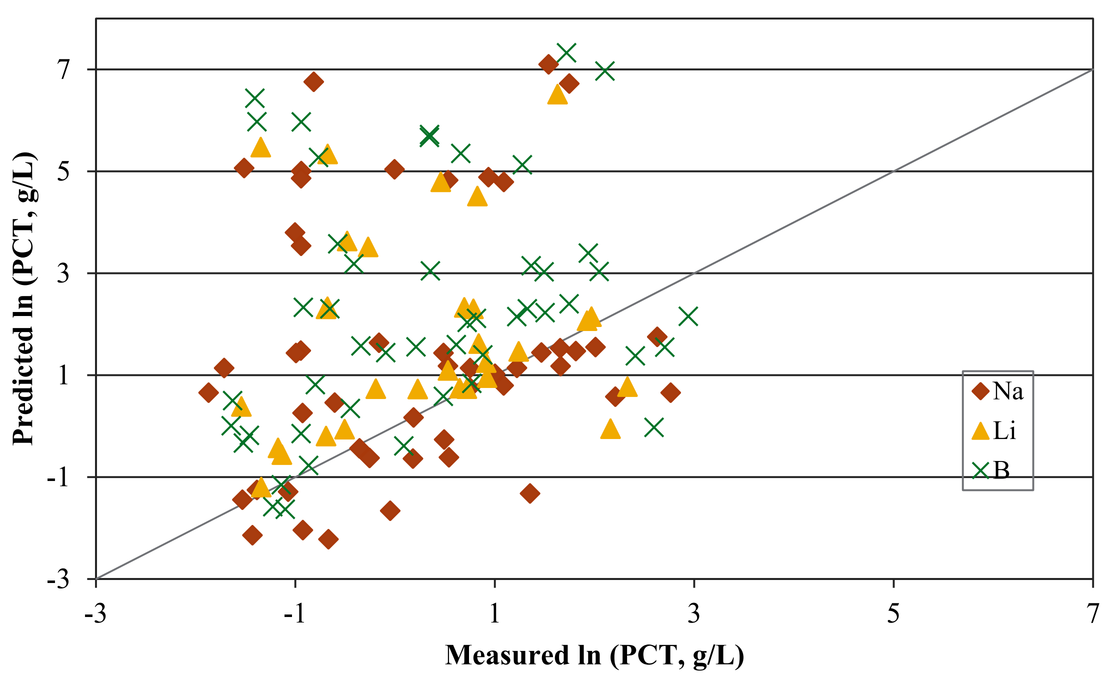

Figure 3.9. Measured versus Predicted PCT Releases (g/L) of Quenched Samples, Using a Previous Model from Piepel et al. (2008)

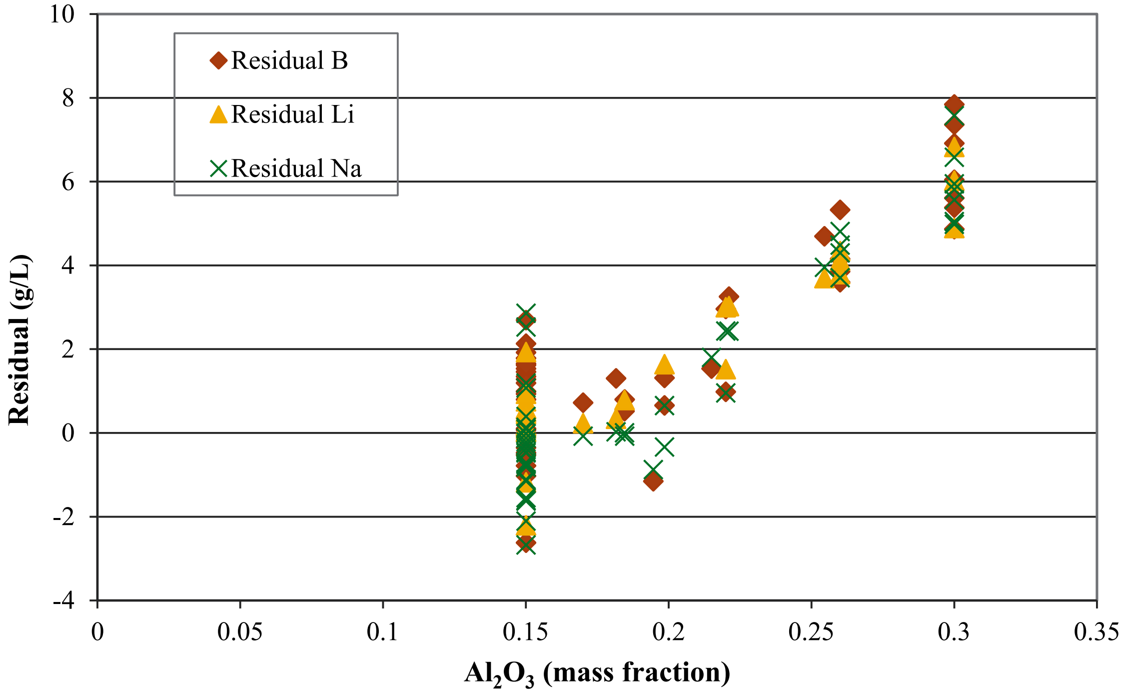

Figure 3.10. **Al_2O_3 mass fraction versus Residual PCT Releases (g/L) of Quenched Samples**

3.8 Toxicity Leaching Characteristic Procedure

This section presents and discusses the TCLP results obtained using the methods discussed in Section 2.6. The TCLP results for Q and CCC glasses are listed in Table 3.9 and Table 3.10, respectively.

Table 3.9. TCLP Results for Quenched Samples of HLW Glasses in the High Alumina Study

Sample ID	As (mg/L)	Ba (mg/L)	Cd (mg/L)	Cr (mg/L)	Pb (mg/L)	Se (mg/L)	Ag (mg/L)	B (mg/L)
EWG-HAI-Centroid-1	<0.02	<0.05	0.161	0.081	0.465	<0.01	0.028	10.1
EWG-HAI-Centroid-2	<0.02	<0.05	0.149	0.091	0.436	<0.01	0.019	15.9
EWG-OL-801	<0.02	<0.05	0.040	<0.005	0.135	<0.01	<0.01	3.35
EWG-OL-1369	<0.02	<0.05	0.020	0.027	0.055	<0.01	<0.01	0.57
EWG-OL-1580	<0.02	<0.05	0.022	0.028	0.055	<0.01	<0.01	0.64
EWG-OL-1672	<0.02	<0.05	0.233	0.276	0.711	<0.01	0.046	34.7
EWG-OL-2463	<0.02	<0.05	0.042	<0.005	0.099	<0.01	<0.01	1.28
EWG-OL-2619	<0.02	<0.05	0.404	0.019	1.18	<0.01	0.071	37.6
EWG-OL-3122	<0.02	<0.05	0.152	2.66	0.899	<0.01	0.030	10.8
EWG-OL-3208	<0.02	<0.05	0.058	0.187	0.131	<0.01	0.014	1.91
EWG-OL-3231	<0.02	<0.05	0.601	0.227	0.833	<0.01	0.094	54.1
EWG-OL-3388	<0.02	<0.05	0.178	0.126	0.453	<0.01	0.046	19.1
EWG-OL-3872	<0.02	<0.05	1.33	<0.005	0.299	<0.01	0.207	53.2
EWG-OL-4099	<0.02	<0.05	0.894	<0.005	1.38	<0.01	0.190	79.6
EWG-OL-5155	<0.02	<0.05	0.143	0.098	0.451	<0.01	0.028	13.3
EWG-OL-5549	<0.02	<0.05	1.65	<0.005	0.322	<0.01	0.164	182
EWG-OL-5801	<0.02	<0.05	0.092	<0.005	0.269	<0.01	0.016	7.57
EWG-OL-6080	<0.02	<0.05	0.154	0.364	0.478	<0.01	0.027	13.4
EWG-OL-6198	<0.02	<0.05	0.061	0.013	0.172	<0.01	<0.01	5.03
EWG-OL-8548	<0.02	<0.05	0.074	0.027	0.234	<0.01	0.010	2.67

Sample ID	As (mg/L)	Ba (mg/L)	Cd (mg/L)	Cr (mg/L)	Pb (mg/L)	Se (mg/L)	Ag (mg/L)	B (mg/L)
EWG-OL-12707	<0.02	<0.05	1.02	<0.005	1.66	<0.01	0.174	89.1
EWG-OL-14827	<0.02	<0.05	1.03	0.235	1.63	<0.01	0.158	98.1
EWG-OL-15968	<0.02	<0.05	1.49	3.52	0.080	<0.01	0.202	186
EWG-OL-16450	<0.02	<0.05	1.89	1.12	0.729	<0.01	0.285	177
EWG-OL-23401	<0.02	<0.05	0.028	0.125	0.089	<0.01	<0.01	1.08
EWG-OL-26012	<0.02	<0.05	0.025	<0.005	0.073	<0.01	<0.01	0.79
EWG-OL-29285	<0.02	<0.05	0.024	<0.005	0.084	<0.01	<0.01	1.69
EWG-OL-31644	<0.02	<0.05	0.023	0.033	0.066	<0.01	<0.01	0.692
EWG-OL-32706	<0.02	<0.05	0.027	<0.005	0.089	<0.01	<0.01	2.31
EWG-OL-33115	<0.02	<0.05	0.051	0.014	0.105	<0.01	<0.01	1.42
EWG-OL-33558	<0.02	<0.05	0.047	<0.005	0.089	<0.01	<0.01	1.35
EWG-OL-33694	<0.02	<0.05	0.117	<0.005	0.393	<0.01	0.020	5.24
EWG-OL-33858	<0.02	<0.05	0.070	<0.005	0.240	<0.01	0.015	3.45
EWG-OL-35387	<0.02	<0.05	0.038	0.058	0.124	<0.01	0.011	1.42
EWG-OL-38081	<0.02	<0.05	0.055	<0.005	0.179	<0.01	0.010	1.76
EWG-OL-38552	<0.02	<0.05	0.047	0.025	0.142	<0.01	<0.01	1.55
EWG-OL-1755 Mod 8% Fe, 10% B	<0.02	<0.05	0.020	0.033	0.053	<0.02	<0.01	0.885
EWG-OL-3063 Mod 1% Zr 3% Li	<0.02	<0.05	0.050	0.022	0.139	<0.02	0.012	4.29
EWG-OL-4744 Mod 7.5% Fe 1% Zr	<0.02	<0.05	0.391	1.03	1.26	<0.02	0.068	17.4
EWG-OL-5385 Mod 12% B 17% Na	<0.02	<0.05	0.377	0.020	1.21	<0.02	0.065	18.7
EWG-OL-6257 Mod 12% B 8% Ca	<0.02	<0.05	0.377	0.190	1.16	<0.02	0.074	17.8
EWG-OL-6311 Mod Reduced Na & K	<0.02	<0.05	0.176	0.222	0.475	<0.02	0.033	8.30
EWG-OL-6489 Mod 11% B 15% Na	<0.02	<0.05	0.136	0.072	0.428	<0.02	0.024	6.31
EWG-OL-8548 Mod 1% Zr	<0.02	<0.05	0.072	0.022	0.231	<0.02	0.010	2.73
EWG-OL-10278 Mod 15% B 1% Zr	<0.02	<0.05	0.360	0.015	1.11	<0.02	0.064	21.0
EWG-OL-11318 Mod 1% Zr	<0.02	<0.05	0.343	0.283	1.10	<0.02	0.064	31.2
EWG-OL-14547 Mod Reduced Alkali 1% Zr	<0.02	<0.05	0.316	1.98	0.994	<0.02	0.064	16.3
EWG-OL-15698 Mod Low Na	<0.02	<0.05	0.306	0.007	0.753	<0.02	0.053	13.1

Table 3.10. TCLP Results for CCC Samples of HLW Glasses in the High Alumina Study

Sample ID	As (mg/L)	Ba (mg/L)	Cd (mg/L)	Cr (mg/L)	Pb (mg/L)	Se (mg/L)	Ag (mg/L)	B (mg/L)
EWG-HAI-Centroid-1	<0.02	<0.05	0.223	0.015	0.656	<0.01	0.034	14.5
EWG-HAI-Centroid-2	<0.02	<0.05	0.193	0.021	0.579	<0.01	0.035	21.3
EWG-OL-801	<0.02	<0.05	0.044	<0.005	0.141	<0.01	<0.01	3.63
EWG-OL-1369	<0.02	<0.05	0.058	0.036	0.110	<0.01	<0.01	1.70
EWG-OL-1580	<0.02	<0.05	0.122	0.019	0.158	<0.01	<0.01	3.68
EWG-OL-1672	<0.02	<0.05	0.141	0.015	0.424	<0.01	0.026	20.4
EWG-OL-2463	<0.02	<0.05	0.407	<0.005	0.021	<0.01	<0.01	569
EWG-OL-2619	<0.02	<0.05	0.795	0.015	2.30	<0.01	0.135	74.9
EWG-OL-3122	<0.02	0.260	2.73	9.65	0.025	<0.01	<0.01	468
EWG-OL-3208	<0.02	<0.05	3.65	6.61	3.10	0.022	0.283	306
EWG-OL-3231	<0.02	<0.05	0.721	0.106	1.10	<0.01	0.106	64.2
EWG-OL-3388	<0.02	<0.05	0.211	0.101	0.746	<0.01	0.092	41.9
EWG-OL-3872	<0.02	<0.05	0.023	0.045	<0.01	<0.01	<0.01	500

Sample ID	As (mg/L)	Ba (mg/L)	Cd (mg/L)	Cr (mg/L)	Pb (mg/L)	Se (mg/L)	Ag (mg/L)	B (mg/L)
EWG-OL-4099	<0.02	<0.05	0.677	0.017	1.37	<0.01	0.139	62.0
EWG-OL-5155	<0.02	<0.05	0.568	0.011	1.78	<0.01	0.071	49.0
EWG-OL-5549	<0.02	<0.05	1.83	<0.005	0.286	<0.01	0.116	203
EWG-OL-5801	<0.02	<0.05	0.176	0.009	0.020	<0.01	0.020	20.8
EWG-OL-6080	<0.02	<0.05	0.215	0.098	0.626	<0.02	0.041	17.6
EWG-OL-6198	0.046	<0.05	0.204	0.007	0.044	<0.01	0.031	22.6
EWG-OL-12707	<0.02	<0.05	0.651	<0.005	0.242	<0.01	0.104	58.8
EWG-OL-14827	<0.02	0.161	1.26	0.171	1.25	<0.01	0.133	120
EWG-OL-15968	<0.02	<0.05	1.48	4.73	0.093	<0.01	0.048	153
EWG-OL-16450	<0.02	<0.05	1.36	0.065	<0.01	<0.01	<0.01	252
EWG-OL-23401	<0.02	<0.05	0.609	1.65	0.520	<0.01	0.084	24.2
EWG-OL-26012	<0.02	<0.05	0.026	<0.005	0.049	<0.01	<0.01	0.819
EWG-OL-29285	<0.02	<0.05	0.023	<0.005	0.059	<0.01	<0.01	1.60
EWG-OL-31644	<0.02	<0.05	0.082	0.011	0.198	<0.01	<0.01	2.48
EWG-OL-32706	<0.02	<0.05	0.031	<0.005	0.085	<0.01	<0.01	2.77
EWG-OL-33115	<0.02	<0.05	0.039	0.022	0.129	<0.01	0.011	2.01
EWG-OL-33558	<0.02	<0.05	0.047	<0.005	0.105	<0.01	0.017	1.98
EWG-OL-33694	<0.02	<0.05	0.042	<0.005	0.109	<0.01	<0.01	3.08
EWG-OL-33858	<0.02	<0.05	0.844	<0.005	2.32	<0.01	0.058	45.8
EWG-OL-35387	<0.02	<0.05	0.065	0.045	0.162	<0.01	0.016	2.47
EWG-OL-38081	<0.02	<0.05	2.72	0.013	0.040	0.059	0.071	308
EWG-OL-38552	<0.02	<0.05	1.88	<0.005	3.35	<0.01	0.016	68.4
EWG-OL-1755 Mod 8% Fe, 10% B	<0.02	<0.05	0.023	0.019	0.064	<0.02	<0.01	0.937
EWG-OL-3063 Mod 1% Zr 3% Li	<0.02	<0.05	0.049	0.013	0.136	<0.02	0.014	4.37
EWG-OL-4744 Mod 7.5% Fe 1% Zr	<0.02	0.066	1.97	11.9	<0.01	<0.02	<0.01	781
EWG-OL-5385 Mod 12% B 17% Na	<0.02	0.164	5.93	0.056	6.54	<0.02	<0.01	350
EWG-OL-6257 Mod 12% B 8% Ca	<0.02	<0.05	1.29	0.288	3.72	<0.02	0.086	63.1
EWG-OL-6311 Mod Reduced Na & K	0.034	0.167	0.071	11.2	0.037	<0.02	0.079	718
EWG-OL-6489 Mod 11% B 15% Na	0.029	<0.05	5.84	1.34	0.161	0.039	0.032	416
EWG-OL-8548 Mod 1% Zr	<0.02	<0.05	1.43	<0.005	0.017	<0.02	0.038	268
EWG-OL-10278 Mod 15% B 1% Zr	<0.02	0.084	5.65	0.008	14.3	<0.02	0.060	373
EWG-OL-11318 Mod 1% Zr	<0.02	<0.05	0.372	0.031	1.18	<0.02	0.065	34.5
EWG-OL-14547 Mod Reduced Alkali 1% Zr	<0.02	<0.05	0.623	<0.005	<0.01	<0.02	<0.01	427
EWG-OL-15698 Mod Low Na	<0.02	0.050	1.33	0.701	<0.01	<0.02	<0.01	751

Toxicity leaching behaviors of Cd, Cr, and Pb were plotted in the normalized form with respect to the B release in Figure 3.11. Cadmium showed congruent leaching behavior with B for all glasses tested with approximately equal normalized releases. Chromium showed incongruent leaching behavior with normalized Cr release, much lower than that of B. Lead exhibited fairly linear release with normalized boron release at lower values. However, above ~7 mg/L B release, the lead release becomes very incongruent.

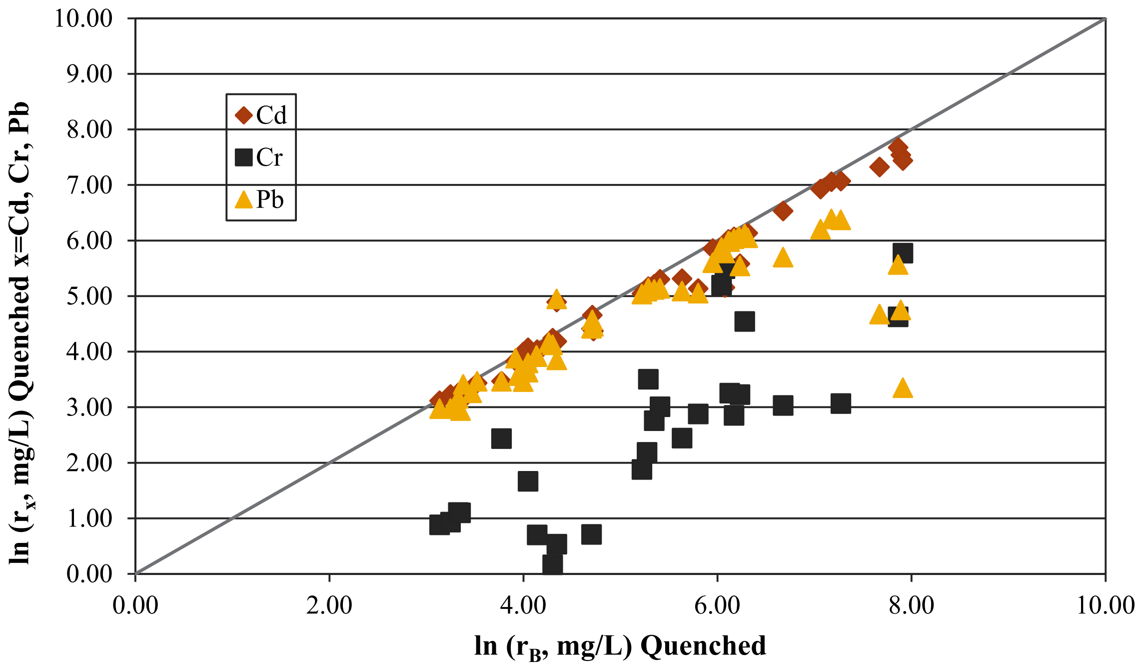

Figure 3.11. TCLP Releases (mg/L) Compared to B Releases (mg/L) for Quenched Samples of HLW Glasses in the High Alumina Study

The TCLP results were compared with predictions from a model from Vienna et al. (2009). This model was developed with older WTP baseline data, which focused on lower waste loadings (i.e., no high alumina glasses). The purpose of the comparison was to assess how well the Vienna et al. (2009) model would predict TCLP results for the HLW glasses in this high alumina study. Vienna et al. (2009) did not develop a separate model for each TCLP normalized elemental release, but rather developed a single model based on the average of normalized B, Ba, and Cd releases. Vienna et al. (2009) developed that model for the purpose of assessing the volume of HLW waste to be produced over the course of the WTP mission. Hence, that model was not intended for direct comparison to the various measured TCLP elemental releases from an experimental study (like the high alumina study). Still, Cd and Ag normalized releases were closest to the model predictions, with the Cr normalized release being the farthest away, as seen in Figure 3.12. In the future, new separate models for each of the important TCLP normalized elemental releases will need to be developed to account for the new data on high alumina glasses.

The TCLP results for quenched and CCC samples of the high alumina study glasses were compared in Figure 3.13. The data were scattered so no clear trend can be ascertained. However, for CCC glasses without crystalline phases, the ratio was close to one, while the ratios were scattered much more at higher crystal fractions. Figure 3.14 shows that when significant crystals containing Al and Si (>5 wt%) are present in the glass, CCC-treated samples can have notably higher TCLP release rates than quenched samples. This may be because the crystals remove the glass formers (Si and Al) from the bulk glass structure and composition, making it less durable (Kim et al. 1995).

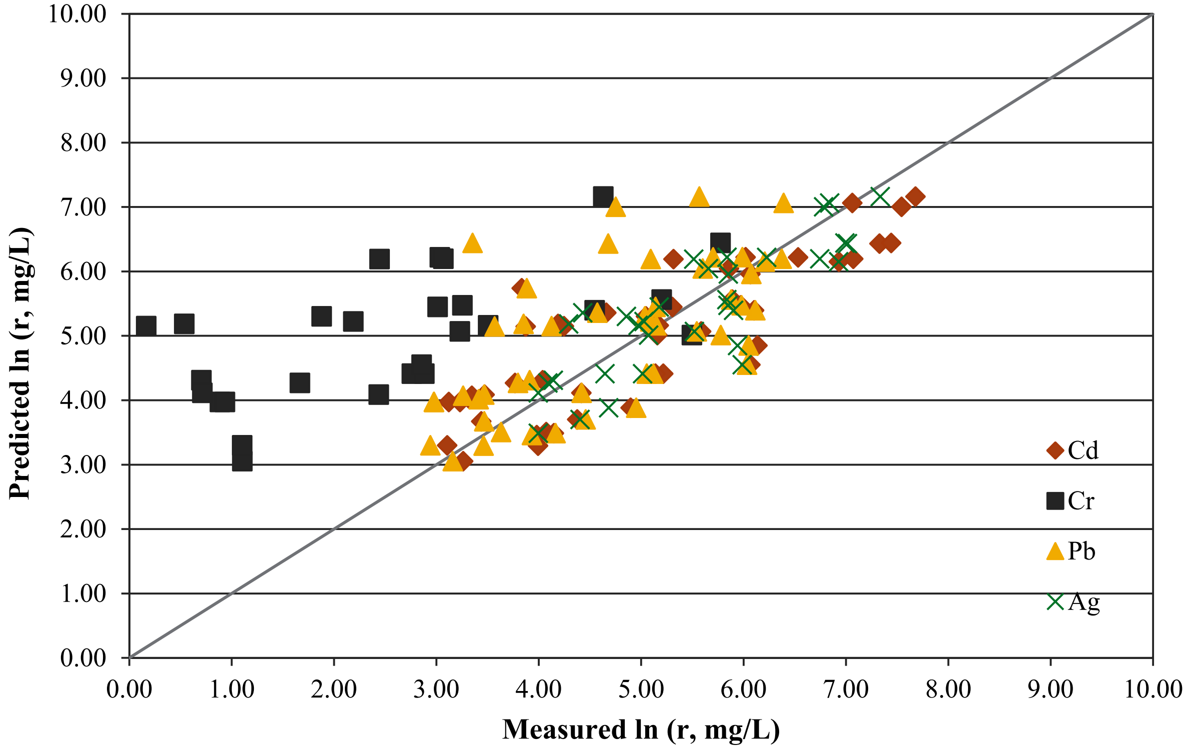

Figure 3.12. TCLP Release (mg/L) of Quenched HLW Glasses from the High Alumina Study Compared to Predicted Release (mg/L) Using the Model of Vienna et al. (2009)

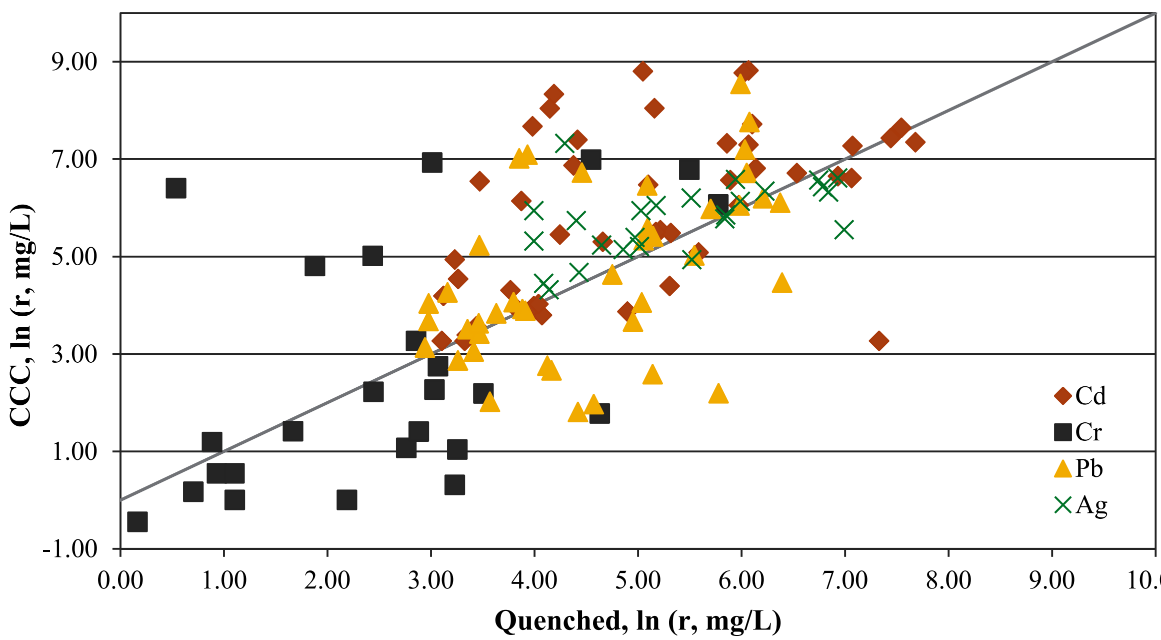

Figure 3.13. TCLP Release (mg/L) of Quenched Glasses Compared to CCC Glasses for HLW Glasses in the High Alumina Study

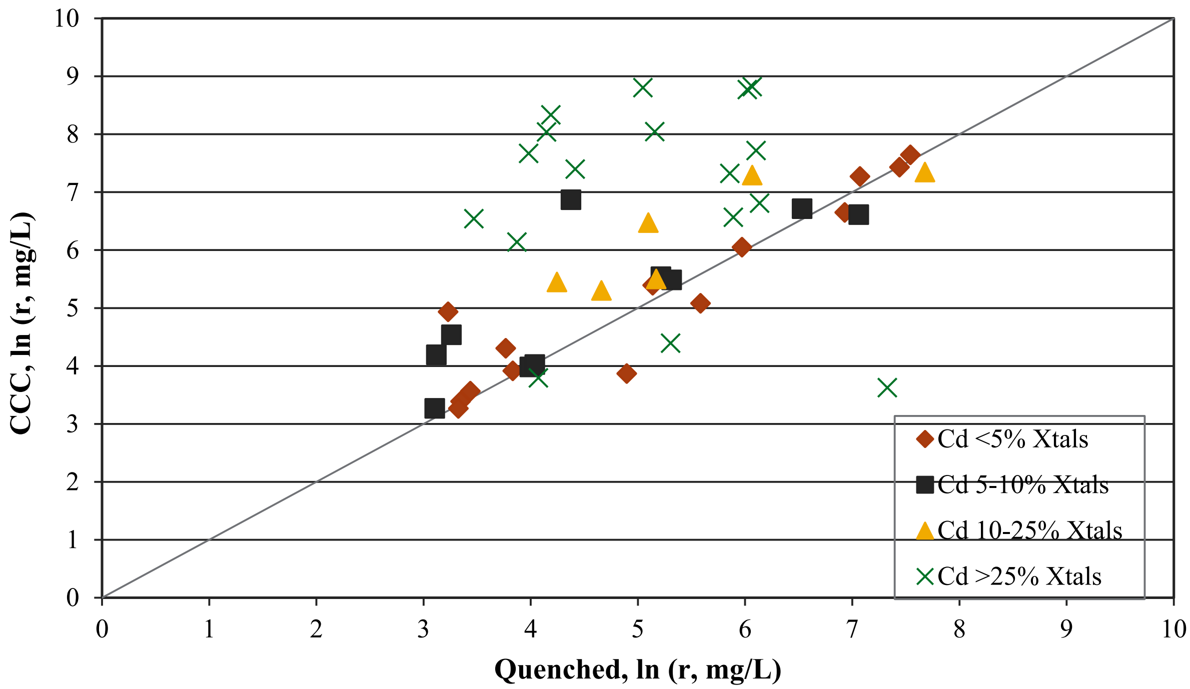

Figure 3.14. Comparison of Natural Logarithm of TCLP Normalized Release (mg/L) of Cd for Quenched and CCC-Treated Samples

4.0 Conclusions

This report documents the EWG compositions and critical glass property results for the first phase of a study that focused on HLWs containing high concentrations of alumina. The objective of this work was to collect data that can be used to develop property-composition models for future treatment of the HLW at the Hanford Site.

The first phase study of enhanced HLW glasses with high alumina collected data on several properties (viscosity, EC, TCLP, PCT, and crystallinity of isothermal and CCC heat treated samples) of 47 glasses in a statistically design test matrix. The test matrix consisted of a subset of 45 extreme vertices of the high alumina EGCR, plus two replicates of a center glass. As was expected, fabricating and measuring properties extreme vertex glasses of the high alumina EGCR led to several glasses that couldn't be successfully fabricated and characterized so needed modification.

A test matrix of glasses was developed as follows. First, an EGCR appropriate for high alumina glasses was specified by SCCs and MCCs on 14 HLW glass components that were to be varied in the study. Next, a statistical experimental design (test matrix) of 47 high alumina (15 to 30 wt%) alkali-borosilicate glasses was generated. The test matrix included 45 of the 39,197 extreme vertices of the EGCR and two replicates of a center glass of the EGCR. The 45 vertices were selected using statistical software to evenly cover the EGCR. It was envisioned that a subsequent phase of the high alumina EWG study would investigate compositions on the interior of the EGCR. Ultimately, the goal was to adequately cover the boundary and interior of the high alumina EGCR with glasses having property values the meet and somewhat exceed planned operating ranges in the WTP vitrification facility. In this way, property-composition models developed from the data would provide for predicting property values inside as well as somewhat outside the WTP operating ranges.

The 47 test-matrix glasses were batched and melted, and the property values were determined. The property values were compared to predictions from baseline WTP models, if available. The existing models are based on a different glass composition region (which does not include high alumina glasses). The prediction performances of the existing models varied considerably. Overall, we concluded that new models are needed for HLW glasses with high alumina content. The conclusions for specific properties are listed in the subsequent subsections.

Glasses were melted at temperatures in the range of 1150°C to 1450ºC. Undesirable features of salt segregation, gross crystallization, phase separation, and undissolved particles were all observed in 12 of the original 47 glasses. For those glasses, modified compositions were selected for characterization based on scoping tests reported by Kroll et al. (2015).

Quenched samples of the 47 test-matrix glasses were chemically analyzed at SRNL to identify potential misbatching and excessive volatility. The sums of measured oxide components were 96.9 wt% to 103.5 wt%, which is a reasonable range compared to the sums of targeted values. One glass was identified as having 53% lower P_2O_5 than the targeted value -- EWG-HAI-Centroid-1. No evidence of substantial volatility was found.

The room temperature density of each glass was measured using a pycnometer. The results of the glass density measurements ranged from approximately 2.4 g/cm^3 to 2.8 g/cm^3. Predicted densities from a previous model compared fairly well to the measured density, although there were indications of some small biases in predictions. Hence, an improved model should be developed in the future including glasses with high alumina.

A total of 84 crystalline phases were identified after CCC treatment of the glasses. Nepheline was present in 12 glasses at >19 wt%. The most common phases found contained alkali-alumino-silicate, alkaline earth-alumino-silicate, alkali-silicate, and spinel.

The glass melt viscosities were found to range from ~1 to 22 Pa-s at 1150°C. The Piepel et al. (2008) viscosity model does not accurately predict the glass melt viscosity of these high alumina glasses. The composition range used to develop this model contained far less alumina than these glasses which may have some effect on this scatter. Therefore, it would be useful to fit a new viscosity model to account for this new data with higher alumina content.

The EC values ranged from 2.5 to 71.5 S/m at 1150°C. Only three glasses (EWG-OL-3208, EWG-OL-26012, and EWG-OL-6489 Mod 11% B 15% Na) deviated from a linear relationship at higher temperatures. Volatility of charge carriers is a potential cause because these three glasses all have relatively low melting temperatures. EC_{1150} values were compared with predictions of EC_{1150} using the Piepel et al. (2008) model. The model tended to over predict this data. This could be because of the different glass composition region that this study explored versus the composition region explored for the EC models in Piepel et al. (2008). Hence, it is recommended that a new model for EC_{1150} exploring a wider composition region should be developed.

Based on crystal fraction of isothermal heat treatment tests, the primary phases identified were classified into the following four groups: 1) spinel (generic form of AB_2O_4), 2) eskolaite (Cr_2O_3), 3) baddeleyite (ZrO_2), and 4) nepheline ($(Na,K)AlSiO_4$). Twenty-four of the glasses had a $T_{1\%}$ above 1150°C, which is the target melting temperature.

An existing model developed in Piepel et al. (2008) assuming all crystals were spinel predicted $T_{1\%}$ poorly for the 47 high alumina HLW glasses. Therefore, a new $T_{1\%}$ model exploring a wider composition region and different crystal structures should be developed to account for the data from the HLW glasses in the high alumina study.

PCT normalized boron release values ranged from 0.097 to 9.444 g/m^2 for quenched and 0.092 to 46.507 g/m^2 for CCC samples. The PCT responses increased significantly for glasses precipitating nepheline and eucryptite during CCC. Plotting normalized PCT releases of Li and Na against B indicated congruent leaching behavior of Q glasses and CCC glasses with low fractions of crystals (<10%). At high crystal fractions (>25%), more glasses (6 of 10) showed incongruent behavior.

The Piepel et al. (2008) model was used to predict the average PCT responses of natural logarithms of Li, Na, and B releases for Q glasses. The predicted values compared poorly to the experimental values, suggesting that a new model should be developed including high alumina glasses.

TCLP releases of B, Cd, Cr, Pb, and Ag were determined for both Q and CCC glasses at SwRI. The results showed that interest, results showed Cd leached congruently with B in both Q and CCC glasses (except for CCC glass with high crystal fractions). Meanwhile, Cr leached at significantly lower concentrations than B and Cd in both the Q and CCC states. For CCC glass samples with higher crystal fractions leaching was found to be higher than for Q samples and less congruent for Pb and Ag.

The existing WTP baseline model was used to predict TCLP releases of Cd for Q glasses. When the measured results for the high alumina glasses were compared with the model predictions, the Cd measured values were closest to predicted values

Future work is needed to further investigate HLW glasses in the high alumina EGCR. Such a second-phase study was envisioned to follow the first-state study discussed in this report. This second phase may likely include glasses with less extreme composition using either an “inner-layer” or “space-filling” approach. Also, additional work should focus on spinel and nepheline formation and prediction because other properties such as viscosity and EC are generally better described as smooth functions of composition. Most of the WTP baseline glass property models were found to poorly predict properties of glasses in this composition region (as was expected). Models will need to be developed to be predictive in this, high alumina, composition region.

5.0 References

40 CFR 268. 2015. "Land Disposal Restrictions." *Code of Federal Regulations*, U.S. Environmental Protection Agency, Washington, DC.

Atkinson AC, AN Donev, and RD Tobias. 2007. *Optimum Experimental Designs, with SAS*, Oxford University Press, Oxford, UK.

ASTM. "Standard Test Methods for Determining Chemical Durability of Nuclear, Hazardous, and Mixed Waste Glasses and Multiphase Glass Ceramics: The Product Consistency Test (PCT)," ASTM C1285, ASTM International, West Conshohocken, PA.

ASTM. "Standard Test Method for Determining Liquidus Temperature of Immobilized Waste Glasses and Simulated Waste Glasses," ASTM C1720, ASTM International, West Conshohocken, PA.

Cornell JA. 2002. Experiments with Mixtures: Designs, Models, and the Analysis of Mixture Data, 3rd Edition, John Wiley and Sons, New York, NY.

Crum, JV, TB Edwards, RL Russell, PJ Workman, M.J. Schweiger, R.F. Schumacher, D.E. Smith, D.K. Peeler, and J.D. Vienna. 2012. "DWPF Startup Frit Viscosity Measurement Round Robin Results," Journal of the American Ceramic Society, 95(7):2196-2205.

DOE. 2012. Memorandum, "Enhanced WTP Glass Composition Envelope Development," to C. Swan, Inter-Entity Work Order M0ORV00020, October 18, 2012, U.S. Department of Energy, Office of River Protection, Richland, WA.

Fox KM and TB Edwards. 2014. *Chemical Composition and PCT Data for the Initial Set of Hanford Enhanced Waste Loading Glasses*. SRNL-STI-2014-00063, Savannah River National Laboratory, Aiken, SC.

Fox KM and TB Edwards. 2015a. Chemical Composition Analysis and Product Consistency Tests to Support Enhanced Hanford Waste Glass Models: Results for the Second Set of High Alumina Outer Layer Matrix Glasses, SRNL-STI-2014-00312, Savannah River National Laboratory, Aiken, SC.

Fox KM and TB Edwards. 2015b. Chemical Composition Analysis and Product Consistency Tests to Support Enhanced Hanford Waste Glass Models: Results for the Third Set of High Alumina Outer Layer Matrix Glasses, SRNL-STI-2015-00652, Savannah River National Laboratory, Aiken, SC.

Hrma P, GF Piepel, MJ Schweiger, DE Smith, DS Kim, PE Redgate, JD Vienna, CA Lopresti, DB Simpson, DK Peeler, and MH Langowski. 1994. *Property/Composition Relationships for Hanford High-Level Waste Glasses Melting at 1150^{0}C*. PNL-10359, Pacific Northwest National Laboratory, Richland, WA.

Jantzen CM, NE Bibler, DC Beam, CL Crawford, and MA Pickett. 1993. Characterization of the Defense Waste Processing Facility (DWPF) Environmental Assessment (EA) Glass Standard Reference Material (U). WSRC-TR-92-346, Rev. 1, Westinghouse Savannah River Company, Aiken, SC.

Kim DS, JD Vienna, PR Hrma, MJ Schweiger, J Matyas, JV Crum, DE Smith, GJ Sevigny, WC Buchmiller, JS Tixier, JD Yeager, and KB Belew. 2003. *Development and Testing of ICV Glasses for Hanford LAW*. PNNL-14351, Pacific Northwest National Laboratory, Richland, WA.

Kim DS, JD Vienna, DK Peeler, KM Fox, AS Aloy, AV Trofimenko, and KD Gerdes. 2008. "Improved Alumina Loading in High-Level Waste Glasses." In WM2008 Conference: Phoenix Rising: Moving Forward in Waste Management, p. Paper No. 8460. WM Symposia, Phoenix, AZ.

Kim DS, MJ Schweiger, CP Rodriguez, WC Lepry, JB Lang, JV Crum, JD Vienna, F Johnson, JC Marra, and DK Peeler. 2011. Formulation and Characterization of Waste Glasses with Varying Processing Temperature. PNNL-20774, Pacific Northwest National Laboratory, Richland, WA.

Kim DS and JD Vienna. 2012. *Preliminary ILAW Formulation Algorithm Description*. 24590-LAW-RPT-RT-04-0003, Rev. 1, River Protection Project, Hanford Tank Waste Treatment and Immobilization Plant, Richland, WA.

Kot WK, K Klatt, H Gan, and IL Pegg, SK Cooley, GF Piepel, and DJ Bates. 2004. *Regulatory Testing of RPP-WTP HLW Glasses to Support Delisting Compliance.* VSL-04R4780-R1, Vitreous State Laboratory, The Catholic University of America, Washington, D.C.

Kroll, JO, MJ Schweiger, and JD Vienna. 2015. "Scoping Melting Studies of High Alumina Waste Glass Compositions," *Advances in Materials Science for Environmental and Energy Technologies IV: Ceramic Transactions*, 253, 37.

Mellinger GB and JL Daniel. 1984. Approved Reference and Testing Materials for Use in Nuclear Waste Management Research and Development Programs. PNL-4955-2, Pacific Northwest Laboratory, Richland, WA.

McCloy, JS and JD Vienna. 2010. *Glass Composition Constraint Recommendations for Use in Life-Cycle Mission Modeling*. PNNL-19372, Pacific Northwest National Laboratory, Richland, WA.

Muller IS, WK Kot, HK Pasieka, K Gilbo, FC Perez-Cardenas, I Joseph, and IL Pegg. 2012. *Compilation and Management of Orp Glass Formulation Database*. VSL-12R2470-1, Vitreous State Laboratory, The Catholic University of America, Washington, DC.

Piepel, GF (2003). MIXSOFT--Software for the Design and Analysis of Mixture and Other Constrained Region Experiments, User's Guide Version 2.4.1, MIXSOFT, Richland, WA.

Piepel GF, SK Cooley, A Heredia-Langner, SM Landmesser, WK Kot, H Gan, and IL Pegg. 2008. *IHLW PCT, VHT, Viscosity, and Electrical Conductivity Model Development*. VSL-07R1240-4, Rev. 0, Vitreous State Laboratory, The Catholic University of America, Washington, D.C.

Rodriguez CP, JS McCloy, MJ Schweiger, JV Crun, A Winschell. 2011. Optical Basicity and Nepheline Crystallization in High Alumina Glasses, PNNL-20184, EMSP-RPT-003, Pacific Northwest National Laboratory, Richland, WA.

Vienna JD, A Fluegal, DS Kim, and P Hrma. 2009. *Glass Property Data and Model for Estimating High-Level Waste Glass Volume*. PNNL-18501, Pacific Northwest National Laboratory, Richland, WA.

Vienna JD, DC Skorski, D Kim, J Matyas, 2013. Glass Property Models and Constraints for Estimating Glass to be Produced at Hanford by Implementing Current Advanced Glass Formulation Efforts, PNNL-22631 Rev.1, ORP-58289, Pacific Northwest National Laboratory, Richland, WA.

Vienna JD. 2014. "Compositional Models of Glass/Melt Properties and their Use for Glass Formulation," *Procedia Materials Science*, 7, 148-155.

Weier, DR and GF Piepel. 2003. *Methodology for Adjusting and Normalizing Analyzed Glass Composition*. PNWD-3260, Battelle Pacific Northwest Division, Richland, WA.

Welch, WJ. 1987. ACED, Algorithms for the Construction of Experimental Designs, User's Guide Version 1.6.1, University of Waterloo, Waterloo, Ontario, Canada.

Appendix A

Morphology/Color of Each Individual Quenched Glass

Appendix A

Morphology/Color of Each Quenched Glass

The photos in this appendix show each glass after melting in a Pt/Rh crucible twice at the specified melt temperature.

Figure A.1. Photo of Glass EWG-HAI-Centroid-2-R1 Morphology of Second Melt at 1150°C for 1 h

Figure A.2. Photo of Glass EWG-OL-1369 Morphology of Second Melt at 1250°C for 0.75 h

Figure A.3. Photo of Glass EWG-OL-1580 Morphology of Second Melt at 1250°C for 1 h

Figure A.4. Photo of Glass EWG-OL-1672 Morphology of Second Melt at 1300°C for 0.83 h

Figure A.5. Photo of Glass EWG-OL-2463 Morphology of Second Melt at 1200°C for 0.83 h

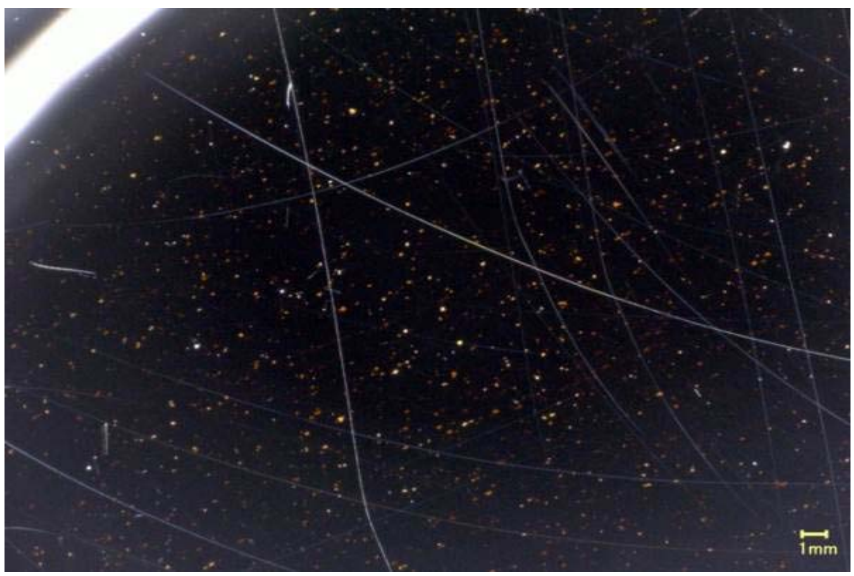

Figure A.6. Photo of Glass EWG-OL-2619 Morphology of Second Melt at 1150°C for 1 h

Figure A.7. Photo of Glass EWG-OL-3122 Morphology of Second Melt at 1450°C for 1 h

Figure A.8. Photo of Glass EWG-OL-3231 Morphology of Second Melt at 1100°C for 1.1 h

Figure A.9. Photo of Glass EWG-OL-3388 Morphology of Second Melt at 1027°C for 1 h

Figure A.10. Photo of Glass EWG-OL-3872 Morphology of Second Melt at 1050°C for 0.9 h

Figure A.11. Photo of Glass EWG-OL-4099 Morphology of Second Melt at 1000°C for 1 h

Figure A.12. Photo of Glass EWG-OL-5549 Morphology of Second Melt at 1050°C for 1 h

Figure A.13. Photo of Glass EWG-OL-5801 Morphology of Second Melt at 1050°C for 1 h

Figure A.14. Photo of Glass EWG-OL-6080 Morphology of Second Melt at 1450°C for 1 h

Figure A.15. Photo of Glass EWG-OL-6198 Morphology of Second Melt at 1150°C for 1 h

Figure A.16. Photo of Glass EWG-OL-12707 Morphology of Second Melt at 1050°C for 0.75 h

Figure A.17. Photo of Glass EWG-OL-14827 Morphology of Second Melt at 980°C for 1.1 h

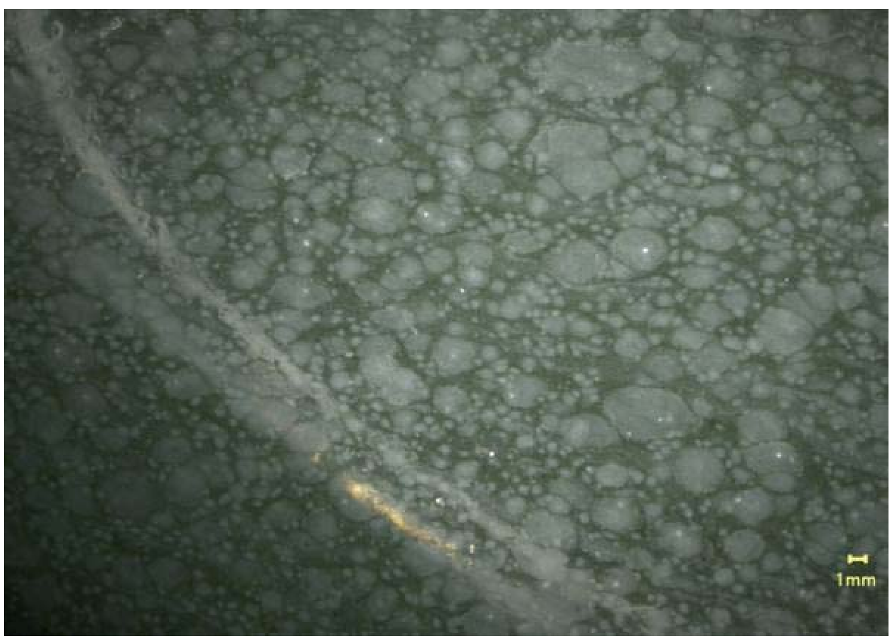

Figure A.18. Photo of Glass EWG-OL-15968 Morphology of Second Melt at 1150°C for 1 h

Figure A.19. Photo of Glass EWG-OL-16450 Morphology of Second Melt at 1025°C for 1 h

Figure A.20. Photo of Glass EWG-OL-23401 Morphology of Second Melt at 1400°C for 1 h

Figure A.21. Photo of Glass EWG-OL-26012 Morphology of Second Melt at 1225°C for 1 h

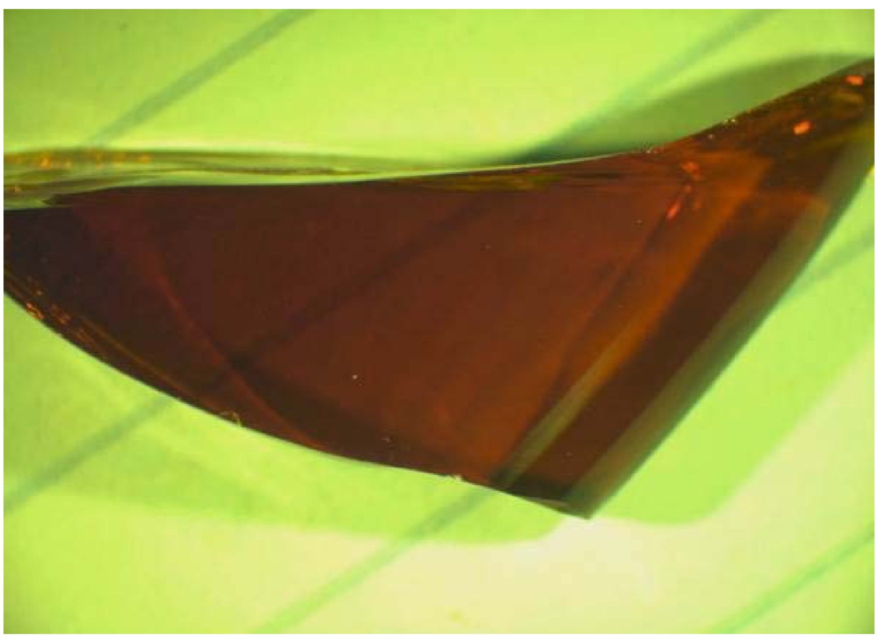

Figure A.22. Photo of Glass EWG-OL-29285 Morphology of Second Melt at 1360°C for 1 h

Figure A.23. Photo of Glass EWG-OL-31644 Morphology of Second Melt at 1350°C for 1 h

Figure A.24. Photo of Glass EWG-OL-32706 Morphology of Second Melt at 1400°C for 1.4 h

Figure A.25. Photo of Glass EWG-OL-33115 Morphology of Second Melt at 1300°C for 1 h

Figure A.26. Photo of Glass EWG-OL-33558 Morphology of Second Melt at 1350°C for 1 h

Figure A.27. Photo of Glass EWG-OL-33694 Morphology of Second Melt at 1450°C for 1 h

Figure A.28. Photo of Glass EWG-OL-38081 Morphology of Second Melt at 1350°C for 1 h

Figure A.29. Photo of Glass EWG-OL-38552 Morphology of Second Melt at 1250°C for 1 h

Figure A.30. Photo of Glass EWG-OL-1755 before Modification Morphology of Third Melt at 1375°C for 1 h

Figure A.31. Photo of Glass EWG-OL-1755 Mod 8% Fe 10% B Morphology of Second Melt at 1275°C for 1 h

Figure A.32. Photo of Glass EWG-OL-3063 before Modification Morphology of Second Melt at 1400°C for 1 h

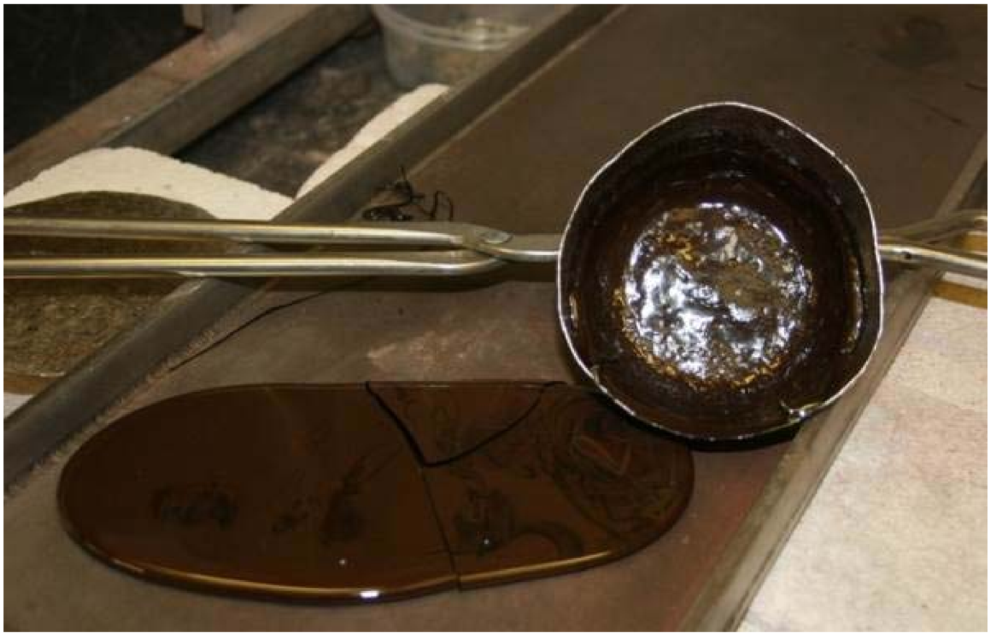

Figure A.33. Photo of Glass EWG-OL-3063 Mod 1% Zr 3% Li Morphology of Second Melt at 1400°C for 0.9 h

Figure A.34. Photo of Glass EWG-OL-4744 Mod 7.5% Fe 1% Zr Morphology of Second Melt at 1250°C for 0.83 h

Figure A.35. Photo of Glass EWG-OL-5385 before Modification Morphology of Second Melt at 1075°C for 0.83 h

Figure A.36. Photo of Glass EWG-OL-6311 Mod Reduced Na & K Morphology of Second Melt at 1125°C for 1 h

Figure A.37. Photo of Glass EWG-OL-6489 before Modification Morphology of First Melt at 1200°C for 0.75 h

Figure A.38. Photo of Glass EWG-OL-6489 Mod 11%B 15%Na Morphology of Second Melt at 1200°C for 1 h

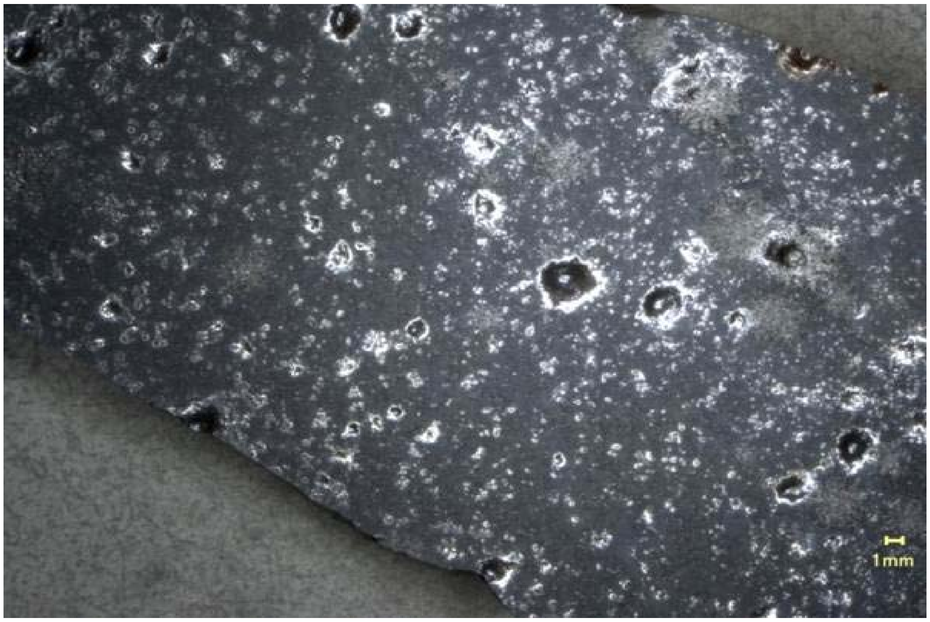

Figure A.39. Photo of Glass EWG-OL-8548 before Modification Morphology of Second Melt at 1350°C for 1.2 h

Figure A.40. Photo of Glass EWG-OL-8548 Mod 1% Zr Morphology of Second Melt at 1300°C for 1.2 h

Figure A.41. Photo of Glass EWG-OL-10278 before Modification Morphology of Second Melt at 1000°C for 1.2 h

Figure A.42. Photo of Glass EWG-OL-10278 Mod 15% B 1% Zr Morphology of Second Melt at 1025°C for 1.1 h

Figure A.43. Photo of Glass EWG-OL-11318 before Modification Morphology of Second Melt at 1250°C for 0.9 h

Figure A.44. Photo of Glass EWG-OL-11318 Mod 1% Zr Morphology of Second Melt at 1250°C for 0.9 h

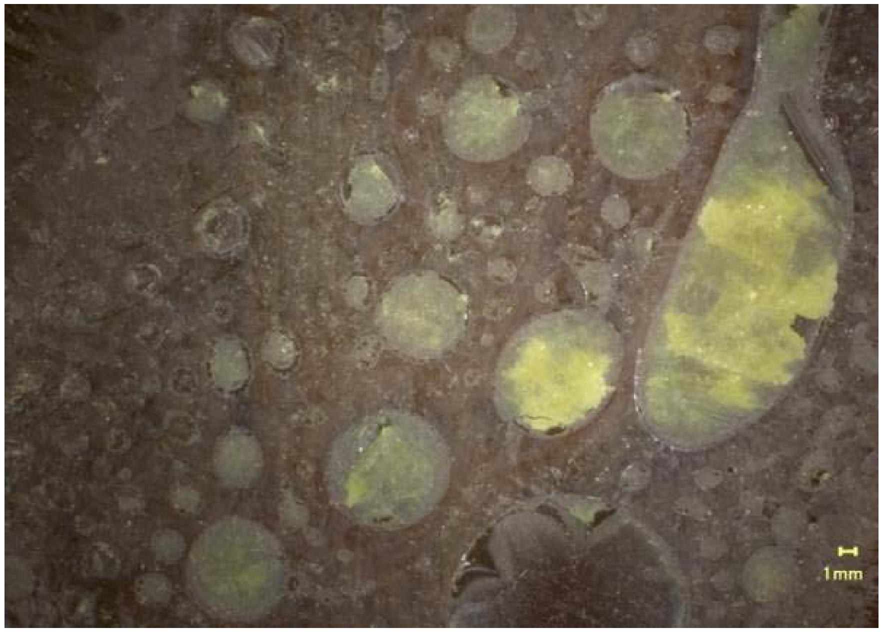

Figure A.45. Photo of Glass EWG-OL-14547 before Modification Morphology of Second Melt at 1150°C for 1.2 h

Figure A.46. Photo of Glass EWG-OL-14547 Mod Reduced Alkali 1% Morphology of Second Melt at 1125°C for 1.1 h

Figure A.47. Photo of Glass EWG-OL-15698 before Modification Morphology of Second Melt at 1000°C for 1 h

Figure A.48. Photo of Glass EWG-OL-15698 Mod Low Na Morphology of Second Melt at 1050°C for 1 h

Appendix B

Analyzed Glass Compositions

Appendix B

Analyzed Glass Compositions

Data in this section compares the targeted glass compositions with the analyzed glass compositions and their percent differences. The percent differences were calculated by subtracting the target value from the analyzed value and dividing by the target value. There appeared to be overall agreement in all samples and the targeted compositions are adequate for use in future work to develop property-composition models except for EWG-HAI-Centroid-1. This glass was mis-batched and the composition was changed to match the analyzed composition in future testing.

Table B.1. Comparison of Targeted and Analyzed HLW Glass Compositions

Glass ID	**EWG-OL-801**			**EWG-OL-1369**			**EWG-OL-1580**			**EWG-OL-1672**		
Component	**Targeted (wt%)**	**Analyzed (wt%)**	**% Diff**	**Targeted (wt%)**	**Analyzed (wt%)**	**% Diff**	**Targeted (wt%)**	**Analyzed (wt%)**	**% Diff**	**Targeted (wt%)**	**Analyzed (wt%)**	**% Diff**
Al_2O_3	30.00	29.52	-1.60	15.00	15.03	0.20	15.00	15.01	0.07	30.00	26.12	-12.93
B_2O_3	21.46	20.99	-2.19	8.00	8.18	2.25	8.00	8.08	1.00	22.00	31.06	41.18
Bi_2O_3	3.00	2.97	-1.00	3.00	2.96	-1.33	0.00	0.11	--	3.00	2.73	-9.00
CaO	0.00	0.14	--	10.00	9.93	-0.70	10.00	10.22	2.20	10.00	8.71	-12.90
CdO	0.10	0.09	-10.00	0.10	0.08	-20.00	0.10	0.09	-10.00	0.10	0.08	-20.00
Cr_2O_3	0.00	0.15	--	1.60	1.51	-5.63	1.60	1.42	-11.25	1.60	1.28	-20.00
Fe_2O_3	0.00	0.14	--	0.00	0.14	--	0.00	0.14	--	0.00	0.14	--
K_2O	0.00	0.01	--	0.00	0.01	--	0.00	0.01	--	0.00	0.01	--
Li_2O	0.00	0.22	--	6.00	5.96	-0.67	6.00	5.95	-0.83	0.00	0.22	--
MgO	0.00	0.17	--	0.00	0.17	--	0.00	0.17	--	0.00	0.17	--
MnO	3.00	3.02	0.67	0.00	0.13	--	3.00	3.08	2.67	3.00	2.59	-13.67
Na_2O	18.00	17.86	-0.78	5.00	5.00	0.00	5.00	5.17	3.40	5.00	4.53	-9.40
NiO	0.40	0.38	-5.00	0.40	0.37	-7.50	0.40	0.37	-7.50	0.40	0.33	-17.50
P_2O_5	3.00	2.75	-8.33	3.00	2.78	-7.33	3.00	2.78	-7.33	3.00	2.41	-19.67
PbO	0.30	0.28	-6.67	0.30	0.27	-10.00	0.30	0.27	-10.00	0.30	0.24	-20.00
RuO_2	0.01	0.013	30.00	0.01	0.013	30.00	0.01	0.01	0.00	0.01	0.01	0.00
SiO_2	20.00	19.74	-1.30	42.86	42.89	0.07	42.86	42.09	-1.80	20.86	18.33	-12.13
SO_3	0.30	0.21	-30.00	0.30	0.25	-16.67	0.30	0.28	-6.67	0.30	0.03	-90.00
SrO	0.12	0.12	0.00	0.12	0.11	-8.33	0.12	0.10	-16.67	0.12	0.11	-8.33
ZrO_2	0.00	0.14	--	4.00	3.97	-0.75	4.00	3.95	-1.25	0.00	0.14	--
Total	99.69	98.89	-0.80	99.69	99.74	0.05	99.69	99.33	-0.36	99.69	99.24	-0.45

Table B.1 (continued)

Glass ID	**EWG-OL-2463**			**EWG-OL-2619**			**EWG-OL-3122**			**EWG-OL-3208**		
Component	**Targeted (wt%)**	**Analyzed (wt%)**	**% Diff**	**Targeted (wt%)**	**Analyzed (wt%)**	**% Diff**	**Targeted (wt%)**	**Analyzed (wt%)**	**% Diff**	**Targeted (wt%)**	**Analyzed (wt%)**	**% Diff**
Al_2O_3	19.46	19.46	0.00	18.46	18.59	0.70	30.00	29.38	-2.07	15.00	14.82	-1.20
B_2O_3	8.00	8.13	1.63	22.00	22.07	0.32	8.00	8.03	0.38	8.00	8.55	6.88
Bi_2O_3	0.00	0.11	--	3.00	3.10	3.33	0.00	<0.11	--	0.00	<0.11	--
CaO	10.00	9.76	-2.40	10.00	10.09	0.90	10.00	10.10	1.00	0.00	<0.14	--
CdO	0.10	0.08	-20.00	0.10	0.09	-10.00	0.10	<0.11	--	0.10	<0.11	--
Cr_2O_3	0.00	0.15	--	0.00	0.15	--	1.60	1.46	-8.75	1.60	1.55	-3.13
Fe_2O_3	10.00	9.93	-0.70	10.00	10.10	1.00	0.00	<0.14	--	0.00	<0.14	--
K_2O	3.00	3.09	3.00	3.00	2.64	-12.00	3.00	2.62	-12.67	3.00	2.96	-1.33
Li_2O	0.00	0.22	--	0.00	0.22	--	0.00	<0.22	--	6.00	6.14	2.33
MgO	0.00	0.17	--	0.00	0.17	--	0.00	<0.17	--	0.00	<0.17	--
MnO	3.00	3.07	2.33	3.00	3.13	4.33	3.00	2.96	-1.33	3.00	3.09	3.00
Na_2O	18.00	18.47	2.61	5.00	4.98	-0.40	18.00	17.83	-0.94	18.00	17.42	-3.22
NiO	0.40	0.36	-10.00	0.40	0.30	-25.00	0.40	0.42	5.00	0.40	0.39	-2.50
P_2O_5	3.00	2.74	-8.67	0.00	0.23	--	0.00	<0.23	--	3.00	2.90	-3.33
PbO	0.30	0.27	-10.00	0.30	0.27	-10.00	0.30	0.22	-26.67	0.30	0.29	-3.33
RuO_2	0.01	0.01	0.00	0.01	0.01	0.00	0.01	<0.13	--	0.01	<0.13	--
SiO_2	20.00	20.14	0.70	20.00	20.36	1.80	24.86	25.40	2.17	40.86	40.86	0.00
SO_3	0.30	0.33	10.00	0.30	0.22	-26.67	0.3	<0.25	--	0.30	0.32	6.67
SrO	0.12	0.12	0.00	0.12	0.12	0.00	0.12	<0.12	--	0.12	0.12	0.00
ZrO_2	4.00	3.90	-2.50	4.00	2.59	-35.25	0.00	<0.14	--	0.00	<0.14	--
Total	99.69	100.48	0.79	99.69	99.42	-0.27	99.69	100.03	0.34	99.69	100.35	0.66

Table B.1 (continued)

Glass ID	EWG-OL-3231			EWG-OL-3388			EWG-OL-3872			EWG-OL-4099		
Component	**Targeted (wt%)**	**Analyzed (wt%)**	**% Diff**	**Targeted (wt%)**	**Analyzed (wt%)**	**% Diff**	**Targeted (wt%)**	**Analyzed (wt%)**	**% Diff**	**Targeted (wt%)**	**Analyzed (wt%)**	**% Diff**
Al_2O_3	15.00	14.71	-1.93	15.00	14.72	-1.87	15.00	14.74	-1.73	15.00	14.57	-2.87
B_2O_3	22.00	22.79	3.59	22.00	22.78	3.55	8.00	8.10	1.25	22.00	22.35	1.59
Bi_2O_3	0.00	<0.11	--	3.00	2.92	-2.67	3.00	3.13	4.33	0.00	<0.11	--
CaO	10.00	10.27	2.70	0.00	<0.15	--	10.00	9.86	-1.40	10.00	10.31	3.10
CdO	0.10	<0.11	--	0.10	<0.11	--	0.10	0.08	-20.00	0.10	<0.11	--
Cr_2O_3	1.60	1.53	-4.38	1.60	1.52	-5.00	0.00	0.15	--	0.00	<0.15	--
Fe_2O_3	0.00	<0.14	--	9.86	9.78	-0.81	0.00	0.14	--	0.00	<0.14	--
K_2O	3.00	2.93	-2.33	3.00	2.98	-0.67	0.00	0.012	--	0.00	<0.12	--
Li_2O	6.00	5.92	-1.33	0	<0.22	--	6.00	5.87	-2.17	6.00	6.07	1.17
MgO	0.00	<0.17	--	0.00	<0.17	--	4.00	3.69	-7.75	4.00	3.67	-8.25
MnO	3.00	3.03	1.00	3.00	3.02	0.67	0.00	0.13	--	3.00	3.02	0.67
Na_2O	5.00	5.38	7.60	18.00	18.00	0.00	18.00	18.57	3.17	5.00	5.41	8.20
NiO	0.40	0.38	-5.00	0.40	0.38	-5.00	0.40	0.37	-7.50	0.40	0.34	-15.00
P_2O_5	3.00	2.78	-7.33	3.00	2.84	-5.33	3.00	2.81	-6.33	3.00	2.92	-2.67
PbO	0.30	0.28	-6.67	0.30	0.28	-6.67	0.30	0.26	-13.33	0.30	0.28	-6.67
RuO_2	0.01	<0.13	--	0.01	<0.13	--	0.01	0.01	0.00	0.01	<0.13	--
SiO_2	29.86	29.9	0.10	20.00	20.56	2.80	31.46	31.02	-1.40	30.46	30.54	0.26
SO_3	0.30	0.32	6.67	0.30	0.25	-16.67	0.30	0.31	3.33	0.30	0.35	16.67
SrO	0.12	0.12	0.00	0.12	0.12	0.00	0.12	0.11	-8.33	0.12	<0.12	--
ZrO_2	0.00	<0.14	--	0.00	<0.14	--	0.00	0.14	--	0.00	<0.14	--
Total	99.69	101.12	1.43	99.69	101.06	1.37	99.69	99.50	-0.19	99.69	100.84	1.15

Table B.1 (continued)

Glass ID	EWG-OL-5155			EWG-OL-5549			EWG-OL-5801			EWG-OL-6080		
Component	**Targeted (wt%)**	**Analyzed (wt%)**	**% Diff**	**Targeted (wt%)**	**Analyzed (wt%)**	**% Diff**	**Targeted (wt%)**	**Analyzed (wt%)**	**% Diff**	**Targeted (wt%)**	**Analyzed (wt%)**	**% Diff**
Al_2O_3	19.86	19.79	-0.35	15.00	14.65	-2.33	18.46	18.23	-1.25	30.00	29.48	-1.73
B_2O_3	22.00	22.16	0.73	22.00	22.60	2.73	22.00	21.70	-1.36	21.86	22.00	0.64
Bi_2O_3	3.00	3.30	10.00	3.00	2.92	-2.67	0.00	0.11	--	0.00	<0.11	--
CaO	0.00	0.14	--	9.46	9.61	1.59	0.00	0.14	--	10.00	10.19	1.90
CdO	0.10	0.09	-10.00	0.10	<0.11	--	0.10	0.09	-10.00	0.10	<0.11	--
Cr_2O_3	1.60	1.07	-33.13	0.00	<0.15	--	0.00	0.15	--	1.60	1.43	-10.63
Fe_2O_3	10.00	9.22	-7.80	0.00	<0.14	--	10.00	9.71	-2.90	0.00	<0.14	--
K_2O	0.00	0.01	--	3.00	2.89	-3.67	3.00	3.13	4.33	3.00	2.55	-15.00
Li_2O	6.00	6.03	0.50	0.00	<0.22	--	6.00	5.94	-1.00	0.00	<0.22	--
MgO	4.00	3.53	-11.75	4.00	3.51	-12.25	4.00	3.58	-10.50	4.00	3.83	-4.25
MnO	3.00	2.97	-1.00	0.00	<0.13	--	3.00	3.04	1.33	0.00	<0.13	--
Na_2O	5.00	5.11	2.20	18.00	17.25	-4.17	5.00	5.09	1.80	5.00	5.28	5.60
NiO	0.40	0.17	-57.5	0.40	0.38	-5.00	0.40	0.37	-7.50	0.40	0.37	-7.50
P_2O_5	0.00	0.23	--	0.00	<0.23	--	3.00	2.74	-8.67	3.00	2.72	-9.33
PbO	0.30	0.28	-6.67	0.30	0.26	-13.33	0.30	0.28	-6.67	0.30	0.27	-10.00
RuO_2	0.01	0.01	0.00	0.01	<0.13	--	0.01	0.01	0.00	0.01	<0.13	--
SiO_2	20.00	20.41	2.05	20.00	20.57	2.85	20.00	19.86	-0.70	20.00	20.26	1.30
SO_3	0.30	0.24	-20.00	0.30	0.31	3.33	0.30	0.32	6.67	0.30	<0.13	--
SrO	0.12	0.12	0.00	0.12	<0.12	--	0.12	0.12	0.00	0.12	<0.12	--
ZrO_2	4.00	3.92	-2.00	4.00	3.74	-6.50	4.00	3.28	-18.00	0.00	<0.14	--
Total	99.69	98.79	-0.90	99.69	99.90	0.21	99.69	97.89	-1.81	99.69	99.58	-0.11

Table B.1 (continued)

Glass ID	EWG-OL-6198			EWG-OL-8548			EWG-OL-12707			EWG-OL-14827		
Component	**Targeted (wt%)**	**Analyzed (wt%)**	**% Diff**	**Targeted (wt%)**	**Analyzed (wt%)**	**% Diff**	**Targeted (wt%)**	**Analyzed (wt%)**	**% Diff**	**Targeted (wt%)**	**Analyzed (wt%)**	**% Diff**
Al_2O_3	15.00	15.06	0.40	20.00	19.56	-2.20	15.00	14.68	-2.13	15.00	15.21	1.40
B_2O_3	22.00	21.92	-0.36	8.00	8.13	1.63	22.00	22.46	2.09	22.00	22.20	0.91
Bi_2O_3	0.00	0.12	--	0.00	<0.11	--	3.00	2.97	-1.00	3.00	2.96	-1.33
CaO	0.00	0.14	--	0.00	<0.14	--	10.00	10.27	2.70	10.00	9.68	-3.20
CdO	0.10	0.09	-10.00	0.10	<0.11	--	0.10	<0.11	--	0.10	0.08	-20.00
Cr_2O_3	1.60	1.53	-4.38	1.60	1.64	2.50	0.00	<0.15	--	1.60	1.51	-5.63
Fe_2O_3	10.00	10.02	0.20	10.00	10.22	2.20	0.00	<0.14	--	0.00	0.14	--
K_2O	3.00	3.03	1.00	0.00	<0.12	--	0.00	<0.12	--	3.00	3.18	6.00
Li_2O	6.00	6.00	0.00	0.00	<0.22	--	0.44	<0.22	--	5.90	5.92	0.34
MgO	4.00	3.54	-11.50	4.00	3.88	-3.00	0.00	<0.17	--	0.00	0.17	--
MnO	0.00	0.13	--	3.00	3.16	5.33	3.00	3.10	3.33	3.00	3.12	4.00
Na_2O	5.00	4.96	-0.80	18.00	18.16	0.89	18.00	18.10	0.56	5.00	5.08	1.60
NiO	0.40	0.10	-75.00	0.40	0.37	-7.50	0.40	0.34	-15.00	0.40	0.29	-27.50
P_2O_5	3.00	2.76	-8.00	3.00	2.72	-9.33	3.00	2.86	-4.67	0.00	0.23	--
PbO	0.30	0.28	-6.67	0.30	0.28	-6.67	0.30	0.25	-16.67	0.30	0.27	-10.00
RuO_2	0.01	0.01	0.00	0.01	<0.13	--	0.01	<0.13	--	0.01	0.01	0.00
SiO_2	24.86	25.03	0.68	26.86	27.01	0.56	20.02	21.40	6.89	29.96	30.65	2.30
SO_3	0.30	0.31	3.33	0.30	0.26	-13.33	0.30	0.36	20.00	0.30	0.31	3.33
SrO	0.12	0.12	0.00	0.12	<0.12	--	0.12	<0.12	--	0.12	0.11	-8.33
ZrO_2	4.00	3.70	-7.50	4.00	3.62	-9.50	4.00	3.91	-2.25	0.00	0.14	--
Total	99.69	98.84	-0.85	99.69	99.96	0.27	99.69	101.85	2.17	99.69	101.24	1.55

Table B.1 (continued)

Glass ID	EWG-OL-15968			EWG-OL-16450			EWG-OL-23401			EWG-OL-26012		
Component	**Targeted (wt%)**	**Analyzed (wt%)**	**% Diff**	**Targeted (wt%)**	**Analyzed (wt%)**	**% Diff**	**Targeted (wt%)**	**Analyzed (wt%)**	**% Diff**	**Targeted (wt%)**	**Analyzed (wt%)**	**% Diff**
Al_2O_3	15.00	14.96	-0.27	15.00	15.06	0.40	15.00	14.91	-0.60	15.00	14.95	-0.33
B_2O_3	22.00	21.77	-1.05	22.00	23.17	5.32	8.00	8.09	1.13	8.00	8.01	0.13
Bi_2O_3	0.00	0.11	--	3.00	2.96	-1.33	0.00	<0.11	--	3.00	3.13	4.33
CaO	0.00	0.14	--	10.00	10.36	3.60	10.00	10.37	3.70	0.00	0.14	--
CdO	0.10	0.08	-20.00	0.10	<0.11	--	0.10	<0.11	--	0.10	0.09	-10.00
Cr_2O_3	1.60	1.38	-13.75	1.60	1.56	-2.50	1.60	1.54	-3.75	0.00	0.15	--
Fe_2O_3	0.00	0.14	--	0.00	<0.14	--	0.00	<0.14	--	0.00	0.14	--
K_2O	0.00	0.01	--	0.00	<0.12	--	0.00	<0.12	--	3.00	3.13	4.33
Li_2O	5.15	5.14	-0.19	0.00	<0.22	--	0.00	<0.22	--	1.68	1.67	-0.60
MgO	4.00	3.76	-6.00	4.00	3.71	-7.25	0.00	<0.17	--	0.00	0.17	--
MnO	0.00	0.13	--	3.00	3.10	3.33	0.00	<0.13	--	0.00	0.13	--
Na_2O	18.00	18.54	3.00	17.77	17.69	-0.45	17.54	17.29	-1.43	18.00	18.13	0.72
NiO	0.40	0.32	-20.00	0.40	0.35	-12.50	0.40	0.34	-15.00	0.40	0.39	-2.50
P_2O_5	0.00	0.23	--	0.00	<0.23	--	0.00	<0.23	--	3.00	2.80	-6.67
PbO	0.30	0.27	-10.00	0.30	0.27	-10.00	0.30	0.27	-10.00	0.30	0.28	-6.67
RuO_2	0.01	0.013	30.00	0.01	<0.13	--	0.01	<0.13	--	0.01	0.013	30.00
SiO_2	28.71	28.93	0.77	22.08	23.48	6.34	42.32	42.79	1.11	42.78	42.57	-0.49
SO_3	0.30	0.30	0.00	0.30	0.35	16.67	0.30	<0.25	--	0.30	0.24	-20.00
SrO	0.12	0.12	0.00	0.12	<0.12	--	0.12	<0.12	--	0.12	0.12	0.00
ZrO_2	4.00	3.96	-1.00	0.00	<0.14	--	4.00	3.84	-4.00	4.00	4.00	0.00
Total	99.69	100.31	0.62	99.68	103.26	3.59	99.69	101.14	1.45	99.69	100.12	0.43

Table B.1 (continued)

Glass ID	EWG-OL-29285			EWG-OL-31644			EWG-OL-32706			EWG-OL-33115		
Component	**Targeted (wt%)**	**Analyzed (wt%)**	**% Diff**	**Targeted (wt%)**	**Analyzed (wt%)**	**% Diff**	**Targeted (wt%)**	**Analyzed (wt%)**	**% Diff**	**Targeted (wt%)**	**Analyzed (wt%)**	**% Diff**
Al_2O_3	15.00	15.05	0.33	15.00	15.22	1.47	15.00	14.81	-1.27	15.00	15.17	1.13
B_2O_3	18.58	18.44	-0.75	8.00	8.20	2.50	22.00	22.29	1.32	8.00	8.26	3.25
Bi_2O_3	0.00	0.11	--	0.00	0.11	--	0.00	<0.11	--	3.00	3.09	3.00
CaO	10.00	10.21	2.10	10.00	10.52	5.20	0.00	<0.15	--	10.00	9.78	-2.20
CdO	0.10	0.09	-10.00	0.10	0.08	-20.00	0.10	<0.11	--	0.10	0.08	-20.00
Cr_2O_3	0.00	0.15	--	1.60	1.45	-9.38	0.00	<0.15	--	0.00	0.15	--
Fe_2O_3	0.00	0.14	--	10.00	9.96	-0.40	0.00	<0.14	--	10.00	10.07	0.70
K_2O	0.00	0.01	--	0.00	0.01	--	3.00	2.90	-3.33	3.00	2.63	-12.33
Li_2O	0.00	0.22	--	1.38	1.40	1.45	1.23	1.09	-11.38	0.00	0.22	--
MgO	4.00	3.47	-13.25	4.00	3.74	-6.50	4.00	3.79	-5.25	4.00	3.65	-8.75
MnO	0.00	0.13	--	3.00	3.10	3.33	0.00	<0.13	--	0.00	0.13	--
Na_2O	5.00	5.06	1.20	5.00	4.92	-1.60	6.23	6.71	7.70	6.56	6.73	2.59
NiO	0.40	0.38	-5.00	0.40	0.29	-27.50	0.40	0.39	-2.50	0.40	0.37	-7.50
P_2O_5	3.00	2.81	-6.33	0.00	0.23	--	0.00	<0.23	--	3.00	2.77	-7.67
PbO	0.30	0.27	-10.00	0.30	0.27	-10.00	0.30	0.29	-3.33	0.30	0.27	-10.00
RuO_2	0.01	0.013	30.00	0.01	0.013	30.00	0.01	<0.13	--	0.01	0.013	30.00
SiO_2	38.88	38.88	0.00	40.48	40.86	0.94	43.00	42.95	-0.12	35.90	36.21	0.86
SO_3	0.30	0.04	-86.67	0.30	0.12	-60.00	0.30	<0.25	--	0.30	0.20	-33.33
SrO	0.12	0.12	0.00	0.12	0.12	0.00	0.12	<0.12	--	0.12	0.11	-8.33
ZrO_2	4.00	4.00	0.00	0.00	0.14	--	4.00	3.95	-1.25	0.00	0.14	--
Total	99.69	99.59	-0.10	99.69	100.76	1.07	99.69	100.67	0.98	99.69	100.03	0.34

Table B.1 (continued)

Glass ID	EWG-OL-33558			EWG-OL-33694			EWG-OL-33858			EWG-OL-35387		
Component	**Targeted (wt%)**	**Analyzed (wt%)**	**% Diff**	**Targeted (wt%)**	**Analyzed (wt%)**	**% Diff**	**Targeted (wt%)**	**Analyzed (wt%)**	**% Diff**	**Targeted (wt%)**	**Analyzed (wt%)**	**% Diff**
Al_2O_3	15.00	14.97	-0.20	15.00	14.91	-0.60	30.00	29.76	-0.80	15.00	15.01	0.07
B_2O_3	8.00	8.57	7.13	22.00	22.36	1.64	9.91	10.27	3.63	8.00	8.40	5.10
Bi_2O_3	0.00	<0.11	--	3.00	2.91	-3.00	3.00	2.90	-3.33	3.00	2.87	-4.33
CaO	10.00	10.29	2.90	0.00	<0.16	--	0.00	<0.21	--	0.00	<0.20	--
CdO	0.10	<0.11	--	0.10	<0.11	--	0.10	<0.11	--	0.10	<0.11	--
Cr_2O_3	0.00	<0.15	--	0.00	<0.15	--	0.00	<0.15	--	1.60	1.52	-5.00
Fe_2O_3	10.00	10.03	0.30	0.00	<0.14	--	0.00	<0.14	--	0.00	<0.14	--
K_2O	3.00	3.02	0.67	3.00	2.92	-2.67	3.00	2.89	-3.67	3.00	2.84	-5.33
Li_2O	0.26	<0.22	--	0.02	<0.22	--	6.00	5.91	-1.50	0.02	<0.22	--
MgO	4.00	3.79	-5.25	4.00	3.79	-5.25	4.00	3.76	-6.00	4.00	3.79	-5.25
MnO	3.00	3.07	2.33	3.00	3.11	3.67	3.00	3.17	5.67	3.00	3.06	2.00
Na_2O	5.00	5.61	12.20	5.44	5.65	3.86	5.00	5.34	6.80	18.00	17.59	-2.28
NiO	0.40	0.38	-5.00	0.40	0.38	-5.00	0.40	0.34	-15.00	0.40	0.36	-10.00
P_2O_5	3.00	2.90	-3.33	0.00	<0.23	--	0.00	<0.23	--	0.00	<0.23	--
PbO	0.30	0.28	-6.67	0.30	0.29	-3.33	0.30	0.27	-10.00	0.30	0.28	-6.67
RuO_2	0.01	<0.13	--	0.01	<0.13	--	0.01	<0.13	--	0.01	<0.13	--
SiO_2	37.19	37.12	-0.19	43.00	43.21	0.49	34.55	35.30	2.17	42.83	42.36	-1.10
SO_3	0.30	<0.25	--	0.30	<0.25	--	0.30	<0.25	--	0.30	<0.25	--
SrO	0.12	<0.12	--	0.12	<0.12	--	0.12	<0.12	--	0.12	<0.12	--
ZrO_2	0.00	<0.14	--	0.00	<0.14	--	0.00	<0.14	--	0.00	<0.14	--
Total	99.68	101.26	1.59	99.69	101.17	1.48	99.69	101.38	1.70	99.68	99.61	-0.07

Table B.1 (continued)

Glass ID	EWG-OL-38081			EWG-OL-38552			EWG-OL-1755 Mod			EWG-OL-3063 Mod		
Component	**Targeted (wt%)**	**Analyzed (wt%)**	**% Diff**	**Targeted (wt%)**	**Analyzed (wt%)**	**% Diff**	**Targeted (wt%)**	**Analyzed (wt%)**	**% Diff**	**Targeted (wt%)**	**Analyzed (wt%)**	**% Diff**
Al_2O_3	26.00	25.84	-0.62	26.00	25.98	-0.08	15.00	14.80	-1.33	15.00	14.83	-1.13
B_2O_3	8.00	8.23	2.88	8.00	8.25	3.13	10.00	10.18	1.80	22.00	21.85	-0.68
Bi_2O_3	3.00	2.90	-3.33	3.00	3.08	2.67	3.00	2.92		3.00	2.92	
CaO	0.00	<0.23	--	0.00	0.14	--	0.00	<0.14	--	0.00	<0.14	--
CdO	0.10	<0.11	--	0.10	0.086	-14.00	0.10	<0.11	--	0.10	<0.11	--
Cr_2O_3	0.00	<0.15	--	0.00	0.15	--	1.60	1.36	-15.00	1.60	1.84	15.00
Fe_2O_3	0.00	<0.14	--	3.62	3.64	0.55	8.00	8.07	0.88	10.00	10.29	2.90
K_2O	3.00	2.96	-1.33	0.00	0.01	--	3.00	3.08	2.67	3.00	2.98	-0.67
Li_2O	6.00	5.59	-6.83	6.00	5.98	-0.33	6.00	5.89	-1.83	3.00	2.87	-4.33
MgO	0.00	<0.17	--	4.00	3.64	-9.00	0.00	<0.17	--	0.00	<0.17	--
MnO	3.00	3.08	2.67	3.00	3.09	3.00	3.00	2.48	-17.33	0.00	<0.13	--
Na_2O	7.96	8.33	4.65	5.00	5.06	1.20	5.00	5.11	2.20	5.00	5.15	3.00
NiO	0.40	0.35	-12.50	0.40	0.37	-7.50	0.40	0.32	-20.00	0.40	0.35	-12.50
P_2O_5	0.00	<0.23	--	3.00	2.74	-8.67	0.00	<0.23	--	3.00	2.71	-9.67
PbO	0.30	0.27	-10.00	0.30	0.27	-10.00	0.30	0.27	-10.00	0.30	0.28	-6.67
RuO_2	0.01	<0.13	--	0.01	0.013	30.00	0.01	<0.13	--	0.01	<0.13	--
SiO_2	37.49	38.29	2.13	32.84	33.16	0.97	42.86	43.59	1.70	31.86	32.30	1.38
SO_3	0.30	<0.25	--	0.30	0.22	-26.67	0.30	0.22	-26.67	0.30	<0.13	--
SrO	0.12	<0.12	--	0.12	0.11	-8.33	0.12	<0.12	--	0.12	<0.12	--
ZrO_2	4.00	3.81	-4.75	4.00	3.17	-20.75	1.00	0.97	-3.00	1.00	0.95	-5.00
Total	99.68	101.18	1.50	99.69	99.16	-0.53	99.69	100.17	0.48	99.69	100.24	0.55

Table B.1 (continued)

Glass ID	EWG-OL-4744 Mod			EWG-OL-5385 Mod			EWG-OL-6257 Mod			EWG-OL-6311 Mod		
Component	**Targeted (wt%)**	**Analyzed (wt%)**	**% Diff**	**Targeted (wt%)**	**Analyzed (wt%)**	**% Diff**	**Targeted (wt%)**	**Analyzed (wt%)**	**% Diff**	**Targeted (wt%)**	**Analyzed (wt%)**	**% Diff**
Al_2O_3	19.86	19.28	-2.92	25.46	24.80	-2.59	30.00	28.15	-6.17	17.00	16.59	-2.41
B_2O_3	10.50	10.64	1.33	12.00	12.12	1.00	12.00	11.75	-2.08	12.00	12.17	1.42
Bi_2O_3	3.00	2.89	-3.67	0.00	<0.11	--	3.00	2.87	-4.33	3.00	2.86	-4.67
CaO	10.00	9.75	-2.50	10.00	9.93	-0.70	8.00	7.77	-2.88	0.00	<0.14	--
CdO	0.10	<0.11	--	0.10	<0.11	--	0.10	<0.11	--	0.10	<0.11	--
Cr_2O_3	1.60	1.58	-1.25	0.00	<0.15	--	1.60	1.51	-5.63	1.60	1.55	-3.13
Fe_2O_3	7.50	7.56	0.80	0.00	<0.14	--	0.00	<0.14	--	10.00	10.11	1.10
K_2O	0.00	<0.12	--	3.00	3.04	1.33	3.00	3.12	4.00	0.00	<0.12	--
Li_2O	0.00	<0.22	--	4.00	3.83	-4.25	6.00	5.63	-6.17	6.00	5.84	-2.67
MgO	4.00	3.72	-7.00	1.00	0.77	-23.00	1.00	0.75	-25.00	4.00	4.03	0.75
MnO	0.00	<0.13	--	0.00	<0.13	--	0.00	<0.13	--	0.00	<0.13	--
Na_2O	18.00	18.37	2.06	17.00	17.12	0.71	5.00	5.21	4.20	15.00	15.30	2.00
NiO	0.40	0.35	-12.50	0.40	0.35	-12.50	0.40	0.34	-15.00	0.40	0.35	-12.50
P_2O_5	0.00	<0.23	--	0.00	<0.23	--	0.00	<0.23	--	3.00	2.66	-11.33
PbO	0.30	0.27	-10.00	0.30	0.25	-16.67	0.30	0.26	-13.33	0.30	0.27	-10.00
RuO_2	0.01	<0.13	--	0.01	<0.13	--	0.01	<0.13	--	0.01	<0.13	--
SiO_2	23.00	23.10	0.43	24.00	24.17	0.71	28.86	28.35	-1.77	26.86	27.12	0.97
SO_3	0.30	0.31	3.33	0.30	0.30	0.00	0.30	0.27	-10.00	0.30	0.33	10.00
SrO	0.12	<0.12	--	0.12	<0.12	--	0.12	<0.12	--	0.12	<0.12	--
ZrO_2	1.00	0.91	-9.00	2.00	1.83	-8.50	0.00	<0.14	--	0.00	<0.14	--
Total	99.69	99.78	0.09	99.69	99.63	-0.06	99.69	96.98	-2.72	99.69	100.04	0.35

Table B.1 (continued)

Glass ID	EWG-OL-6489 Mod			EWG-OL-8548 Mod			EWG-OL-10278 Mod			EWG-OL-11318 Mod		
Component	**Targeted (wt%)**	**Analyzed (wt%)**	**% Diff**	**Targeted (wt%)**	**Analyzed (wt%)**	**% Diff**	**Targeted (wt%)**	**Analyzed (wt%)**	**% Diff**	**Targeted (wt%)**	**Analyzed (wt%)**	**% Diff**
Al_2O_3	30.00	28.30	-5.67	21.50	20.74	-3.53	26.00	24.52	-5.69	26.00	24.89	-4.27
B_2O_3	11.00	10.86	-1.27	8.00	8.03	0.38	15.00	14.63	-2.47	22.00	21.53	-2.14
Bi_2O_3	0.00	<0.11	--	0.00	<0.11	--	0.00	<0.11	--	0.00	<0.11	--
CaO	0.00	<0.19	--	0.00	<0.18	--	10.00	9.67	-3.30	0.00	<0.14	--
CdO	0.10	<0.11	--	0.10	<0.11	--	0.10	<0.11	--	0.10	<0.11	--
Cr_2O_3	1.60	1.56	-2.50	1.60	1.56	-2.50	0.00	<0.15	--	1.60	1.56	-2.50
Fe_2O_3	0.00	<0.14	--	10.00	10.00	0.00	0.00	<0.14	--	0.00	<0.14	--
K_2O	3.00	3.08	2.67	0.00	<0.12	--	3.00	3.09	3.00	0.00	<0.12	--
Li_2O	4.00	3.77	-5.75	0.00	<0.22	--	5.00	4.70	-6.00	0.00	<0.22	--
MgO	4.00	3.84	-4.00	4.00	4.01	0.25	0.00	<0.17	--	2.00	1.75	-12.50
MnO	3.00	3.05	1.67	3.00	3.13	4.33	1.50	1.49	-0.67	3.00	3.10	3.33
Na_2O	15.00	15.47	3.13	18.00	18.10	0.56	15.00	15.20	1.33	17.86	18.06	1.12
NiO	0.40	0.40	0.00	0.40	0.35	-12.50	0.40	0.35	-12.5	0.40	0.35	-12.50
P_2O_5	3.00	2.73	-9.10	3.00	2.72	-9.33	0.00	<0.23	--	0.00	<0.23	--
PbO	0.30	0.26	-13.33	0.30	0.27	-10.00	0.30	0.26	-13.33	0.30	0.28	-6.67
RuO_2	0.01	<0.13	--	0.01	<0.13	--	0.01	<0.13	--	0.01	<0.13	--
SiO_2	23.86	23.21	-2.72	28.36	28.24	-0.42	21.96	21.23	-3.32	25.00	24.66	-1.36
SO_3	0.30	0.31	3.33	0.30	0.26	-13.33	0.30	0.32	6.67	0.30	0.20	-33.33
SrO	0.12	<0.12	--	0.12	<0.12	--	0.12	<0.12	--	0.12	<0.12	--
ZrO_2	0.00	<0.14	--	1.00	0.95	-5.00	1.00	0.95	-5.00	1.00	0.96	-4.00
Total	99.69	97.77	-1.93	99.69	99.35	-0.34	99.69	97.55	-2.15	99.69	98.67	-1.02

Table B.1 (continued)

Glass ID	EWG-OL-14547 Mod			EWG-OL-15698 Mod			EWG- Centroid-1			EWG-Centroid-2-R1		
Component	**Targeted (wt%)**	**Analyzed (wt%)**	**% Diff**	**Targeted (wt%)**	**Analyzed (wt%)**	**% Diff**	**Targeted (wt%)**	**Analyzed (wt%)**	**% Diff**	**Targeted (wt%)**	**Analyzed (wt%)**	**% Diff**
Al_2O_3	18.15	17.06	-6.01	15.00	14.88	-0.80	22.00	22.11	0.50	22.00	21.40	-2.73
B_2O_3	12.50	12.24	-2.08	11.00	11.46	4.18	15.50	15.33	-1.10	15.50	15.89	2.52
Bi_2O_3	3.00	2.85	-5.00	3.00	2.92	-2.67	1.00	0.98	-2.00	1.00	1.00	0.00
CaO	10.00	9.57	-4.30	10.00	9.95	-0.50	3.50	3.77	7.71	3.50	3.73	6.57
CdO	0.10	<0.11	--	0.10	<0.11	--	0.10	0.087	-13.00	0.10	<0.11	--
Cr_2O_3	1.60	1.49	-6.88	0.00	<0.15	--	0.75	0.72	-4.00	0.75	0.72	-4.00
Fe_2O_3	10.00	9.67	-3.30	10.00	9.87	-1.30	5.50	5.60	1.82	5.50	5.50	0.00
K_2O	1.50	1.53	2.00	0.00	<0.12	--	0.70	0.68	-2.86	0.70	0.67	-4.29
Li_2O	4.00	3.73	-6.75	2.90	2.80	-3.45	3.00	3.07	2.33	3.00	2.82	-6.00
MgO	0.00	<0.17	--	4.00	3.77	-5.75	0.50	0.23	-54.00	0.50	0.32	-36.00
MnO	0.00	<0.13	--	3.00	3.07	2.33	1.00	0.99	-1.00	1.00	1.00	0.00
Na_2O	13.70	13.78	0.58	15.00	15.33	2.20	11.50	11.89	3.39	11.50	11.99	4.26
NiO	0.40	0.34	-15.00	0.40	0.29	-27.50	0.40	0.17	-57.5	0.40	0.38	-5.00
P_2O_5	0.00	<0.23	--	3.00	2.80	-6.67	0.50	0.47	-6.00	1.00	1.02	2.00
PbO	0.30	0.26	-13.33	0.30	0.27	-10.00	0.30	0.27	-10.00	0.30	0.27	-10.00
RuO_2	0.01	<0.13	--	0.01	<0.13	--	0.01	<0.13	--	0.01	<0.13	--
SiO_2	23.00	22.25	-3.26	21.55	22.25	3.25	31.50	31.61	0.35	31.50	31.72	0.70
SO_3	0.30	0.30	0.00	0.30	0.35	16.67	0.30	0.24	-20.00	0.30	0.28	-6.67
SrO	0.12	<0.12	--	0.12	<0.12	--	0.12	<0.12	--	0.12	<0.12	--
ZrO_2	1.00	0.92	-8.00	0.00	<0.14	--	1.00	0.91	-9.00	1.00	0.92	-8.00
Total	99.68	96.87	-2.82	99.68	100.76	1.08	99.18	99.25	0.07	99.68	99.98	0.30

Appendix C

Photographs of Modified Composition Glasses after CCC Treatment

Appendix C

Photographs of Modified Composition Glasses after CCC Treatment

The photos in this appendix show the modified composition glasses after CCC treatment.

Figure C.1. Photo of Glass EWG-OL-4744 Mod 7.5% Fe 1% Zr after CCC Treatment

Figure C.2. Photo of Glass EWG-OL-5385 Mod 12% B 17% Na after CCC Treatment

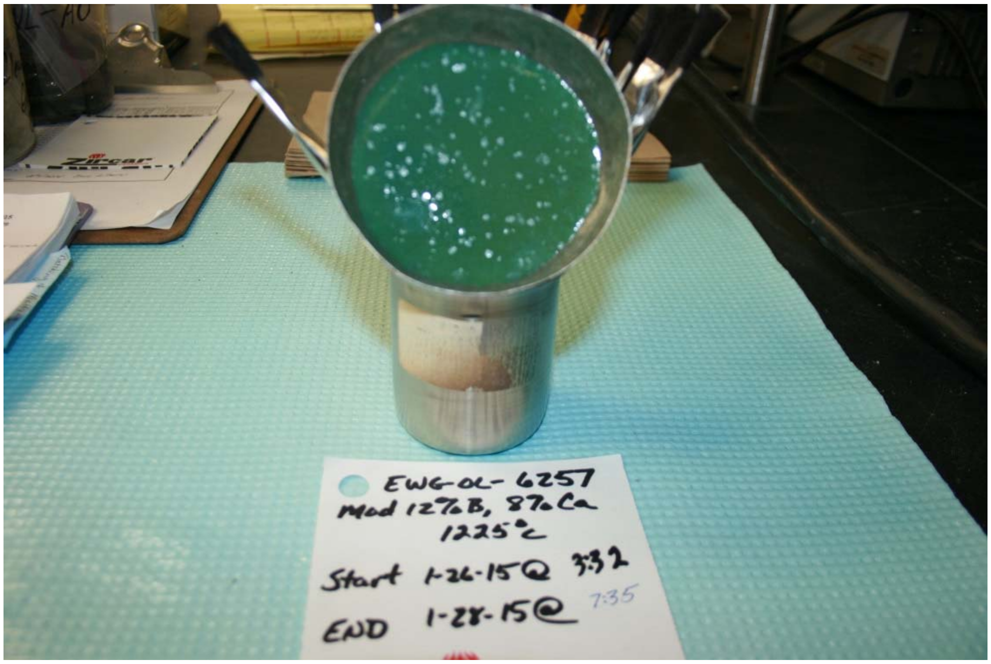

Figure C.3. Photo of Glass EWG-OL-6257 Mod 12% B 8% Ca after CCC Treatment

Figure C.4. Photo of Glass EWG-OL-6311 Mod Reduced Na & K after CCC Treatment

Figure C.5. Photo of Glass EWG-OL-6489 Mod 11% B 15% Na after CCC Treatment

Figure C.6. Photo of Glass EWG-OL-8548 Mod 1% Zr after CCC Treatment

Figure C.7. Photo of Glass EWG-OL-10278 Mod 15% B 1% Zr after CCC Treatment

Figure C.8. Photo of Glass EWG-OL-11318 Mod 1% Zr after CCC Treatment

Figure C.9. Photo of Glass EWG-OL-14547 Mod Reduced Alkali 1% Zr after CCC Treatment

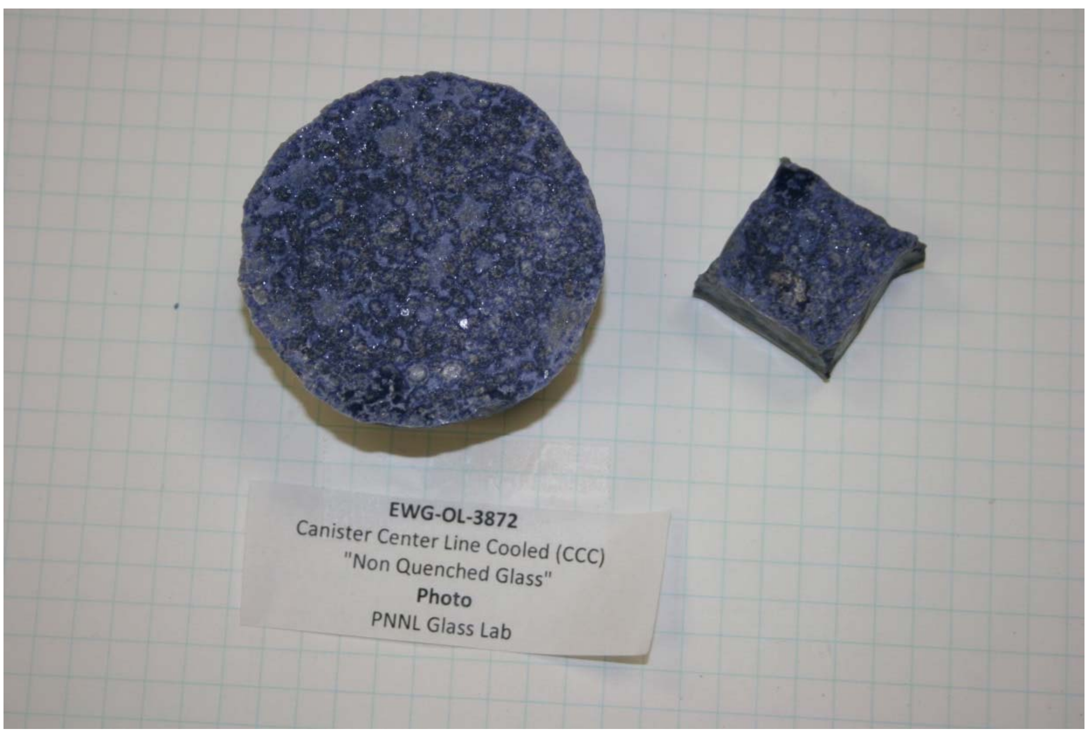

Figure C.10. Photo of Glass EWG-OL-3872 after CCC Treatment

Appendix D

XRD Patterns with Weight Percentages of Identified Crystalline Phases of CCC Glasses

Appendix D

XRD Patterns with Weight Percentages of Identified Crystalline Phases of CCC Glasses

This appendix shows the XRD patterns obtained from each glass after CCC treatment and the weight percentages of each identified crystalline phase. Only four glasses had no crystals identified and remained amorphous after CCC treatment (EWG-OL-801, EWG-OL-5549, EWG-OL-26012, and EWG-OL-33694).

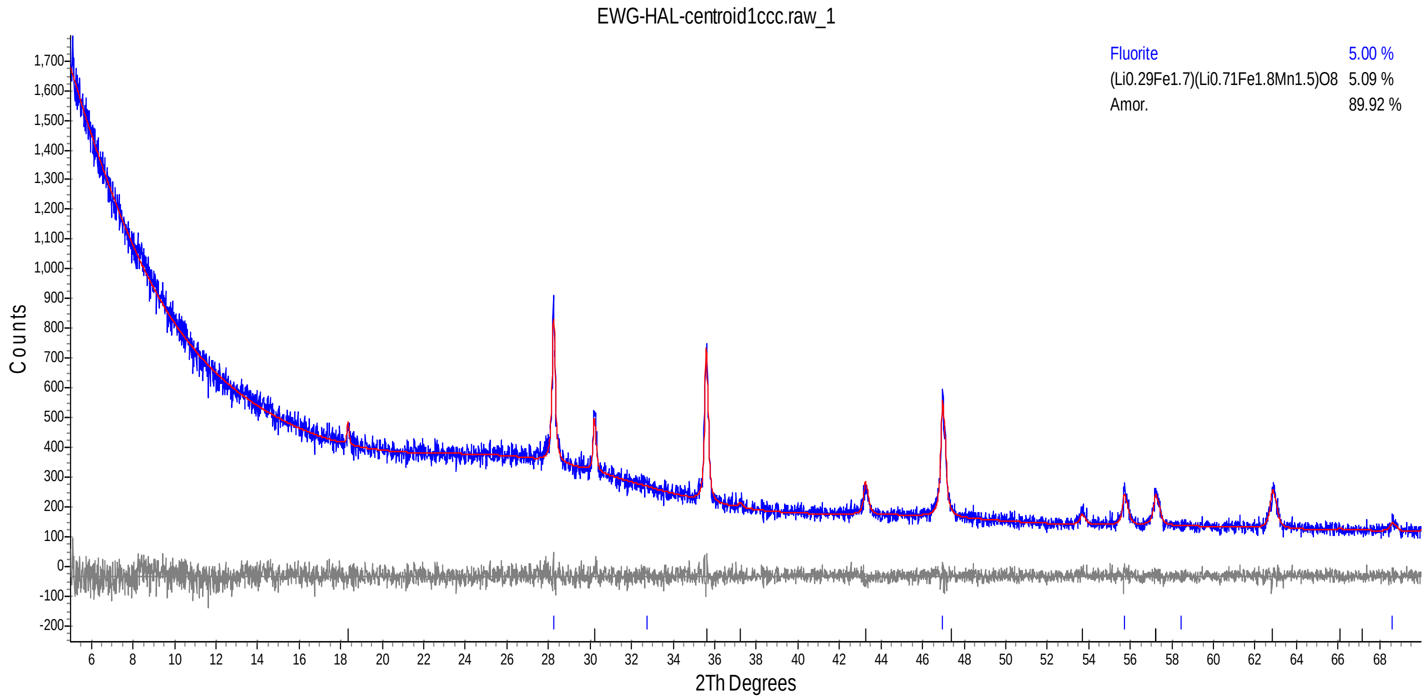

	Phase Name	Wt% of Spiked	Wt% in Spiked sample	Wt% in Original sample
1	CaF2_44618_(70-1469)	4.996	4.996	0
2	(Li0.29Fe1.7)(Li0.71Fe1.8Mn1.5)O8	0	5.088	5.356

Figure D.1. XRD Pattern of Glass EWG-Centroid-1 with the Weight % of Crystalline Phases after CCC Treatment

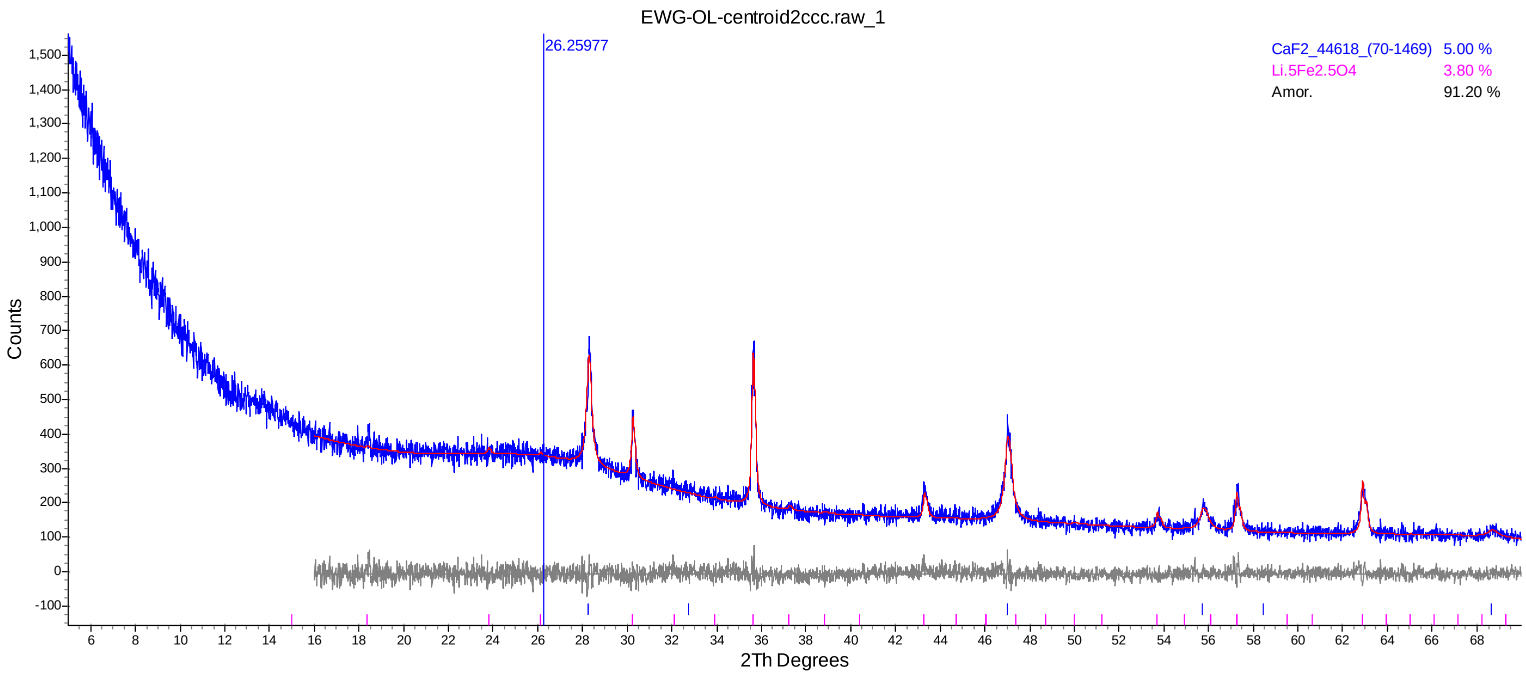

	Phase Name	Wt% of Spiked	Wt% in Spiked sample	Wt% in Original sample
1	CaF2_44618_(70-1469)	5	5	0
2	(Li0.29Fe1.7)(Li0.71Fe1.8Mn1.5)O8	0	3.803	4.003

Figure D.2. XRD Pattern of Glass EWG-Centroid-2 with the Weight % of Crystalline Phases after CCC Treatment

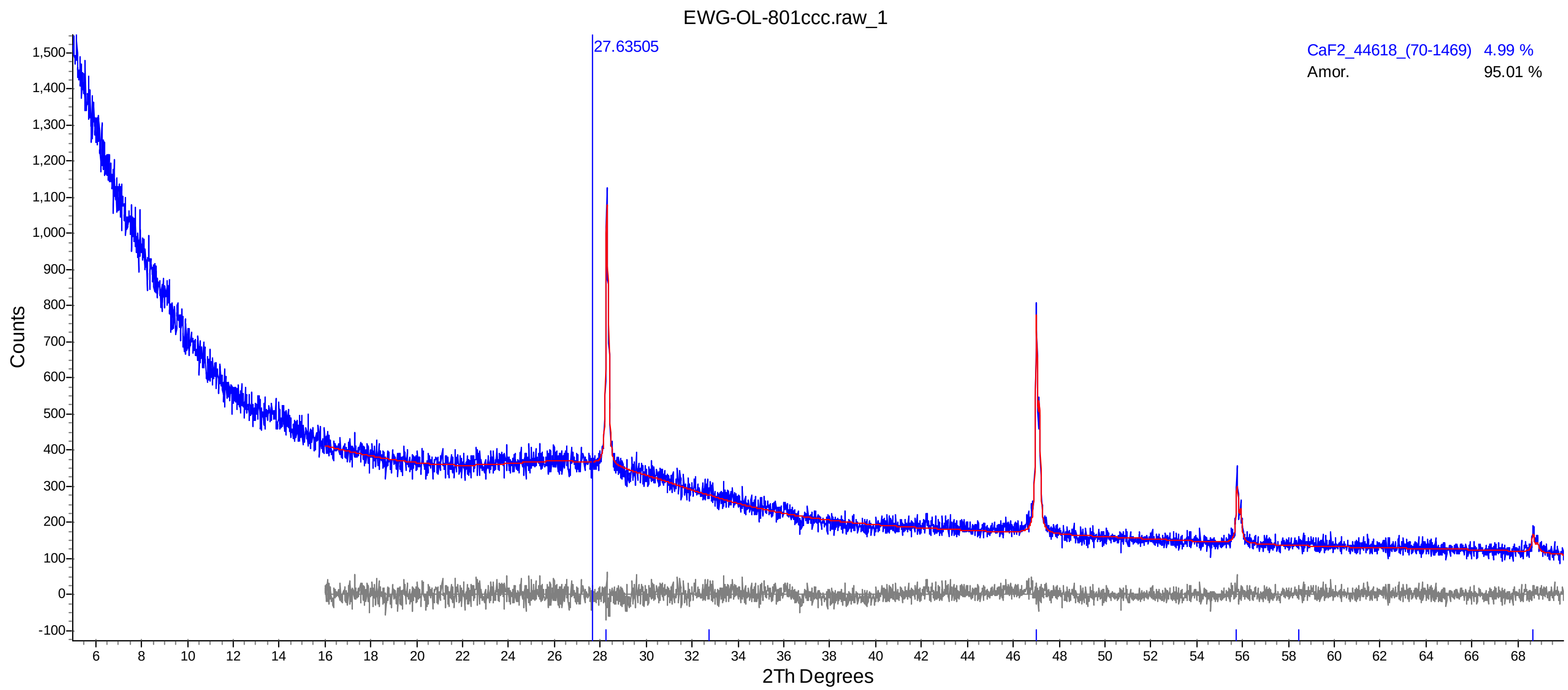

Note: No Crystalline Phase (Except the Added CaF_2) was identified.

Figure D.3. XRD Pattern of Glass EWG-OL-801 with the Weight % of Crystalline Phases after CCC Treatment

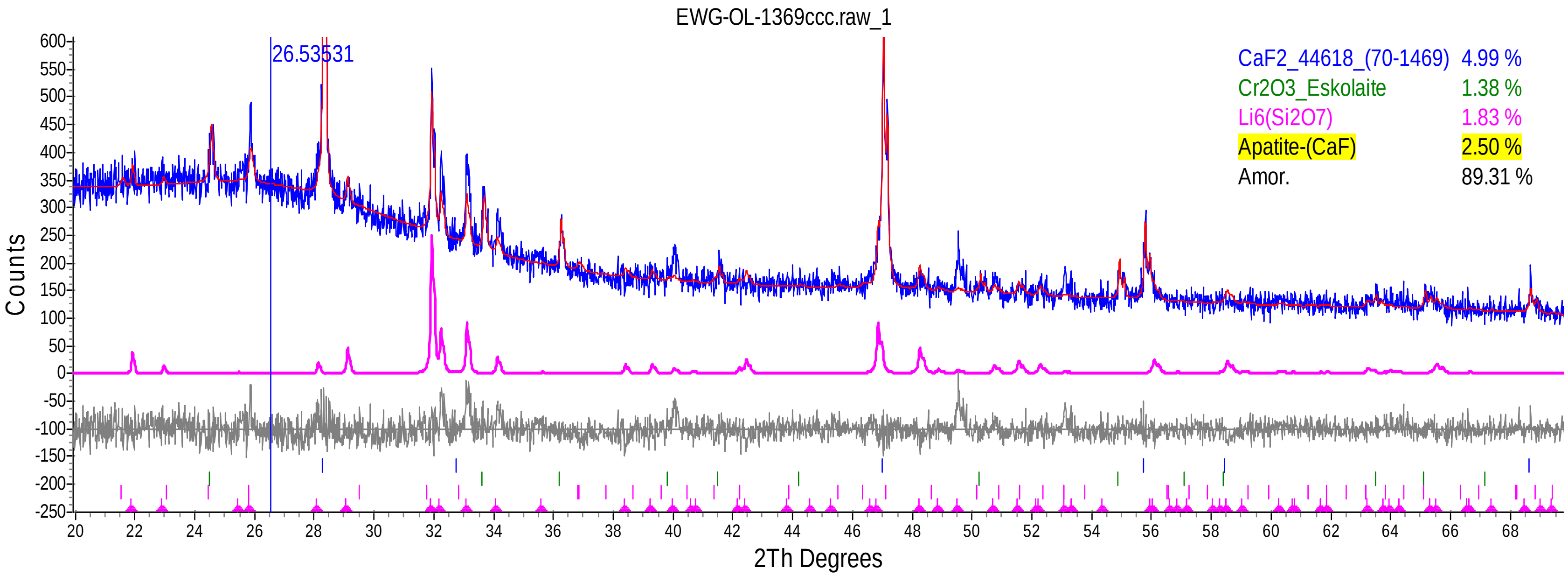

	Phase Name	Wt% of Spiked	Wt% in Spiked sample	Wt% in Original sample
1	Fluorite	4.986	4.986	0
2	Eskolaite	0	1.377	1.449
3	Li6(Si2O7)	0	1.828	1.924
4	Apatite-(CaF)	0	2.501	2.632

Figure D.4. XRD Pattern of Glass EWG-OL-1369 with the Weight % of Crystalline Phases after CCC Treatment

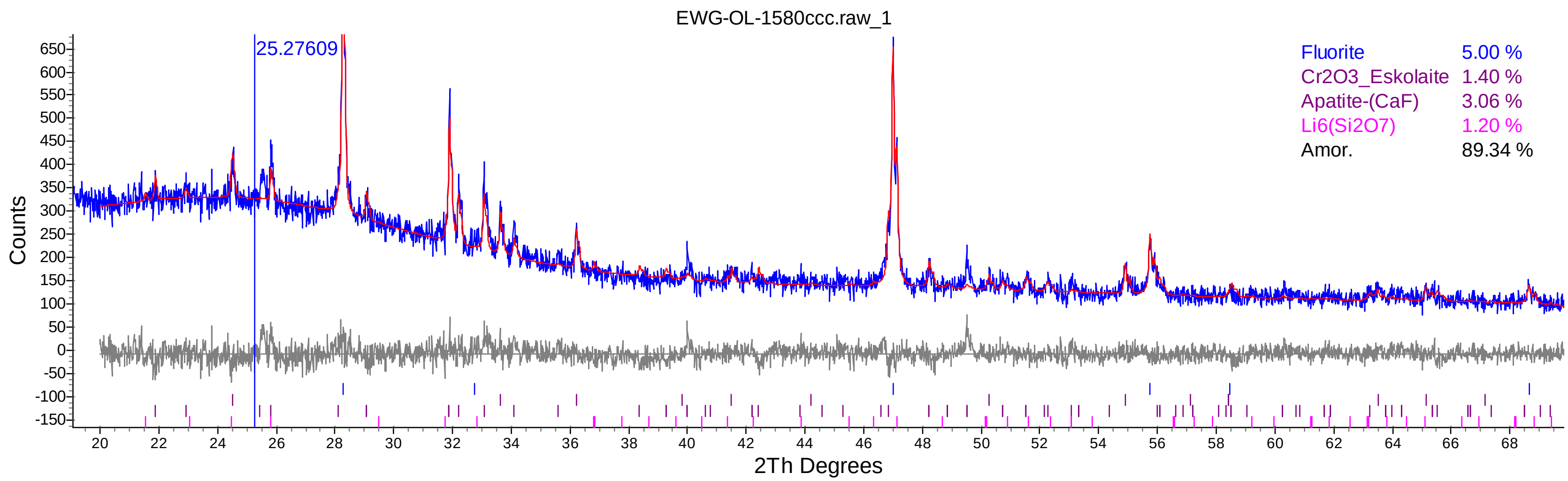

	Phase Name	Wt% of Spiked	Wt% in Spiked sample	Wt% in Original sample
1	Fluorite	4.996	4.996	0
2	Li6(Si2O7)	0	1.204	1.267
3	Apatite-(CaF)	0	3.06	3.221
4	Cr2O3_Eskolaite	0	1.396	1.469

Figure D.5. XRD Pattern of Glass EWG-OL-1580 with the Weight % of Crystalline Phases after CCC Treatment

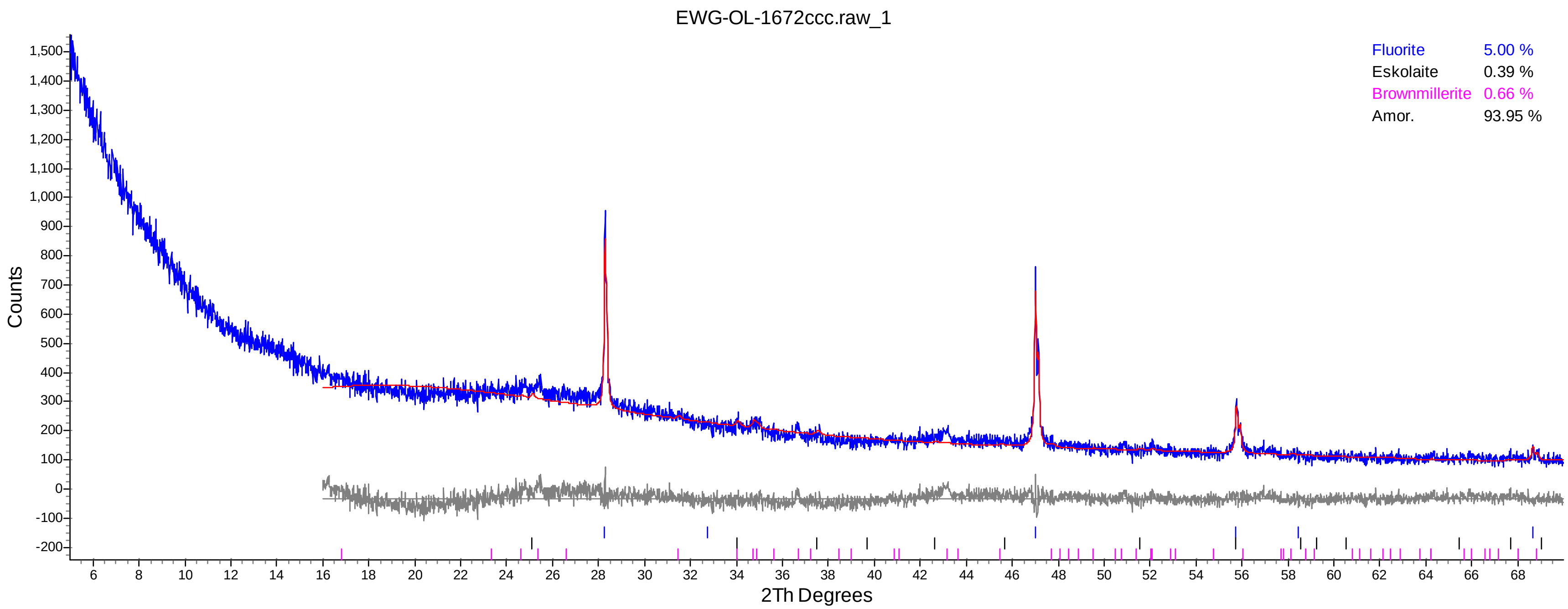

	Phase Name	Wt% of Spiked	Wt% in Spiked sample	Wt% in Original sample
1	Fluorite	5	5	0
2	Eskolaite	0	0.39	0.411
3	Brownmillerite	0	0.662	0.697

Figure D.6. XRD Pattern of Glass EWG-OL-1672 with the Weight % of Crystalline Phases after CCC Treatment

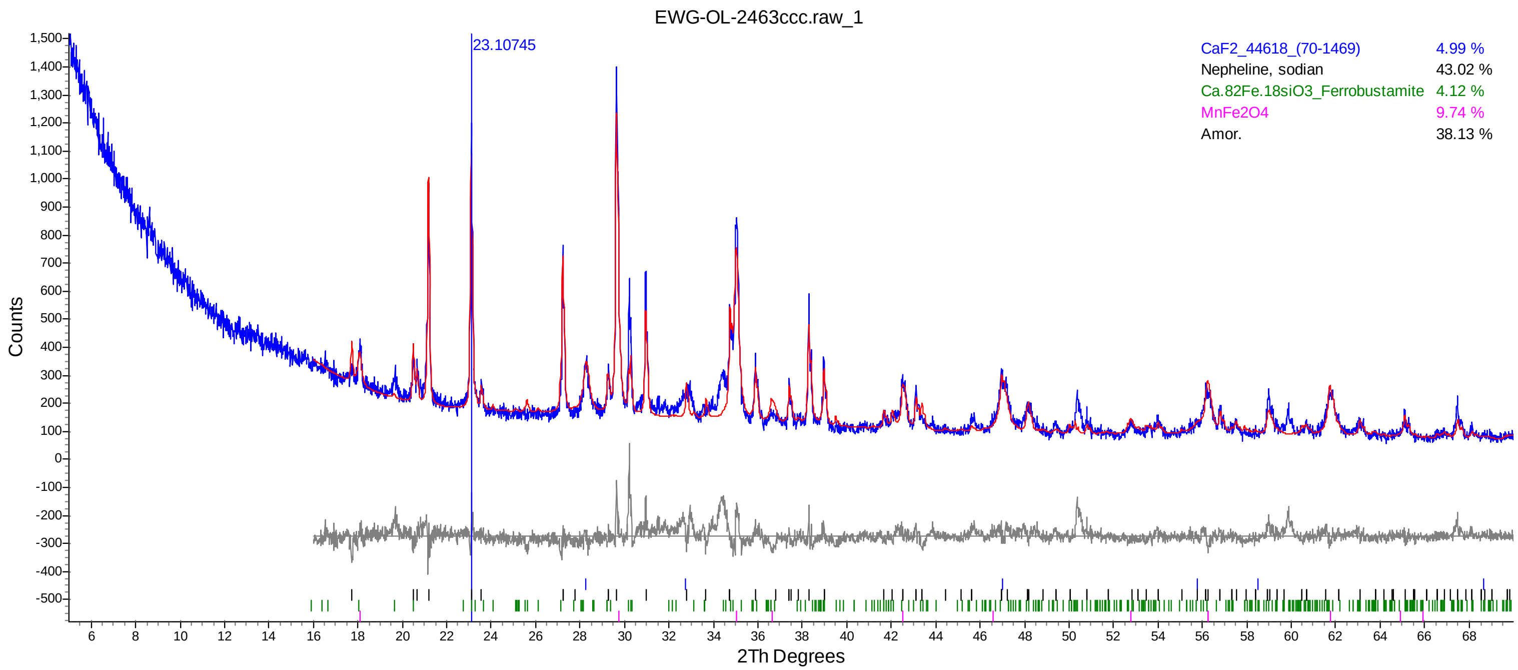

	Phase Name	Wt% of Spiked	Wt% in Spiked sample	Wt% in Original sample
1	CaF2_44618_(70-1469)	4.986	4.986	0
2	Nepheline, sodian	0	43.022	45.28
3	Ca.82Fe.18SiO3	0	4.12	4.337
4	MnFe2O4	0	9.742	10.253

Figure D.7. XRD Pattern of Glass EWG-OL-2463 with the Weight % of Crystalline Phases after CCC Treatment

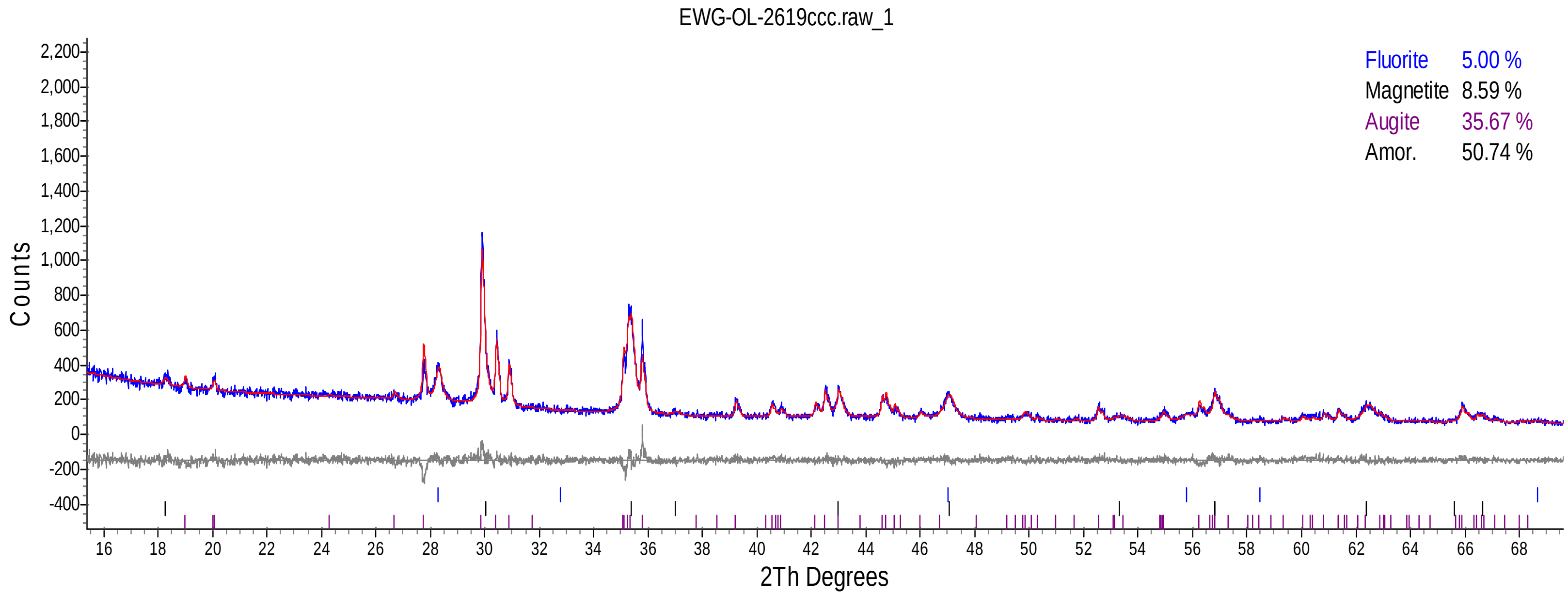

	Phase Name	Wt% of Spiked	Wt% in Spiked sample	Wt% in Original sample
1	Fluorite	5.002	5.002	0
2	Augite	0	35.673	37.551
3	Magnetite	0	8.585	9.037

Figure D.8. XRD Pattern of Glass EWG-OL-2619 with the Weight % of Crystalline Phases after CCC Treatment

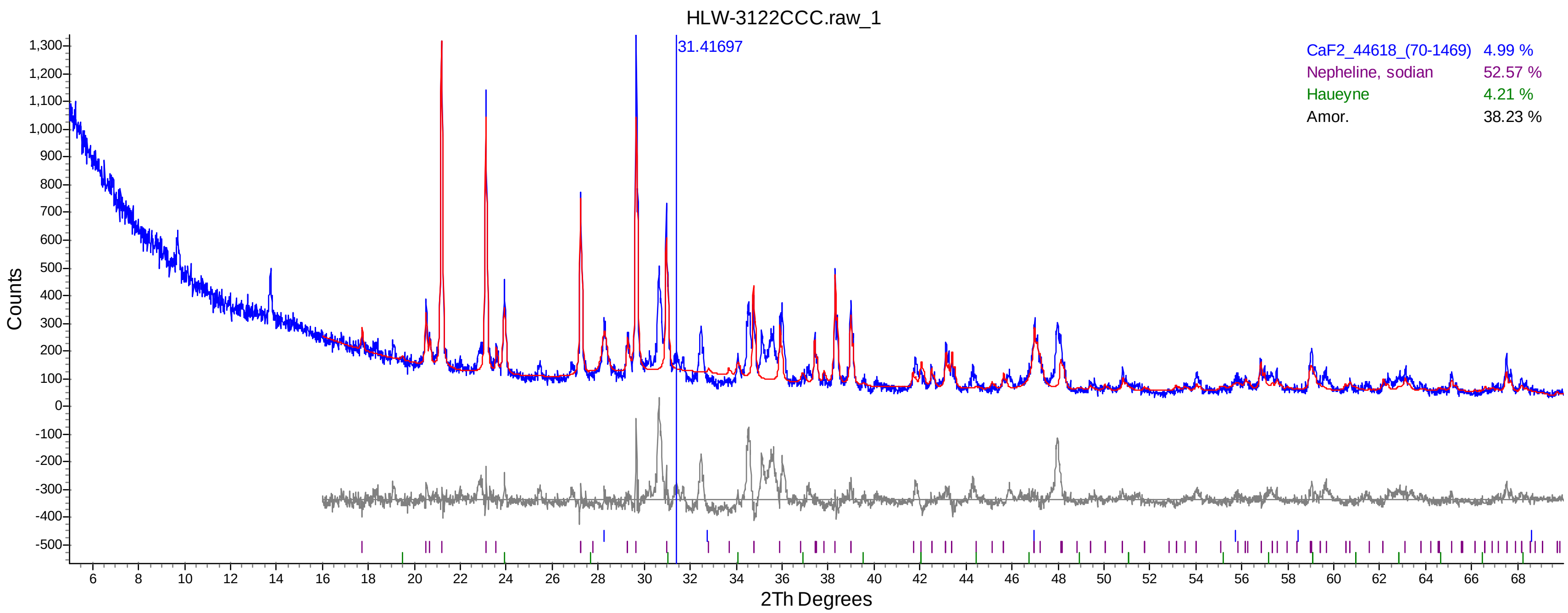

	Phase Name	Wt% of Spiked	Wt% in Spiked sample	Wt% in Original sample
1	CaF2_44618_(70-1469)	4.986	4.986	0
2	Nepheline, sodian	0	52.574	55.332
3	Haueyne	0	4.207	4.428

Figure D.9. XRD Pattern of Glass EWG-OL-3122 with the Weight % of Crystalline Phases after CCC Treatment

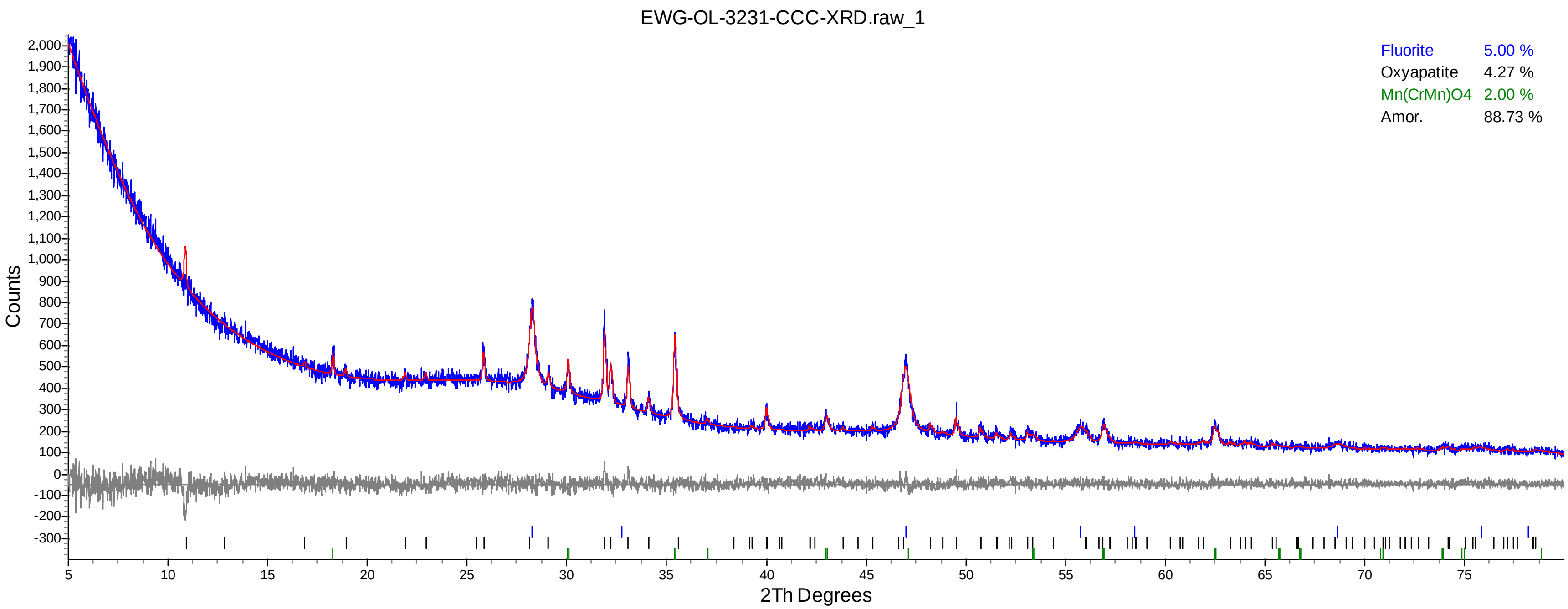

	Phase Name	Wt% of Spiked	Wt% in Spiked sample	Wt% in Original sample
1	Fluorite	4.995	4.995	0
2	Oxyapatite	0	4.272	4.497
3	Mn(CrMn)O4	0	2	2.106

Figure D.10. XRD Pattern of Glass EWG-OL-3231 with the Weight % of Crystalline Phases after CCC Treatment

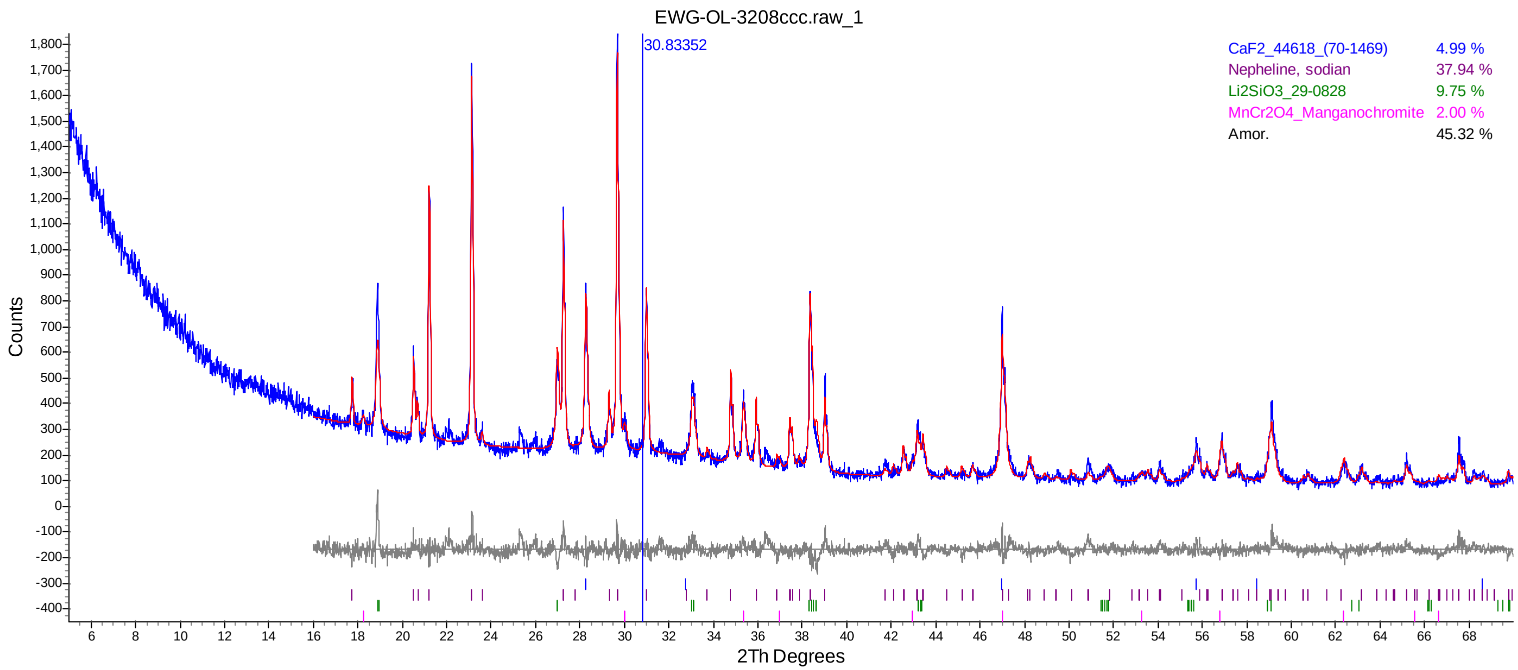

	Phase Name	Wt% of Spiked	Wt% in Spiked sample	Wt% in Original sample
1	CaF2_44618_(70-1469)	4.986	4.986	0
2	Nepheline, sodian	0	37.945	39.936
3	Li2SiO3 29-0828	0	9.748	10.26
4	MnCr2O4_Manganochromate	0	2.002	2.107

Figure D.11. XRD Pattern of Glass EWG-OL-3208 with the Weight % of Crystalline Phases after CCC Treatment

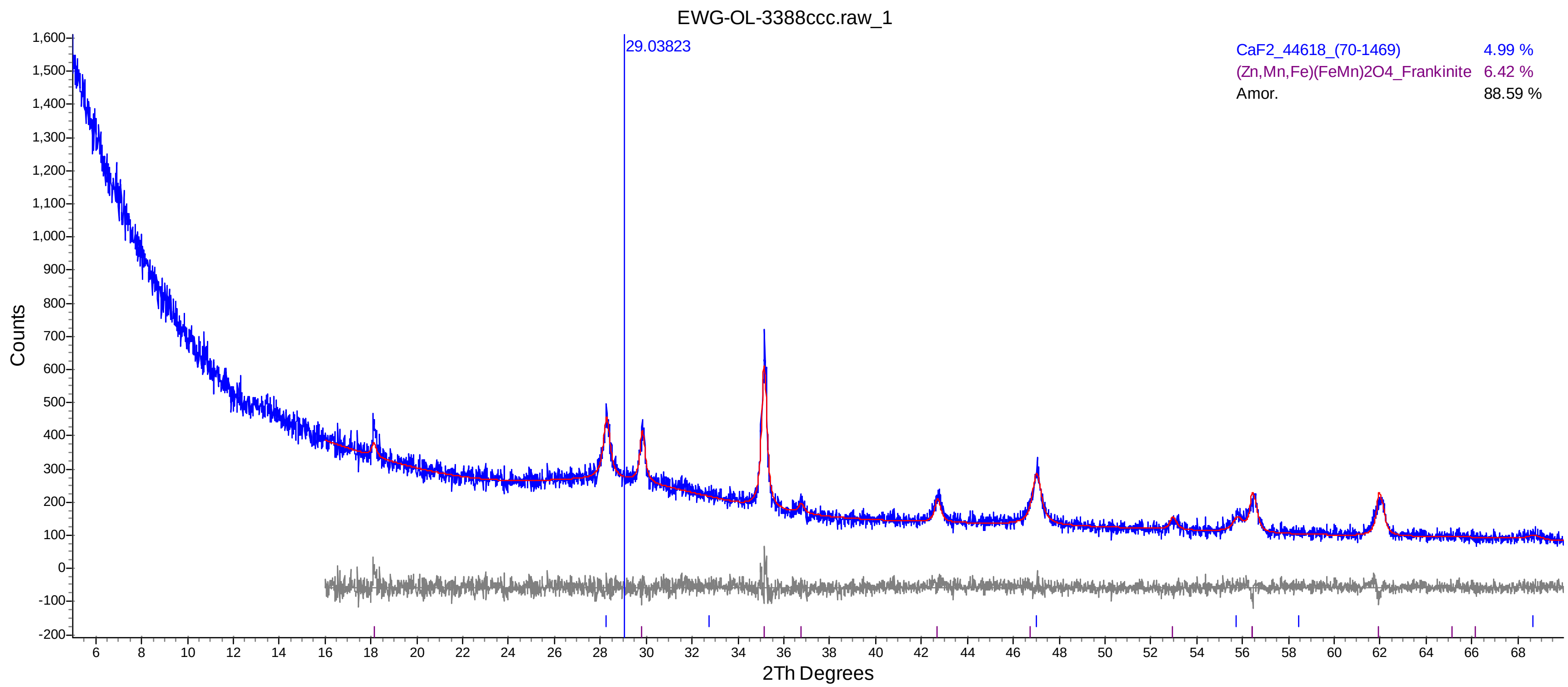

	Phase Name	Wt% of Spiked	Wt% in Spiked sample	Wt% in Original sample
1	CaF2_44618_(70-1469)	4.986	4.986	0
2	(Zn, Mn,Fe)(FeMn)2O4	0	6.423	6.76

Figure D.12. XRD Pattern of Glass EWG-OL-3388 with the Weight % of Crystalline Phases after CCC Treatment

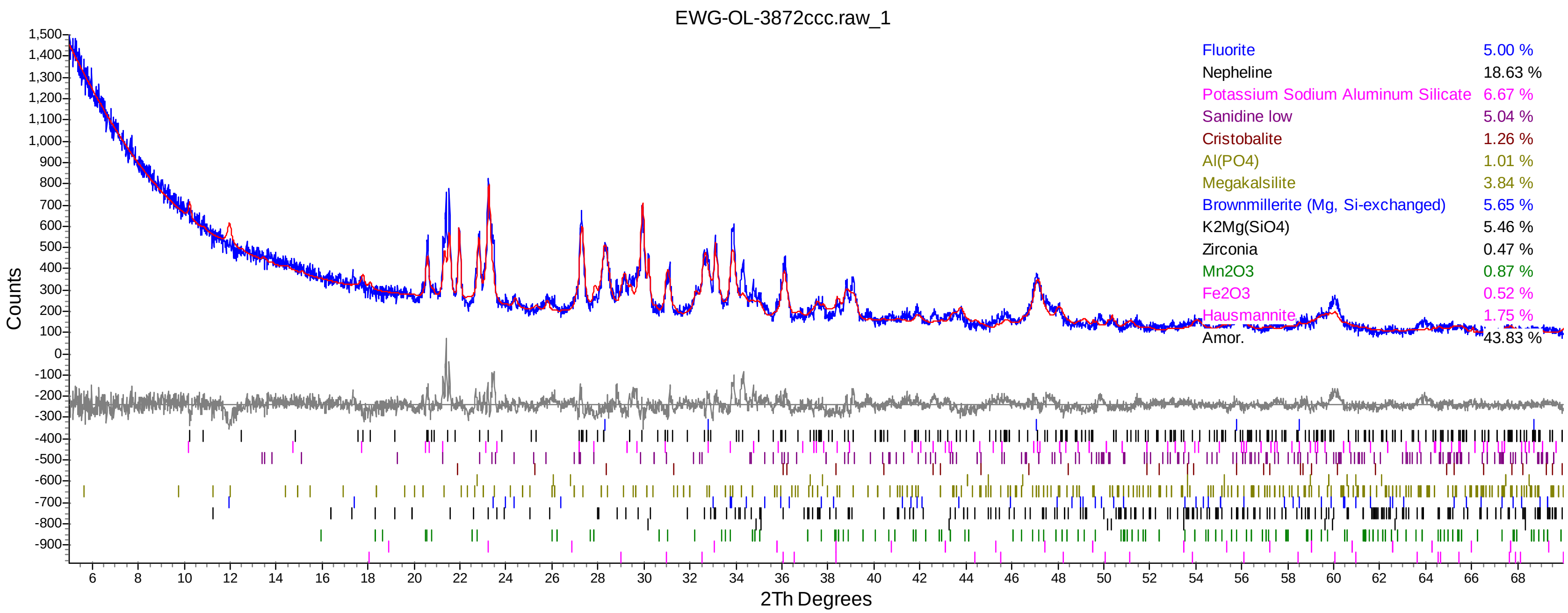

	Phase Name	Wt% of Spiked	Wt% in Spiked sample	Wt% in Original sample
1	Fluorite	5	5	0
2	Nepheline	0	18.632	19.613
3	Potassium Sodium Aluminum Silicate	0	6.673	7.024
4	Sanidine low	0	5.04	5.306
5	Cristobalite	0	1.262	1.328
6	Al(PO4)	0	1.01	1.063
7	Megakalsilite	0	3.837	4.039
8	Brownmillerite (Mg, Si-exchanged)	0	5.647	5.945
9	K2Mg(SiO4)	0	5.464	5.752
10	Zirconia	0	0.473	0.498
11	Mn2O3	0	0.865	0.911
12	Fe2O3	0	0.522	0.549
13	Hausmannite	0	1.746	1.837

Figure D.13. XRD Pattern of Glass EWG-OL-3872 with the Weight % of Crystalline Phases after CCC Treatment

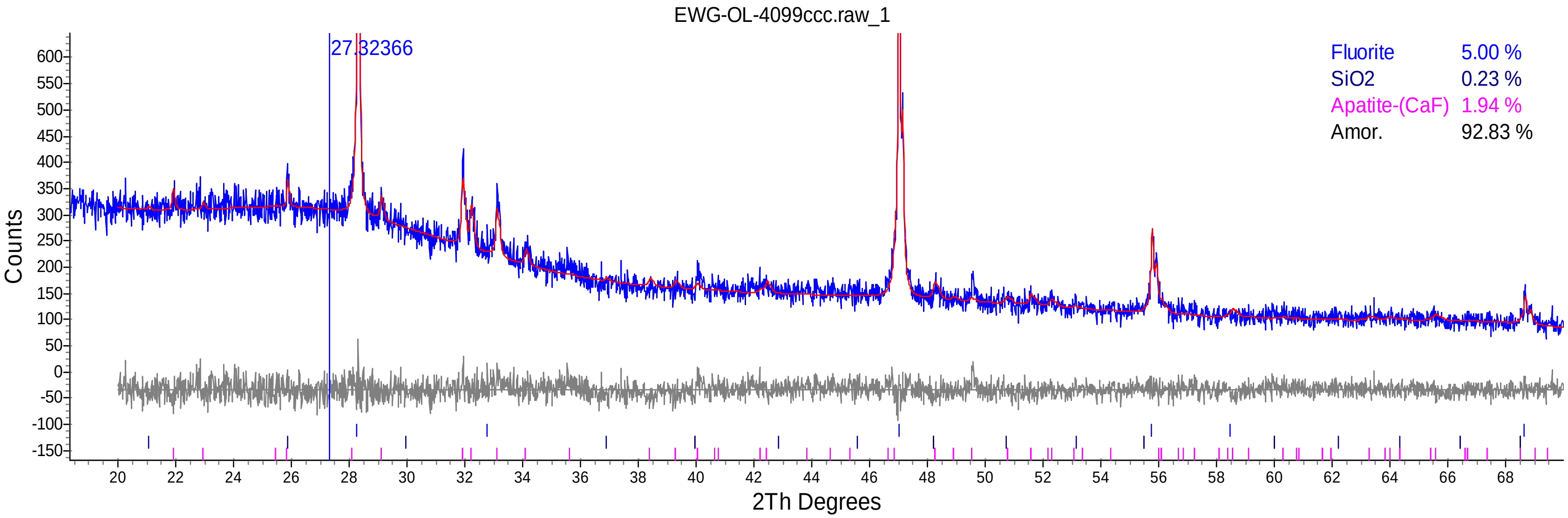

	Phase Name	Wt% of Spiked	Wt% in Spiked sample	Wt% in Original sample
1	Fluorite	5	5	0
2	Braurite 1Q	0	0.788	0.829
3	Apatite-(CaF)	0	1.935	2.037
4	SiO2	0	0.234	0.247

Figure D.14. XRD Pattern of Glass EWG-OL-4099 with the Weight % of Crystalline Phases after CCC Treatment

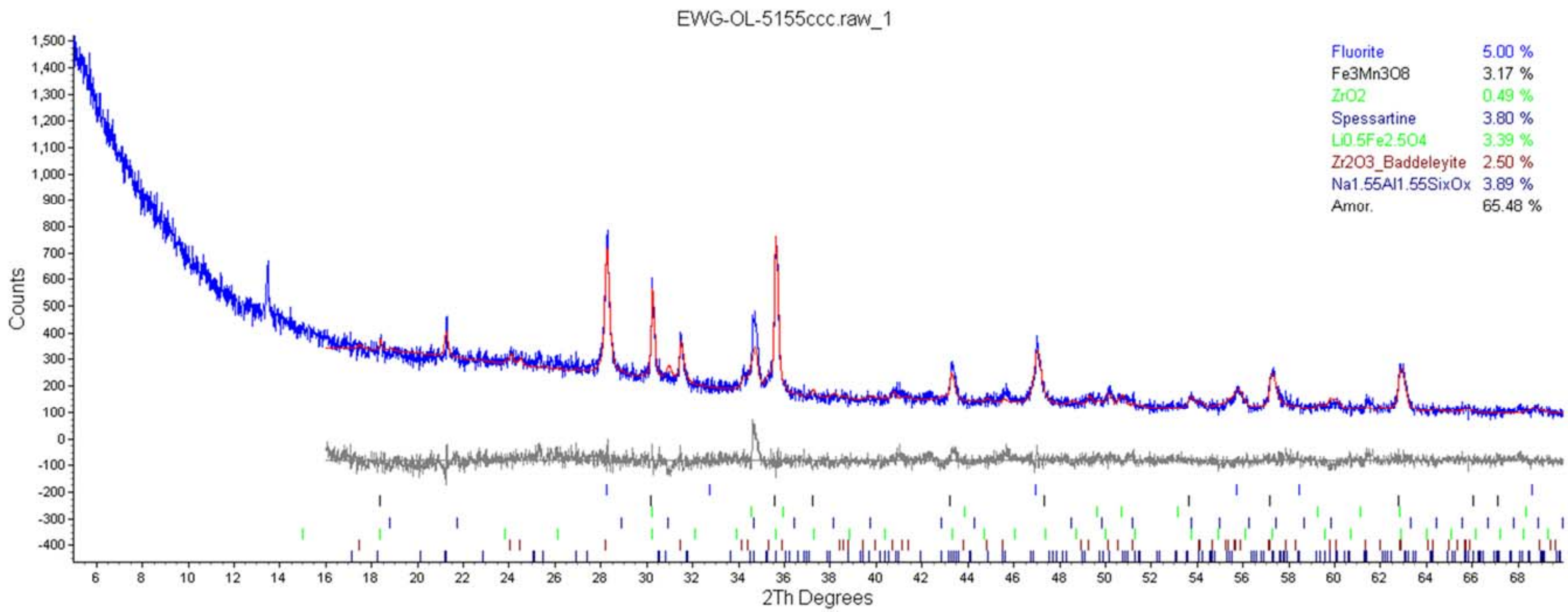

	Phase Name	Wt% of Spiked	Wt% in Spiked sample	Wt% in Original sample
1	Fluorite	5	5	0
2	Fe3Mn3O8	0	3.167	3.333
3	ZrO2	0	0.49	0.515
4	Spessarine	0	3.801	4.002
5	Li0.5Fe2.5O4	0	3.387	3.565
6	ZrO2_Baddeleyite	0	2.499	2.631
7	Na1.55Al1.55SixOx	0	3.892	4.097

Figure D.15. XRD Pattern of Glass EWG-OL-5155 with the Weight % of Crystalline Phases after CCC Treatment

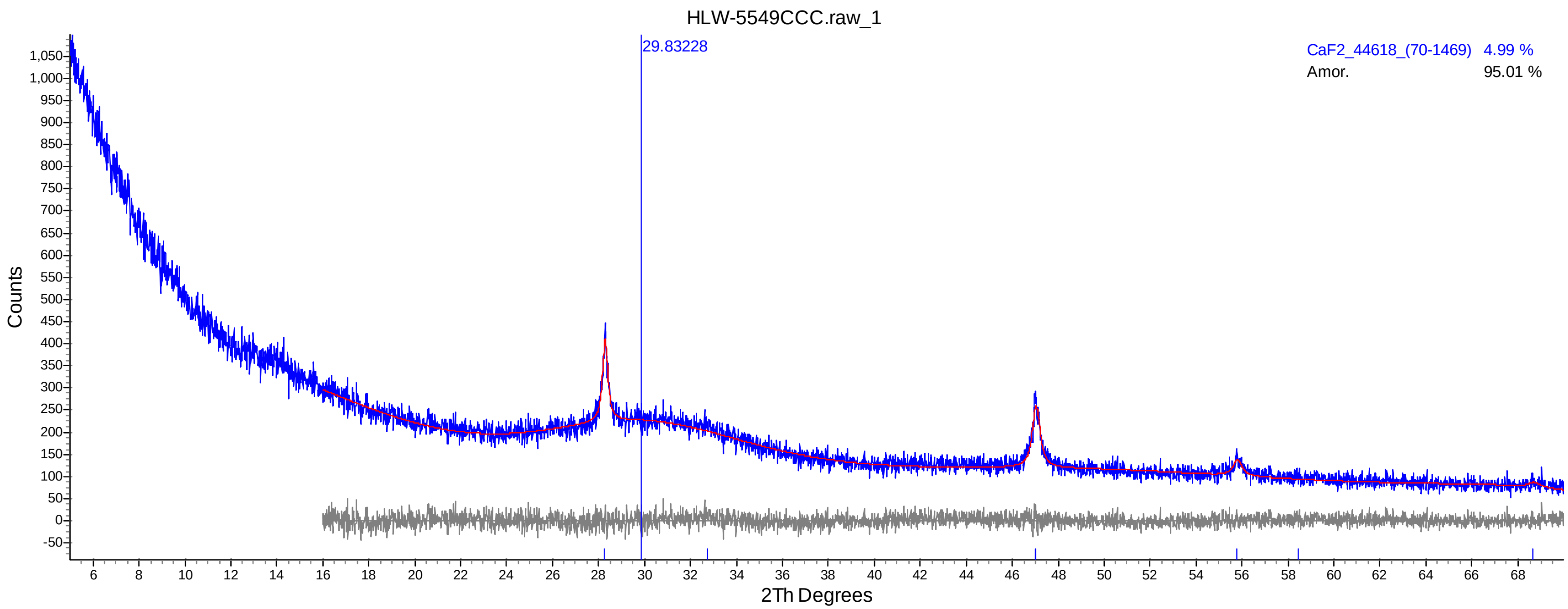

Note: No Crystalline Phase (Except the Added CaF_2) was identified.

Figure D.16. XRD Pattern of Glass EWG-OL-5549 with the Weight % of Crystalline Phases after CCC Treatment

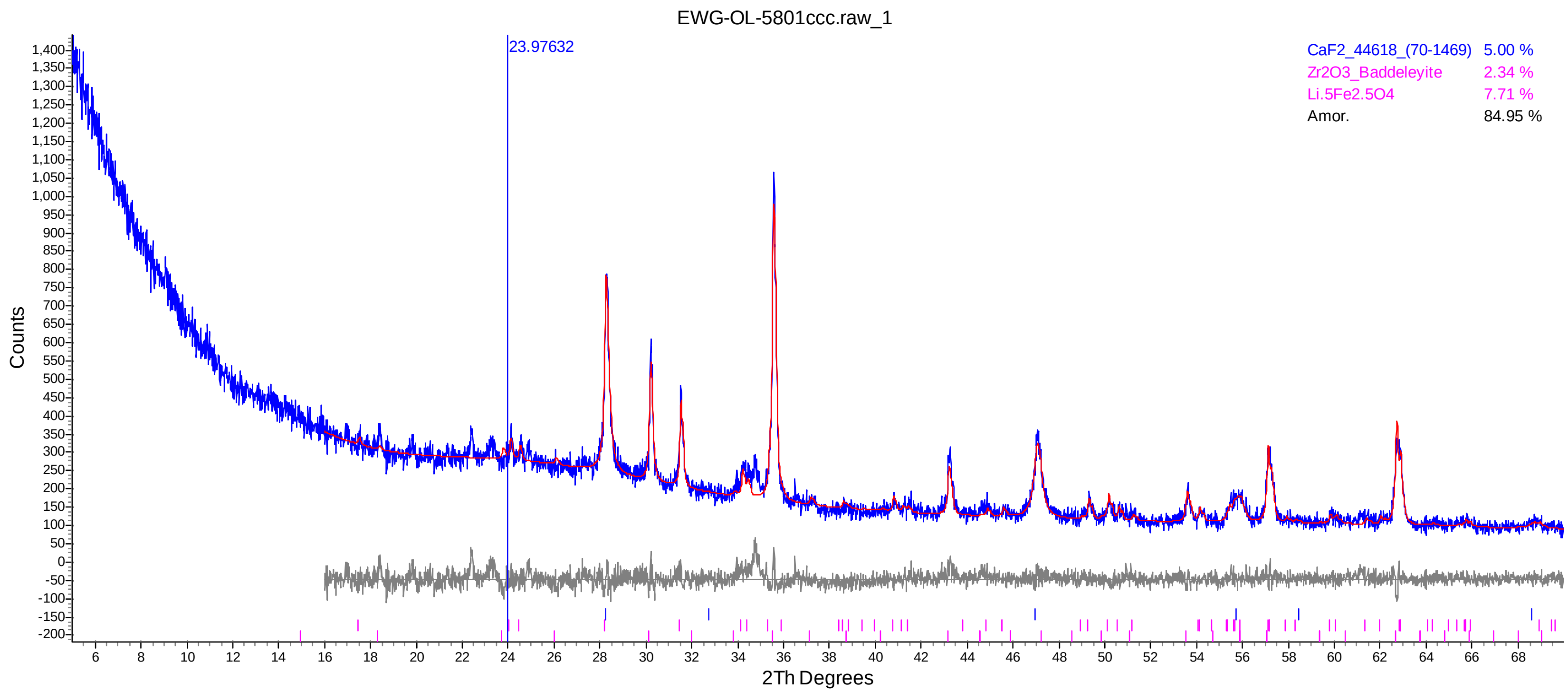

	Phase Name	Wt% of Spiked	Wt% in Spiked sample	Wt% in Original sample
1	CaF2_44618_(70-1469)	5	5	0
2	ZrO2_Baddeleyite	0	2.339	2.462
3	Li0.5Fe2.5O4	0	7.708	8.114

Figure D.17. XRD Pattern of Glass EWG-OL-5801 with the Weight % of Crystalline Phases after CCC Treatment

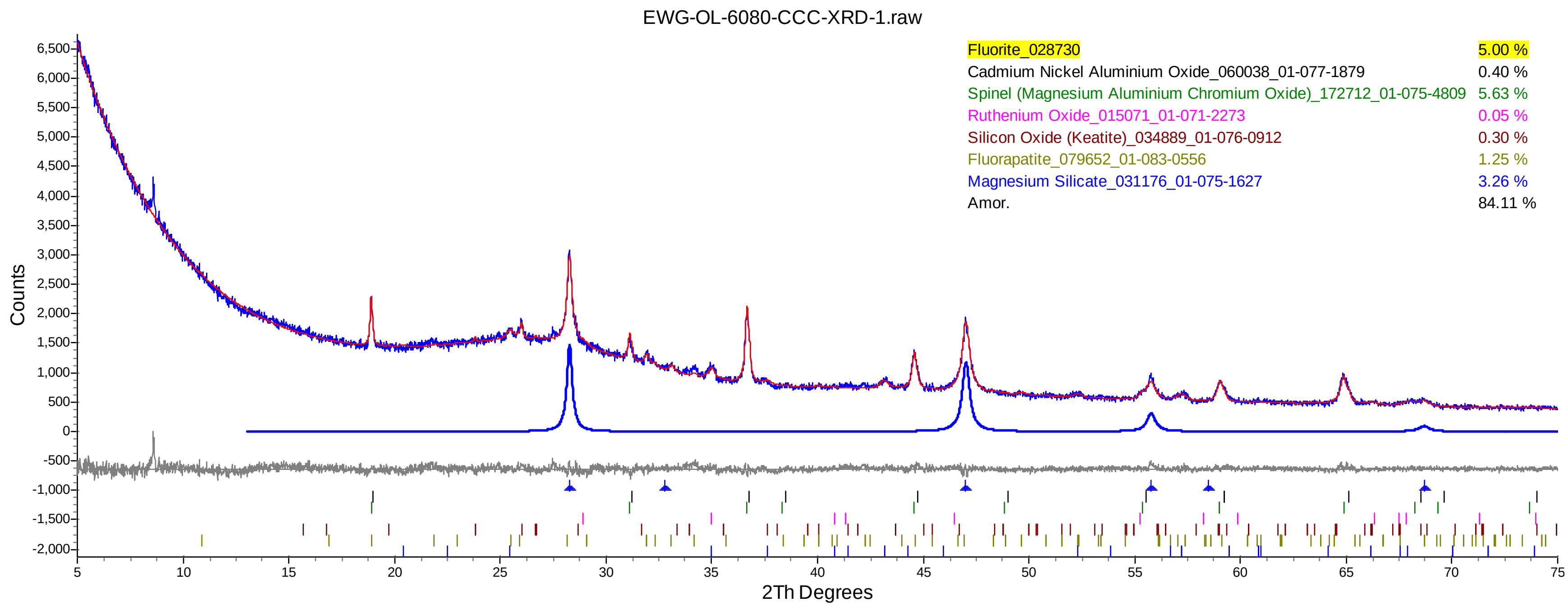

	Phase Name	Wt% of Spiked	Wt% in Spiked sample	Wt% in Original sample
1	Fluorite 028730	5	5	0
2	Cadmium Nickel Aluminum Oxide	0	0.405	0.426
3	Spinel (Magnesium Aluminum Chromium Oxide)	0	5.628	5.925
4	Ruthenium Oxide	0	0.046	0.048
5	Silicon Dioxide	0	0.299	0.314
6	Fluorapatite	0	1.251	1.317
7	Magnesium Silicate	0	3.263	3.435

Figure D.18. XRD Pattern of Glass EWG-OL-6080 with the Weight % of Crystalline Phases after CCC Treatment

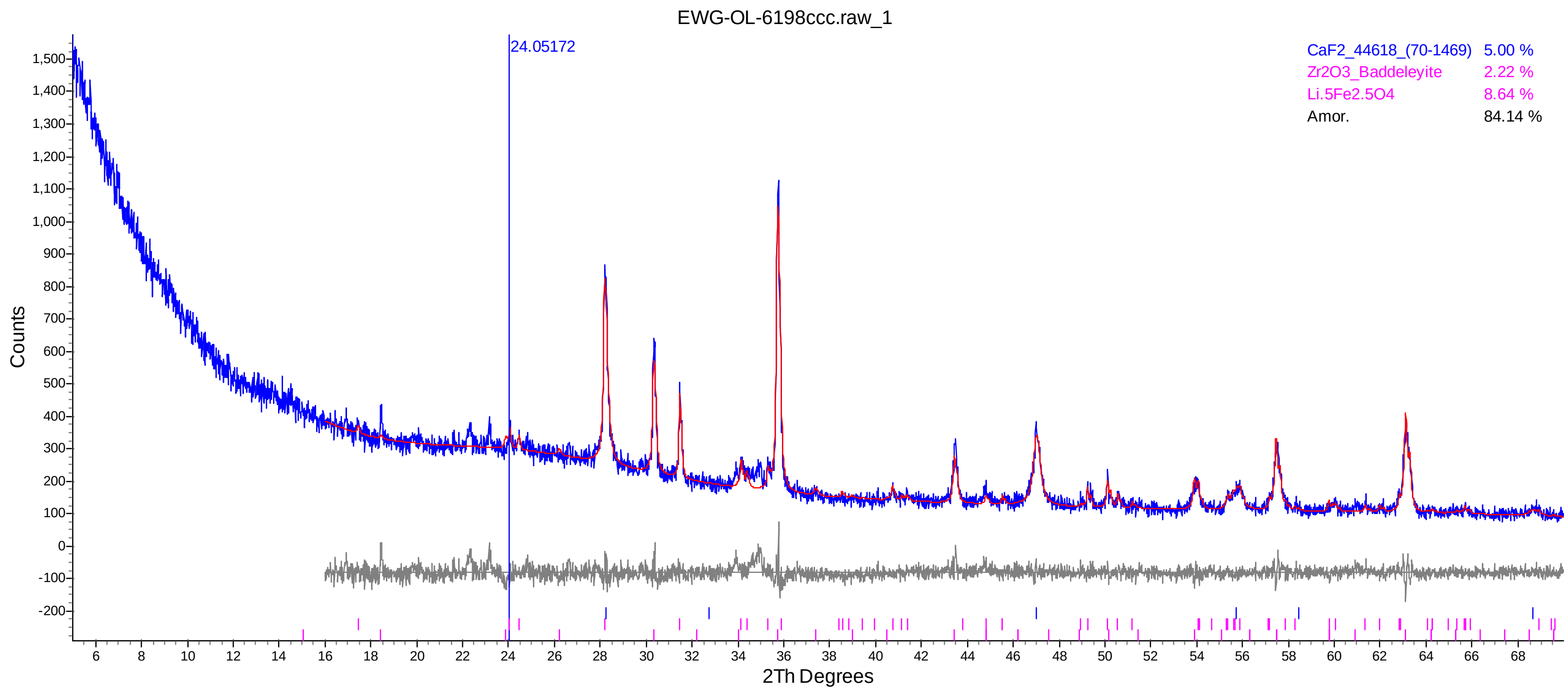

	Phase Name	Wt% of Spiked	Wt% in Spiked sample	Wt% in Original sample
1	CaF2_44618_(70-1469)	5	5	0
2	ZrO2_Baddeleyite	0	2.221	2.337
3	Li0.5Fe2.5O4	0	8.64	9.095

Figure D.19. XRD Pattern of Glass EWG-OL-6198 with the Weight % of Crystalline Phases after CCC Treatment

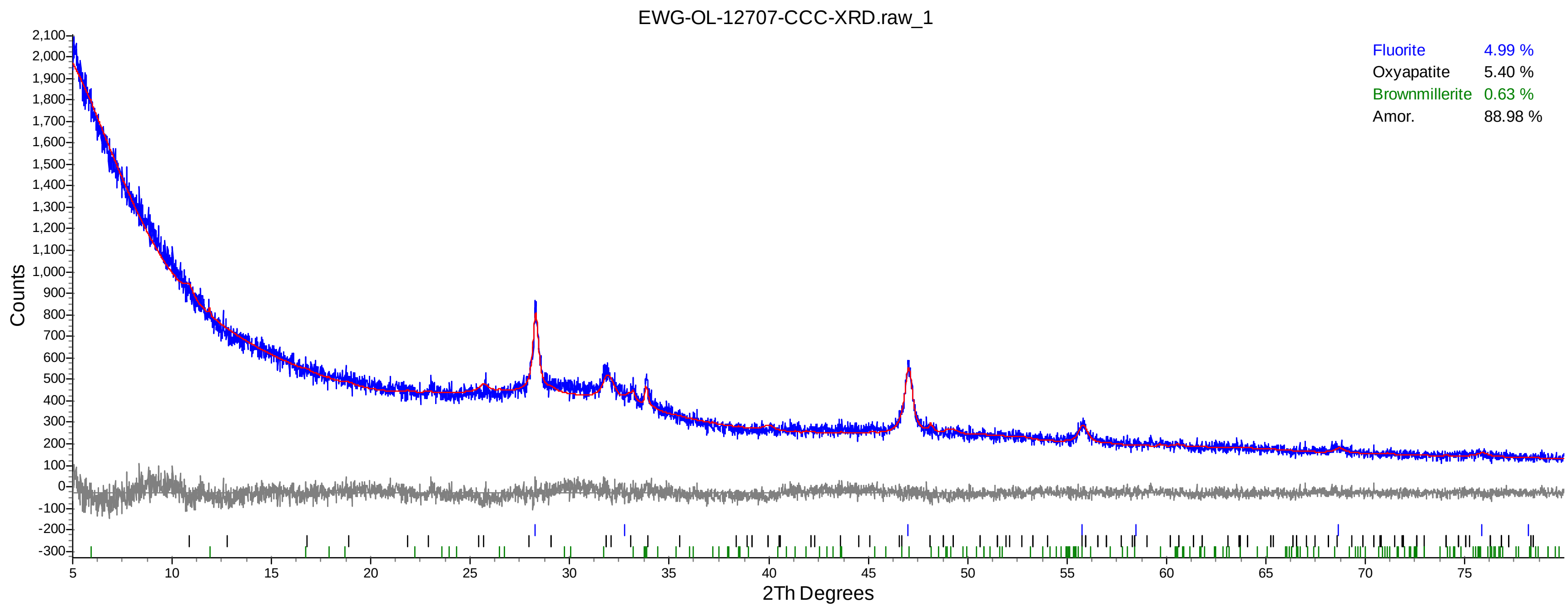

	Phase Name	Wt% of Spiked	Wt% in Spiked sample	Wt% in Original sample
1	Fluorite	4.992	4.992	0
2	Oxyapatite	0	5.401	5.685
3	Brownmillerite	0	0.626	0.659

Figure D.20. XRD Pattern of Glass EWG-OL-12707 with the Weight % of Crystalline Phases after CCC Treatment

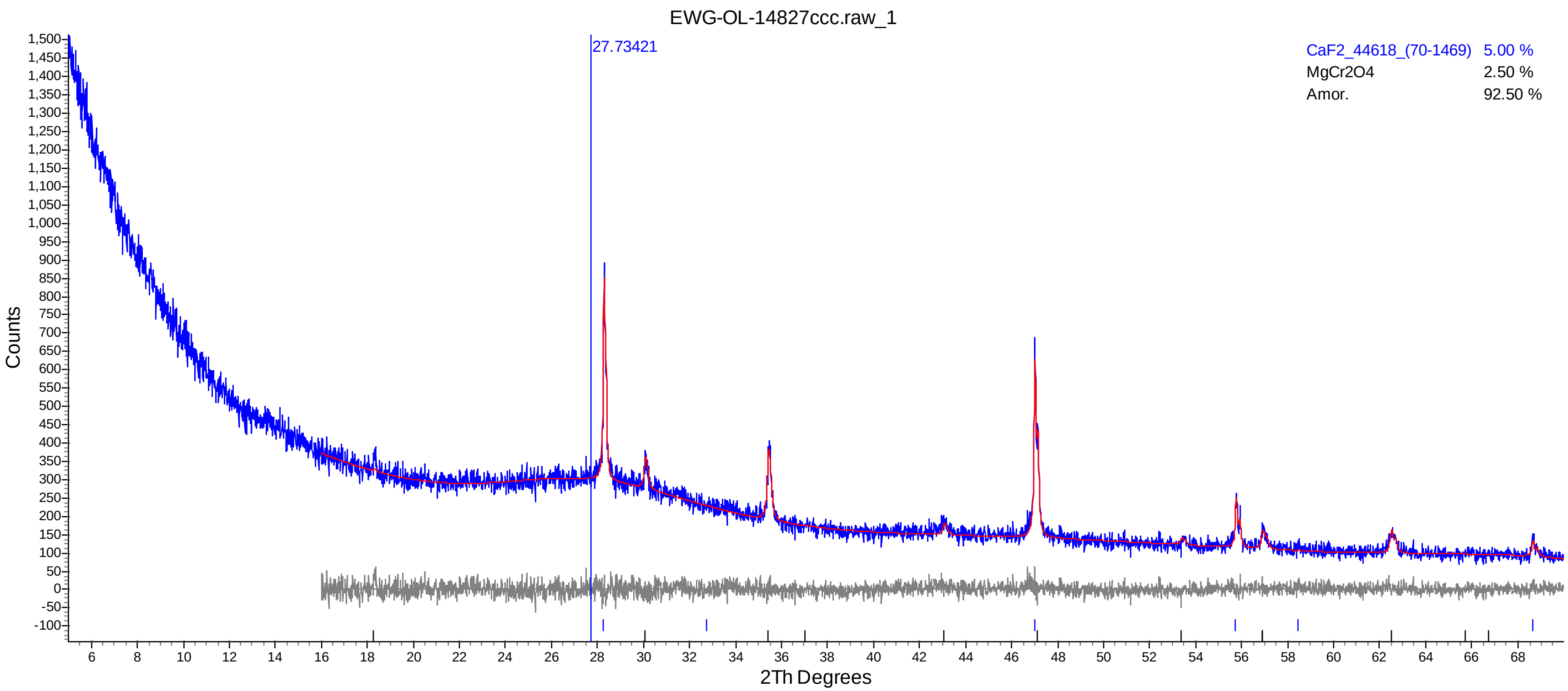

	Phase Name	Wt% of Spiked	Wt% in Spiked sample	Wt% in Original sample
1	CaF2_44618_(70-1469)	5	5	0
2	MgCr2O4	0	2.499	2.631

Figure D.21. XRD Pattern of Glass EWG-OL-14827 with the Weight % of Crystalline Phases after CCC Treatment

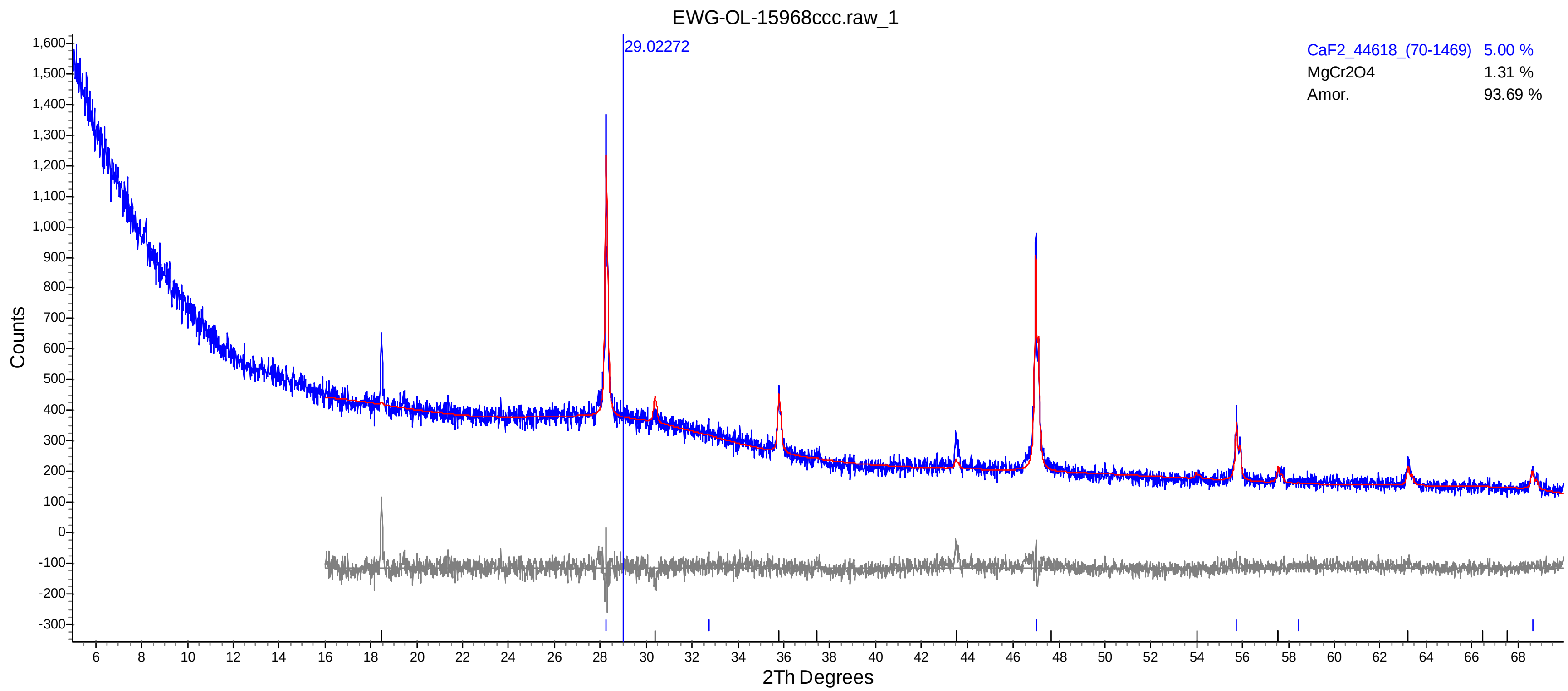

	Phase Name	Wt% of Spiked	Wt% in Spiked sample	Wt% in Original sample
1	CaF2_44618_(70-1469)	5	5	0
2	MgCr2O4	0	1.306	1.375

Figure D.22. XRD Pattern of Glass EWG-OL-15968 with the Weight % of Crystalline Phases after CCC Treatment

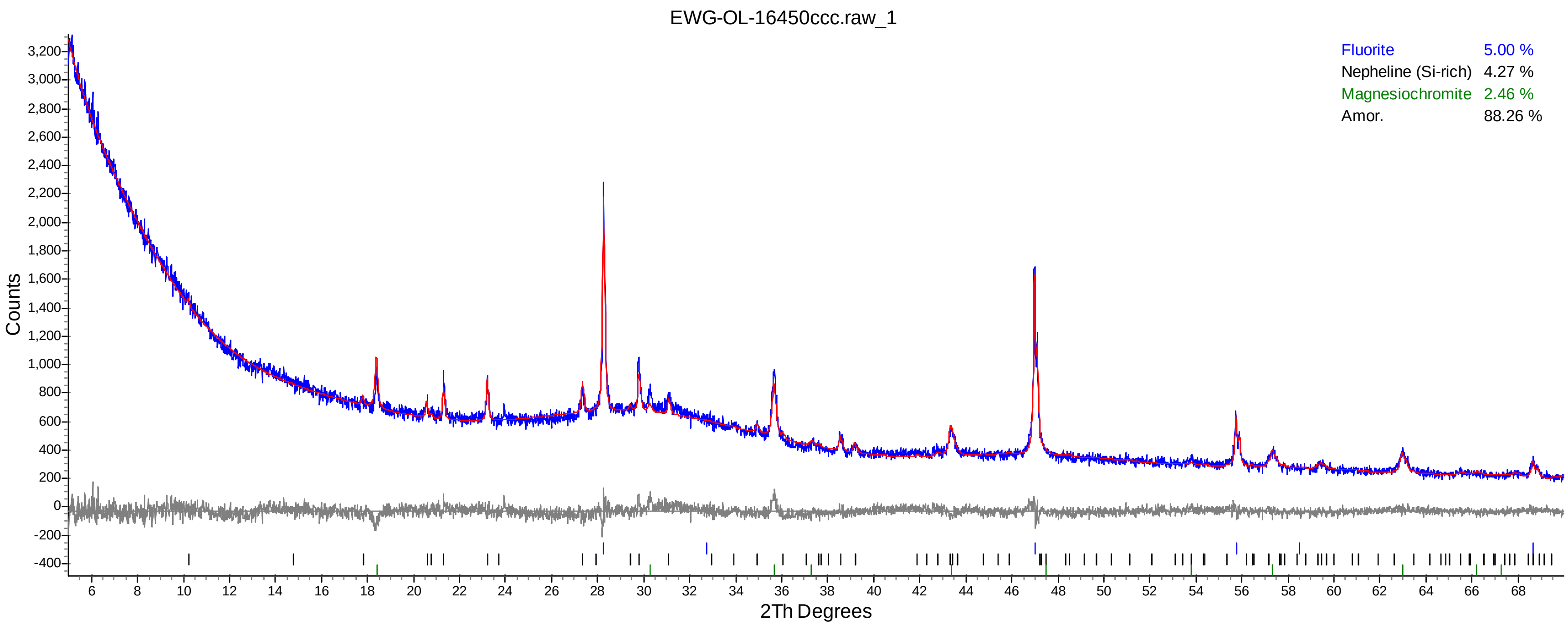

	Phase Name	Wt% of Spiked	Wt% in Spiked sample	Wt% in Original sample
1	Fluorite	5	5	0
2	Nepheline (Si-rich)	0	4.273	4.498
3	Magnesiochromite	0	2.463	2.592

Figure D.23. XRD Pattern of Glass EWG-OL-16450 with the Weight % of Crystalline Phases after CCC Treatment

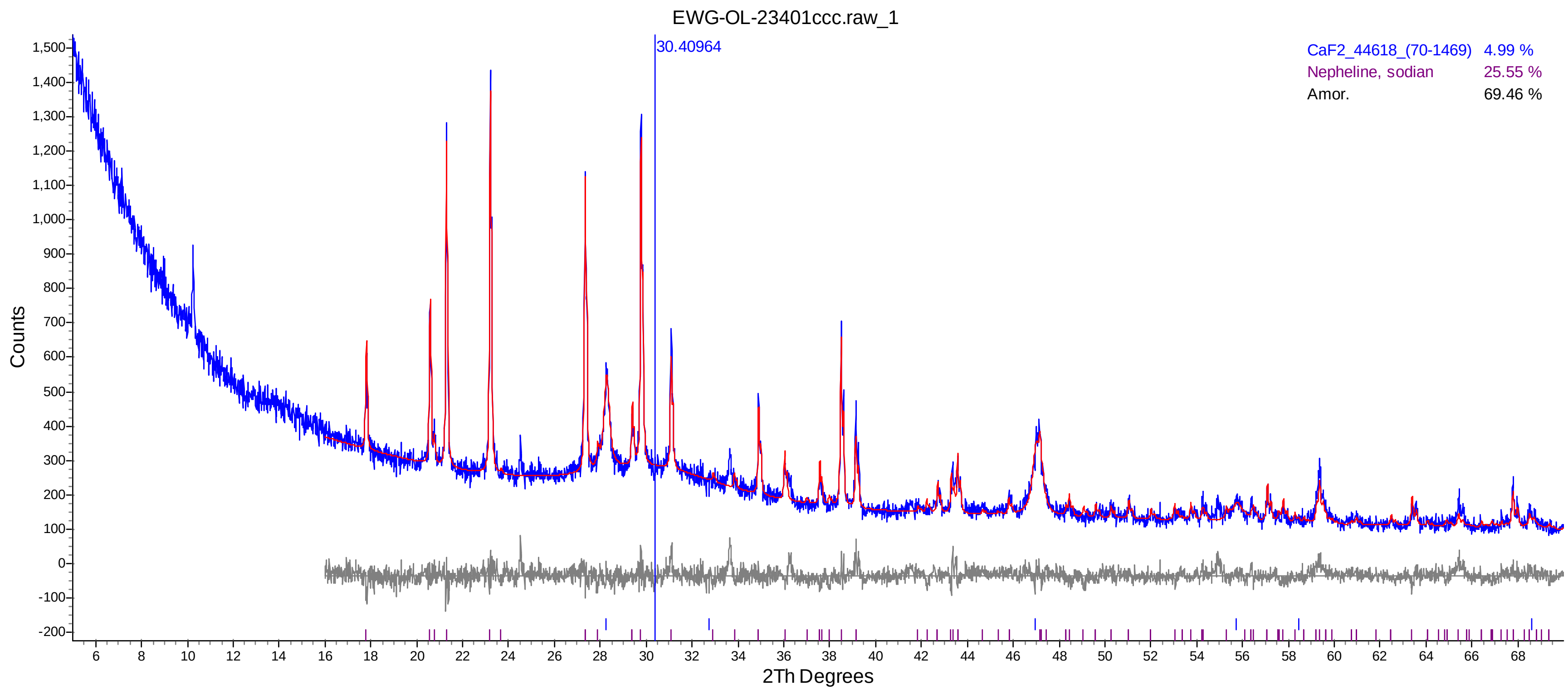

	Phase Name	Wt% of Spiked	Wt% in Spiked sample	Wt% in Original sample
1	CaF2_44618_(70-1469)	4.986	4.986	0
2	Nepheline, sodian	0	25.552	26.893

Figure D.24. XRD Pattern of Glass EWG-OL-23401 with the Weight % of Crystalline Phases after CCC Treatment

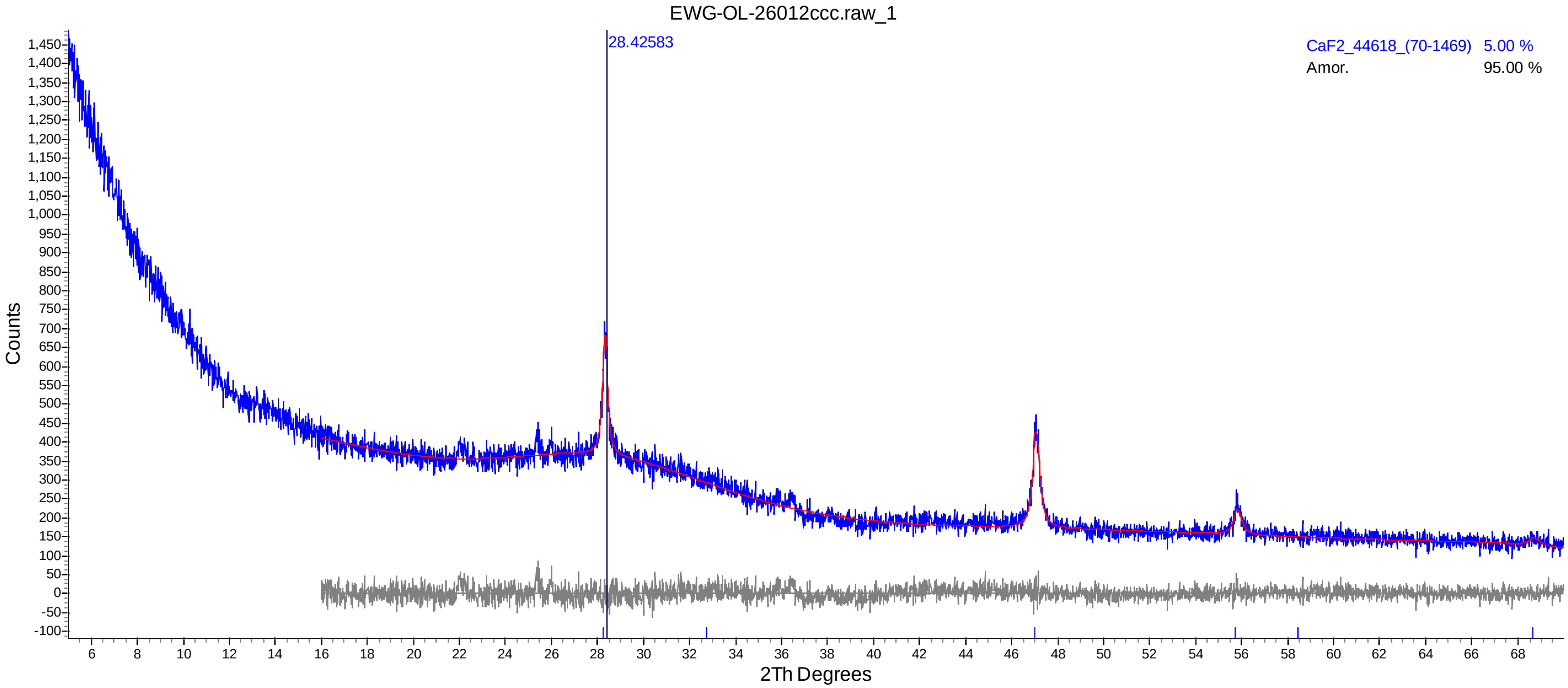

Note: No Crystalline Phase (Except the Added CaF_2) was identified.

Figure D.25. XRD Pattern of Glass EWG-OL-26012 with the Weight % of Crystalline Phases after CCC Treatment

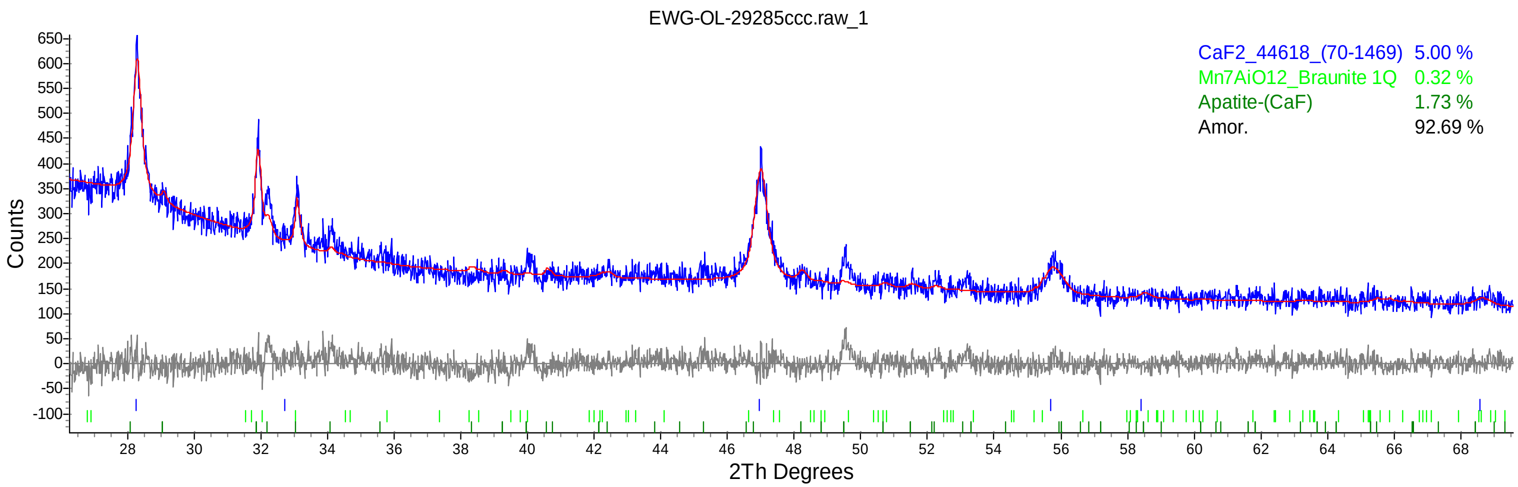

	Phase Name	Wt% of Spiked	Wt% in Spiked sample	Wt% in Original sample
1	CaF2_44618_(70-1469)	4.998	4.998	0
2	Apatite-(CaF)	0	1.726	1.816
3	Mn7AlO12 Braunite 1Q	0	0.315	0.332

Figure D.26. XRD Pattern of Glass EWG-OL-29285 with the Weight % of Crystalline Phases after CCC Treatment

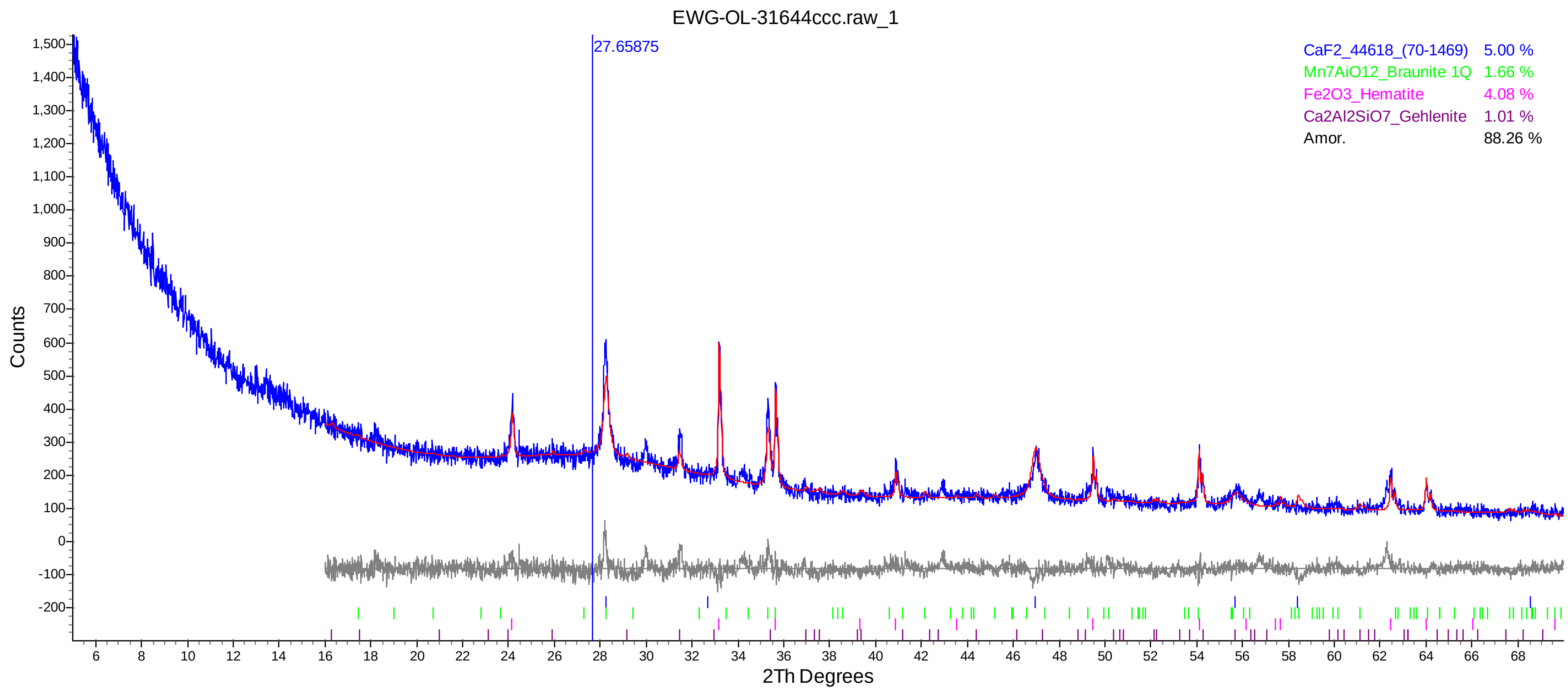

	Phase Name	Wt% of Spiked	Wt% in Spiked sample	Wt% in Original sample
1	CaF2_44618_(70-1469)	5	5	0
2	Mn7AlO12 Braunite 1Q	0	1.657	1.744
3	Fe2O3 Hematite	0	4.078	4.292
4	Ca2Al2SiO7 Gehlenite	0	1.009	1.062

Figure D.27. XRD Pattern of Glass EWG-OL-31644 with the Weight % of Crystalline Phases after CCC Treatment

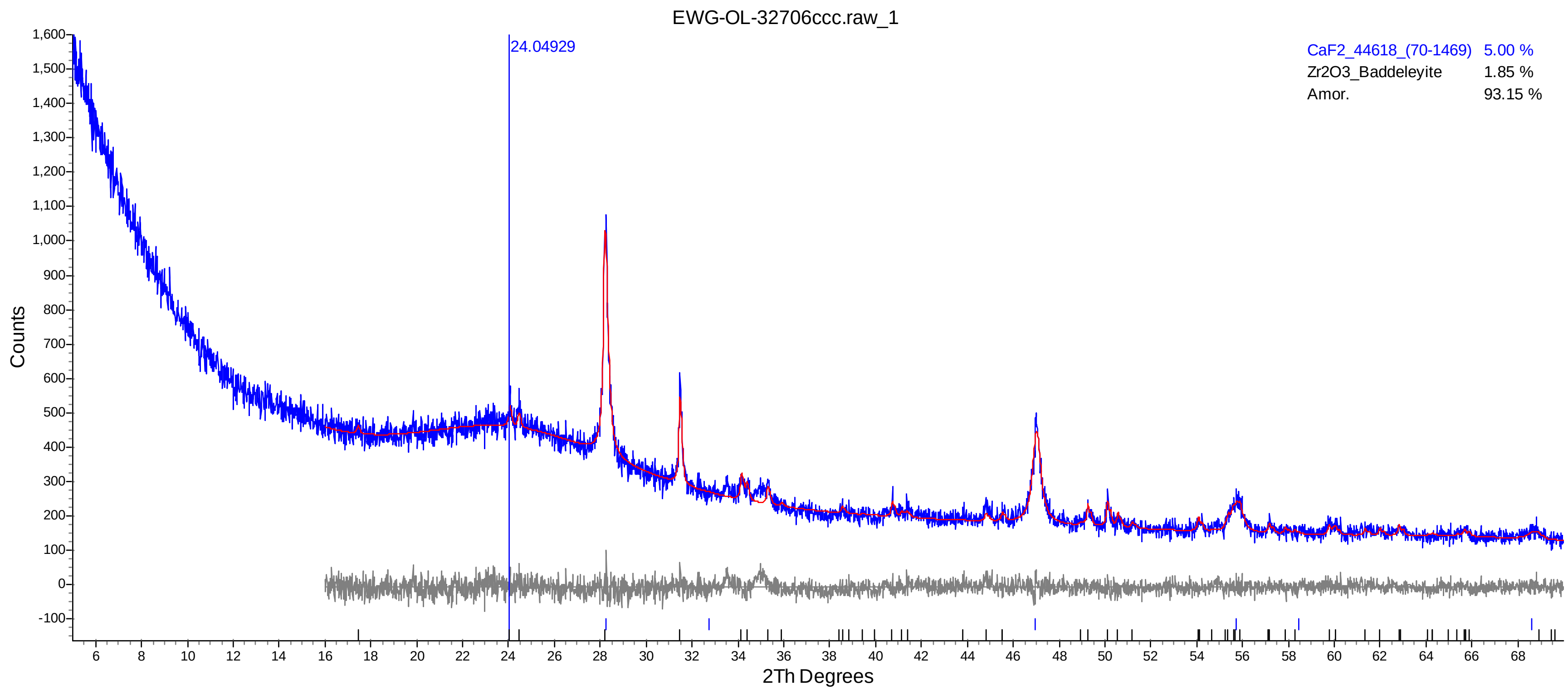

	Phase Name	Wt% of Spiked	Wt% in Spiked sample	Wt% in Original sample
1	CaF2_44618_(70-1469)	5	5	0
2	ZrO2 Baddeleyite	0	1.847	1.945

Figure D.28. XRD Pattern of Glass EWG-OL-32706 with the Weight % of Crystalline Phases after CCC Treatment

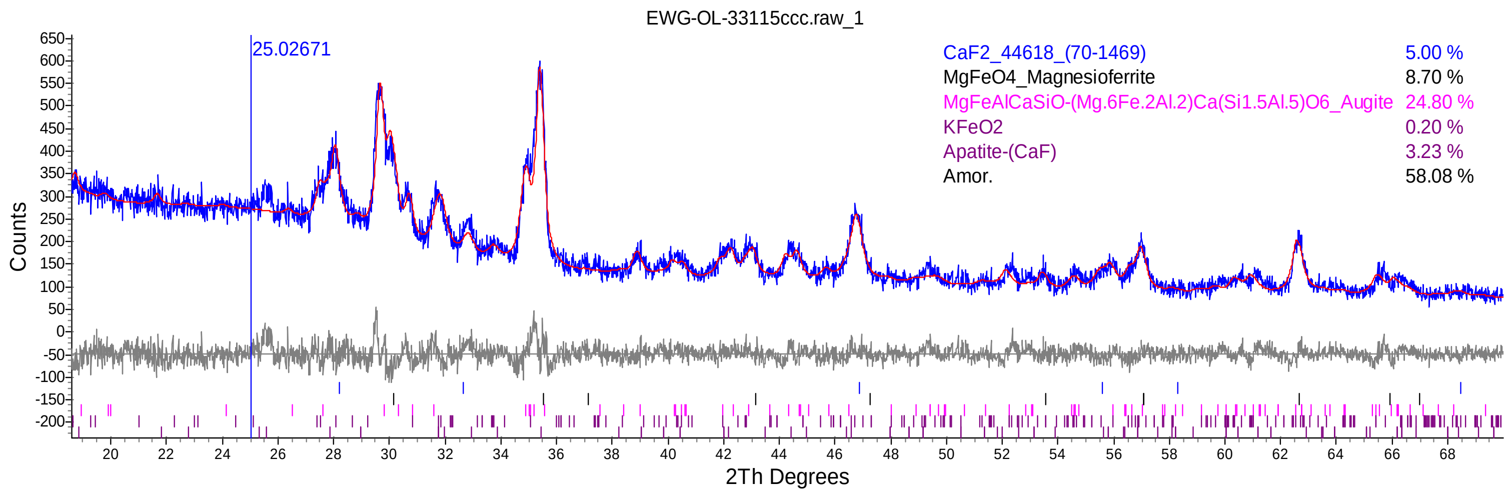

	Phase Name	Wt% of Spiked	Wt% in Spiked sample	Wt% in Original sample
1	CaF2_44618_(70-1469)	5.004	5.004	0
2	MgFeO4_Magnesioferrite	0	8.699	9.157
3	MgFeAlCaSiO-(Mg.6Fe.2Al.2)Ca(Si1.5Al.5)O6 Augite	0	24.796	26.101
4	Apatite-(CaF)	0	3.227	3.397
5	KFeO2	0	0.199	0.210

Figure D.29. XRD Pattern of Glass EWG-OL-33115 with the Weight % of Crystalline Phases after CCC Treatment

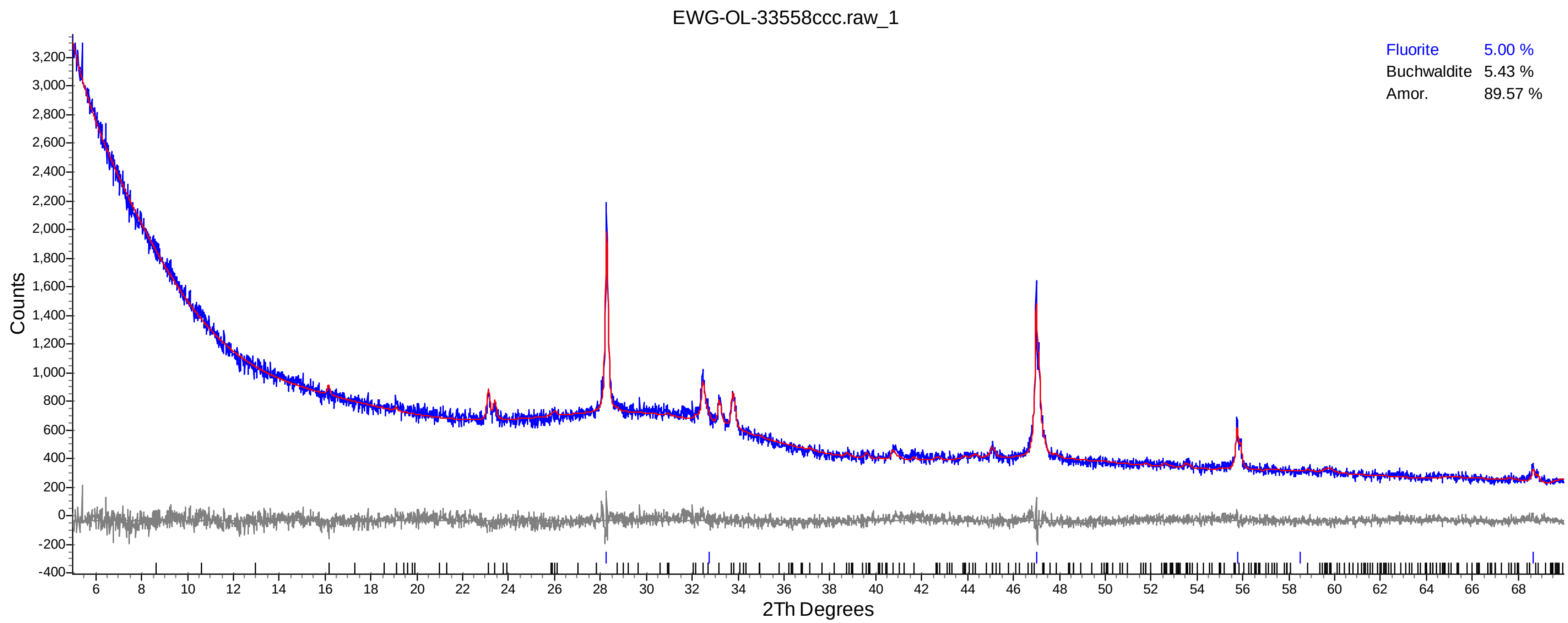

	Phase Name	Wt% of Spiked	Wt% in Spiked sample	Wt% in Original sample
1	Fluorite	5	5	0
2	Buchwaldite	0	5.434	5.72

Figure D.30. XRD Pattern of Glass EWG-OL-33558 with the Weight % of Crystalline Phases after CCC Treatment

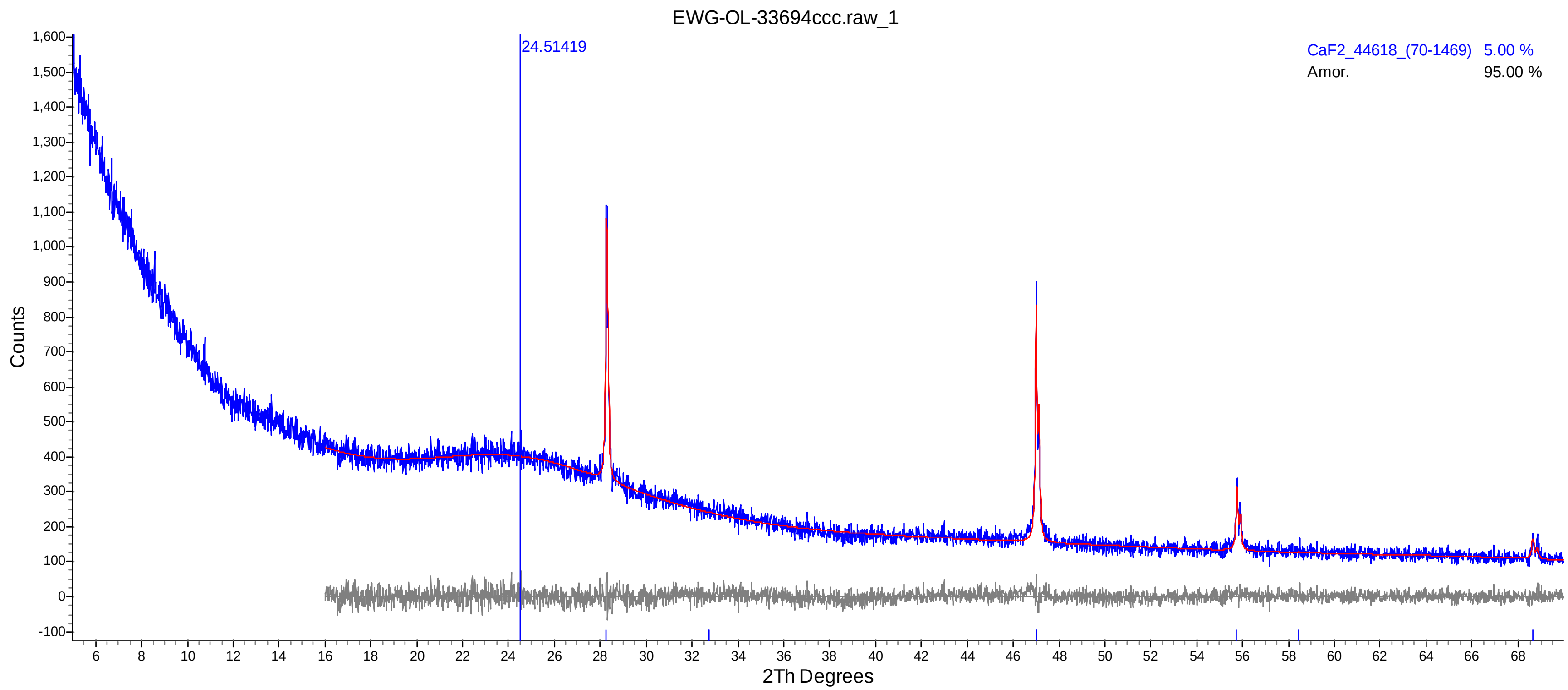

Note: No Crystalline Phase (Except the Added CaF_2) was identified.

Figure D.31. XRD Pattern of Glass EWG-OL-33694 with the Weight % of Crystalline Phases after CCC Treatment

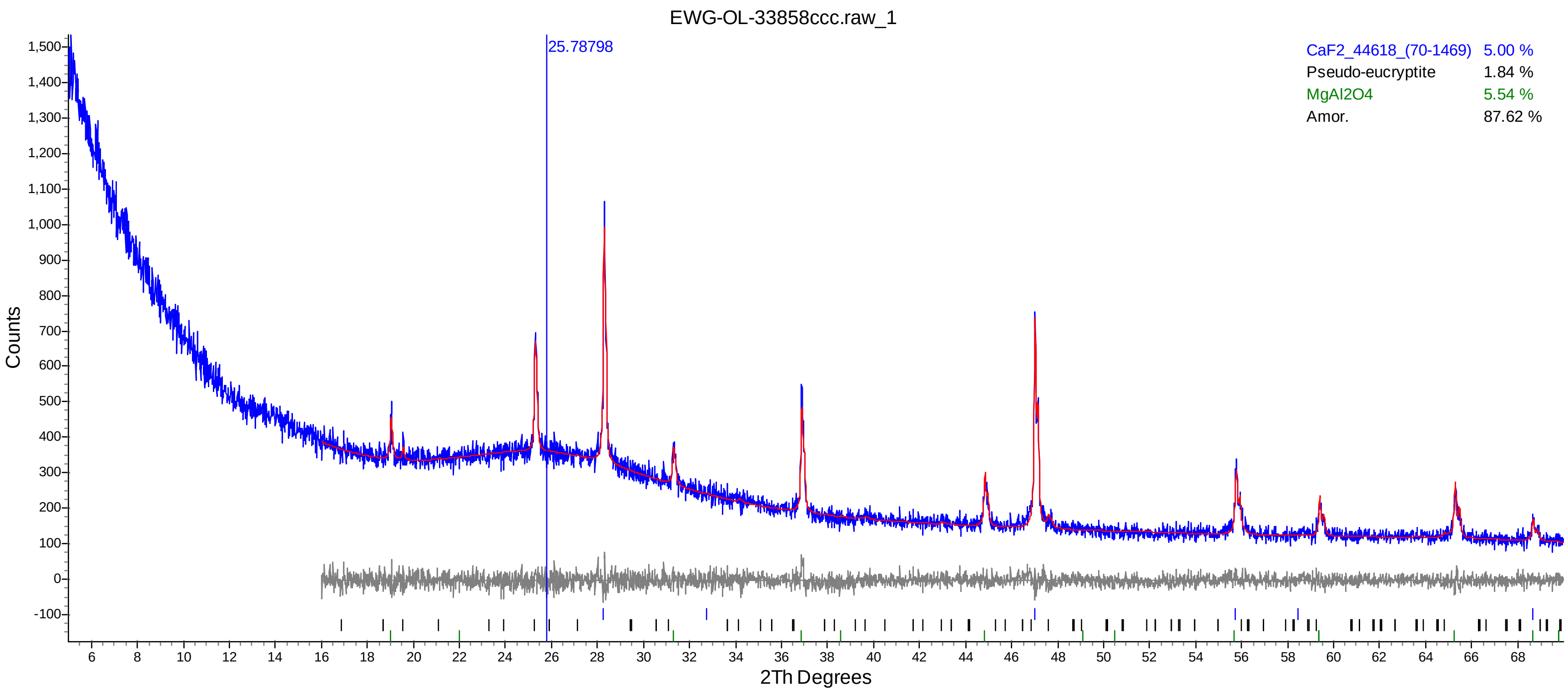

	Phase Name	Wt% of Spiked	Wt% in Spiked sample	Wt% in Original sample
1	CaF2_44618_(70-1469)	5	5	0
2	Psuedo-eucryptite	0	1.841	1.938
3	MgAl2O4	0	5.536	5.827

Figure D.32. XRD Pattern of Glass EWG-OL-33858 with the Weight % of Crystalline Phases after CCC Treatment

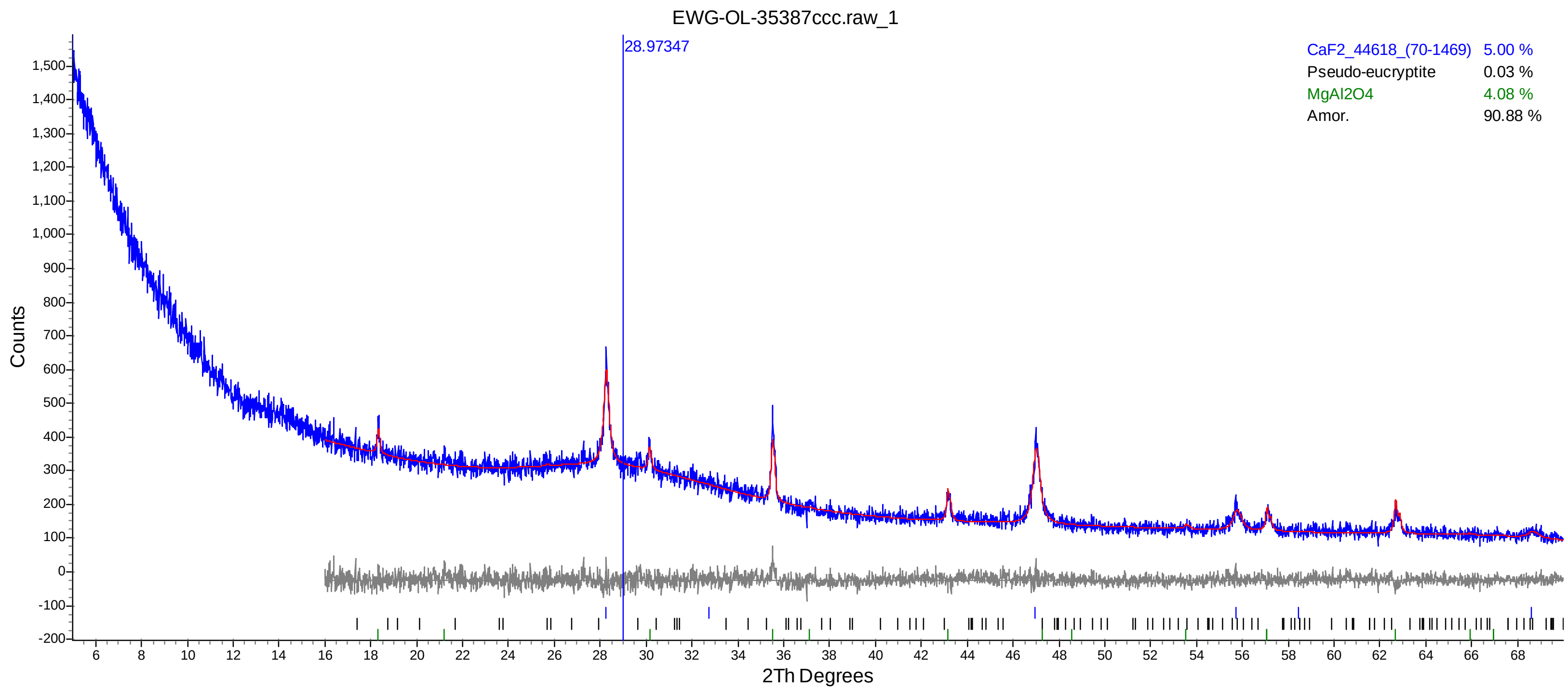

	Phase Name	Wt% of Spiked	Wt% in Spiked sample	Wt% in Original sample
1	CaF2_44618_(70-1469)	5	5	0
2	Psuedo-eucryptite	0	0.035	0.037
3	MgAl2O4	0	4.082	4.297

Figure D.33. XRD Pattern of Glass EWG-OL-35387 with the Weight % of Crystalline Phases after CCC Treatment

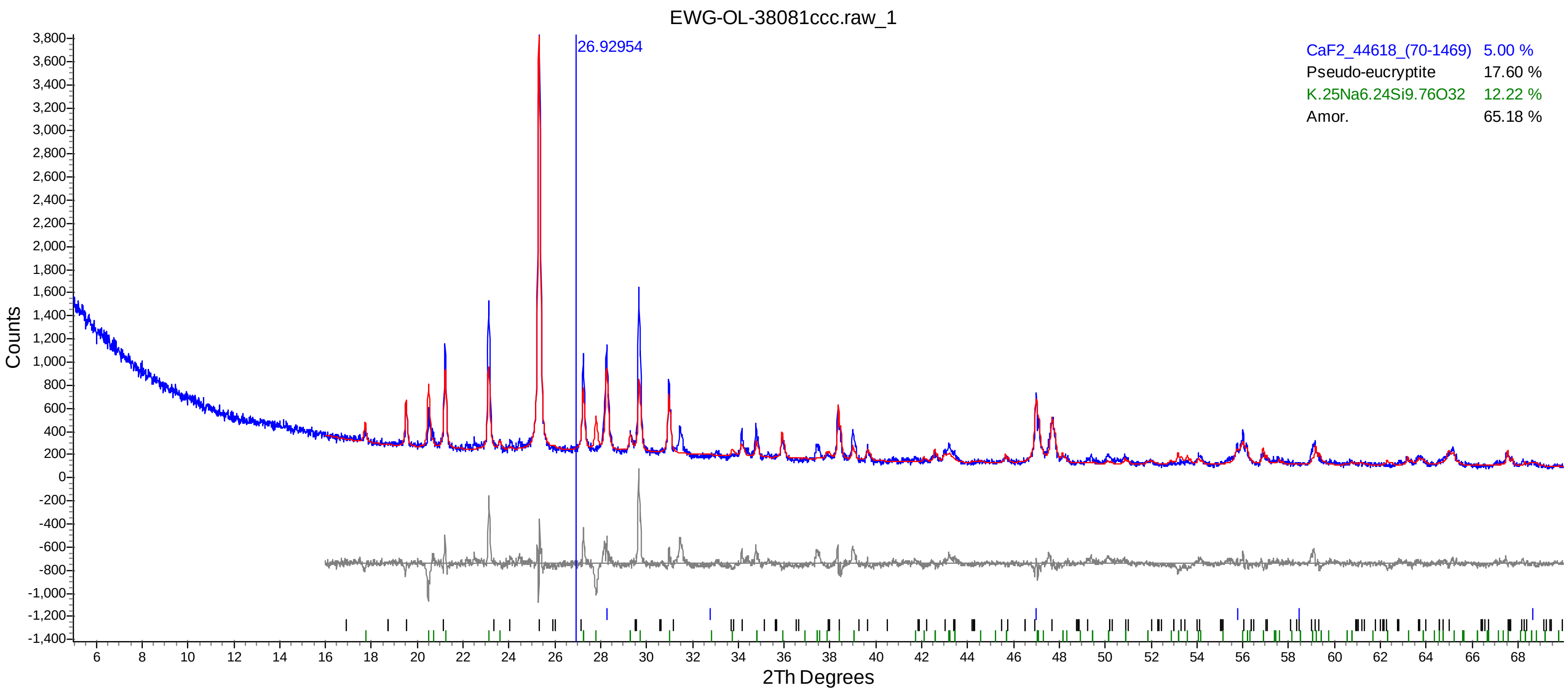

	Phase Name	Wt% of Spiked	Wt% in Spiked sample	Wt% in Original sample
1	CaF2_44618_(70-1469)	5	5	0
2	Psuedo-eucryptite	0	17.6	18.526
3	K.25Na6.24Si9.76O32	0	12.225	12.868

Figure D.34. XRD Pattern of Glass EWG-OL-38081 with the Weight % of Crystalline Phases after CCC Treatment

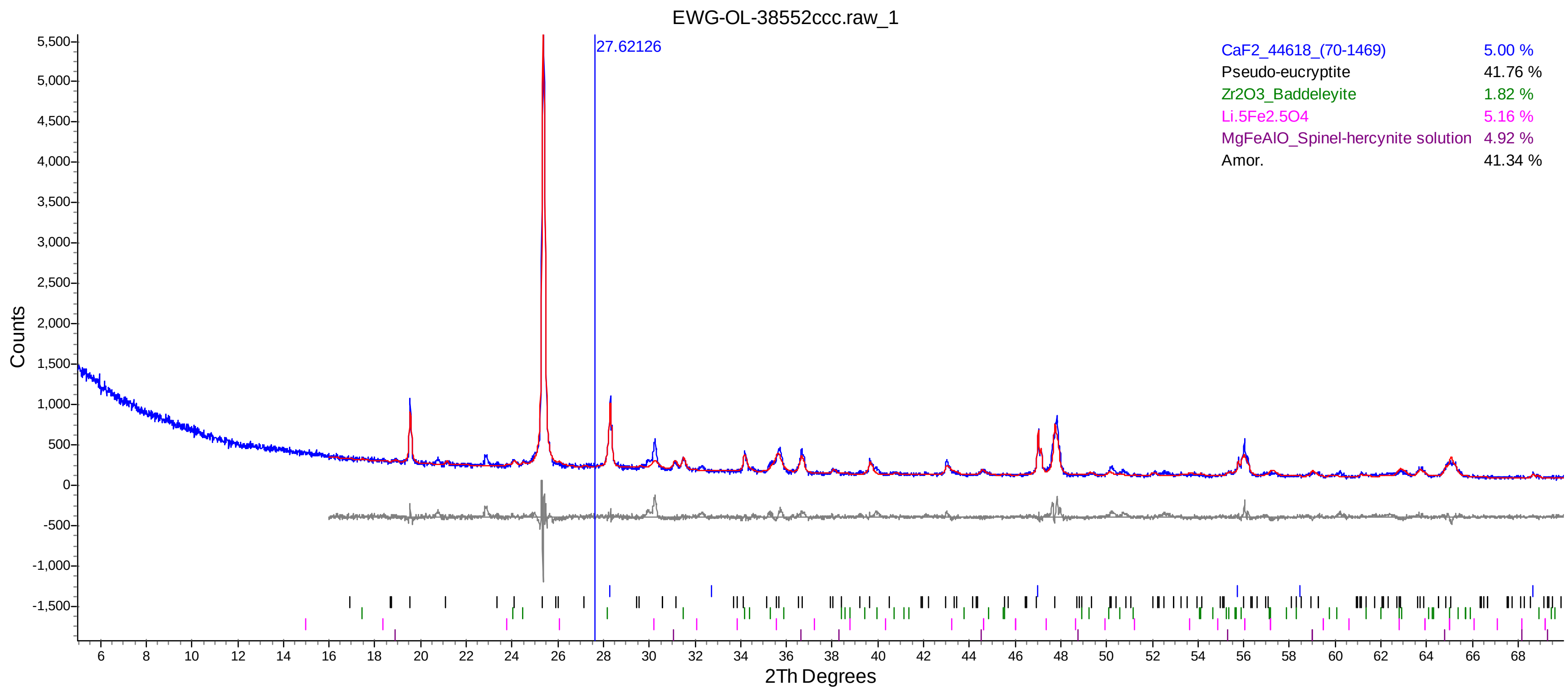

	Phase Name	Wt% of Spiked	Wt% in Spiked sample	Wt% in Original sample
1	CaF2_44618_(70-1469)	5	5	0
2	Psuedo-eucryptite	0	41.758	43.956
3	ZrO2_Baddeleyite	0	1.817	1.913
4	Li.5Fe2.5O4	0	5.161	5.432
5	MgFeAlO Spinel-hercynite solution	0	4.924	5.183

Figure D.35. XRD Pattern of Glass EWG-OL-38552 with the Weight % of Crystalline Phases after CCC Treatment

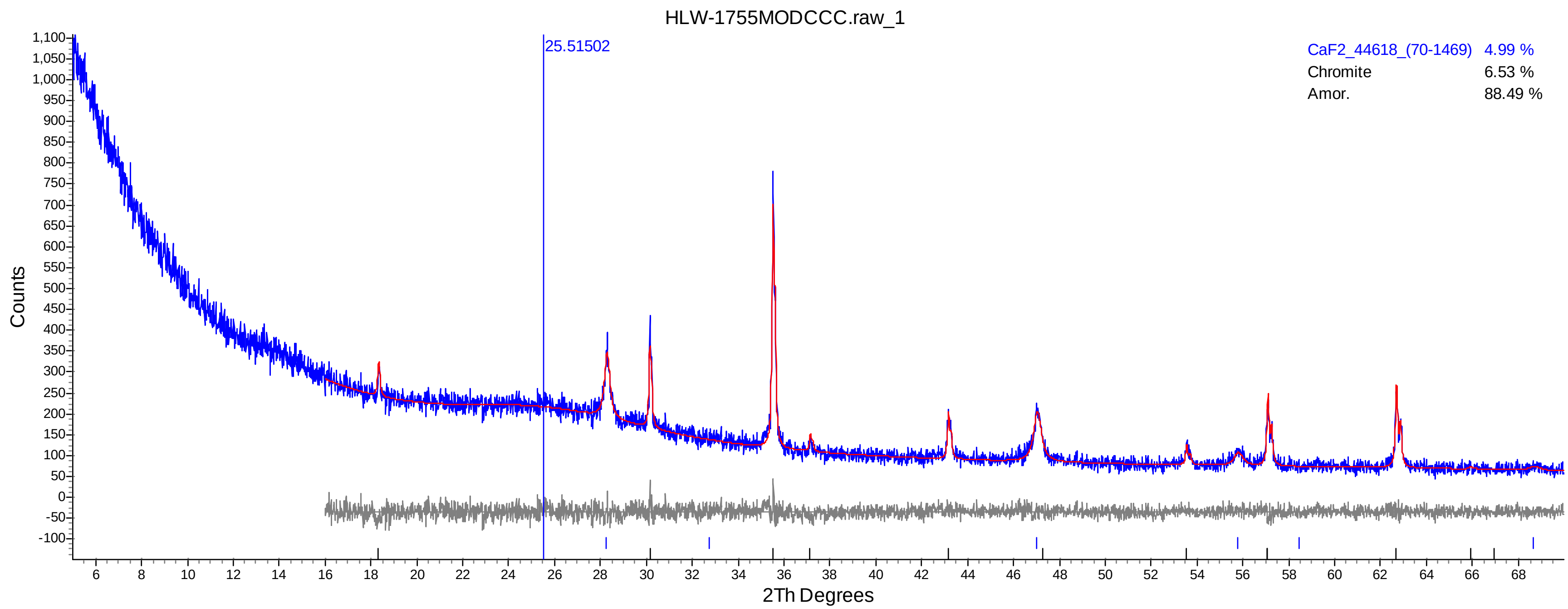

	Phase Name	Wt% of Spiked	Wt% in Spiked sample	Wt% in Original sample
1	CaF2_44618_(70-1469)	4.986	4.986	0
2	Chromite	0	6.529	6.871

Figure D.36. XRD Pattern of Glass EWG-OL-1755 Mod 8% Fe 10% B with the Weight % of Crystalline Phases after CCC Treatment

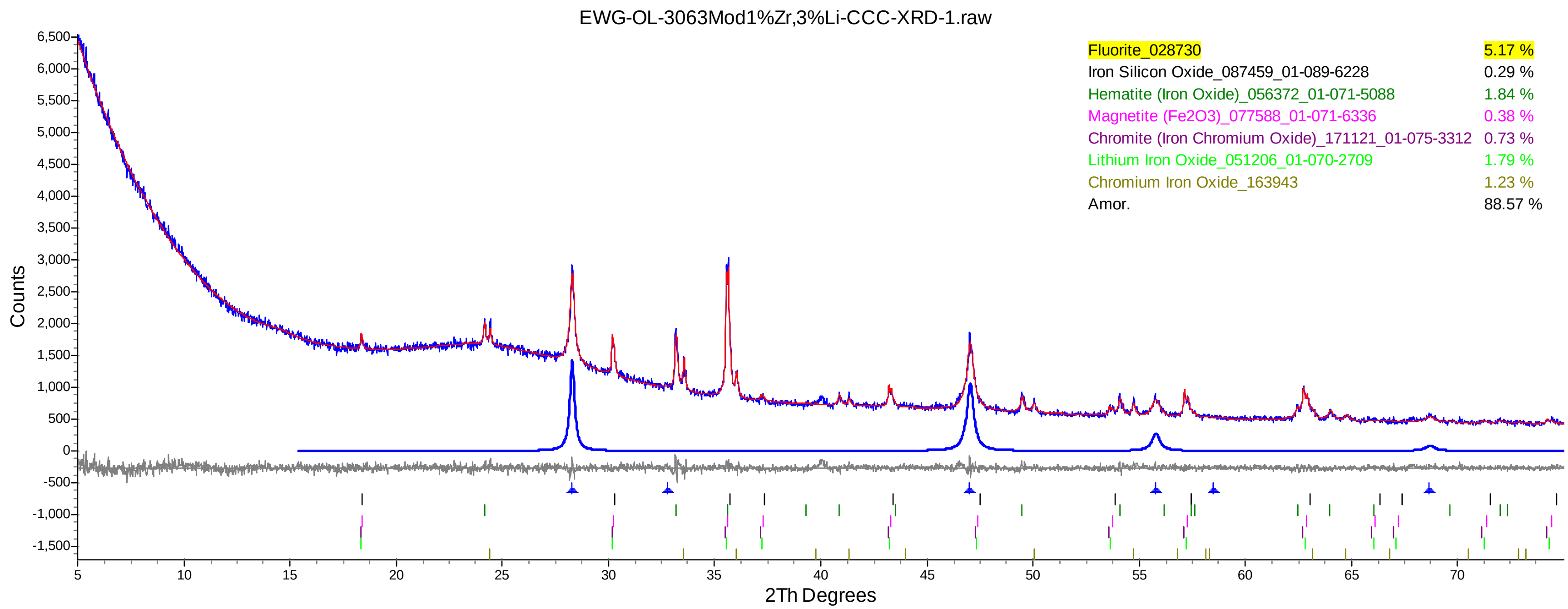

	Phase Name	Wt% of Spiked	Wt% in Spiked sample	Wt% in Original sample
1	Fluorite_028730	5.171	5.171	0
2	Iron Silicon Oxide	0	0.289	0.305
3	Hematite (Iron Oxide)	0	1.843	1.943
4	Magnetite (Fe2O3)	0	0.38	0.401
5	Chromite (Iron Chromium Oxide)	0	0.725	0.765
6	Lithium Iron Oxide	0	1.792	1.89
7	Chromium Iron Oxide	0	1.23	1.298

Figure D.37. XRD Pattern of Glass EWG-OL-3063 Mod 1% Zr 3% Li with the Weight % of Crystalline Phases after CCC Treatment

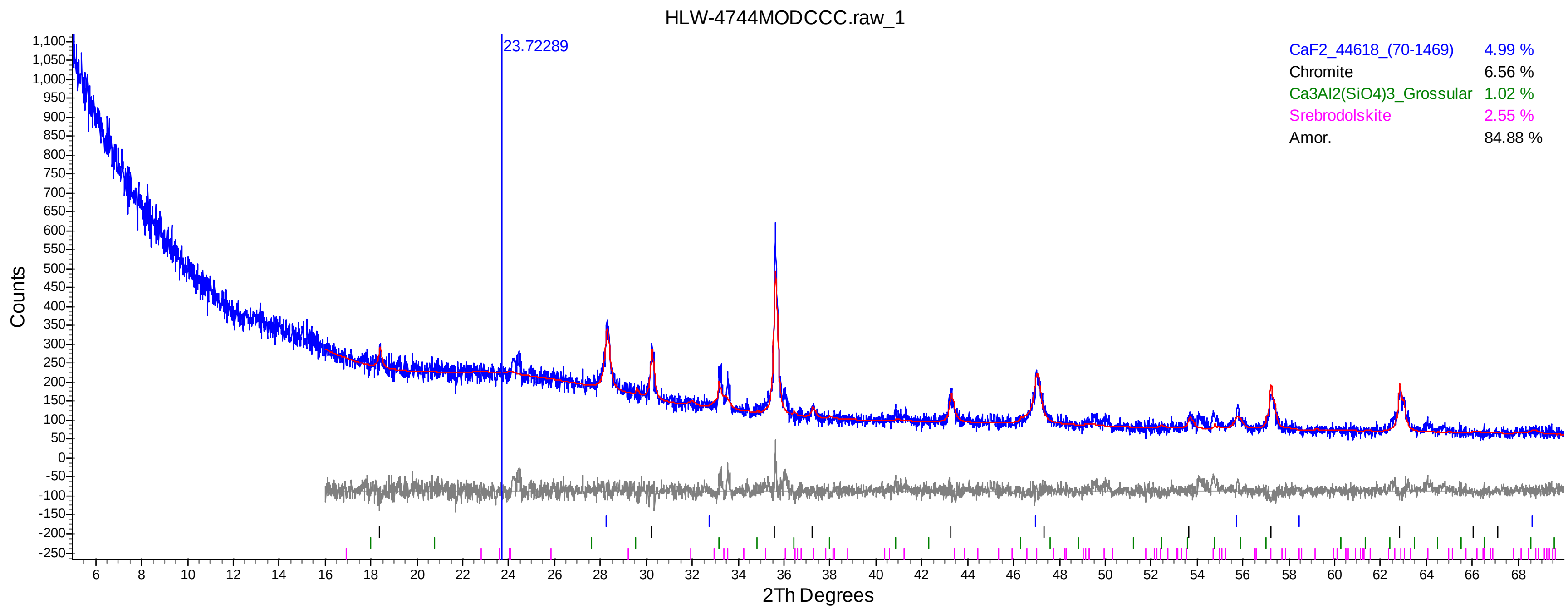

	Phase Name	Wt% of Spiked	Wt% in Spiked sample	Wt% in Original sample
1	CaF2_44618_(70-1469)	4.986	4.986	0
2	Chromite	0	6.564	6.908
3	Ca3Al2(SiO4)3_Grossular	0	1.017	1.07
4	Srebrodolskite	0	2.553	2.687

Figure D.38. XRD Pattern of Glass EWG-OL-4744 Mod 7.5% Fe 1% Zr with the Weight % of Crystalline Phases after CCC Treatment

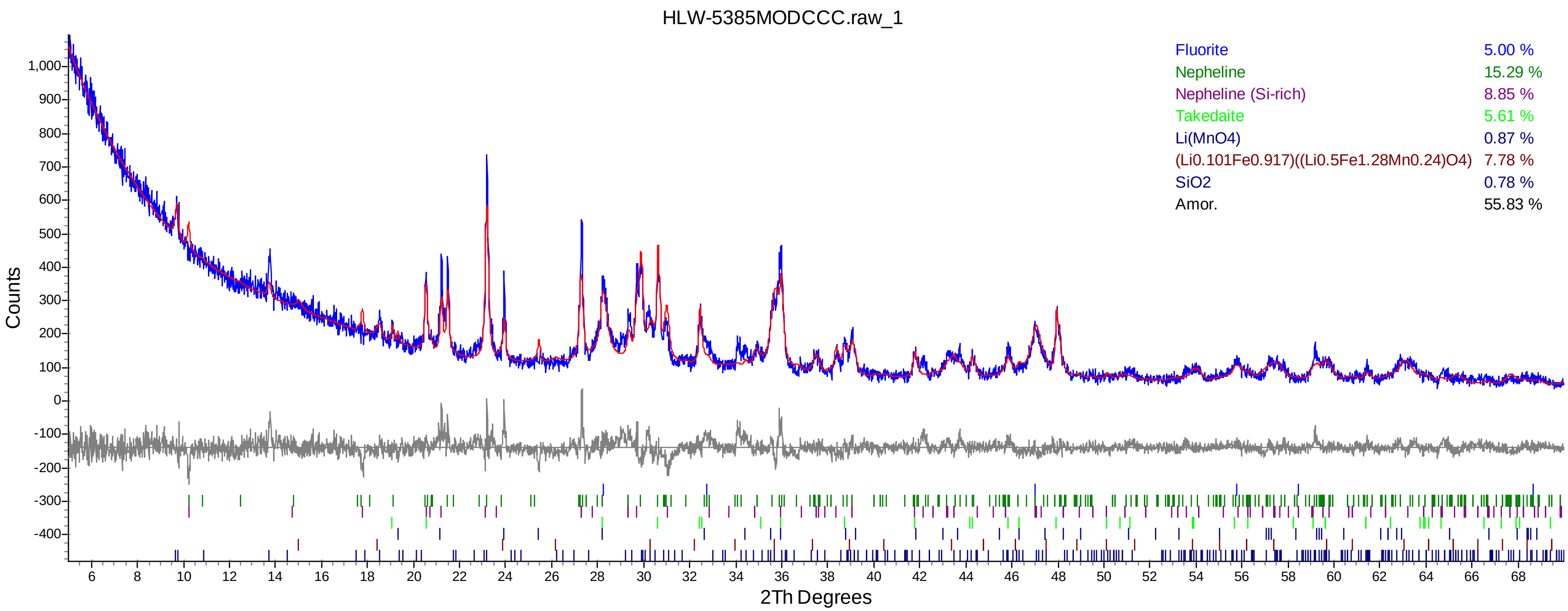

	Phase Name	Wt% of Spiked	Wt% in Spiked sample	Wt% in Original sample
1	Fluorite	5	5	0
2	Nepheline	0	15.29	16.094
3	Nepheline (Si-rich)	0	8.846	9.312
4	Takedaite	0	5.607	5.902
5	Li(MnO4)	0	0.872	0.918
6	(Li0.101Fe0.917)((Li0.5Fe1.28Mn0.24)O4)	0	7.784	8.193
7	SiO2	0	0.775	0.816

Figure D.39. XRD Pattern of Glass EWG-OL-5385 Mod 12% B 17% Na with the Weight % of Crystalline Phases after CCC Treatment

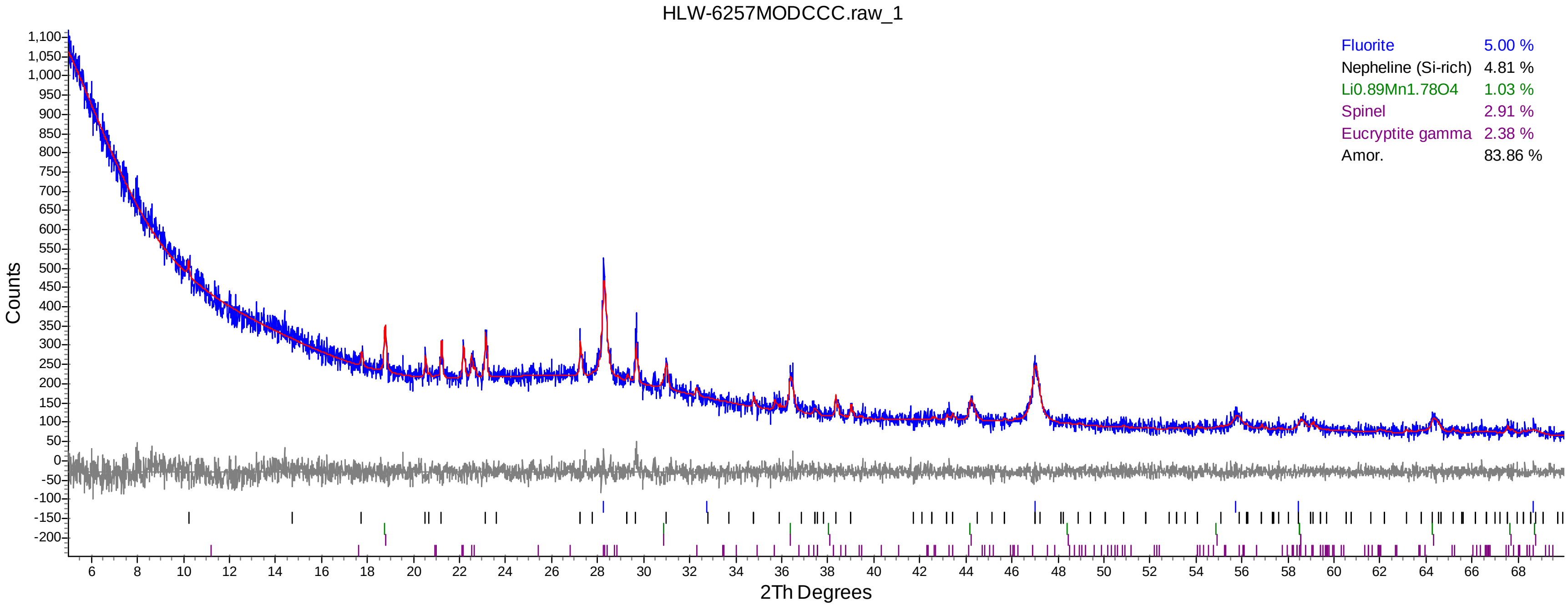

	Phase Name	Wt% of Spiked	Wt% in Spiked sample	Wt% in Original sample
1	Fluorite	5	5	0
2	Nepheline (Si-rich)	0	4.812	5.065
3	Li0.89Mn1.78O4	0	1.033	1.087
4	Spinel	0	2.913	3.066
5	Eucryptite gamma	0	2.379	2.504

Figure D.40. XRD Pattern of Glass EWG-OL-6257 Mod 12% B 8% Ca with the Weight % of Crystalline Phases after CCC Treatment

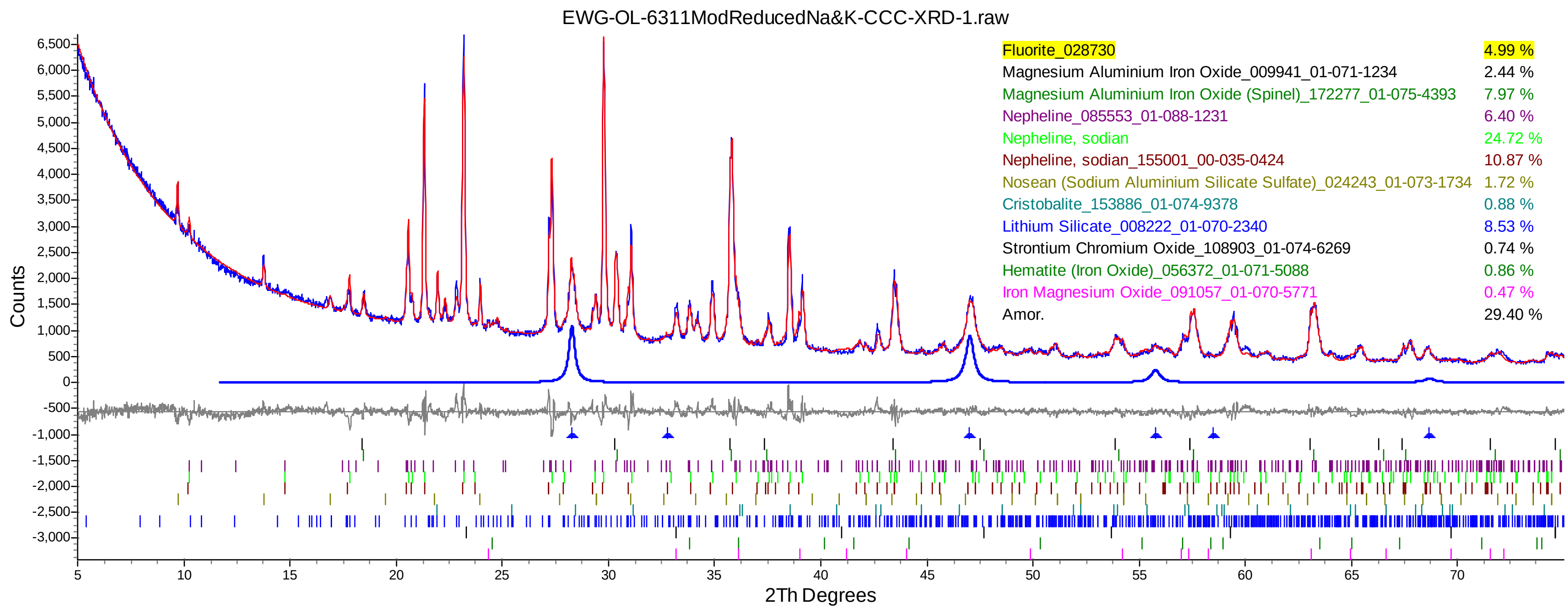

	Phase Name	Wt% of Spiked	Wt% in Spiked sample	Wt% in Original sample
1	Fluorite_028730	4.99	4.99	0
2	Magnesium Aluminum Iron Oxide	0	2.439	2.567
3	Magnesium Aluminum Iron Oxide (Spinel)	0	7.97	8.388
4	Nepheline	0	6.404	6.741
5	Nepheline, sodian	0	24.724	26.022
6	Nepheline, sodian_155001_00-035-0424	0	10.869	11.44
7	Nosean (Sodium Aluminum Silicate Sulfate)	0	1.721	1.812
8	Cristobalite	0	0.882	0.929
9	Lithium Silicate	0	8.532	8.98
10	Strontium Chromium Oxide	0	0.736	0.775
11	Hematite (Iron Oxide)	0	0.862	0.907
12	Iron Magnesium Oxide	0	0.472	0.497

Figure D.41. XRD Pattern of Glass EWG-OL-6311 Mod Reduced Na & K with the Weight % of Crystalline Phases after CCC Treatment

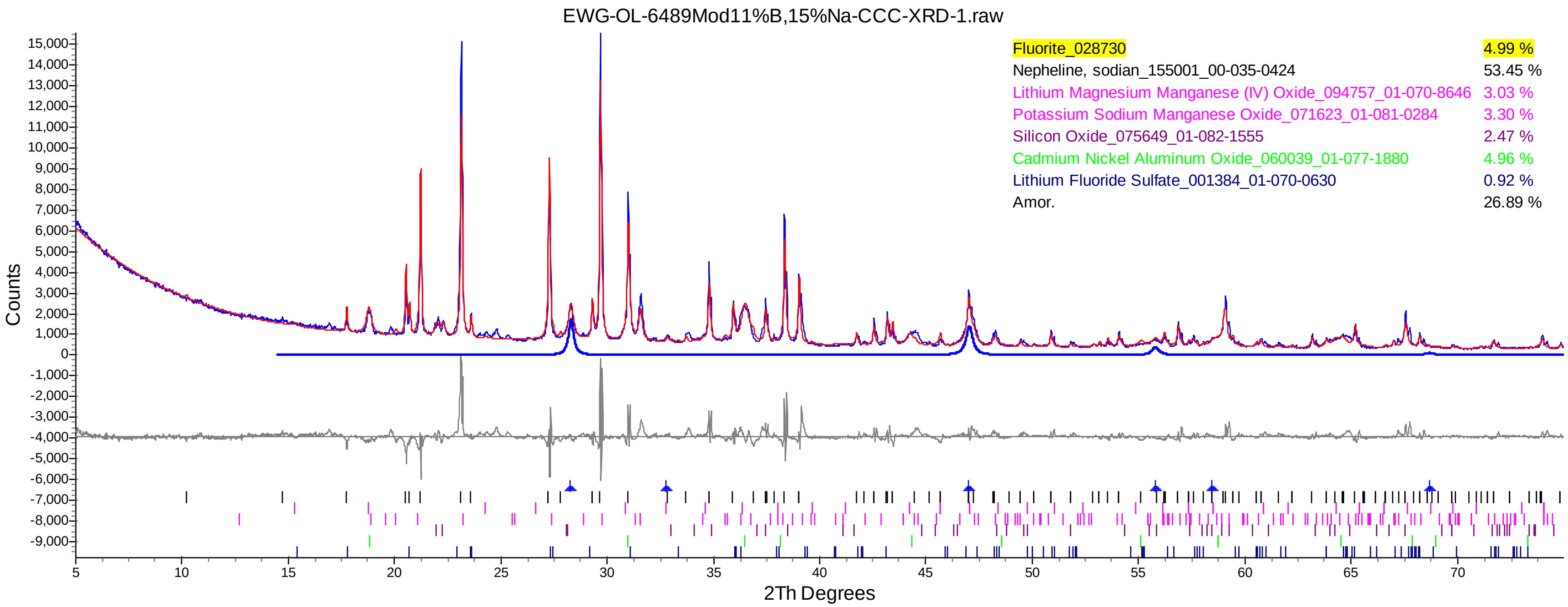

	Phase Name	Wt% of Spiked	Wt% in Spiked sample	Wt% in Original sample
1	Fluorite_028730	4.99	4.99	0
2	Nepheline, sodian	0	53.445	56.252
3	Lithium Magnesium Manganese(IV) Oxide	0	3.028	3.187
4	Potassium Sodium Manganese Oxide	0	3.299	3.472
5	Silicon Oxide	0	2.467	2.597
6	Cadmium Nickel Aluminum Oxide	0	4.964	5.225
7	Lithium Fluoride Sulfate	0	0.918	0.967

Figure D.42. XRD Pattern of Glass EWG-OL-6489 Mod 11% B 15% Na with the Weight % of Crystalline Phases after CCC Treatment

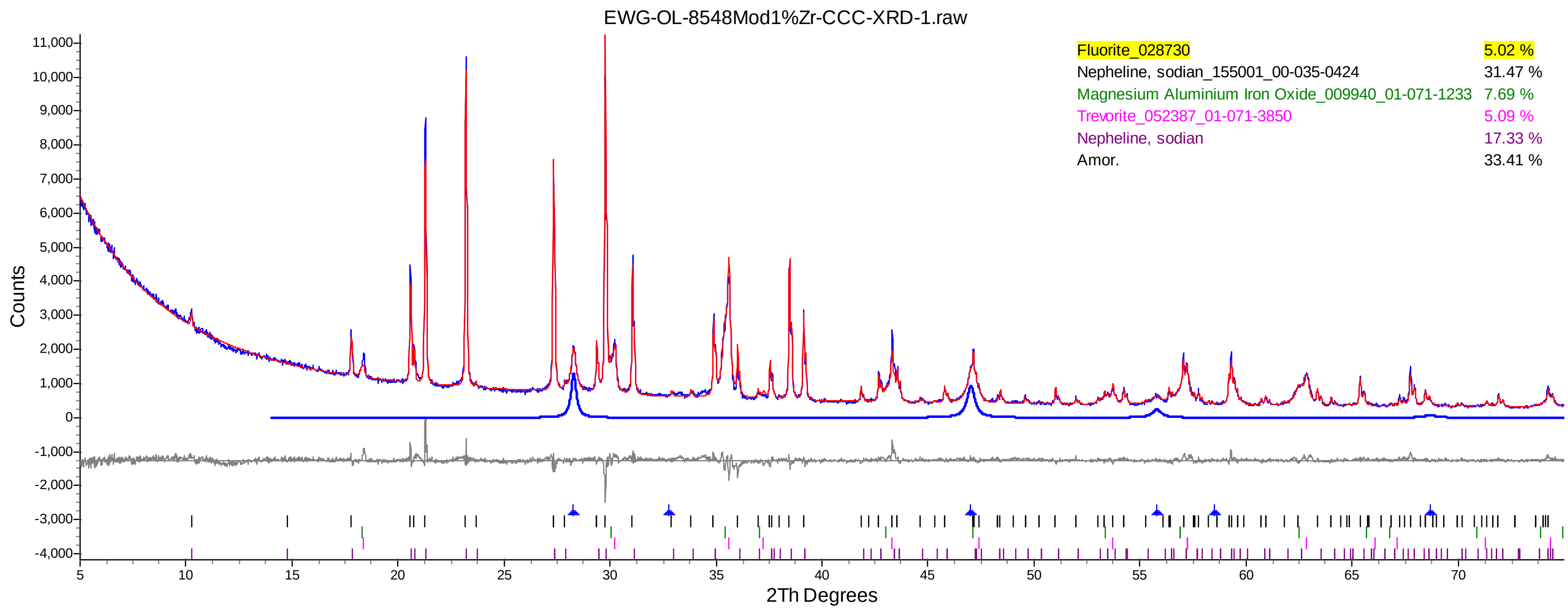

	Phase Name	Wt% of Spiked	Wt% in Spiked sample	Wt% in Original sample
1	Fluorite_028730	5.02	5.02	0
2	Nepheline, sodian_155001 00-035-0424	0	31.468	33.131
3	Magnesium Aluminum Iron Oxide	0	7.687	8.094
4	Trevorite	0	5.087	5.356
5	Nepheline, sodian	0	17.329	18.245

Figure D.43. XRD Pattern of Glass EWG-OL-8548 Mod 1% Zr with the Weight % of Crystalline Phases after CCC Treatment

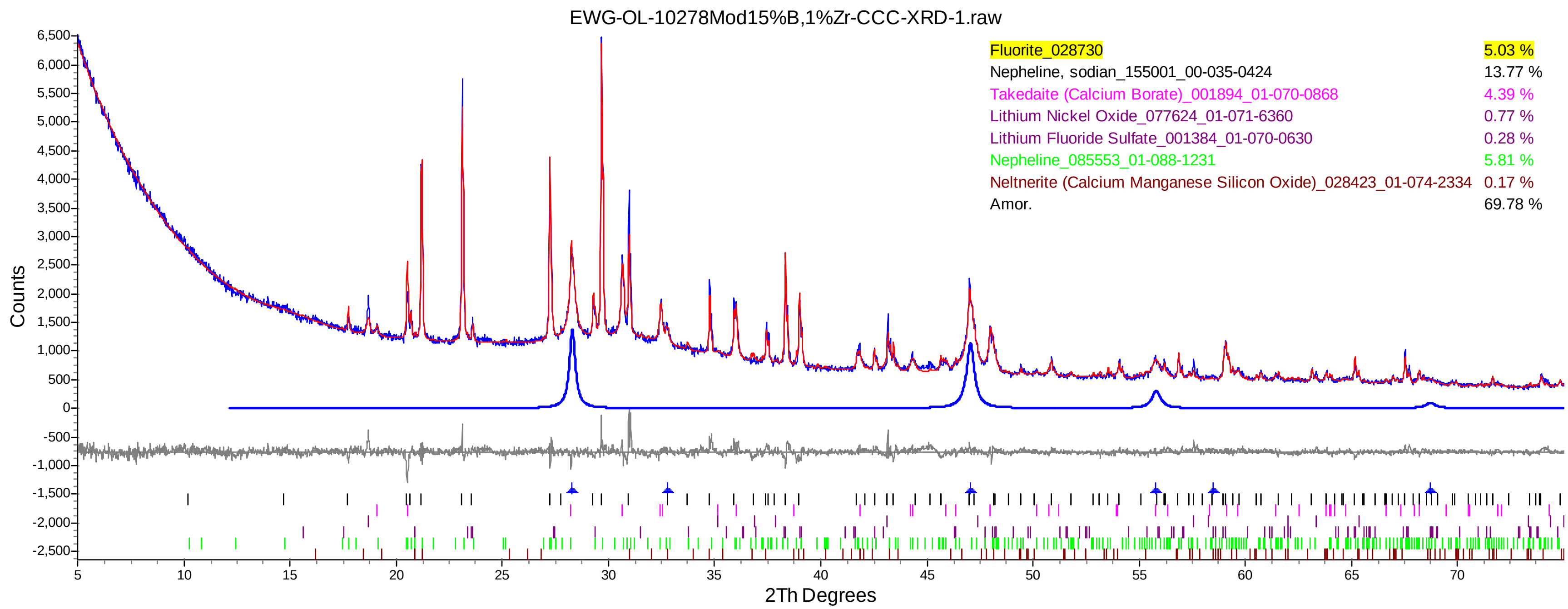

	Phase Name	Wt% of Spiked	Wt% in Spiked sample	Wt% in Original sample
1	Fluorite_028730	5.03	5.03	0
2	Nepheline, sodian_155001 00-035-0424	0	13.773	14.503
3	Takedaite (Calcium Borate)	0	4.387	4.62
4	Lithium Nickel Oxide	0	0.766	0.806
5	Lithium Fluoride Sulfate	0	0.28	0.295
6	Nepheline	0	5.809	6.117
7	Neltnerite (Calcium Manganese Silicon Oxide)	0	0.174	0.183

Figure D.44. XRD Pattern of Glass EWG-OL-10278 Mod 15% B 1% Zr with the Weight % of Crystalline Phases after CCC Treatment

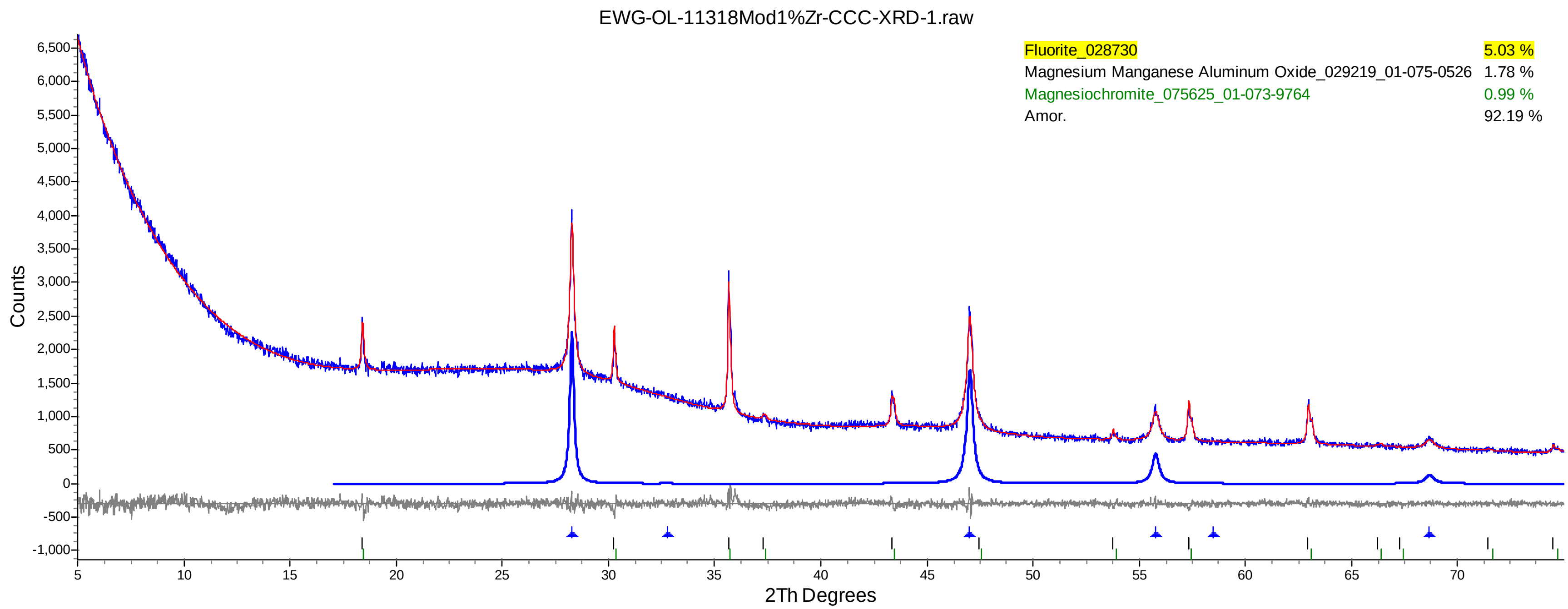

	Phase Name	Wt% of Spiked	Wt% in Spiked sample	Wt% in Original sample
1	Fluorite_028730	5.03	5.03	0
2	Magnesium Manganese Aluminum Oxide	0	1.784	1.879
3	Magnesiochromite	0	0.992	1.045

Figure D.45. XRD Pattern of Glass EWG-OL-11318 Mod 1% Zr with the Weight % of Crystalline Phases after CCC Treatment

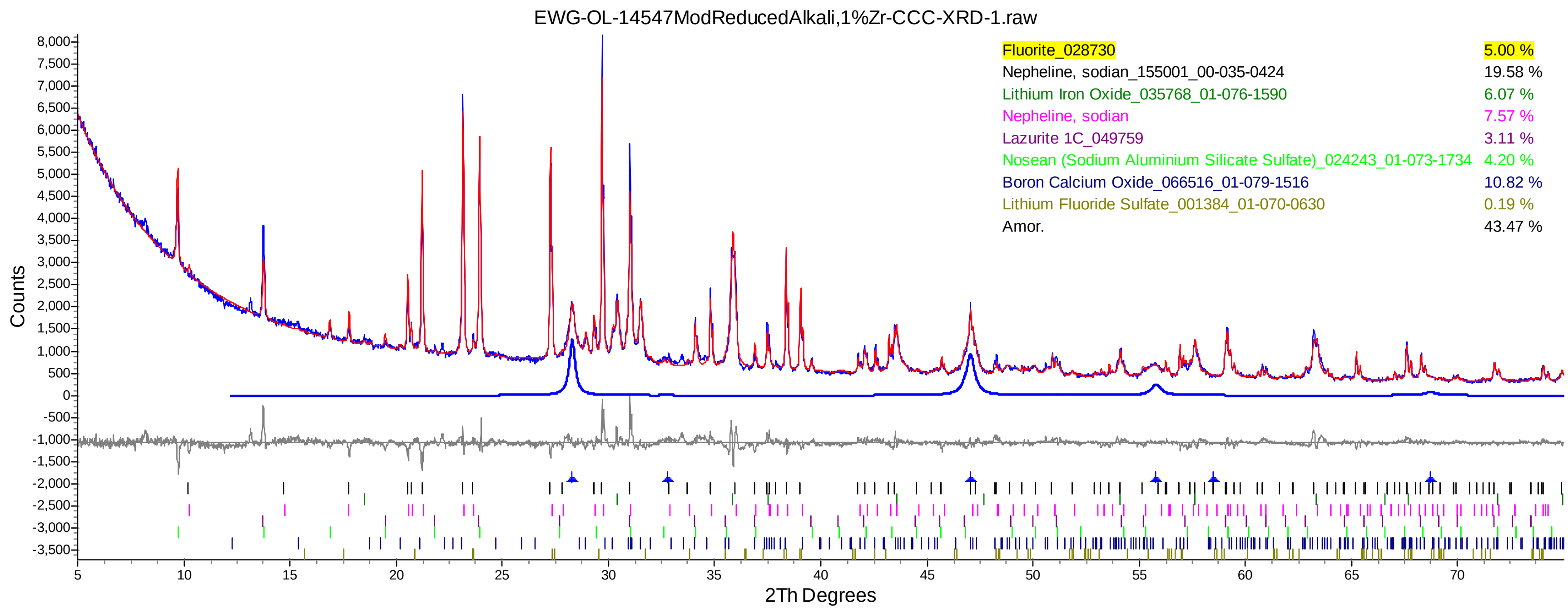

	Phase Name	Wt% of Spiked	Wt% in Spiked sample	Wt% in Original sample
1	Fluorite_028730	5	5	0
2	Nepheline, sodian_155001 00-035-0424	0	19.578	20.608
3	Lithium Iron Oxide	0	6.073	6.393
4	Nepheline, sodian	0	7.568	7.967
5	Lazurite 1C	0	3.106	3.269
6	Nosean (Sodium Aluminum Silicate Sulfate)	0	4.2	4.421
7	Boron Calcium Oxide	0	10.818	11.388
8	Silicon Oxide (Chabazite)	0	0.953	1.003
9	Lithium Fluoride Sulfate	0	0.188	0.198

Figure D.46. XRD Pattern of Glass EWG-OL-14547 Mod Reduced Alkali & 1% Zr with the Weight % of Crystalline Phases after CCC Treatment

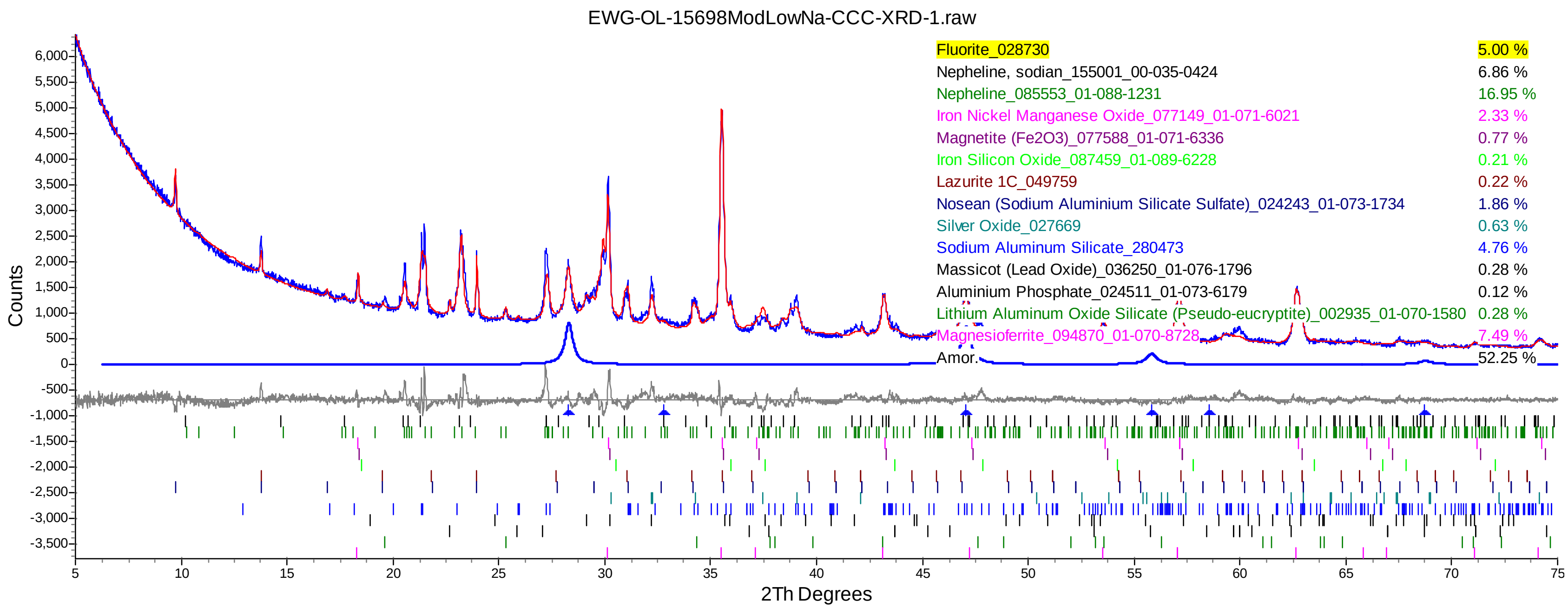

	Phase Name	Wt% of Spiked	Wt% in Spiked sample	Wt% in Original sample
1	Fluorite_028730	5	5	0
2	Nepheline, sodian_155001 00-035-0424	0	6.86	7.221
3	Nepheline	0	16.946	17.838
4	Iron Nickel Manganese Oxide	0	2.332	2.454
5	Magnetite	0	0.766	0.807
6	Iron Silicon Oxide	0	0.212	0.223
7	Lazurite 1C	0	0.221	0.233
8	Nosean (Sodium Aluminum Silicate Sulfate)	0	1.858	1.956
9	Silver Oxide	0	0.628	0.661
10	Sodium Aluminum Silicate	0	4.762	5.013
11	Massicot (Lead Oxide)	0	0.284	0.299
12	Aluminum Phosphate	0	0.124	0.13
13	Lithium Aluminum Oxide	0	0.275	0.29
14	Magnesioferrite	0	7.485	7.879

Figure D.47. XRD Pattern of Glass EWG-OL-15698 Mod Low Na with the Weight % of Crystalline Phases after CCC Treatment

Appendix E

Viscosity Data and Plots

Appendix E

Viscosity Data and Plots

This appendix contains the measured viscosity data for each of the glasses in this matrix. The plots shown in this appendix are fitted to the Arrhenius equation

$$\ln(\eta) = A + \frac{B}{T_K} \tag{E.1}$$

where *A* and *B* are independent of temperature and temperature (T_K) is in K (T(°C) + 273.15). However, some of the plots showed curvature and would be better fit to the Vogel - Fulcher - Tamman (VFT) model

$$\ln(\eta) = E + \frac{F}{T_k - T_0} \tag{E.2}$$

where *E*, *F*, and T_0 are temperature independent and composition dependent coefficients and T_K is the temperature in K (T(°C) + 273.15). The intent of the figures and Arrhenius equation fits shown in this appendix are mainly to assess trends of the data and provide some observations about whether there may be sufficient curvature in the data to consider VFT fits in the subsequent work that will decide between fitting the viscosity-temperature data to the Arrhenius or VFT equations.

There does appear to be some indication of possible small curvature in several of the viscosity plots because the middle data points are slightly below the fitted line, and end points are slightly above the fitted line. The curvature is still slight but the Arrhenius equation may not be adequate for all glasses. For the glasses with the largest curvature, the curved fit is also shown in the plots.

E.1 EWG-HAI-Centroid-1 Viscosity Data

Table E.1. Viscosity Data for Glass EWG-HAI-Centroid-1

Temperature, °C	Viscosity, Pa·s	1/(T+273.15) × 10,000 , K^{-1}	ln η, Pa·s
1150	6.32	7.03	1.84
1050	17.30	7.56	2.85
950	55.68	8.18	4.02
1150	6.10	7.03	1.81
1250	2.49	6.57	0.91
1150	5.97	7.03	1.79

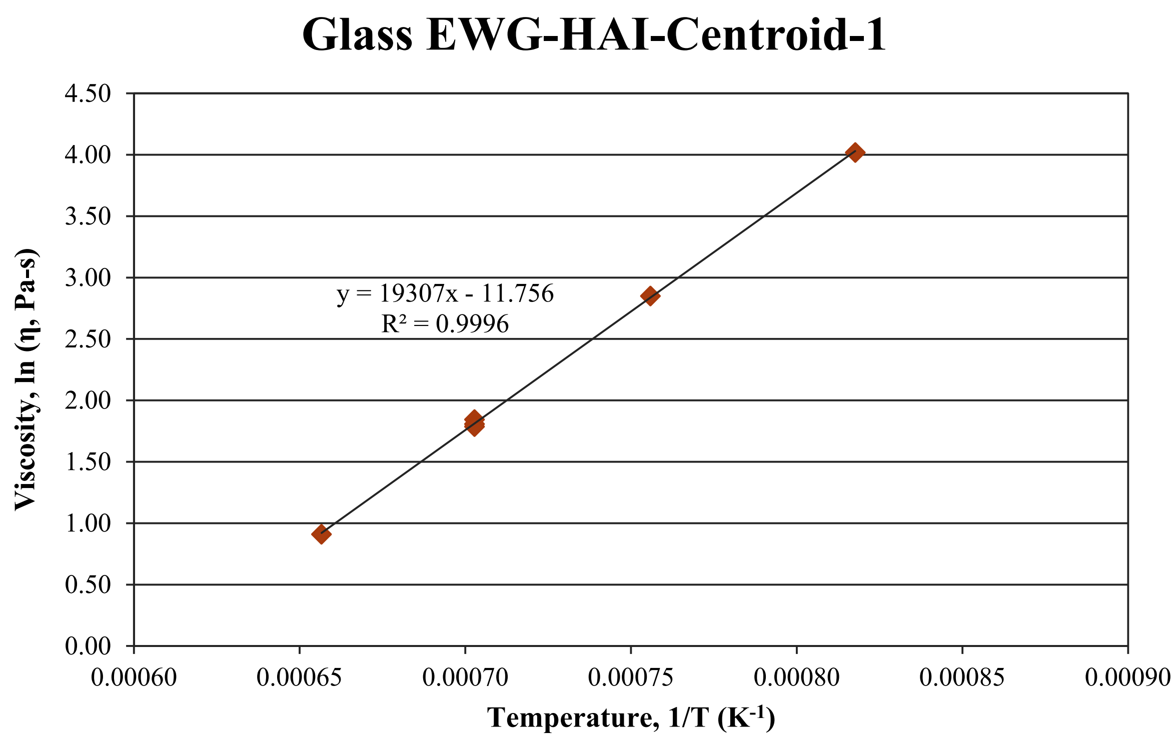

Figure E.1. Viscosity-Temperature Data and Arrhenius Equation Fit for Glass EWG-HAI-Centroid-1

E.2 Glass EWG-HAI-Centroid-2 Viscosity Data

Table E.2. Viscosity Data for Glass EWG-HAI-Centroid-2

Temperature, °C	Viscosity, Pa·s	1/(T+273.15) × 10,000 , K^{-1}	ln η, Pa·s
1050	22.26	7.56	3.10
950	75.75	8.18	4.33
900	156.18	8.53	5.05
1050	22.52	7.56	3.11
1150	8.01	7.03	2.08
1050	22.81	7.56	3.13

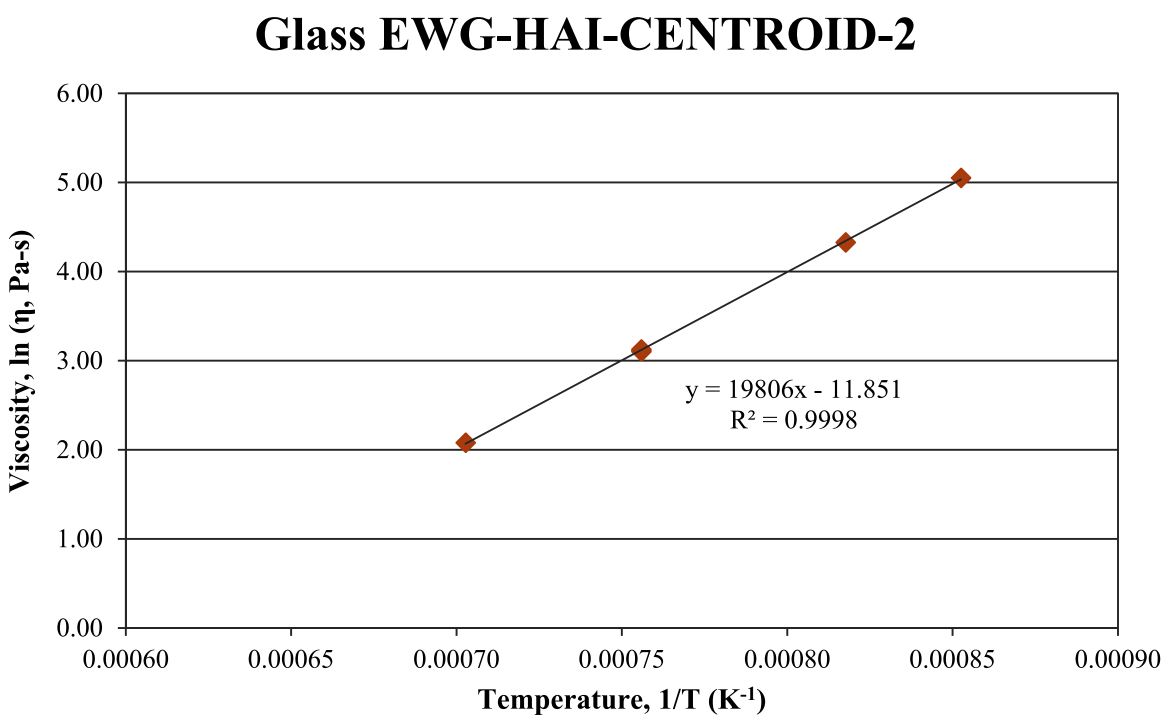

Figure E.2. Viscosity-Temperature Data and Arrhenius Equation Fit for Glass EWG-HAI-Centroid-2

E.3 Glass EWG-OL-801 Viscosity Data

Table E.3. Viscosity Data for Glass EWG-OL-801

Temperature, °C	Viscosity, Pa·s	1/(T+273.15) × 10,000 , K^{-1}	ln η, Pa·s
1250	4.04	6.57	1.40
1150	10.60	7.03	2.36
1050	33.01	7.56	3.50
1250	4.08	6.57	1.41
1300	2.67	6.36	0.98
1250	4.16	6.57	1.42

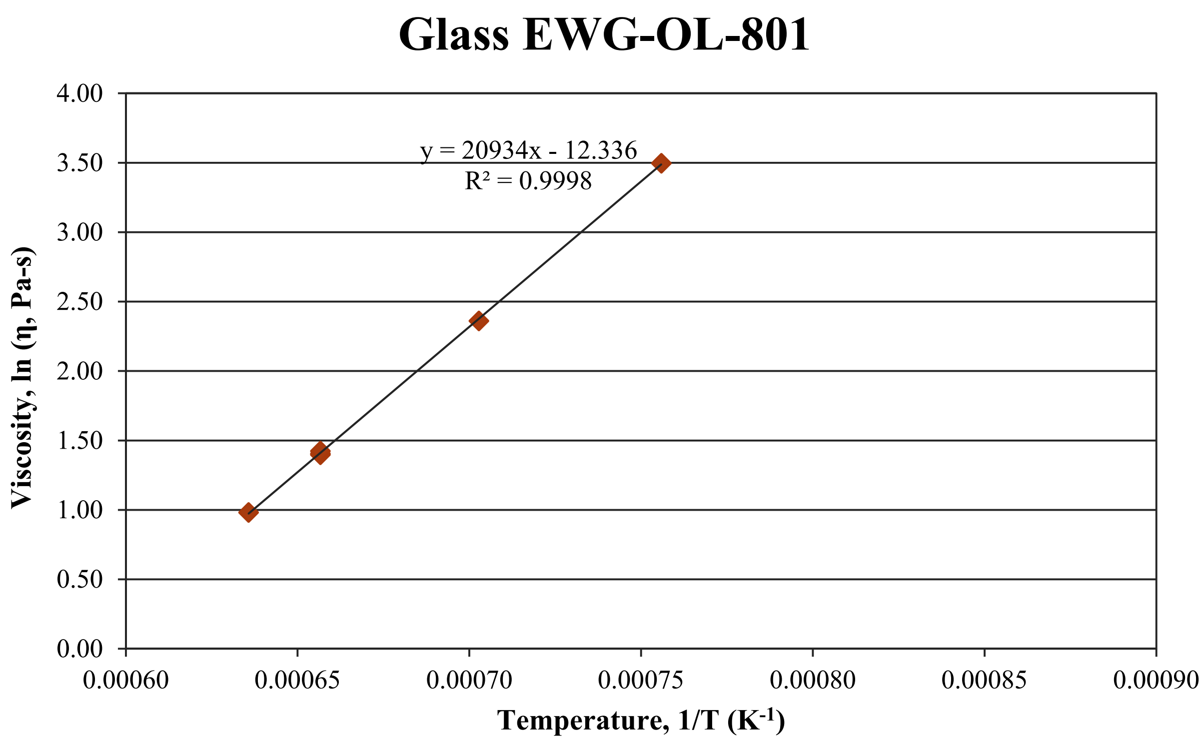

Figure E.3. Viscosity-Temperature Data and Arrhenius Equation Fit for Glass EWG-OL-801

E.4 Glass EWG-OL-1369 Viscosity Data

Table E.4. Viscosity Data for Glass EWG-OL-1369

Temperature, °C	Viscosity, Pa·s	1/(T+273.15) × 10,000 , K^{-1}	ln η, Pa·s
1250	5.29	6.57	1.67
1150	8.66	7.03	2.16
1050	23.92	7.56	3.17
1250	4.22	6.57	1.44
1300	2.54	6.36	0.93
1250	3.73	6.57	1.32

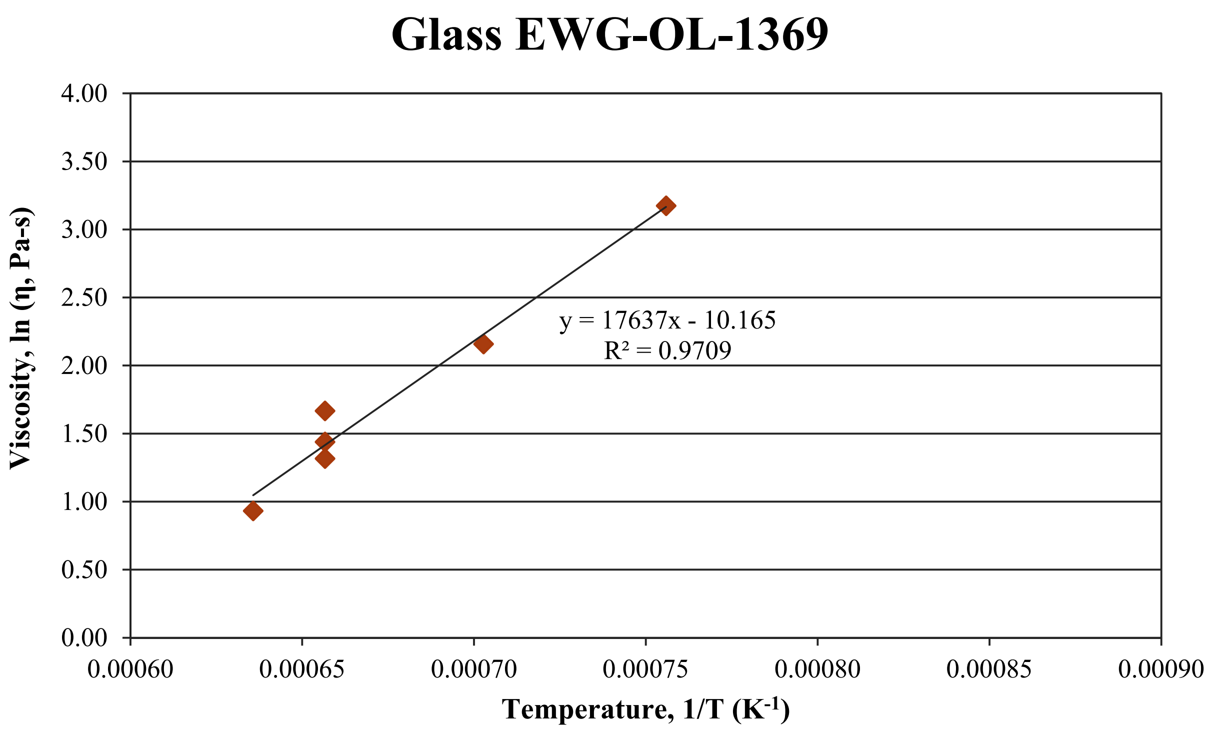

Figure E.4. Viscosity-Temperature Data and Arrhenius Equation Fit for Glass EWG-OL-1369

E.5 Glass EWG-OL-1580 Viscosity Data

Table E.5. Viscosity Data for Glass EWG-OL-1580

Temperature, °C	Viscosity, Pa·s	1/(T+273.15) × 10,000 , K^{-1}	ln η, Pa·s
1240	3.20	6.61	1.16
1140	7.20	7.08	1.97
1040	19.70	7.62	2.98
1240	3.25	6.61	1.18
1340	1.50	6.20	0.40
1240	3.26	6.61	1.18

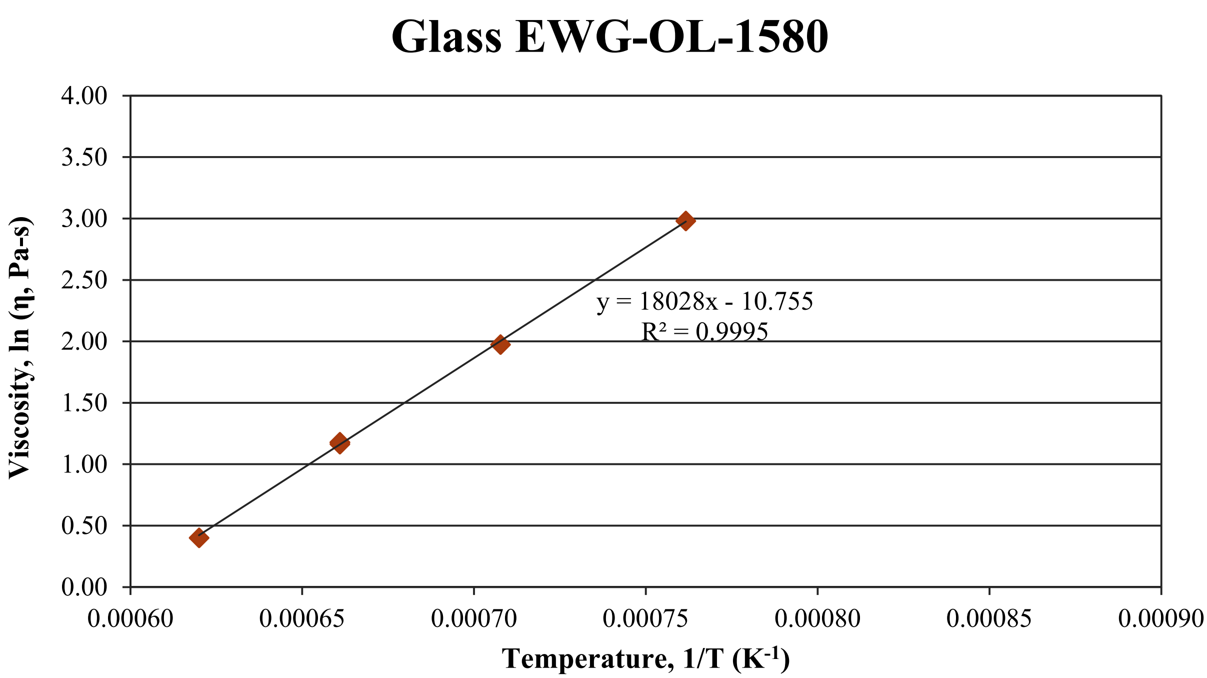

Figure E.5. Viscosity-Temperature Data and Arrhenius Equation Fit for Glass EWG-OL-1580

E.6 Glass EWG-OL-1672 Viscosity Data

Table E.6. Viscosity Data for Glass EWG-OL-1672

Temperature, °C	Viscosity, Pa·s	1/(T+273.15) × 10,000 , K^{-1}	ln η, Pa·s
1300	3.51	6.36	1.25
1200	5.18	6.79	1.65
1100	11.32	7.28	2.43
1300	3.64	6.36	1.29
1390	3.40	6.01	1.22
1300	3.77	6.36	1.33

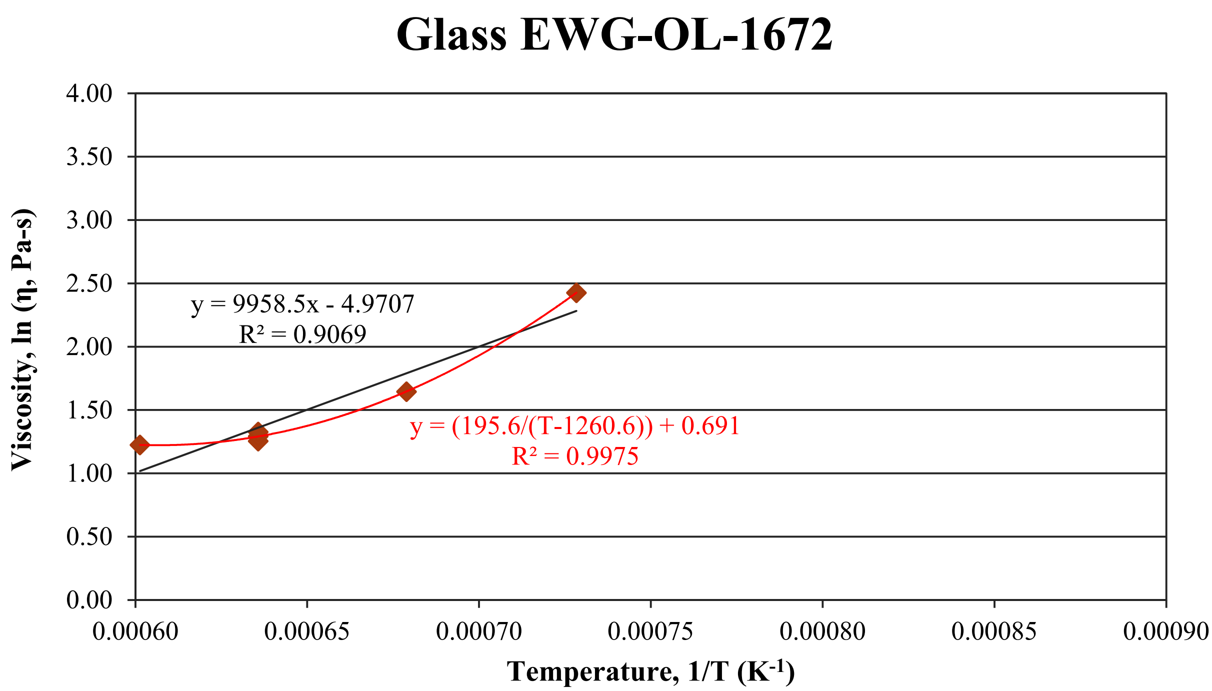

Figure E.6. Viscosity-Temperature Data and Arrhenius Equation Fit for Glass EWG-OL-1672

E.7 Glass EWG-OL-2463 Viscosity Data

Table E.7. Viscosity Data for Glass EWG-OL-2463

Temperature, °C	Viscosity, Pa·s	1/(T+273.15) × 10,000 , K^{-1}	ln η, Pa·s
1200	1.75	6.79	0.56
1100	4.84	7.28	1.58
1000	57.52	7.86	4.05
1200	1.71	6.79	0.54

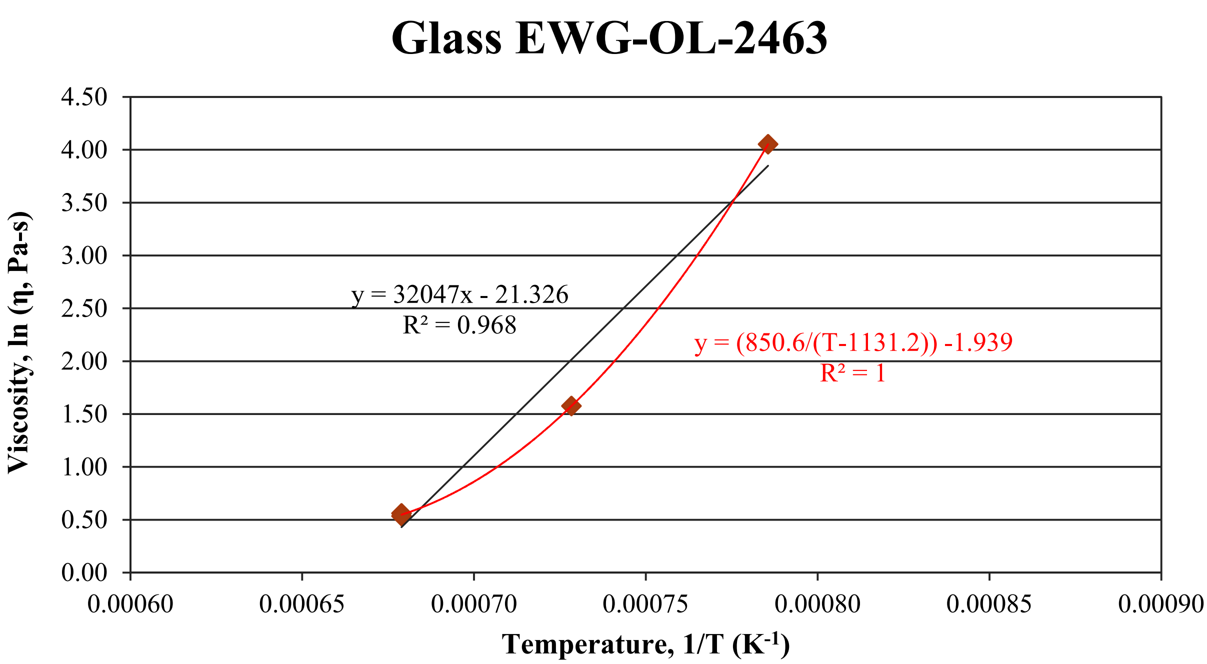

Figure E.7. Viscosity-Temperature Data and Arrhenius Equation Fit for Glass EWG-OL-2463

E.8 Glass EWG-OL-2619 Viscosity Data

Table E.8. Viscosity Data for Glass EWG-OL-2619

Temperature, °C	Viscosity, Pa·s	1/(T+273.15) × 10,000 , K^{-1}	ln η, Pa·s
1150	1.43	7.03	0.36
1050	4.12	7.56	1.42
950	28.86	8.18	3.36
1150	1.44	7.03	0.36
1250	0.62	6.57	-0.48
1150	1.45	7.03	0.37

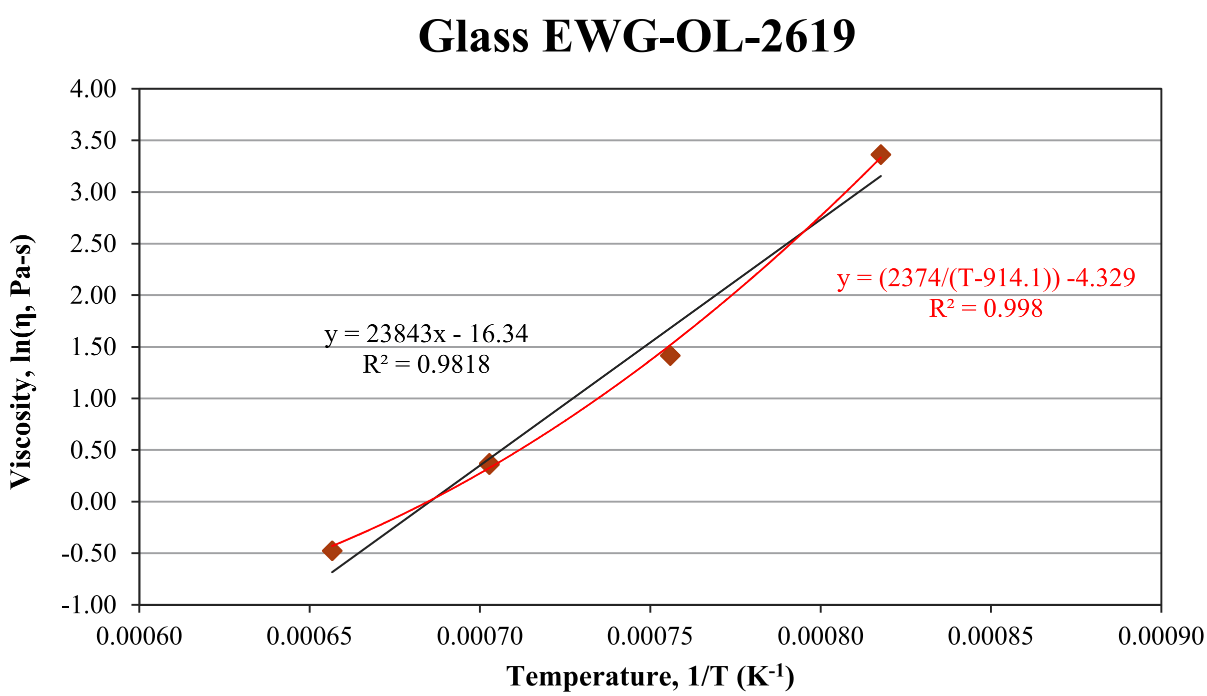

Figure E.8. Viscosity-Temperature Data and Arrhenius Equation Fit for Glass EWG-OL-2619

E.9 Glass EWG-OL-3122 Viscosity Data

Table E.9. Viscosity Data for Glass EWG-OL-3122

Temperature, °C	Viscosity, Pa·s	1/(T+273.15) × 10,000 , K^{-1}	ln η, Pa·s
1390	1.58	6.01	0.46
1300	3.78	6.36	1.33
1200	9.75	6.79	2.28
1100	75.41	7.28	4.32
1390	1.60	6.01	0.47

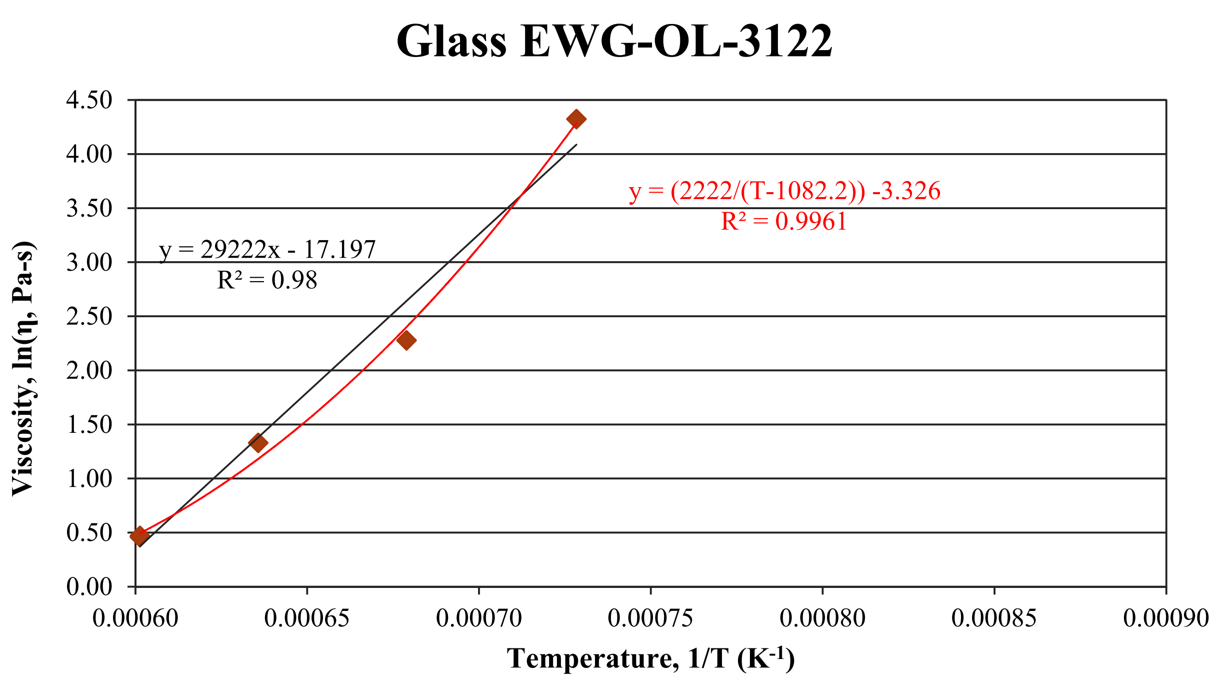

Figure E.9. Viscosity-Temperature Data and Arrhenius Equation Fit for Glass EWG-OL-3122

E.10 Glass EWG-OL-3208 Viscosity Data

Table E.10. Viscosity Data for Glass EWG-OL-3208

Temperature, °C	Viscosity, Pa·s	1/(T+273.15) × 10,000 , K^{-1}	ln η, Pa·s
1100	5.34	7.28	1.68
1000	12.00	7.86	2.48
900	32.25	8.53	3.47
1100	5.38	7.28	1.68
1200	2.66	6.79	0.98
1100	5.30	7.28	1.67

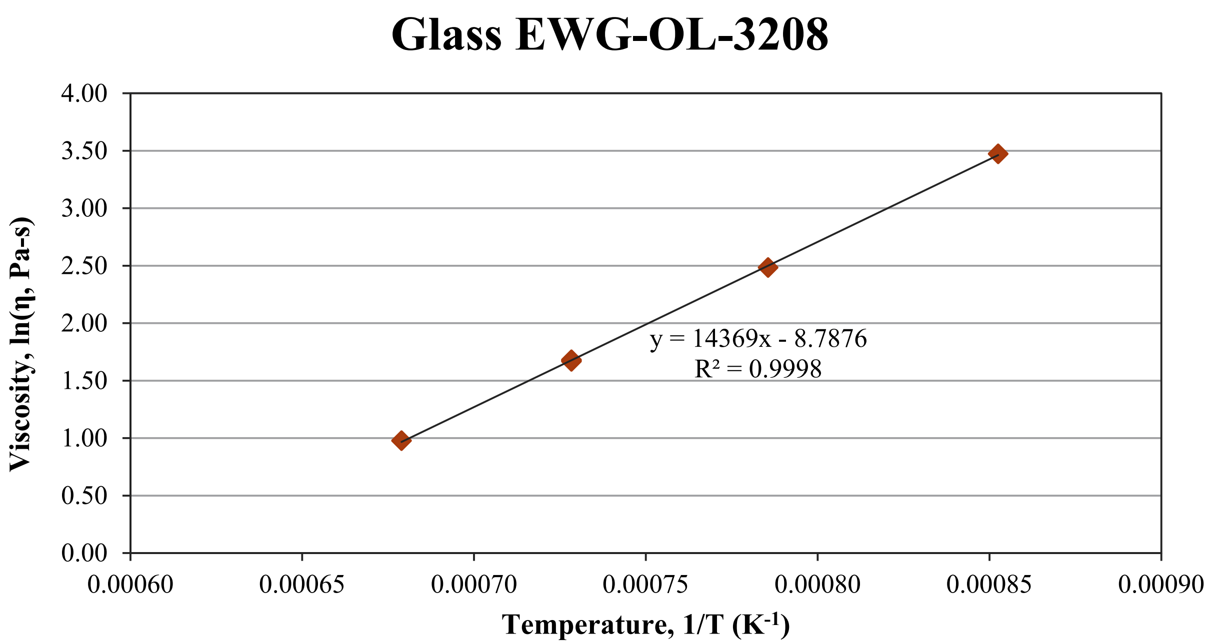

Figure E.10. Viscosity-Temperature Data and Arrhenius Equation Fit for Glass EWG-OL-3208

E.11 Glass EWG-OL-3231 Viscosity Data

Table E.11. Viscosity Data for Glass EWG-OL-3231

Temperature, °C	Viscosity, Pa·s	1/(T+273.15) × 10,000 , K^{-1}	ln η, Pa·s
1100	1.42	7.28	0.35
1000	3.23	7.86	1.17
900	24.01	8.53	3.18
1100	1.44	7.28	0.36
1200	1.22	6.79	0.20
1100	2.09	7.28	0.74

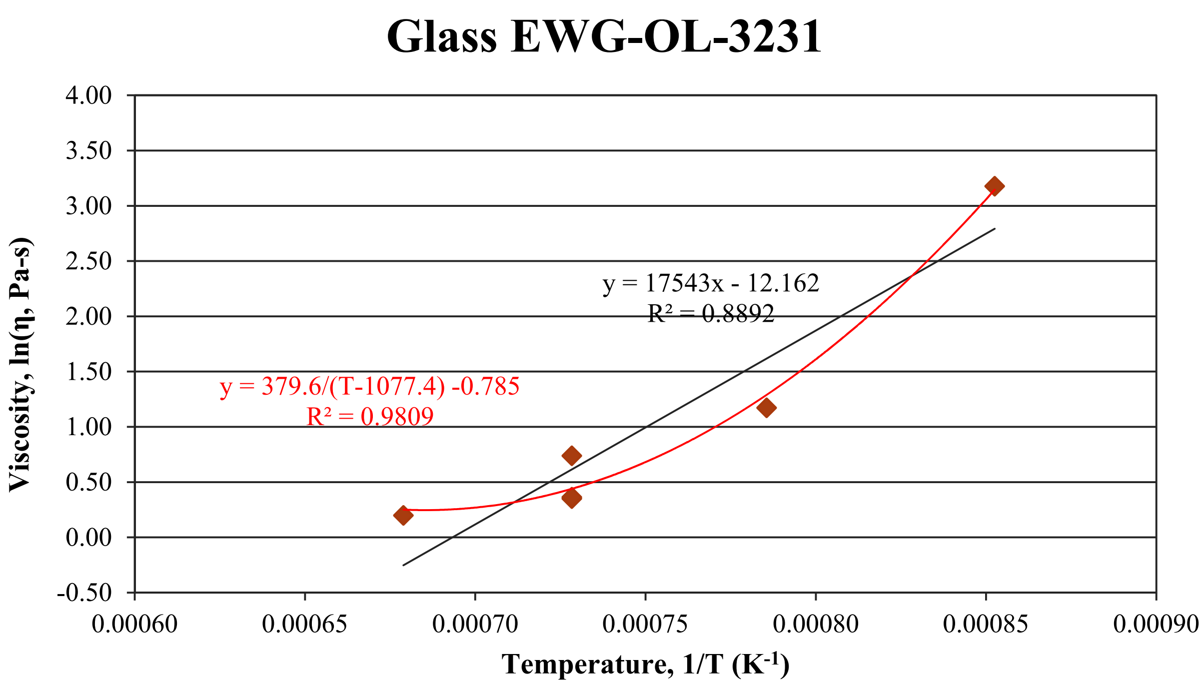

Figure E.11. Viscosity-Temperature Data and Arrhenius Equation Fit for Glass EWG-OL-3231

E.12 Glass EWG-OL-3388 Viscosity Data

Table E.12. Viscosity Data for Glass EWG-OL-3388

Temperature, °C	Viscosity, Pa·s	1/(T+273.15) × 10,000 , K^{-1}	ln η, Pa·s
1025	4.50	7.70	1.50
950	8.54	8.18	2.14
850	27.16	8.90	3.30
1025	4.60	7.70	1.53
1125	2.24	7.15	0.81
1025	4.53	7.70	1.51

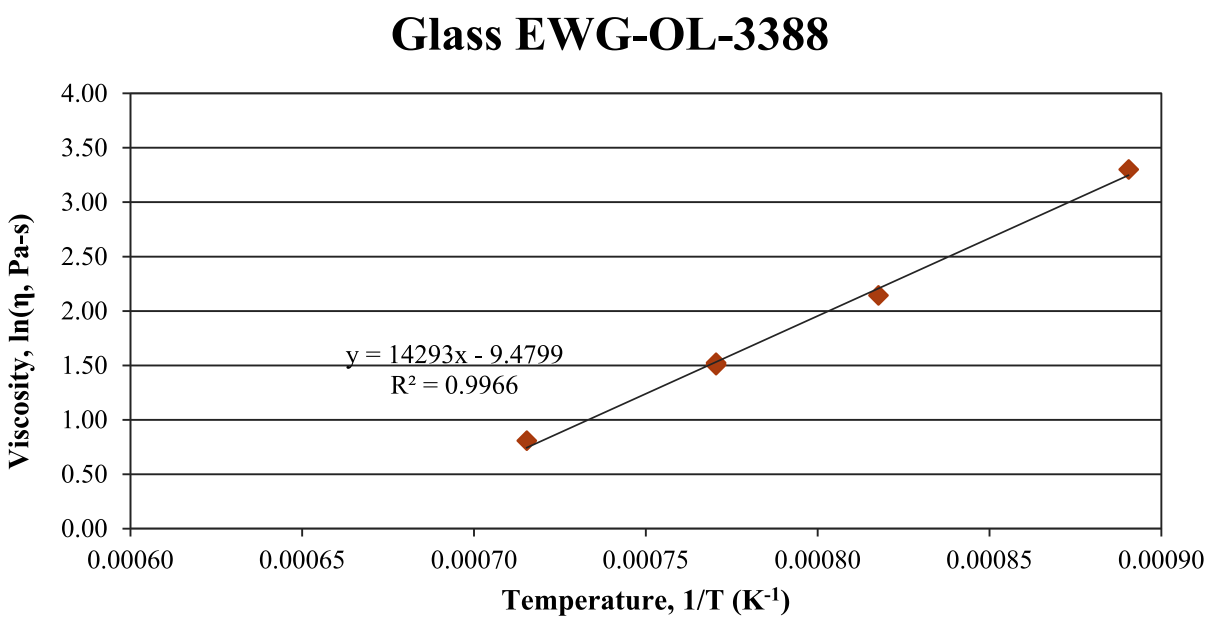

Figure E.12. Viscosity-Temperature Data and Arrhenius Equation Fit for Glass EWG-OL-3388

E.13 Glass EWG-OL-3872 Viscosity Data

Table E.13. Viscosity Data for Glass EWG-OL-3872

Temperature, °C	Viscosity, Pa·s	1/(T+273.15) × 10,000 , K^{-1}	ln η, Pa·s
1050	2.31	7.56	0.84
950	6.02	8.18	1.79
900	10.70	8.53	2.37
1050	2.33	7.56	0.85
1150	1.06	7.03	0.06
1050	2.32	7.56	0.84

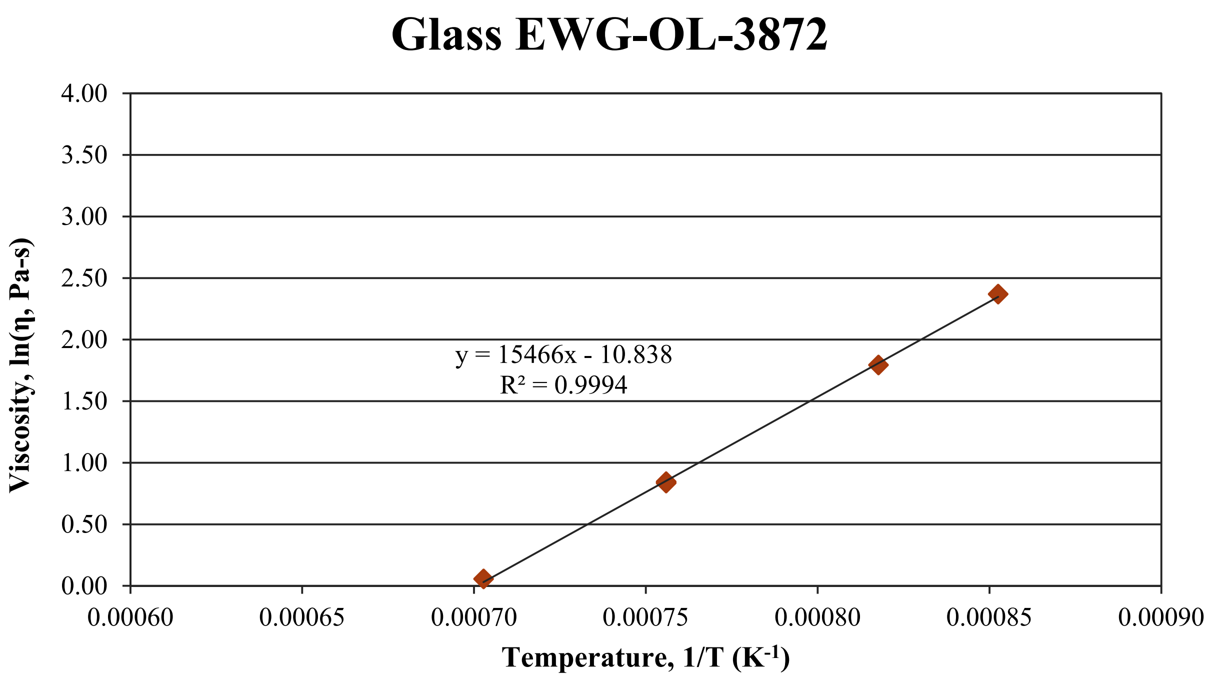

Figure E.13. Viscosity-Temperature Data and Arrhenius Equation Fit for Glass EWG-OL-3872

E.14 Glass EWG-OL-4099 Viscosity Data

Table E.14. Viscosity Data for Glass EWG-OL-4099

Temperature, °C	Viscosity, Pa·s	1/(T+273.15) × 10,000 , K^{-1}	ln η, Pa·s
1000	2.74	7.86	1.01
950	4.72	8.18	1.55
850	34.43	8.90	3.54
1000	2.74	7.86	1.01
1100	1.16	7.28	0.15
1000	2.80	7.86	1.03

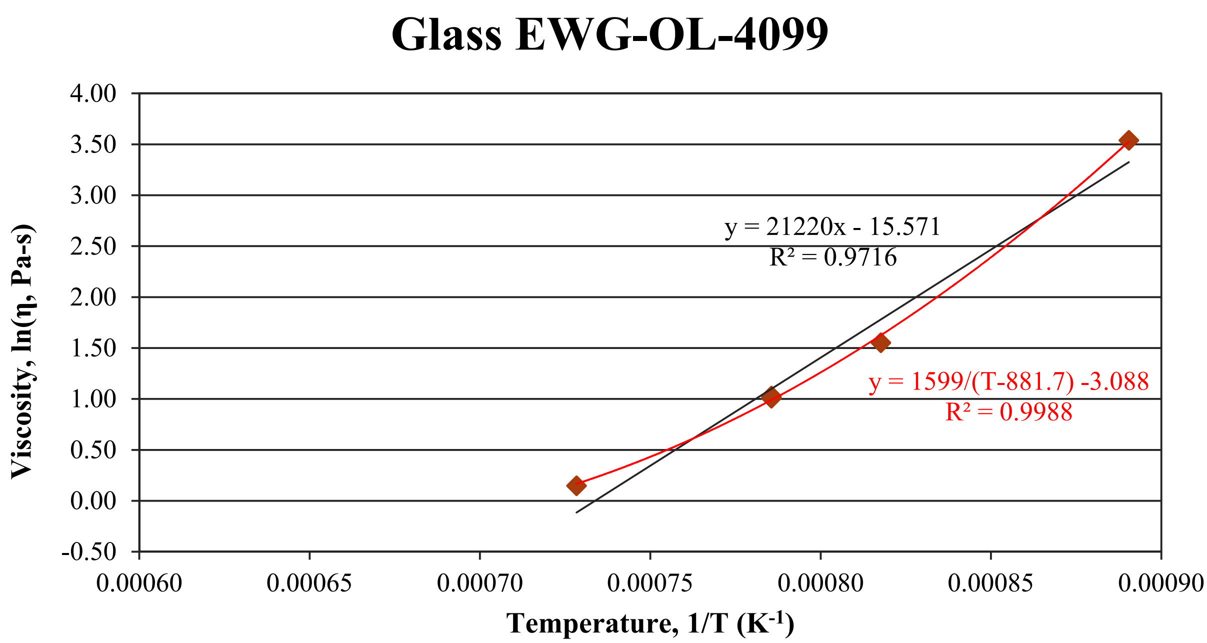

Figure E.14. Viscosity-Temperature Data and Arrhenius Equation Fit for Glass EWG-OL-4099

E.15 Glass EWG-OL-5155 Viscosity Data

Table E.15. Viscosity Data for Glass EWG-OL-5155

Temperature, °C	Viscosity, Pa·s	1/(T+273.15) × 10,000 , K^{-1}	ln η, Pa·s
1225	0.79	6.68	-0.23
1125	3.11	7.15	1.13
1025	7.01	7.70	1.95
1025	7.01	7.70	1.95
1025	7.01	7.70	1.95
1025	6.30	7.70	1.84

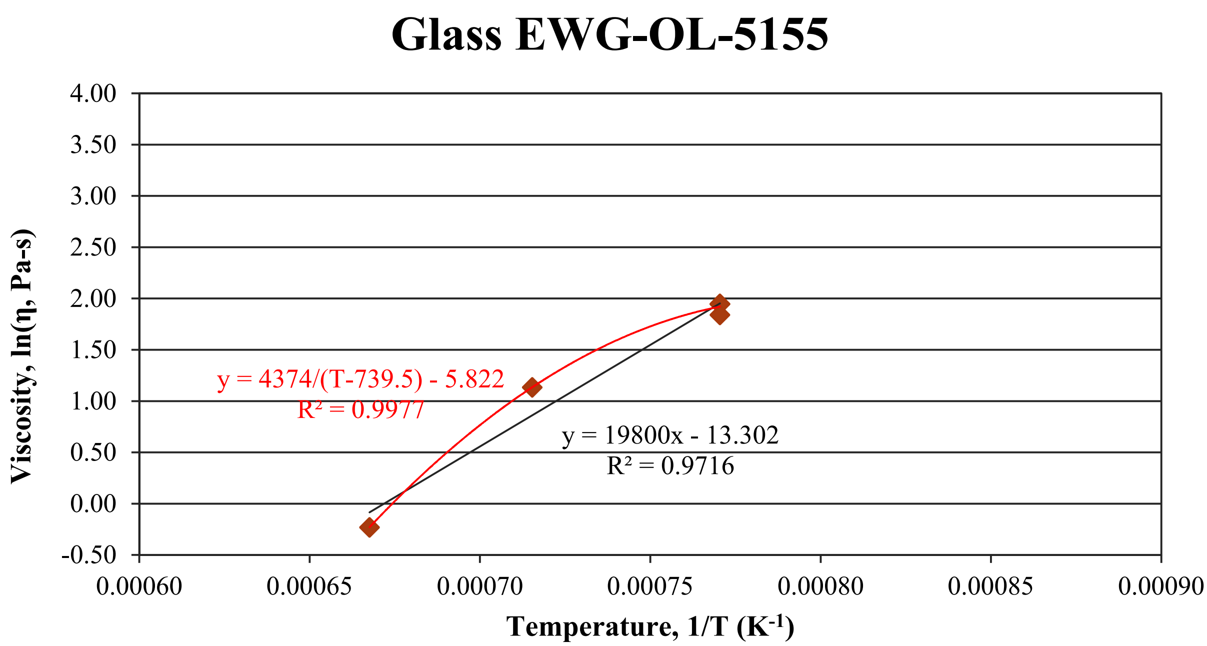

Figure E.15. Viscosity-Temperature Data and Arrhenius Equation Fit for Glass EWG-OL-5155

E.16 Glass EWG-OL-5549 Viscosity Data

Table E.16. Viscosity Data for Glass EWG-OL-5549

Temperature, °C	Viscosity, Pa·s	1/(T+273.15) × 10,000 , K^{-1}	ln η, Pa·s
1050	4.67	7.56	1.54
950	5.97	8.18	1.79
900	8.78	8.53	2.17
1050	4.13	7.56	1.42
1150	4.51	7.03	1.51
1050	4.33	7.56	1.47

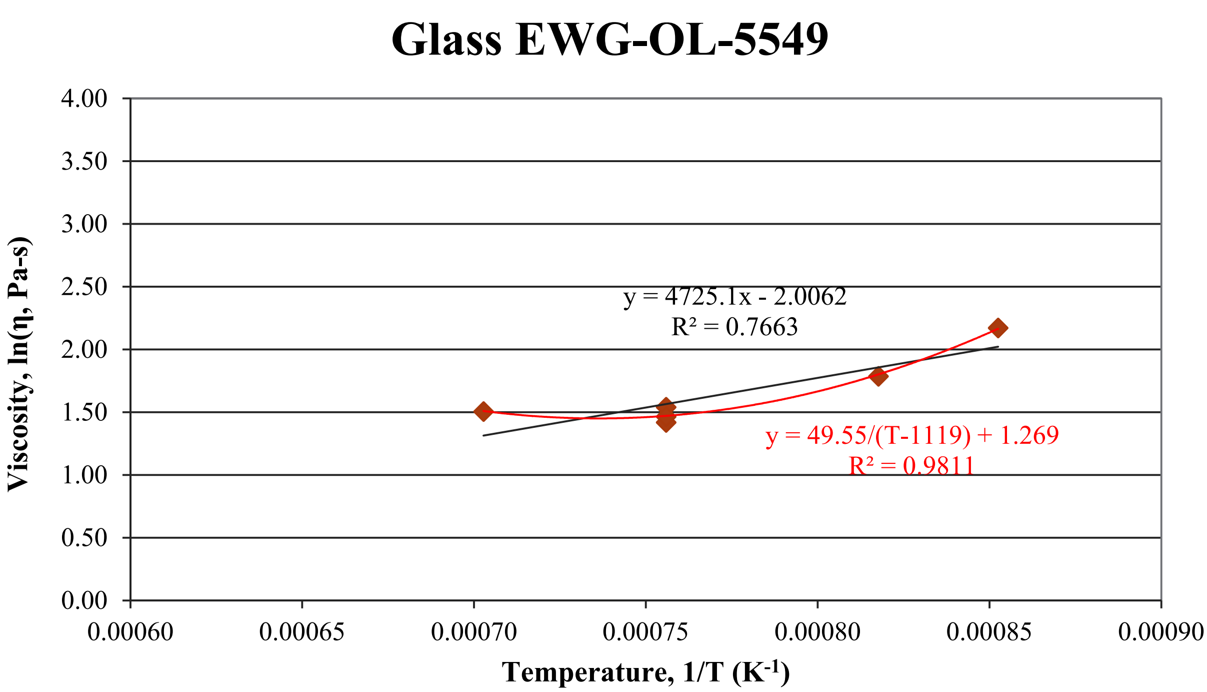

Figure E.16. Viscosity-Temperature Data and Arrhenius Equation Fit for Glass EWG-OL-5549

E.17 Glass EWG-OL-5801 Viscosity Data

Table E.17. Viscosity Data for Glass EWG-OL-5801

Temperature, °C	Viscosity, Pa·s	1/(T+273.15) × 10,000 , K^{-1}	ln η, Pa·s
1050	1.33	7.56	0.28
950	4.47	8.18	1.50
900	25.08	8.53	3.22
1050	1.31	7.56	0.27
1100	0.85	7.28	-0.16
1050	1.28	7.56	0.25

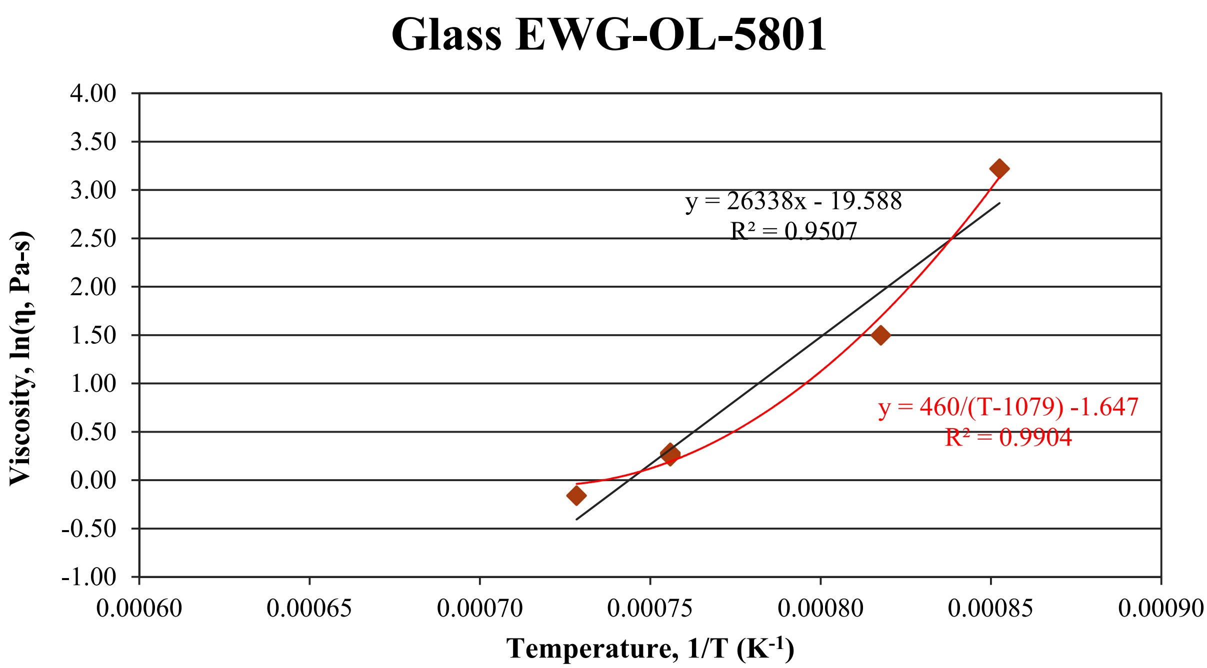

Figure E.17. Viscosity-Temperature Data and Arrhenius Equation Fit for Glass EWG-OL-5801

E.18 Glass EWG-OL-6080 Viscosity Data

Table E.18. Viscosity Data for Glass EWG-OL-6080

Temperature, °C	Viscosity, Pa·s	1/(T+273.15) × 10,000 , K^{-1}	ln η, Pa·s
1390	1.54	6.01	0.43
1300	3.16	6.36	1.15
1200	7.64	6.79	2.03
1100	24.15	7.28	3.18
1390	1.45	6.01	0.37

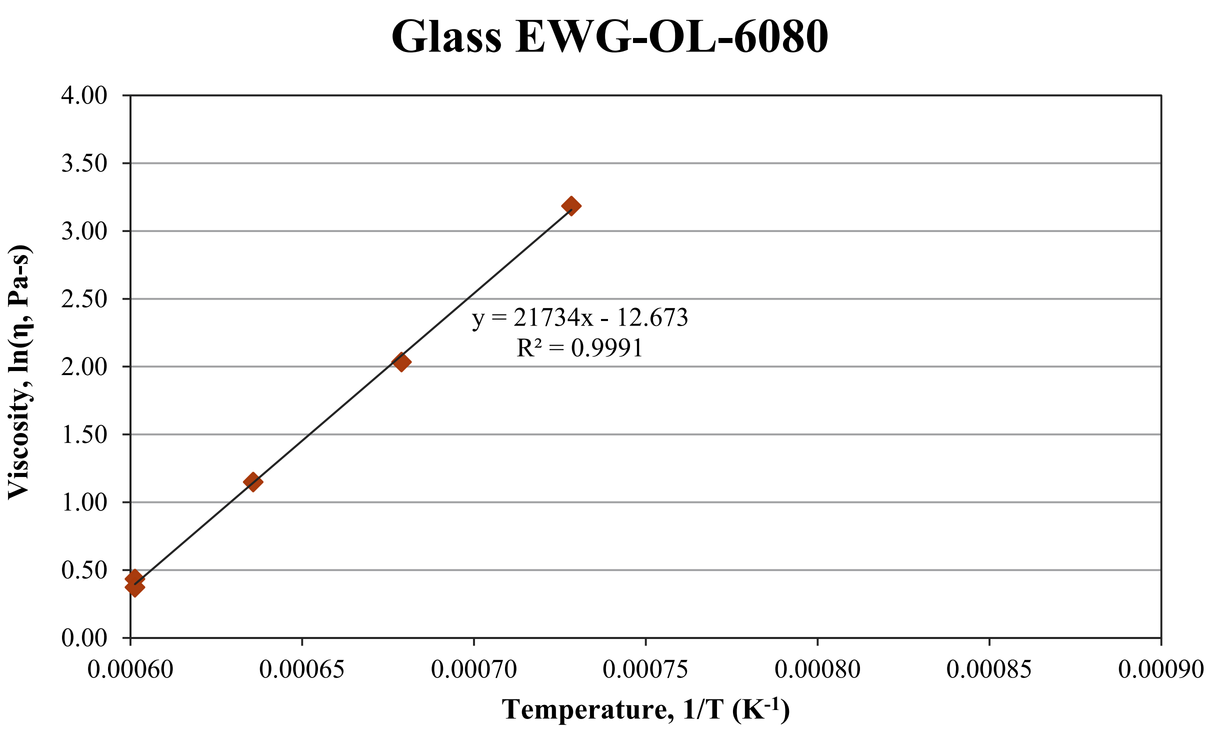

Figure E.18. Viscosity-Temperature Data and Arrhenius Equation Fit for Glass EWG-OL-6080

E.19 Glass EWG-OL-6198 Viscosity Data

Table E.19. Viscosity Data for Glass EWG-OL-6198

Temperature, °C	Viscosity, Pa·s	1/(T+273.15) × 10,000 , K^{-1}	ln η, Pa·s
1100	4.77	7.28	1.56
1000	12.23	7.86	2.50
900	31.26	8.53	3.44
1100	4.92	7.28	1.59

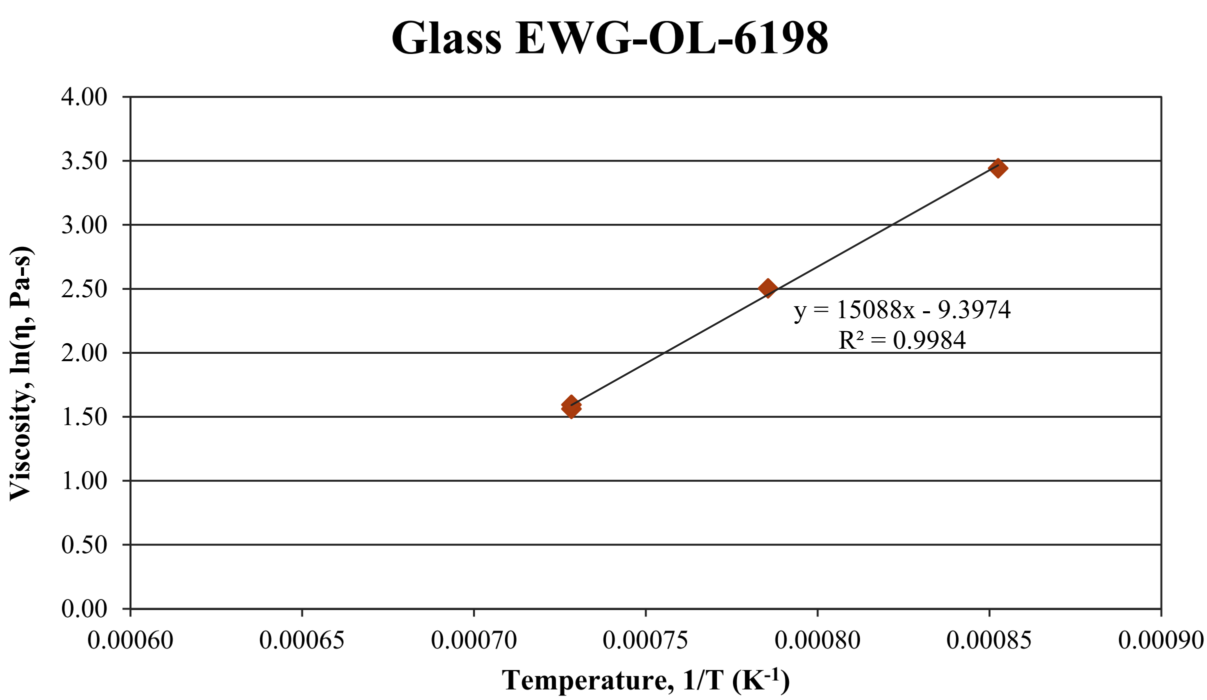

Figure E.19. Viscosity-Temperature Data and Arrhenius Equation Fit for Glass EWG-OL-6198

E.20 Glass EWG-OL-6311 Viscosity Data

Table E.20. Viscosity Data for Glass EWG-OL-6311

Temperature, °C	Viscosity, Pa·s	1/(T+273.15) × 10,000 , K^{-1}	ln η, Pa·s
1050	7.76	7.56	2.05
950	15.51	8.18	2.74
900	18.58	8.53	2.92
1050	8.23	7.56	2.11
1050	7.59	7.56	2.03
1050	7.59	7.56	2.03

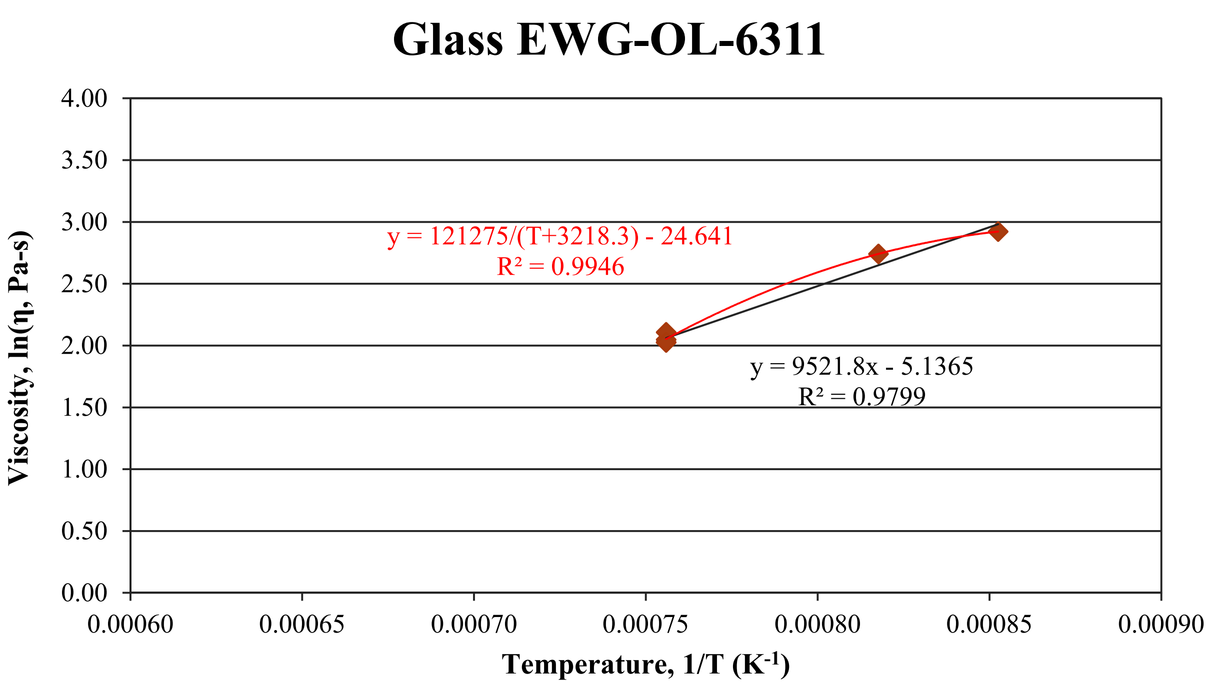

Figure E.20. Viscosity-Temperature Data and Arrhenius Equation Fit for Glass EWG-OL-6311

E.21 Glass EWG-OL-12707 Viscosity Data

Table E.21. Viscosity Data for Glass EWG-OL-12707

Temperature, °C	Viscosity, Pa·s	1/(T+273.15) × 10,000 , K^{-1}	ln η, Pa·s
1050	1.55	7.56	0.44
950	6.94	8.18	1.94
900	14.66	8.53	2.69
1050	1.49	7.56	0.40
1150	0.69	7.03	-0.37
1050	1.49	7.56	0.40

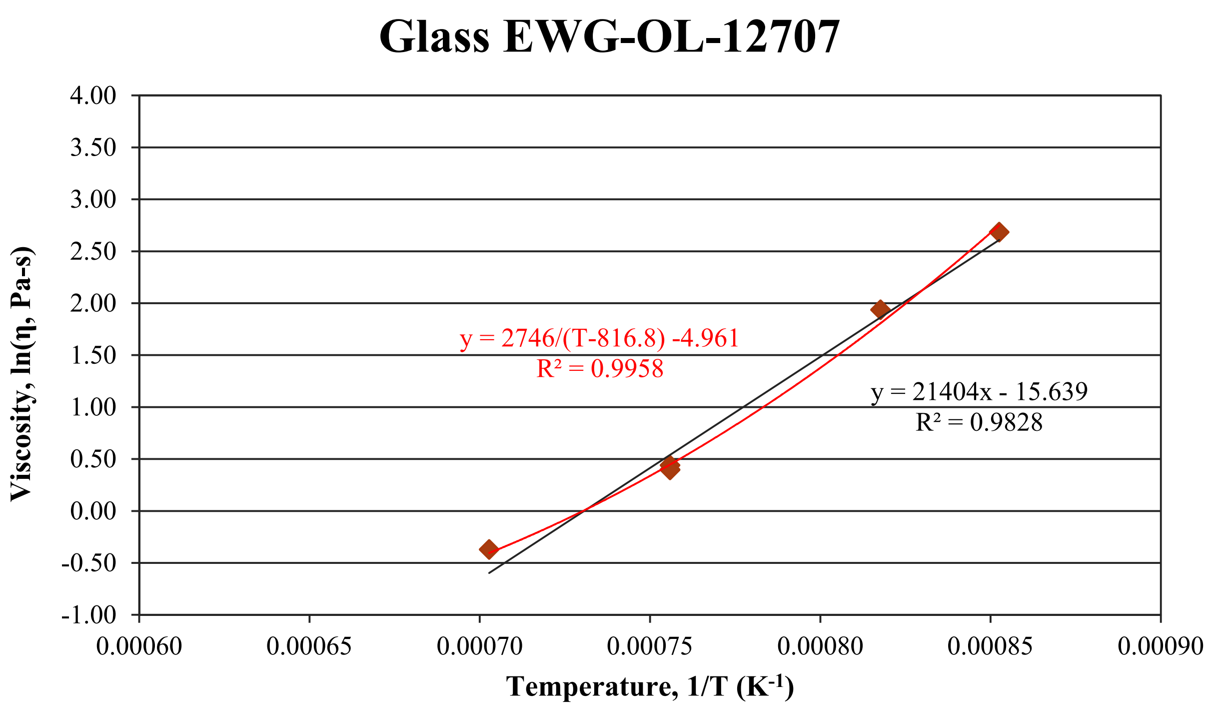

Figure E.21. Viscosity-Temperature Data and Arrhenius Equation Fit for Glass EWG-OL-12707

E.22 Glass EWG-OL-14827 Viscosity Data

Table E.22. Viscosity Data for Glass EWG-OL-14827

Temperature, °C	Viscosity, Pa·s	1/(T+273.15) × 10,000 , K^{-1}	ln η, Pa·s
980	3.02	7.98	1.10
900	7.34	8.53	1.99
850	15.00	8.90	2.71
975	3.18	8.01	1.16
1025	2.08	7.70	0.73
980	3.14	7.98	1.14

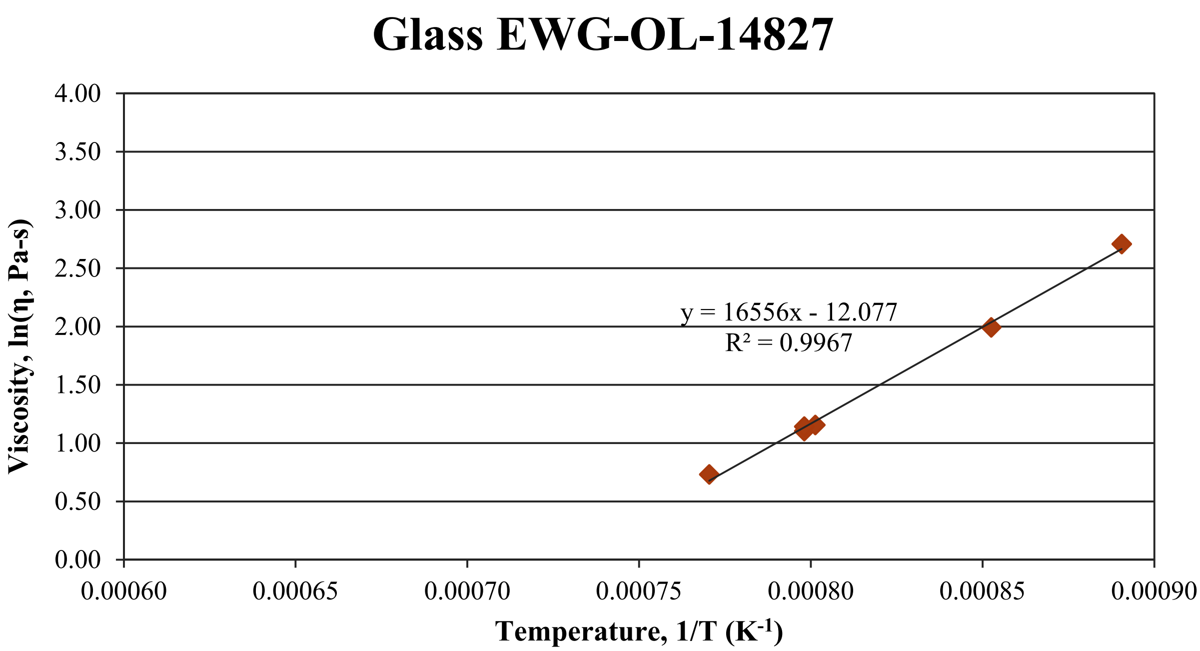

Figure E.22. Viscosity-Temperature Data and Arrhenius Equation Fit for Glass EWG-OL-14827

E.23 Glass EWG-OL-15968 Viscosity Data

Table E.23. Viscosity Data for Glass EWG-OL-15968

Temperature, °C	Viscosity, Pa·s	1/(T+273.15) × 10,000 , K^{-1}	ln η, Pa·s
1150	1.03	7.03	0.03
1050	1.90	7.56	0.64
950	4.32	8.18	1.46
1150	0.95	7.03	-0.05
1250	0.51	6.57	-0.68
1150	0.91	7.03	-0.09

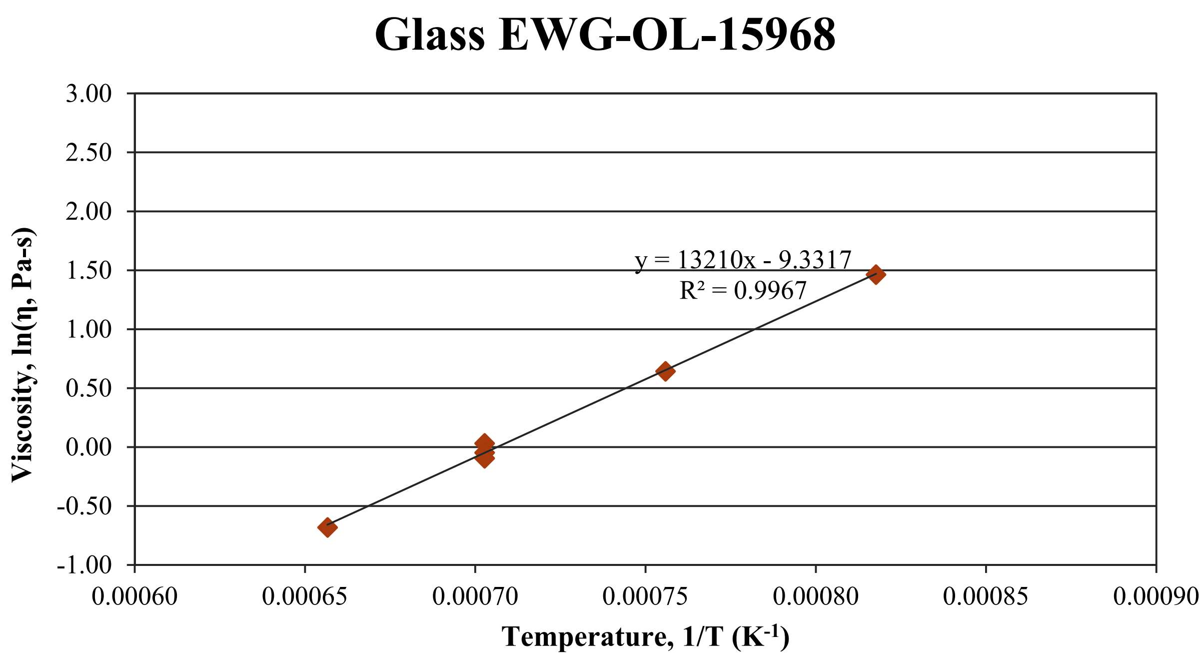

Figure E.23. Viscosity-Temperature Data and Arrhenius Equation Fit for Glass EWG-OL-15968

E.24 Glass EWG-OL-16450 Viscosity Data

Table E.24. Viscosity Data for EWG-OL-16450

Temperature, °C	Viscosity, Pa·s	1/(T+273.15) × 10,000 , K^{-1}	ln η, Pa·s
975	3.67	8.01	1.30
900	9.48	8.53	2.25
850	24.65	8.90	3.20
975	3.80	8.01	1.34
1025	2.39	7.70	0.87
975	3.98	8.01	1.38

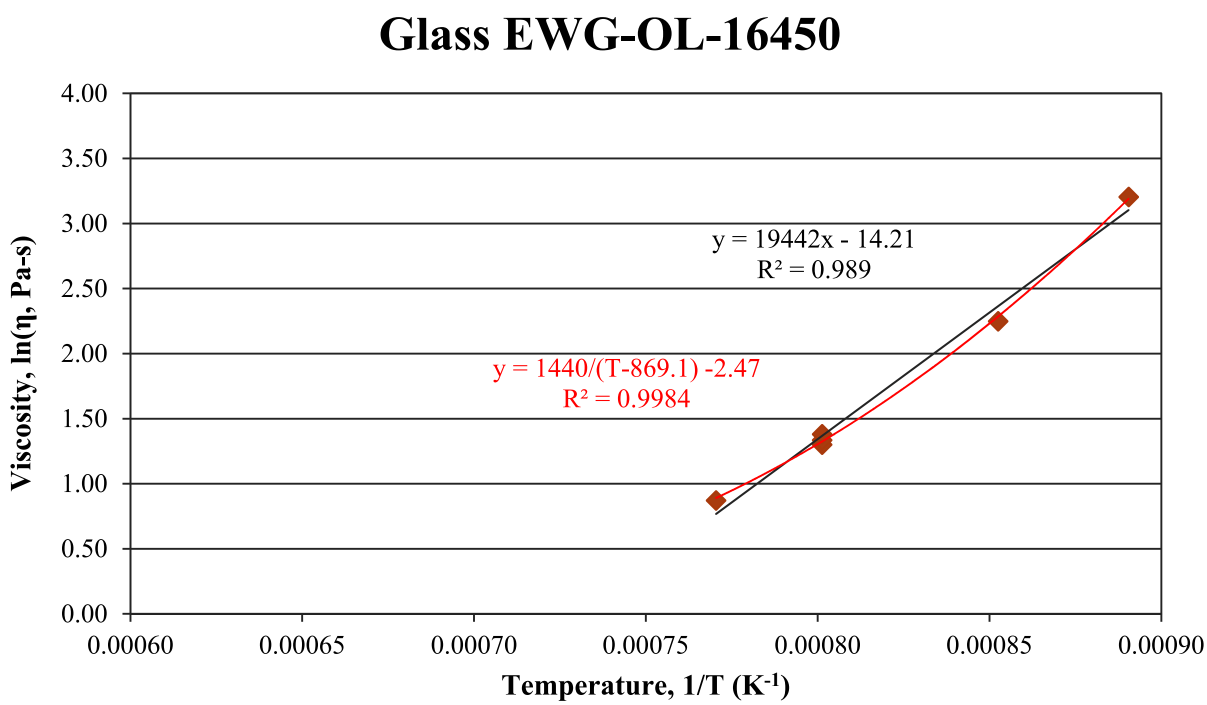

Figure E.24. Viscosity-Temperature Data and Arrhenius Equation Fit for Glass EWG-OL-16450

E.25 Glass EWG-OL-23401 Viscosity Data

Table E.25. Viscosity Data for Glass EWG-OL-23401

Temperature, °C	Viscosity, Pa·s	1/(T+273.15) × 10,000 , K^{-1}	ln η, Pa·s
1390	2.11	6.01	0.75
1300	4.34	6.36	1.47
1200	10.70	6.79	2.37
1100	31.61	7.28	3.45
1390	2.07	6.01	0.73

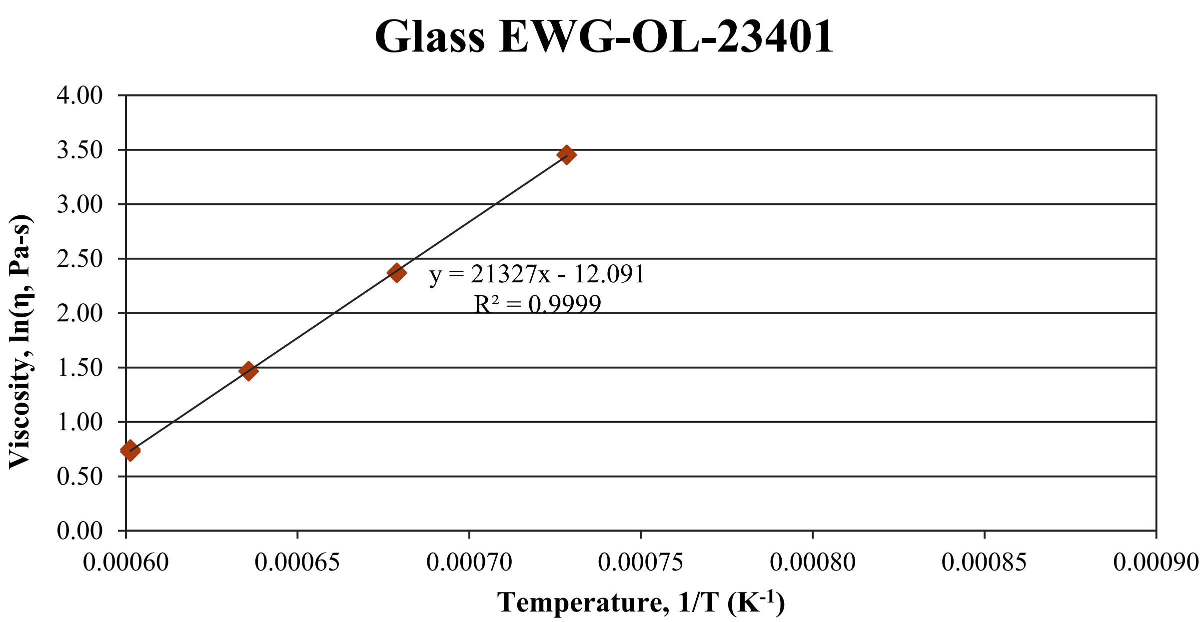

Figure E.25. Viscosity-Temperature Data and Arrhenius Equation Fit for Glass EWG-OL-23401

E.26 Glass EWG-OL-26012 Viscosity Data

Table E.26. Viscosity Data for Glass EWG-OL-26012

Temperature, °C	Viscosity, Pa·s	1/(T+273.15) × 10,000 , K^{-1}	ln η, Pa·s
1250	9.03	6.57	2.20
1150	21.08	7.03	3.05
1050	57.47	7.56	4.05
1250	9.14	6.57	2.21
1300	6.23	6.36	1.83
1250	9.17	6.57	2.22

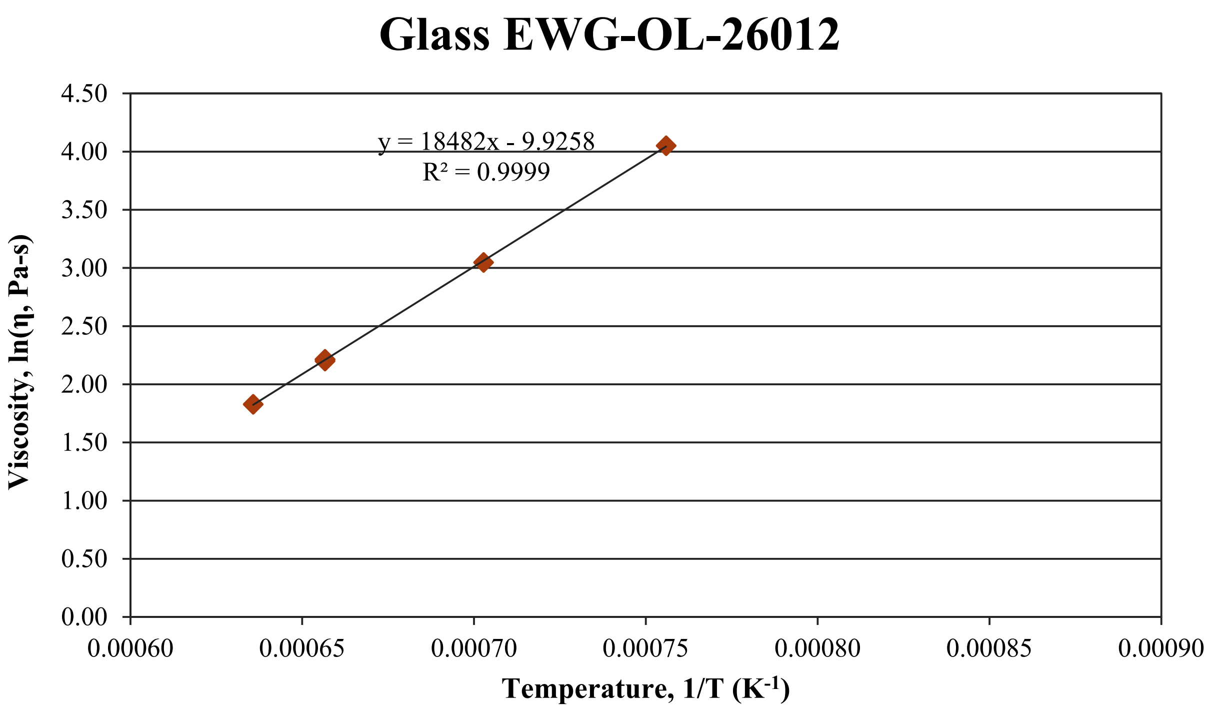

Figure E.26. Viscosity-Temperature Data and Arrhenius Equation Fit for Glass EWG-OL-26012

E.27 Glass EWG-OL-29285 Viscosity Data

Table E.27. Viscosity Data for Glass EWG-OL-29285

Temperature, °C	Viscosity, Pa·s	1/(T+273.15) × 10,000 , K^{-1}	ln η, Pa·s
1360	4.85	6.12	1.58
1260	8.05	6.52	2.09
1160	23.90	6.98	3.17
1360	3.20	6.12	1.16
1390	2.48	6.01	0.91
1360	3.15	6.12	1.15

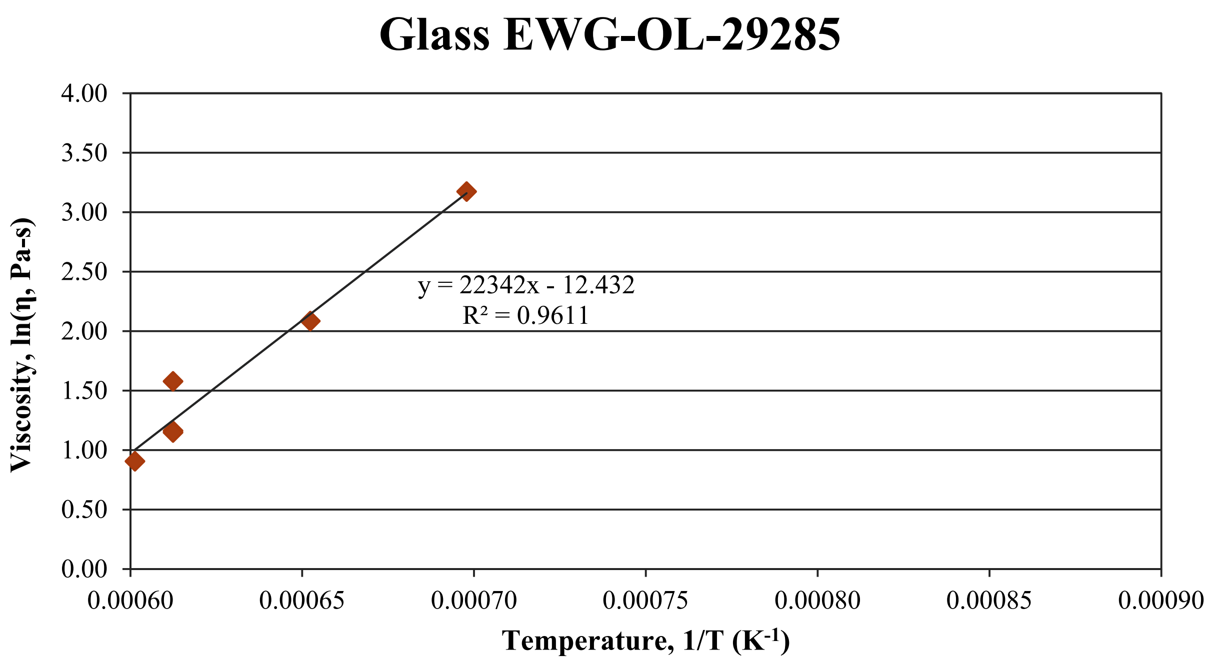

Figure E.27. Viscosity-Temperature Data and Arrhenius Equation Fit for Glass EWG-OL-29285

E.28 Glass EWG-OL-31644 Viscosity Data

Table E.28. Viscosity Data for Glass EWG-OL-31644

Temperature, °C	Viscosity, Pa·s	1/(T+273.15) × 10,000 , K^{-1}	ln η, Pa·s
1375	3.29	6.07	1.19
1275	7.98	6.46	2.08
1175	17.84	6.91	2.88
1375	4.00	6.07	1.39

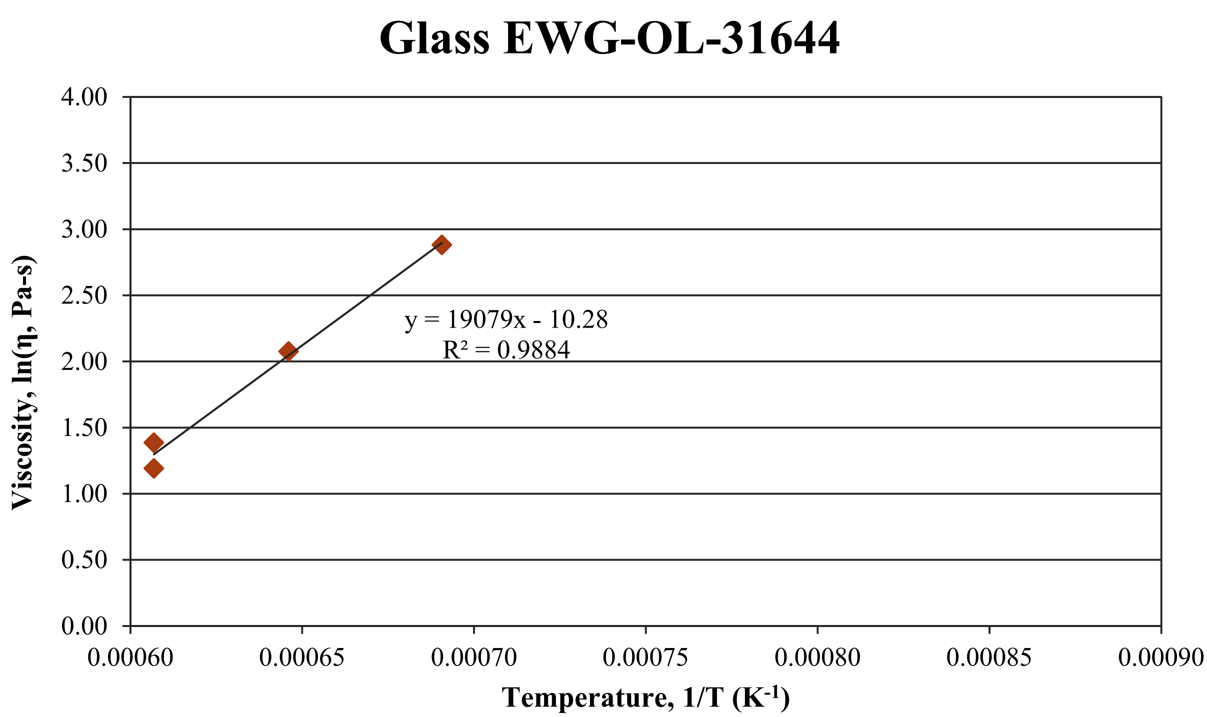

Figure E.28. Viscosity-Temperature Data and Arrhenius Equation Fit for Glass EWG-OL-31644

E.29 Glass EWG-OL-32706 Viscosity Data

Table E.29. Viscosity Data for Glass EWG-OL-32706

Temperature, °C	Viscosity, Pa·s	1/(T+273.15) × 10,000 , K^{-1}	ln η, Pa·s
1390	4.61	6.01	1.53
1300	9.41	6.36	2.24
1200	23.07	6.79	3.14
1100	76.05	7.28	4.33
1390	4.61	6.01	1.53

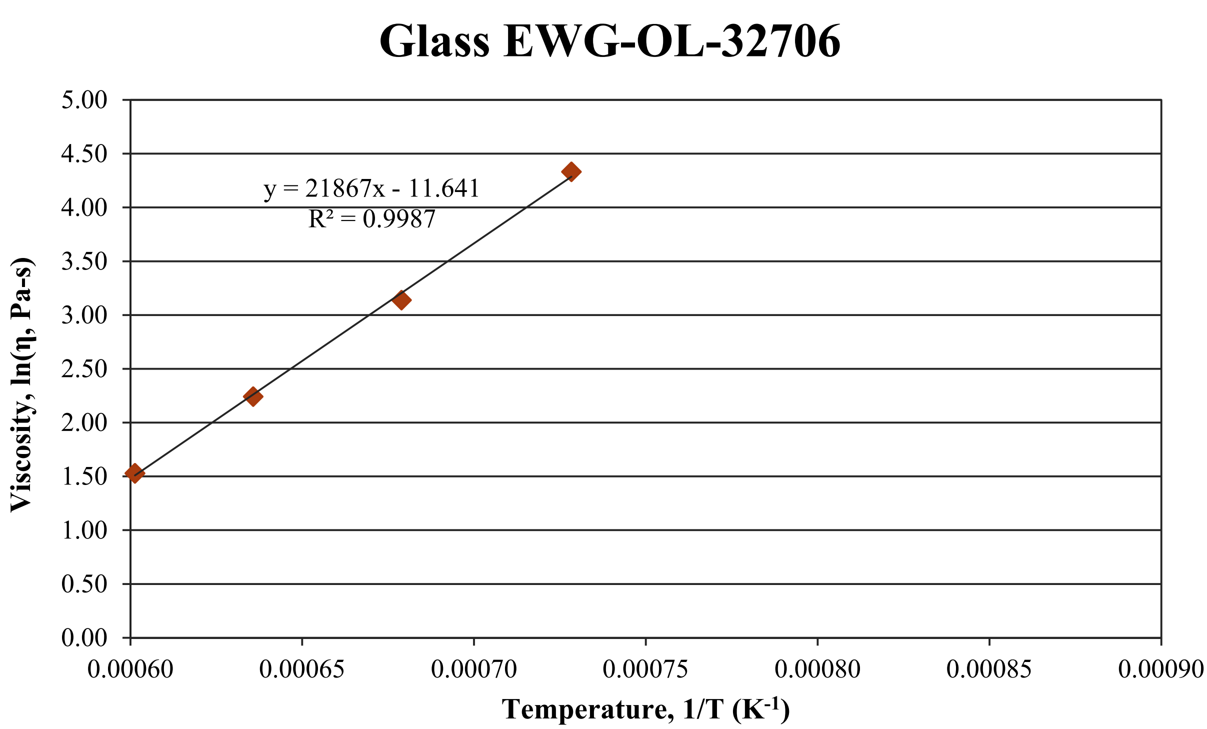

Figure E.29. Viscosity-Temperature Data and Arrhenius Equation Fit for Glass EWG-OL-32706

E.30 Glass EWG-OL-33115 Viscosity Data

Table E.30. Viscosity Data for Glass EWG-OL-33115

Temperature, °C	Viscosity, Pa·s	1/(T+273.15) × 10,000 , K^{-1}	ln η, Pa·s
1300	3.22	6.36	1.17
1200	8.35	6.79	2.12
1100	32.89	7.28	3.49
1300	3.17	6.36	1.15

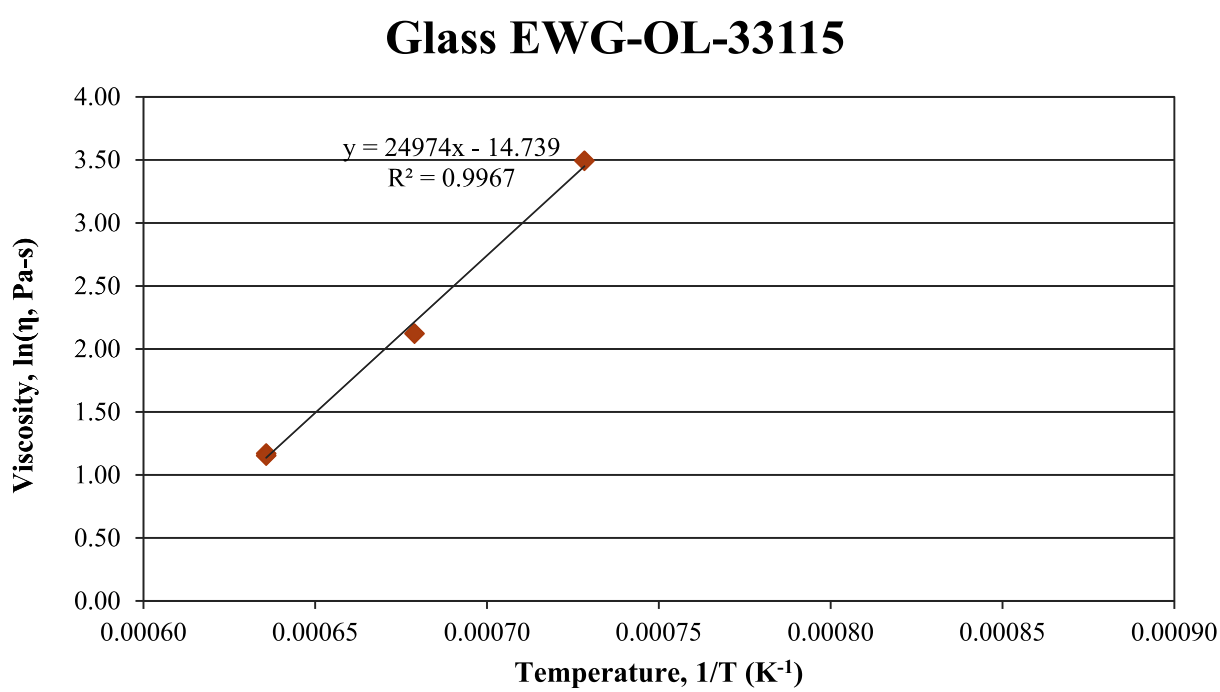

Figure E.30. Viscosity -Temperature Data and Arrhenius Equation Fit for Glass EWG-OL-33115

E.31 Glass EWG-OL-33558 Viscosity Data

Table E.31. Viscosity Data for Glass EWG-OL-33558

Temperature, °C	Viscosity, Pa·s	1/(T+273.15) × 10,000 , K^{-1}	ln η, Pa·s
1350	1.92	6.16	0.65
1250	4.70	6.57	1.55
1150	13.80	7.03	2.62
1350	1.93	6.16	0.66

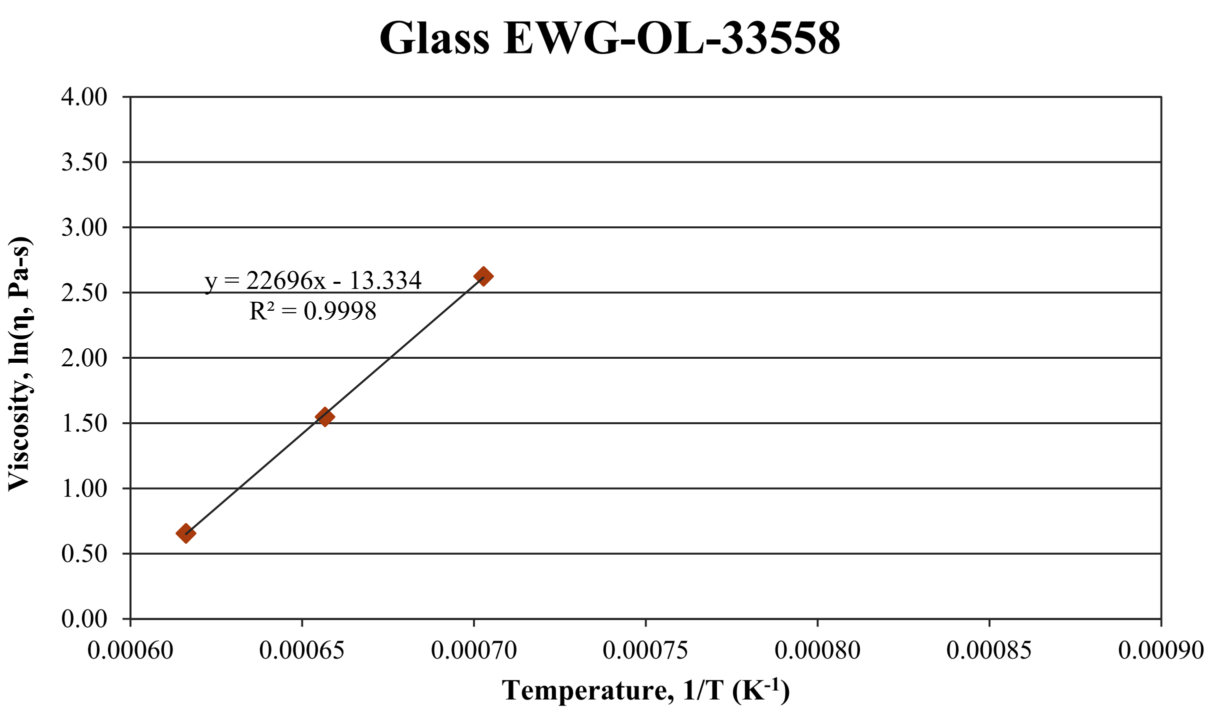

Figure E.31. Viscosity-Temperature Data and Arrhenius Equation Fit for Glass EWG-OL-33558

E.32 Glass EWG-OL-33694 Viscosity Data

Table E.32. Viscosity Data for Glass EWG-OL-33694

Temperature, °C	Viscosity, Pa·s	1/(T+273.15) × 10,000 , K^{-1}	ln η, Pa·s
1390	6.70	6.01	1.90
1300	14.41	6.36	2.67
1200	38.05	6.79	3.64
1100	115.00	7.28	4.74
1390	6.71	6.01	1.90

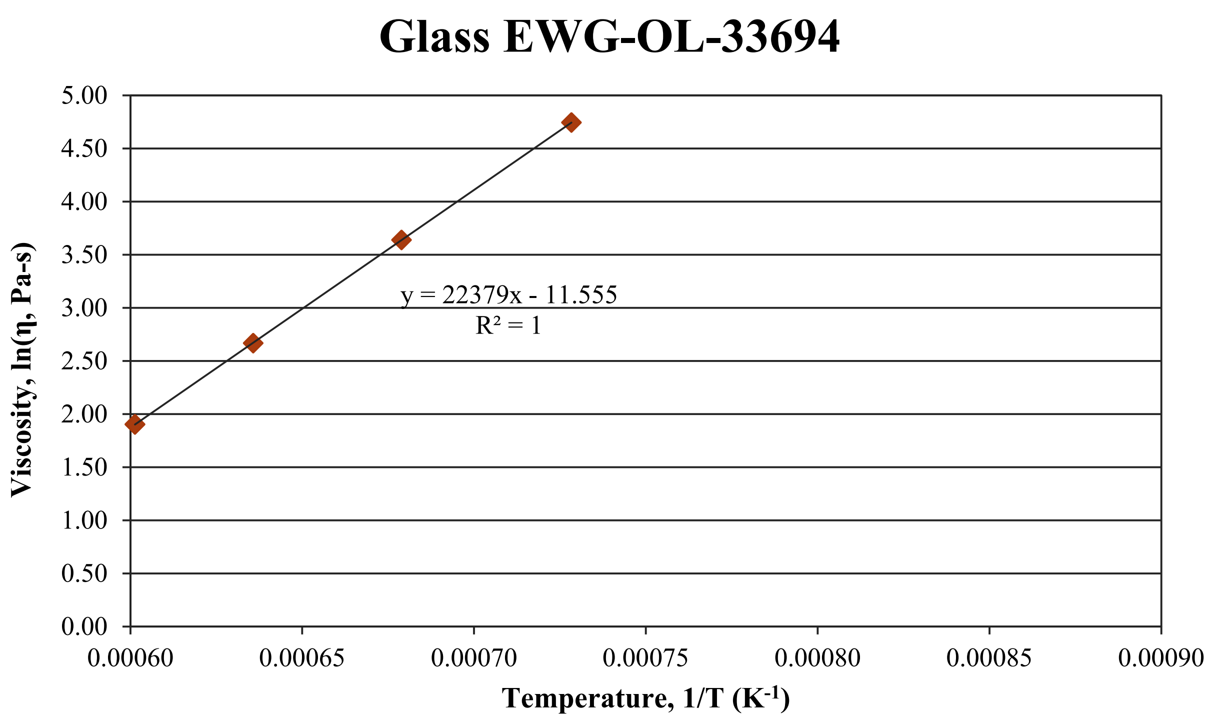

Figure E.32. Viscosity-Temperature Data and Arrhenius Equation Fit for Glass EWG-OL-33694

E.33 Glass EWG-OL-33858 Viscosity Data

Table E.33. Viscosity Data for Glass EWG-OL-33858

Temperature, °C	Viscosity, Pa·s	1/(T+273.15) × 10,000 , K^{-1}	ln η, Pa·s
1300	3.28	6.36	1.19
1200	7.75	6.79	2.05
1100	21.50	7.28	3.07
1300	3.30	6.36	1.19
1390	1.59	6.01	0.46
1300	3.27	6.36	1.18

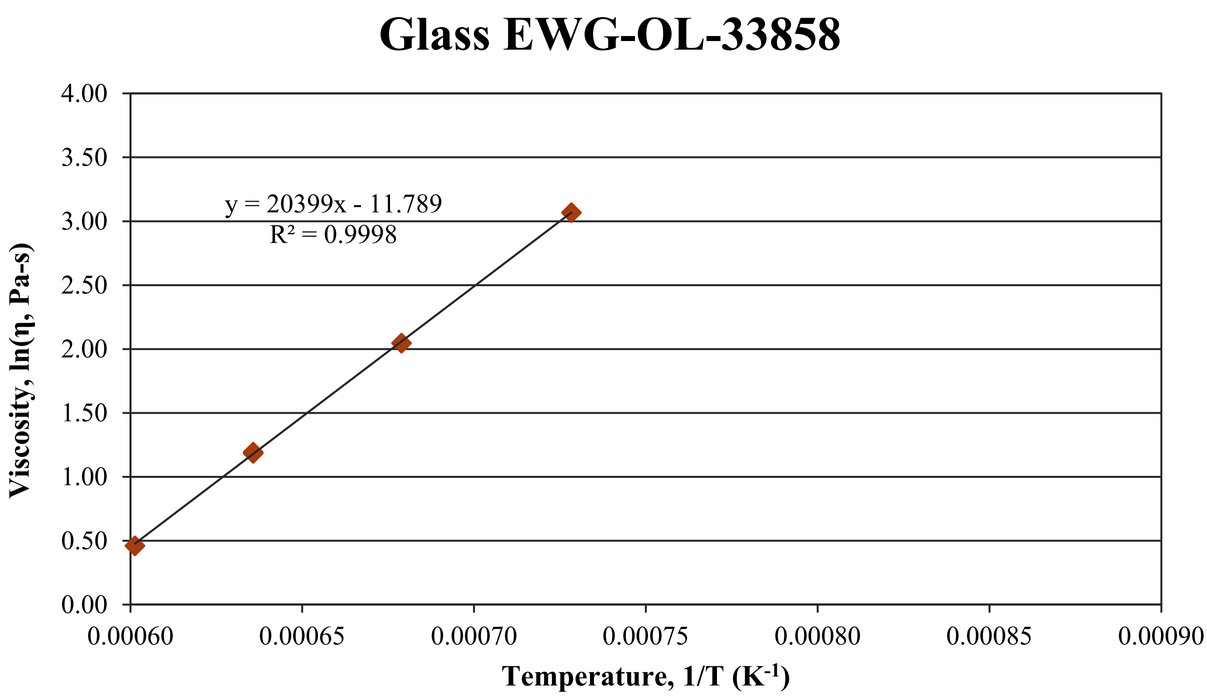

Figure E.33. Viscosity-Temperature Data and Arrhenius Equation Fit for Glass EWG-OL-33858

E.34 Glass EWG-OL-35387 Viscosity Data

Table E.34. Viscosity Data for Glass EWG-OL-35387

Temperature, °C	Viscosity, Pa·s	1/(T+273.15) × 10,000 , K^{-1}	ln η, Pa·s
1350	4.38	6.16	1.48
1250	9.36	6.57	2.24
1150	21.98	7.03	3.09
1350	4.42	6.16	1.49
1390	3.25	6.01	1.18
1350	4.48	6.16	1.50

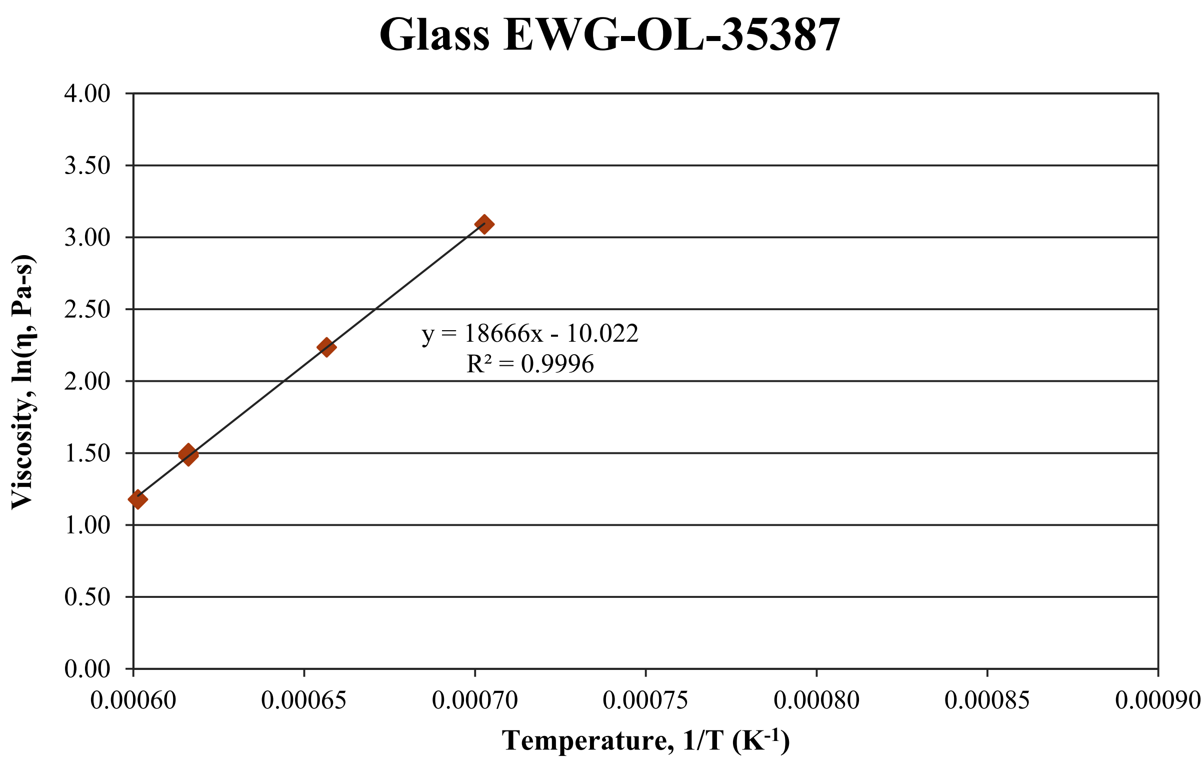

Figure E.34. Viscosity-Temperature Data and Arrhenius Equation Fit for Glass EWG-OL-35387

E.35 Glass EWG-OL-38081 Viscosity Data

Table E.35. Viscosity Data for Glass EWG-OL-38081

Temperature, °C	Viscosity, Pa·s	1/(T+273.15) × 10,000 , K^{-1}	ln η, Pa·s
1350	8.24	6.16	2.11
1250	7.24	6.57	1.98
1150	20.83	7.03	3.04
1350	4.43	6.16	1.49
1390	3.66	6.01	1.30
1350	3.45	6.16	1.24

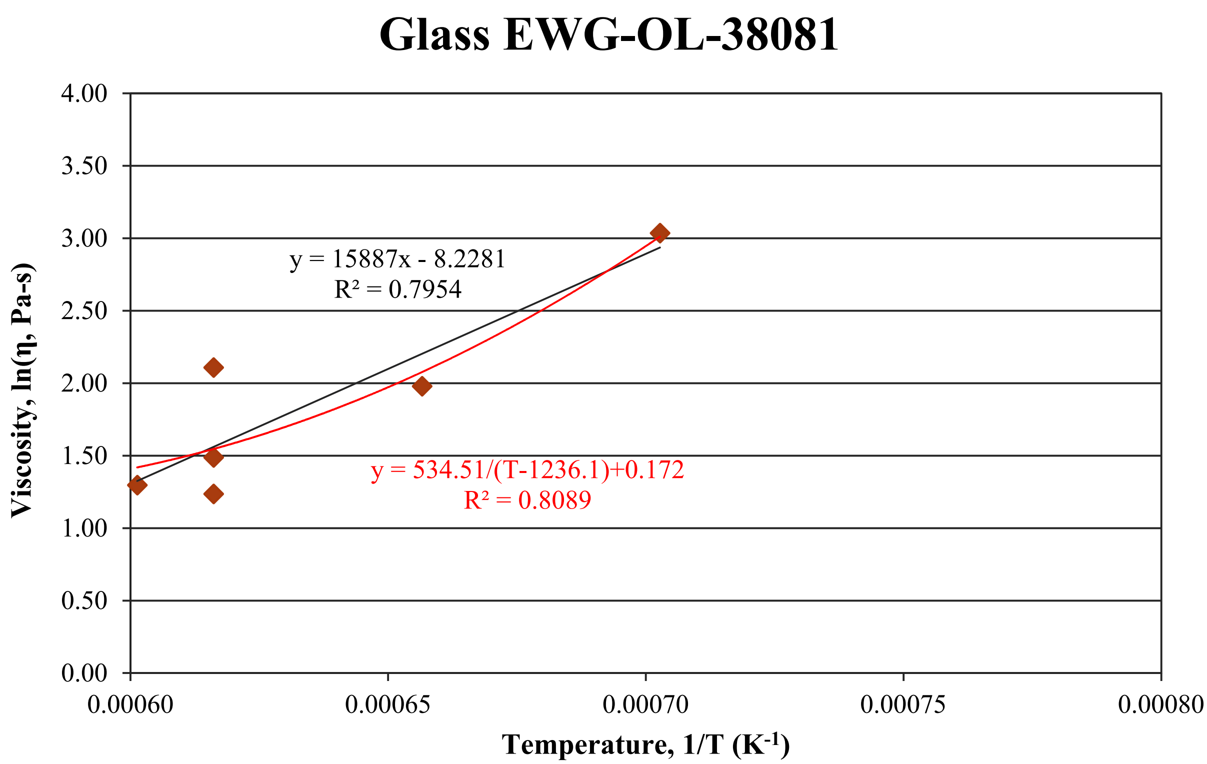

Figure E.35. Viscosity-Temperature Data and Arrhenius Equation Fit for Glass EWG-OL-38081

E.36 Glass EWG-OL-38552 Viscosity Data

Table E.36. Viscosity Data for Glass EWG-OL-38552

Temperature, °C	Viscosity, Pa·s	1/(T+273.15) × 10,000 , K^{-1}	ln η, Pa·s
1250	3.72	6.57	1.31
1150	11.38	7.03	2.43
1050	41.41	7.56	3.72
1250	3.77	6.57	1.33

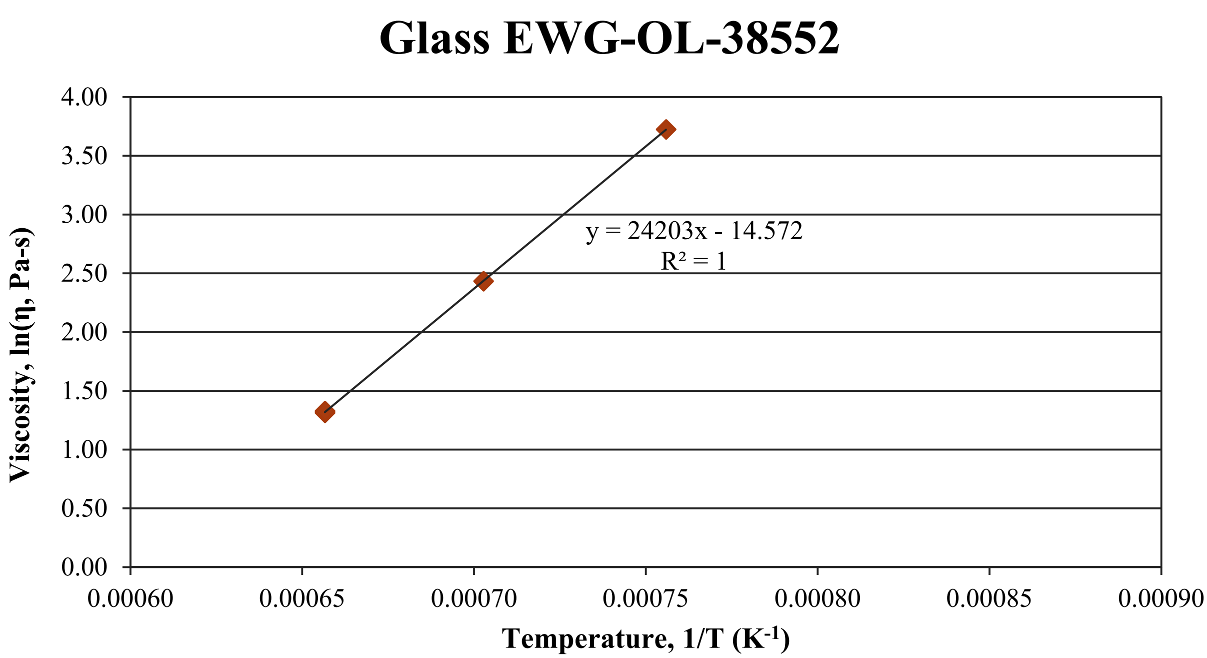

Figure E.36. Viscosity-Temperature Data and Arrhenius Equation Fit for Glass EWG-OL-38552

E.37 Glass EWG-OL-1755 Mod 8% Fe 10% B Viscosity Data

Table E.37. Viscosity Data for Glass EWG-OL-1755 Mod 8% Fe 10% B

Temperature, °C	Viscosity, Pa·s	1/(T+273.15) × 10,000 , K^{-1}	ln η, Pa·s
1275	4.19	6.46	1.43
1175	10.19	6.91	2.32
1075	24.10	7.42	3.18
1275	4.28	6.46	1.45

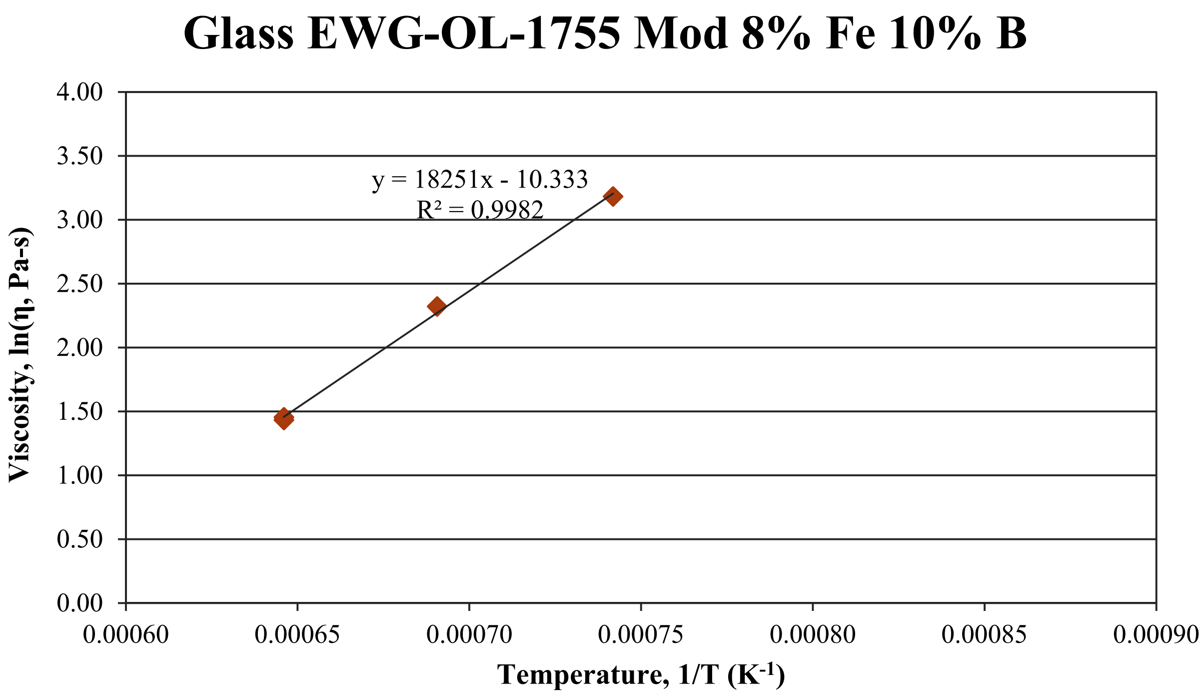

Figure E.37. Viscosity-Temperature Data and Arrhenius Equation Fit for Glass EWG-OL-1755 Mod 8% Fe 10% B

E.38 Glass EWG-OL-3063 Mod 1% Zr 3% Li Viscosity Data

Table E.38. Viscosity Data for Glass EWG-OL-3063 Mod 1% Zr 3% Li

Temperature, °C	Viscosity, Pa·s	1/(T+273.15) × 10,000 , K^{-1}	ln η, Pa·s
1375	2.02	6.07	0.70
1275	3.91	6.46	1.36
1175	8.30	6.91	2.12
1375	1.83	6.07	0.61

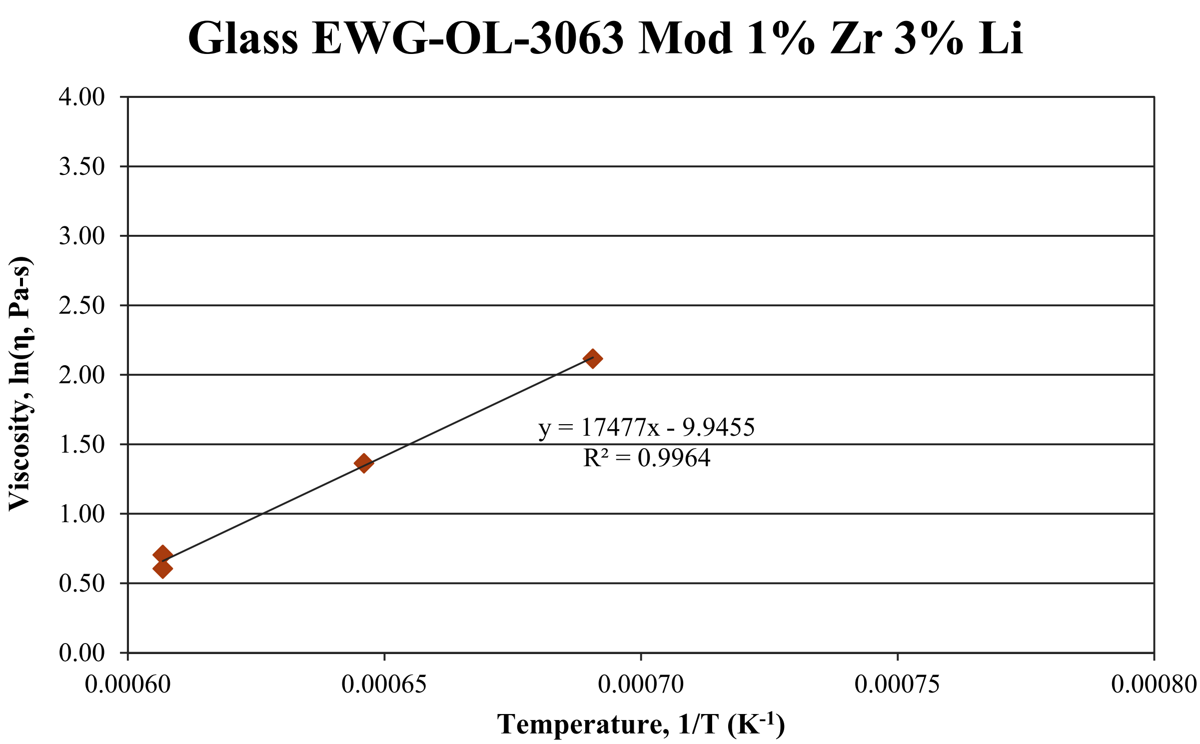

Figure E.38. Viscosity-Temperature Data and Arrhenius Equation Fit for Glass EWG-OL-3063 Mod 1% Zr 3% Li

E.39 Glass EWG-OL-4744 Mod 7.5% Fe 1% Zr Viscosity Data

Table E.39. Viscosity Data for Glass EWG-OL-4744 Mod 7.5% Fe 1% Zr

Temperature, °C	Viscosity, Pa·s	1/(T+273.15) × 10,000 , K^{-1}	ln η, Pa·s
1250	2.08	6.57	0.73
1150	4.60	7.03	1.53
1050	13.10	7.56	2.57
1250	1.98	6.57	0.68

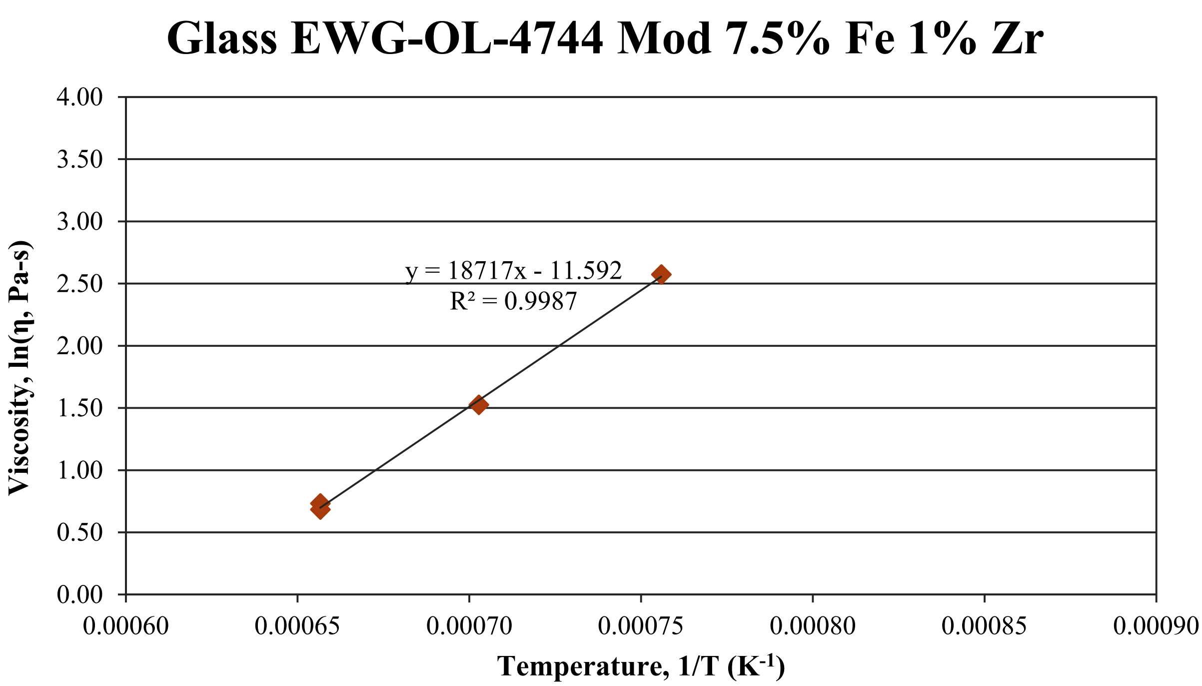

Figure E.39. Viscosity-Temperature Data and Arrhenius Equation Fit for Glass EWG-OL-4744 Mod 7.5% Fe 1% Zr

E.40 Glass EWG-OL-5385 Mod 12% B 17% Na Viscosity Data

Table E.40. Viscosity Data for Glass EWG-OL-5385 Mod 12% B 17% Na

Temperature, °C	Viscosity, Pa·s	1/(T+273.15) × 10,000 , K^{-1}	ln η, Pa·s
1225	1.88	6.68	0.63
1125	2.77	7.15	1.02
1025	6.76	7.70	1.91
1225	1.66	6.68	0.51
1325	1.43	6.26	0.36
1225	1.86	6.68	0.62

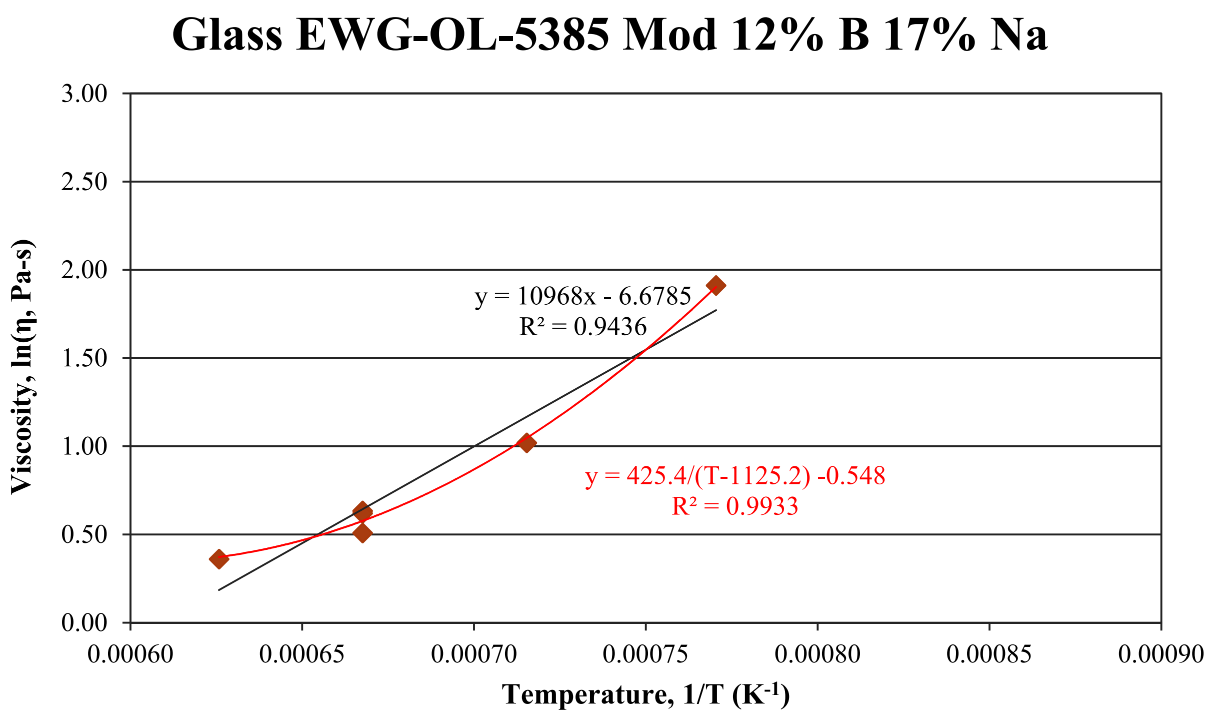

Figure E.40. Viscosity-Temperature Data and Arrhenius Equation Fit for Glass EWG-OL-5385Mod 12% B 17% Na

E.41 Glass EWG-OL-6257 Mod 12% B 8% Ca Viscosity Data

Table E.41. Viscosity Data for Glass EWG-OL-6257 Mod 12% B 8% Ca

Temperature, °C	Viscosity, Pa·s	1/(T+273.15) × 10,000 , K^{-1}	ln η, Pa·s
1225	4.98	6.68	1.61
1125	11.01	7.15	2.40
1025	27.94	7.70	3.33
1225	5.38	6.68	1.68

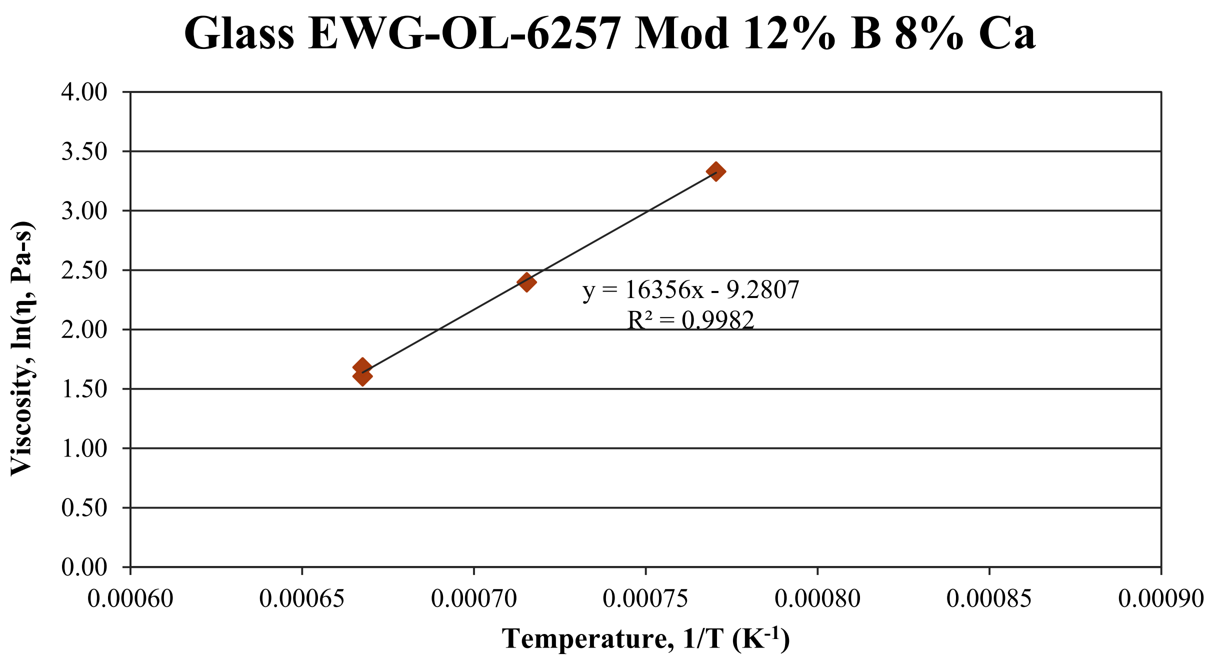

Figure E.41. Viscosity-Temperature Data and Arrhenius Equation Fit for Glass EWG-OL-6257 Mod 12% B 8% Ca

E.42 Glass EWG-OL-6311 Mod Reduced Na & K Viscosity Data

Table E.42. Viscosity Data for Glass EWG-OL-6311 Mod Reduced Na and K

Temperature, °C	Viscosity, Pa·s	1/(T+273.15) × 10,000 , K^{-1}	ln η, Pa·s
1125	3.39	7.15	1.22
1025	8.22	7.70	2.11
925	18.60	8.35	2.92
1125	3.67	7.15	1.30
1225	1.73	6.68	0.55
1125	4.15	7.15	1.42

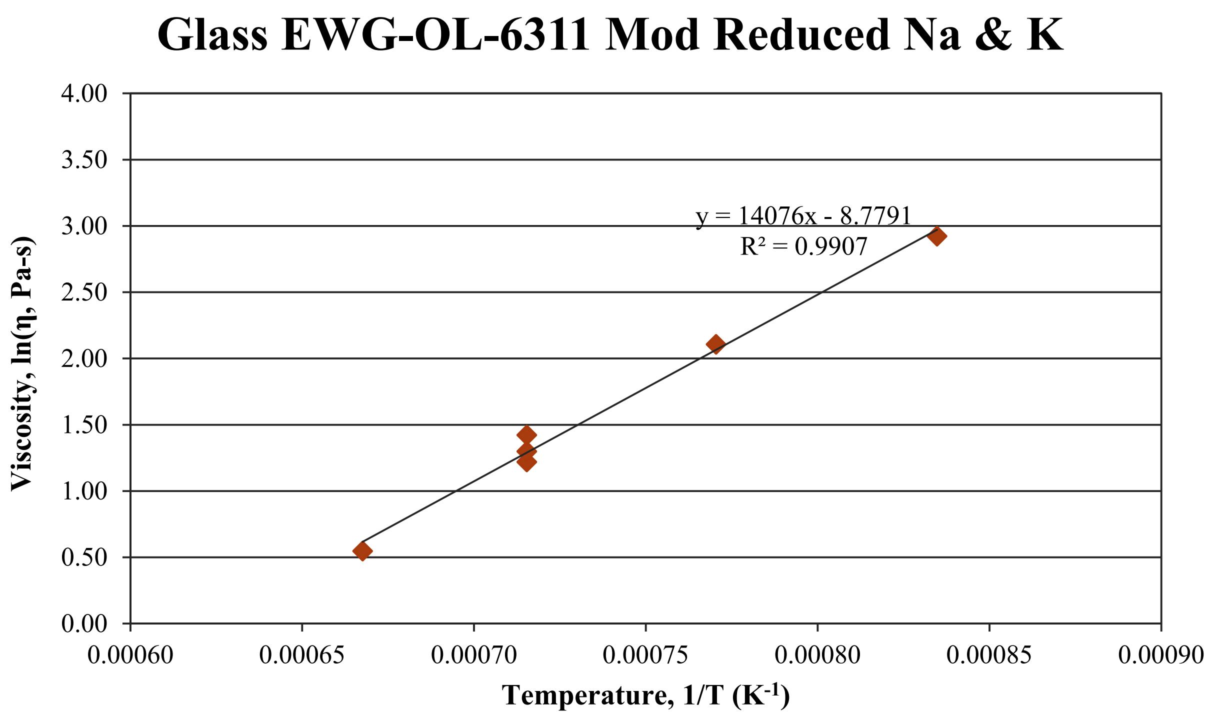

Figure E.42. Viscosity-Temperature Data and Arrhenius Equation Fit for Glass EWG-OL-6311 Mod Reduced Na and K

E.43 Glass EWG-OL-6489 Mod 11% B 15% Na Viscosity Data

Table E.43. Viscosity Data for Glass EWG-OL-6489 Mod 11% B 15% Na

Temperature, °C	Viscosity, Pa·s	1/(T+273.15) × 10,000 , K^{-1}	ln η, Pa·s
1200	10.79	6.79	2.38
1100	24.34	7.28	3.19
1000	56.82	7.86	4.04
1200	14.16	6.79	2.65
1300	8.06	6.36	2.09
1200	15.60	6.79	2.75

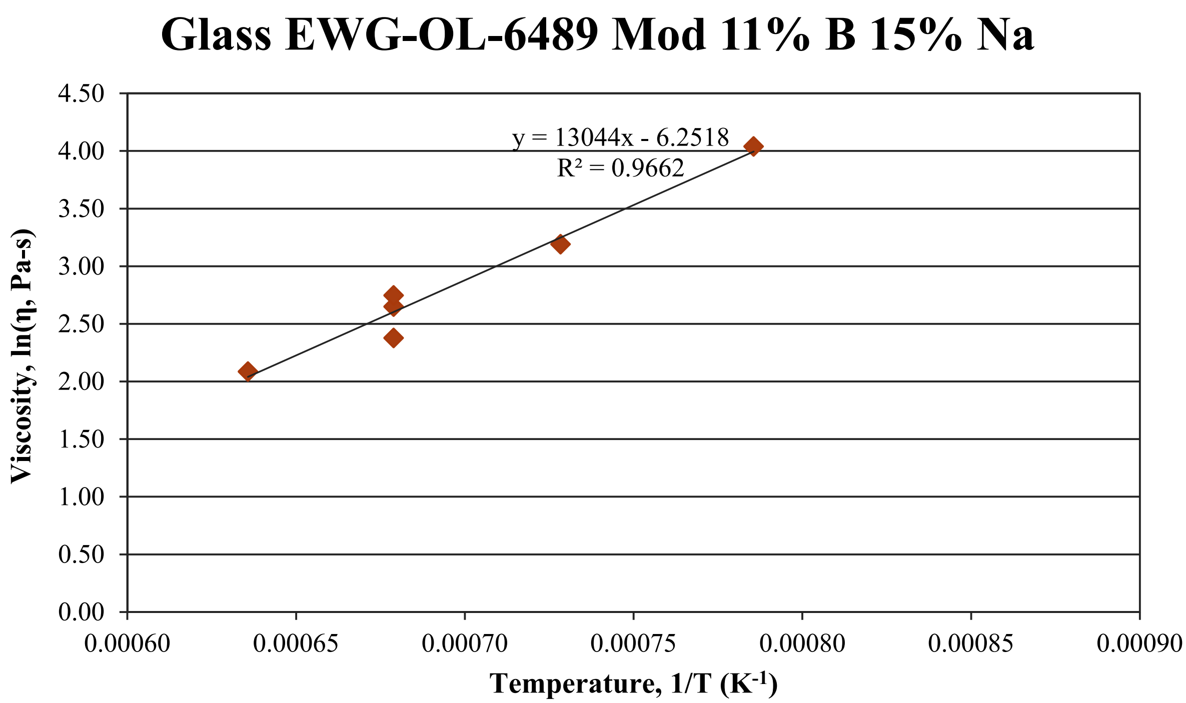

Figure E.43. Viscosity-Temperature Data and Arrhenius Equation Fit for Glass EWG-OL-6489 Mod 11% B 15% Na

E.44 Glass EWG-OL-8548 Mod 1% Zr Viscosity Data

Table E.44. Viscosity Data for Glass EWG-OL-8548 Mod 1% Zr

Temperature, °C	Viscosity, Pa·s	1/(T+273.15) × 10,000 , K^{-1}	ln η, Pa·s
1300	13.16	6.36	2.58
1200	40.02	6.79	3.69
1100	117.00	7.28	4.76
1300	10.93	6.36	2.39

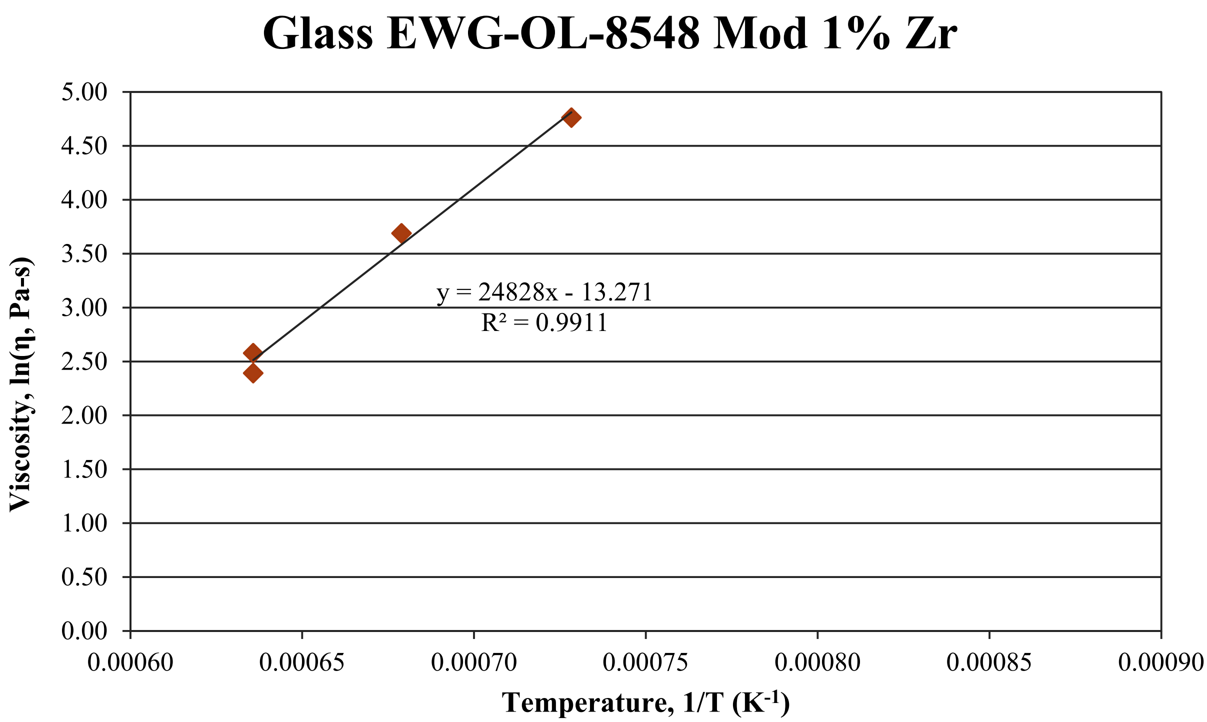

Figure E.44. Viscosity-Temperature Data and Arrhenius Equation Fit for Glass EWG-OL-8548 Mod 1% Zr

E.45 Glass EWG-OL-10278 Mod 15% B 1% Zr Viscosity Data

Table E.45. Viscosity Data for Glass EWG-OL-10278 Mod 15% B 1% Zr

Temperature, °C	Viscosity, Pa·s	1/(T+273.15) × 10,000 , K^{-1}	ln η, Pa·s
1025	3.86	7.70	1.35
950	8.32	8.18	2.12
850	29.33	8.90	3.38
1025	3.85	7.70	1.35
1125	1.67	7.15	0.51
1025	3.88	7.70	1.36

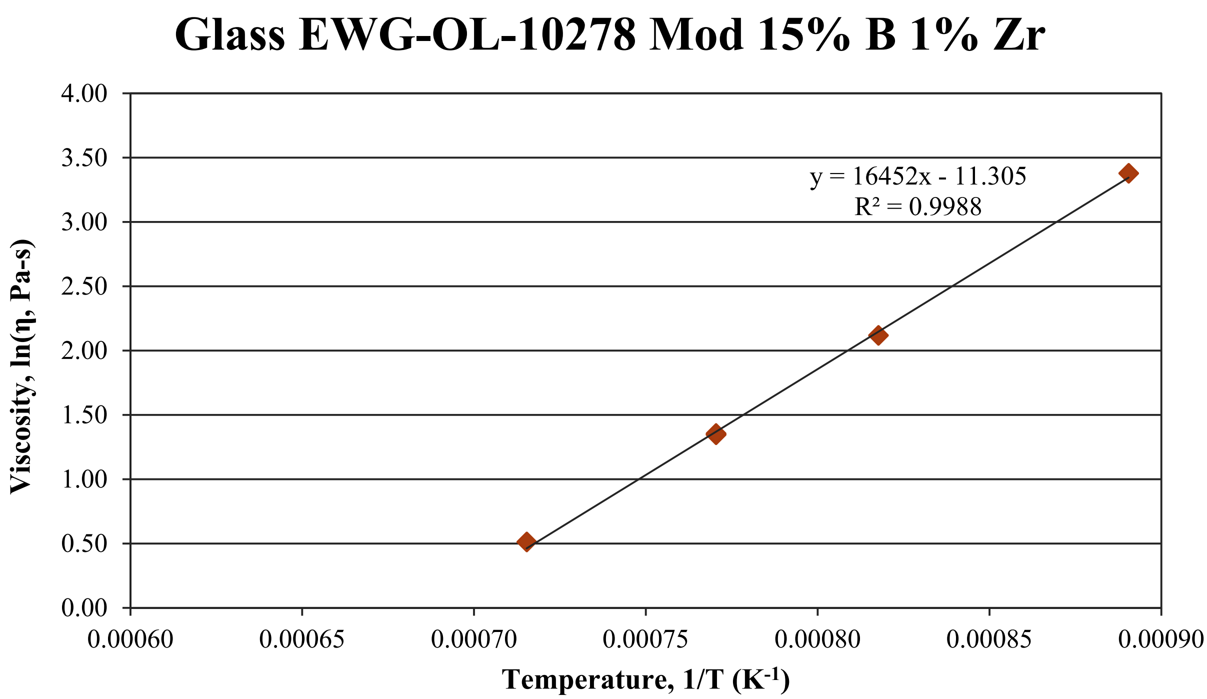

Figure E.45. Viscosity-Temperature Data and Arrhenius Equation Fit for Glass EWG-OL-10278 Mod 15% B 1% Zr

E.46 Glass EWG-OL-11318 Mod 1% Zr Viscosity Data

Table E.46. Viscosity Data for Glass EWG-OL-11318 Mod 1% Zr

Temperature, °C	Viscosity, Pa·s	1/(T+273.15) × 10,000 , K^{-1}	ln η, Pa·s
1250	5.57	6.57	1.72
1150	12.25	7.03	2.51
1050	32.01	7.56	3.47
1250	5.50	6.57	1.70
1300	3.86	6.36	1.35
1250	5.57	6.57	1.72

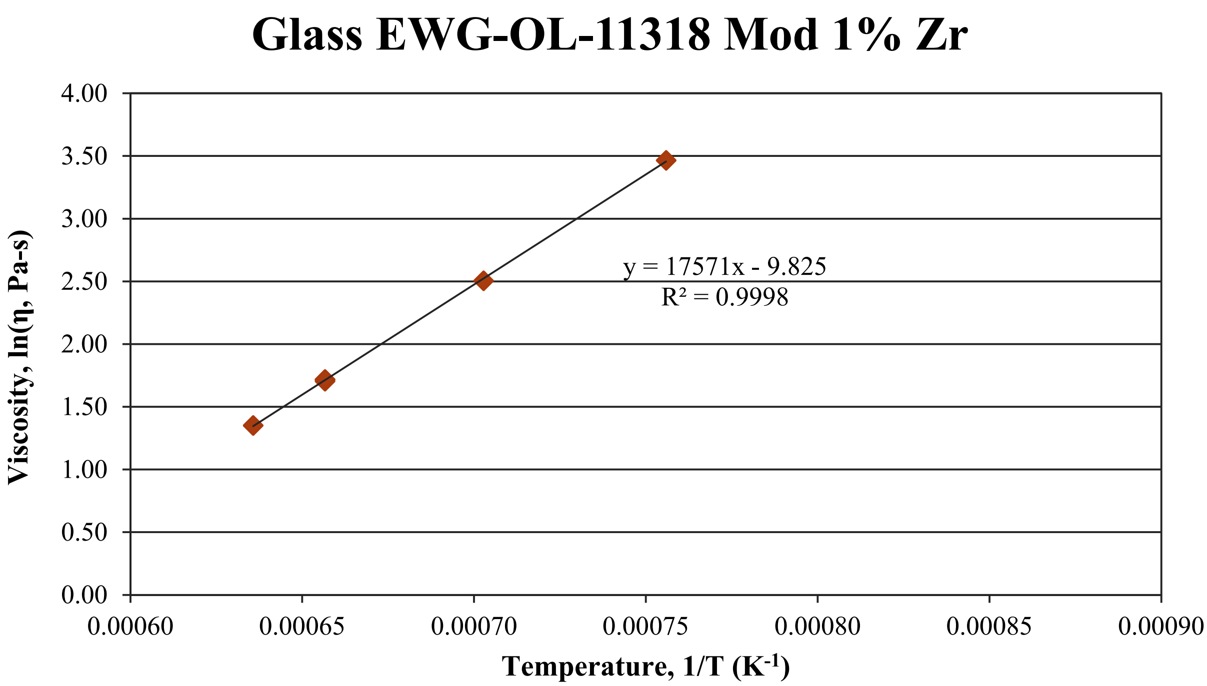

Figure E.46. Viscosity-Temperature Data and Arrhenius Equation Fit for Glass EWG-OL-11318 Mod 1% Zr

E.47 Glass EWG-OL-14547 Mod Reduced Alkali 1% Zr Viscosity Data

Table E.47. Viscosity Data for Glass EWG-OL-14547 Mod Reduced Alkali 1% Zr

Temperature, °C	Viscosity, Pa·s	1/(T+273.15) × 10,000 , K^{-1}	ln η, Pa·s
1125	1.53	7.15	0.43
1025	3.73	7.70	1.32
925	15.07	8.35	2.71
1125	1.63	7.15	0.49

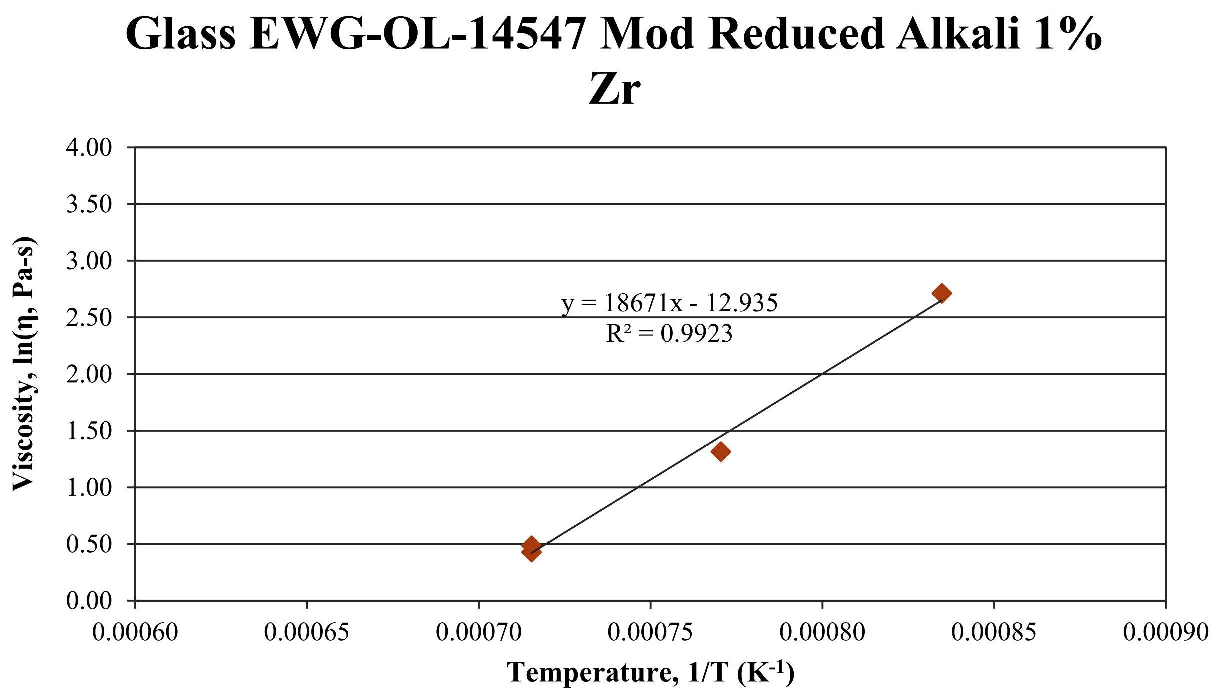

Figure E.47. Viscosity-Temperature Data and Arrhenius Equation Fit for Glass EWG-OL-14547 Mod Reduced Alkali 1% Zr

E.48 Glass EWG-OL-15698 Mod Low Na Viscosity Data

Table E.48. Viscosity Data for Glass EWG-OL-15698 Mod Low Na

Temperature, °C	Viscosity, Pa·s	1/(T+273.15) × 10,000 , K^{-1}	ln η, Pa·s
1050	4.14	7.56	1.42
950	13.30	8.18	2.59
900	24.25	8.53	3.19
1050	3.41	7.56	1.23

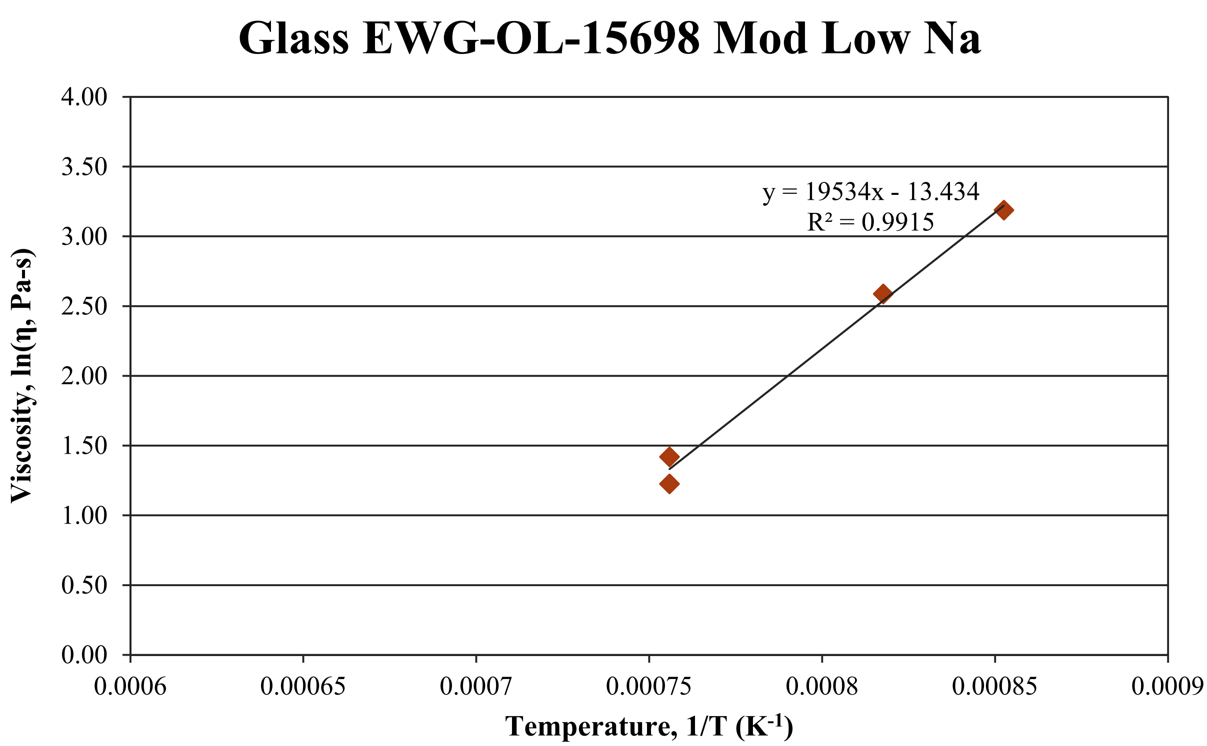

Figure E.48. Viscosity-Temperature Data and Arrhenius Equation Fit for Glass EWG-OL-15698 Mod Low Na

Appendix F

Electrical Conductivity Data and Plots

Appendix F

Electrical Conductivity Data and Plots

This appendix contains the measured electrical conductivity data for each of the glasses in this matrix. The plots shown in this appendix are fitted to the Arrhenius equation (Eq. F.1):

$$\ln(\varepsilon) = A + \frac{B}{T_K} \quad \text{(F.1)}$$

where *A* and *B* are independent of temperature and temperature (T_K) is in K (T(°C) + 273.15). However, some of the plots showed curvature and would be better fit to the Vogel -Fulcher-Tamman (VFT) model (Equation F.2)

$$\ln(\varepsilon) = \text{E} + \frac{\text{F}}{T_K - T_0} \quad \text{(F.2)}$$

where *E*, *F*, and T_0 are temperature independent and composition dependent coefficients and T_K is in K (T(°C) + 273.15). The intent of the figures and Arrhenius equation fits shown in this appendix are mainly to assess trends of the data and provide some observations about whether there may be sufficient curvature in the data to consider VFT fits in the subsequent work that will decide between fitting the data to the Arrhenius or VFT equations for the electrical conductivity-temperature data for each glass that is being made in subsequent work.

F.1 Glass EWG-HAI-Centroid-1 Electrical Conductivity Data

Table F.1. Electrical Conductivity Data for Glass EWG-HAI-Centroid-1

Temperature, °C	Conductivity, S/m	1/(T+273.15), K^{-1}	ln ε (S/m)
850	6.23	0.00089	1.83
850	6.28	0.00089	1.84
1150	27.60	0.00070	3.32
1050	19.33	0.00076	2.96
1050	19.38	0.00076	2.96
950	11.91	0.00082	2.48
950	11.97	0.00082	2.48

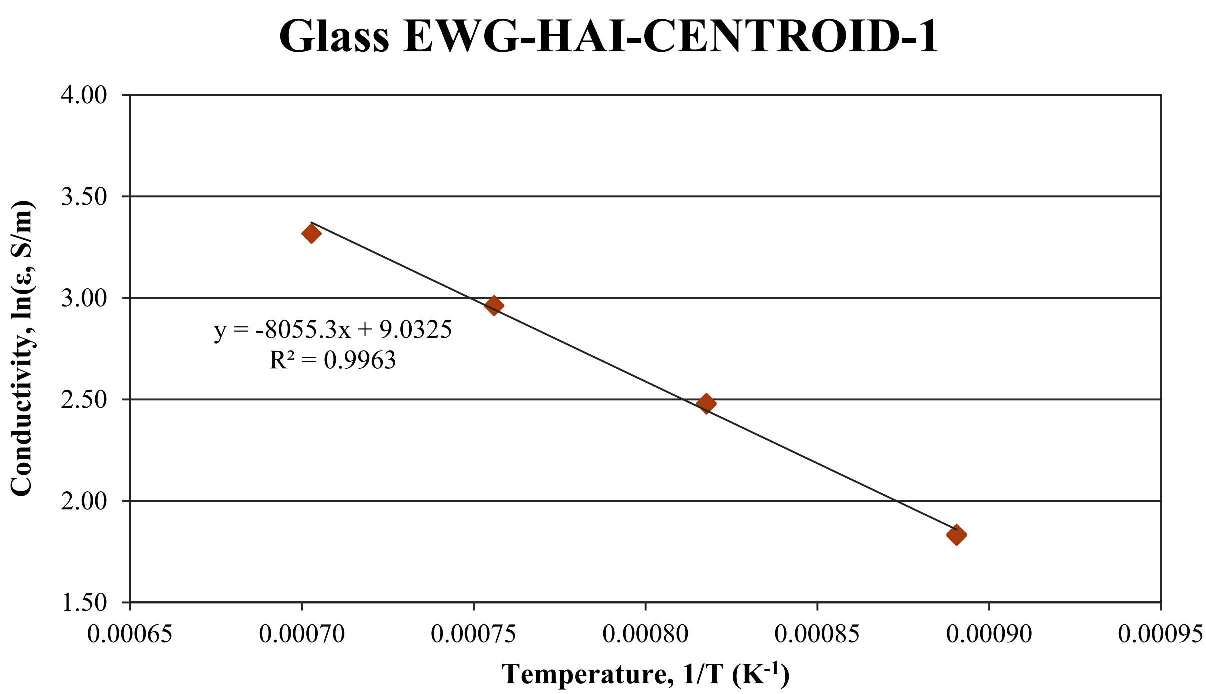

Figure F.1. Electrical Conductivity-Temperature Data and Arrhenius Equation Fit for Glass EWG-HAI-Centroid-1

F.2 Glass EWG-HAI-Centroid-2 Electrical Conductivity Data

Table F.2. Electrical Conductivity Data for Glass EWG-HAI-Centroid-2

Temperature, °C	Conductivity, S/m	1/(T+273.15), K^{-1}	ln(ε, S/m)
1153	27.34	0.00070	3.31
1152	27.13	0.00070	3.30
866	6.21	0.00088	1.83
867	6.29	0.00088	1.84
962	11.71	0.00081	2.46
963	11.81	0.00081	2.47
1059	19.08	0.00075	2.95
1060	19.19	0.00075	2.95

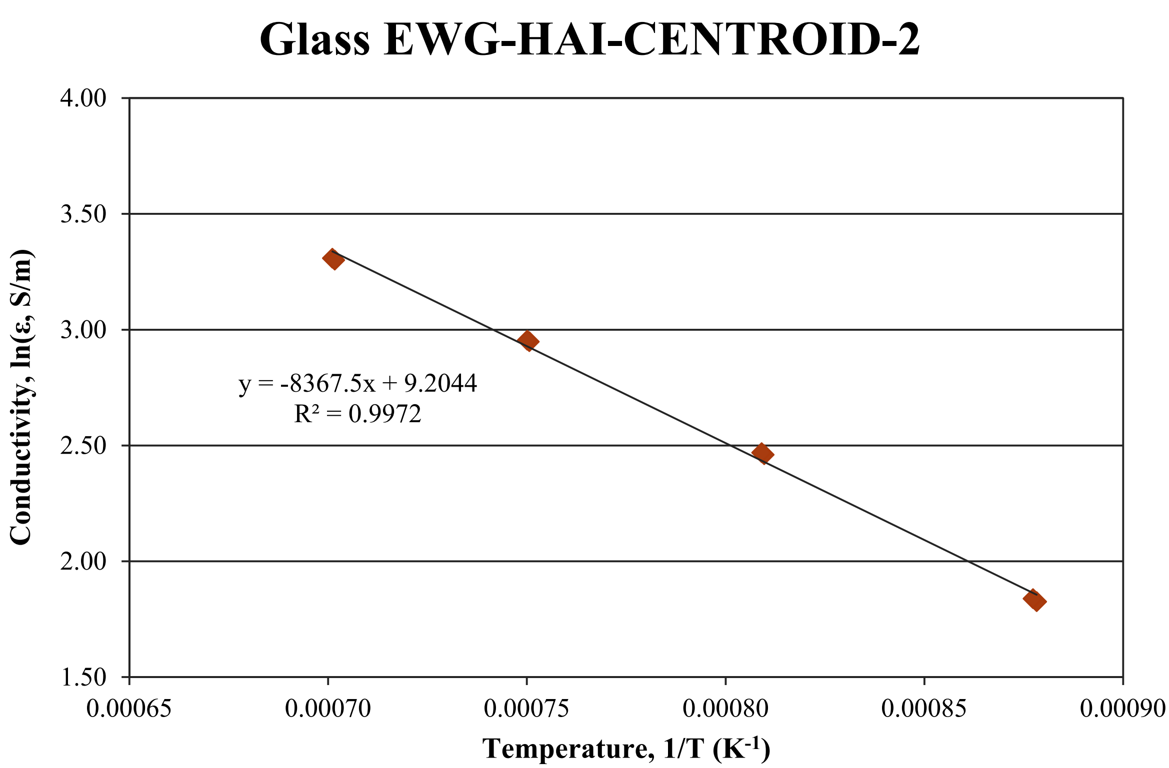

Figure F.2. Electrical Conductivity -Temperature Data and Arrhenius Equation Fit for Glass EWG-HAI-Centroid-2

F.3 Glass EWG-OL-801 Electrical Conductivity Data

Table F.3. Electrical Conductivity Data for Glass EWG-OL-801

Temperature, °C	Conductivity, S/m	1/(T+273.15), K^{-1}	ln(ε, S/m)
950	15.36	0.00082	2.73
950	15.51	0.00082	2.74
1250	41.55	0.00066	3.73
1150	32.36	0.00070	3.48
1150	32.43	0.00070	3.48
1050	23.37	0.00076	3.15
1050	23.46	0.00076	3.16

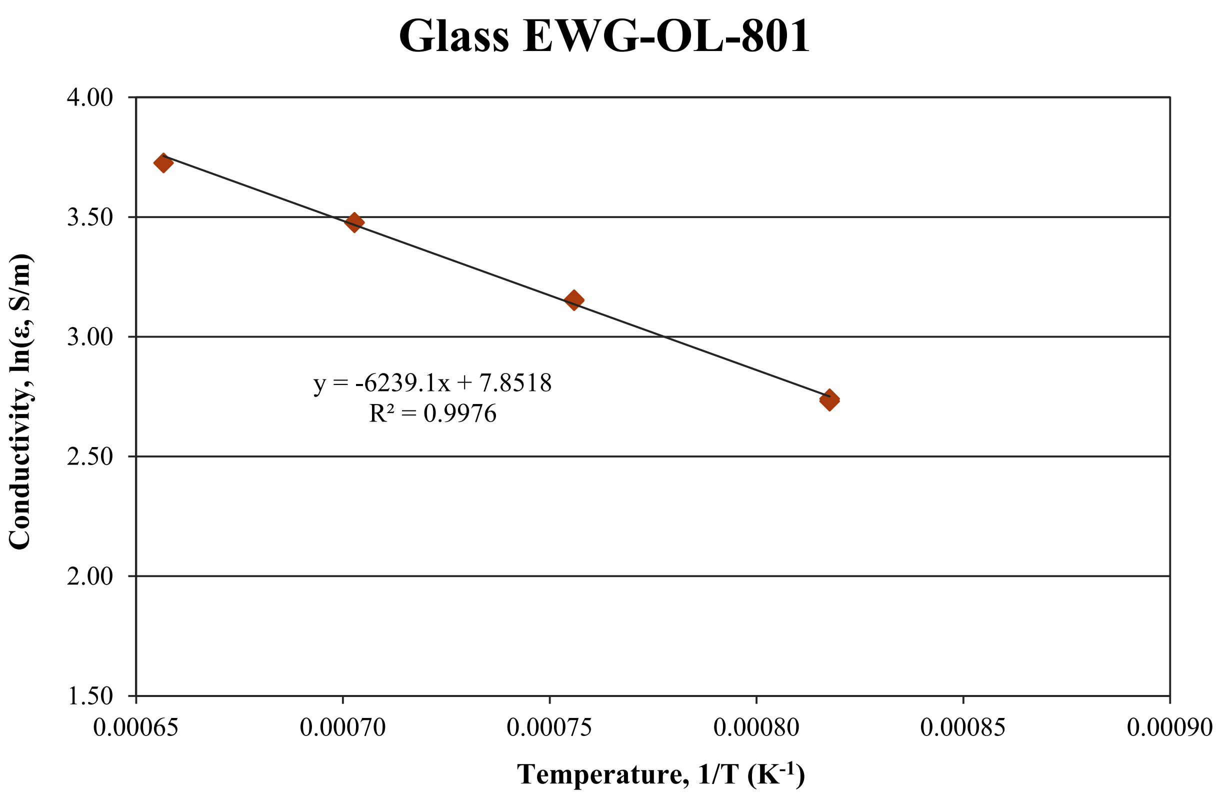

Figure F.3. Electrical Conductivity -Temperature Data and Arrhenius Equation Fit for Glass EWG-OL-801

F.4 Glass EWG-OL-1369 Electrical Conductivity Data

Table F.4. Electrical Conductivity Data for Glass EWG-OL-1369

Temperature, °C	Conductivity, S/m	1/(T+273.15), K^{-1}	ln(ε, S/m)
950	11.59	0.00082	2.45
950	11.65	0.00082	2.46
1250	40.16	0.00066	3.69
1250	39.96	0.00066	3.69
1150	29.45	0.00070	3.38
1150	29.50	0.00070	3.38
1050	19.61	0.00076	2.98
1050	19.66	0.00076	2.98

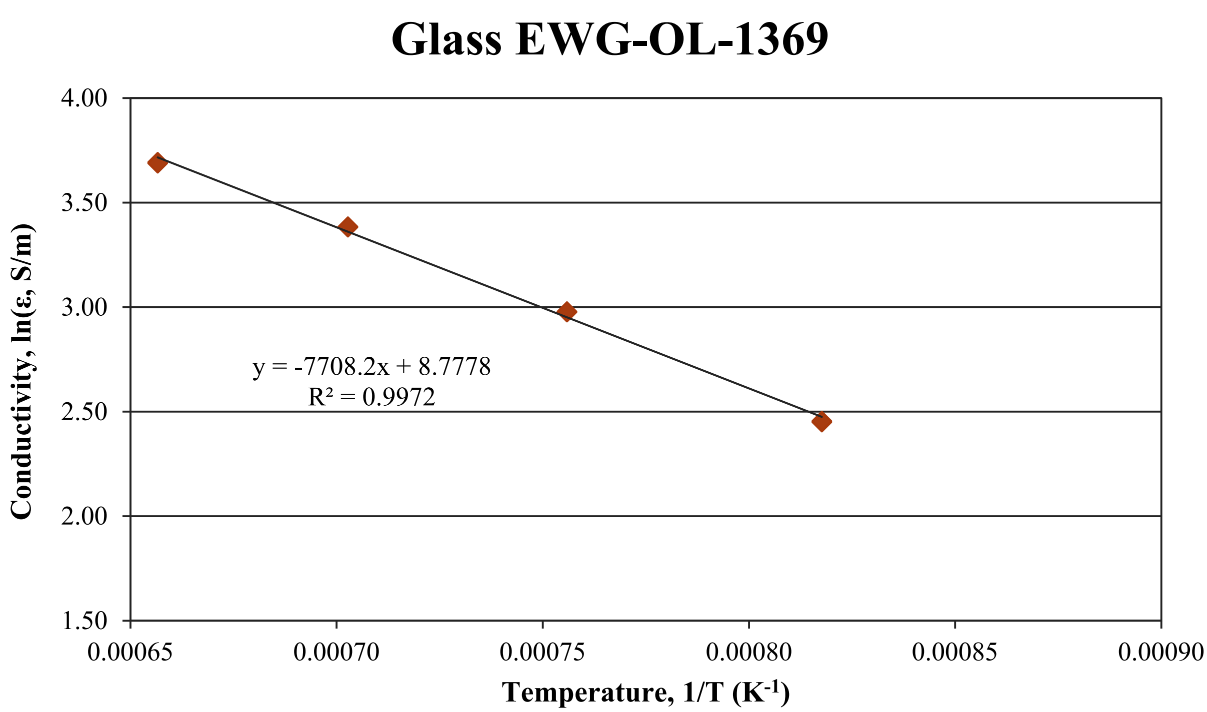

Figure F.4. Electrical Conductivity -Temperature Data and Arrhenius Equation Fit for Glass EWG-OL-1369

F.5 Glass EWG-OL-1580 Electrical Conductivity Data

Table F.5. Electrical Conductivity Data for Glass EWG-OL-1580

Temperature, °C	Conductivity, S/m	1/(T+273.15), K^{-1}	ln(ε, S/m)
940	11.94	0.00082	2.48
940	12.02	0.00082	2.49
1240	42.24	0.00066	3.74
1240	42.03	0.00066	3.74
1140	30.85	0.00071	3.43
1140	30.91	0.00071	3.43
1040	20.45	0.00076	3.02
1040	20.52	0.00076	3.02

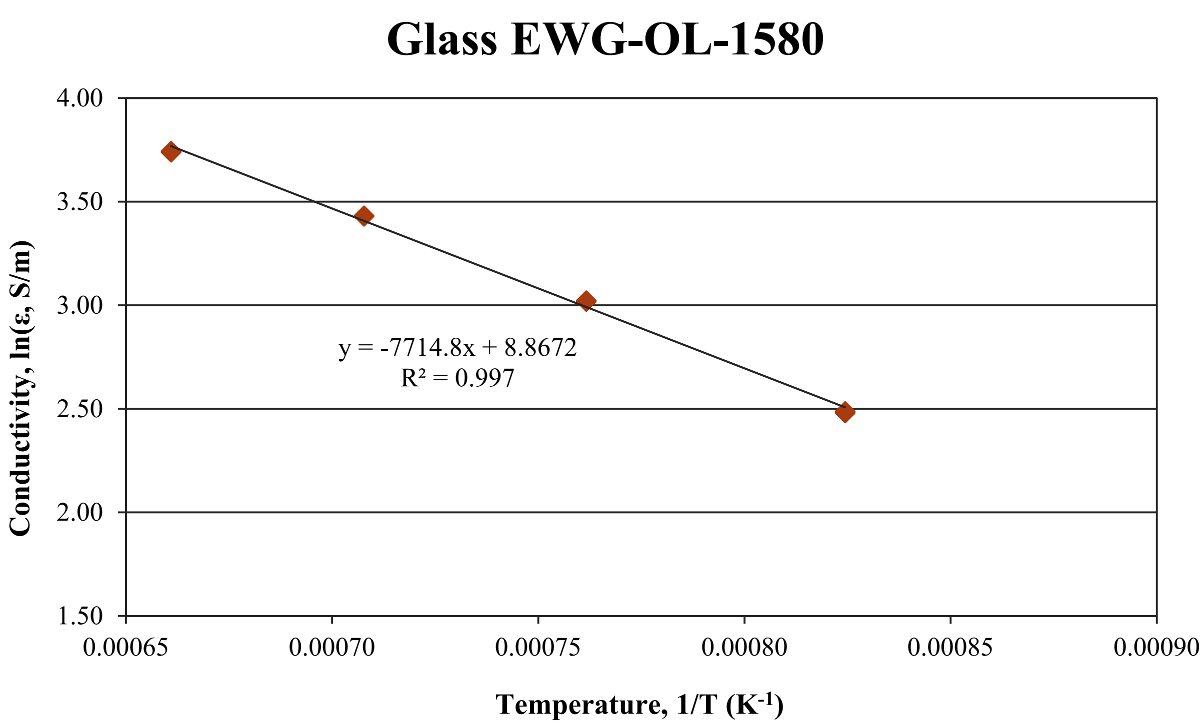

Figure F.5. Electrical Conductivity -Temperature Data and Arrhenius Equation Fit for Glass EWG-OL-1580

F.6 Glass EWG-OL-1672 Electrical Conductivity Data

Table F.6. Electrical Conductivity Data for Glass EWG-OL-1672

Temperature, °C	Conductivity, S/m	1/(T+273.15), K^{-1}	ln(ε, S/m)
1000	0.84	0.00079	-0.18
1000	0.84	0.00079	-0.17
1300	7.70	0.00064	2.04
1200	4.37	0.00068	1.47
1100	2.08	0.00073	0.73
1100	2.09	0.00073	0.74

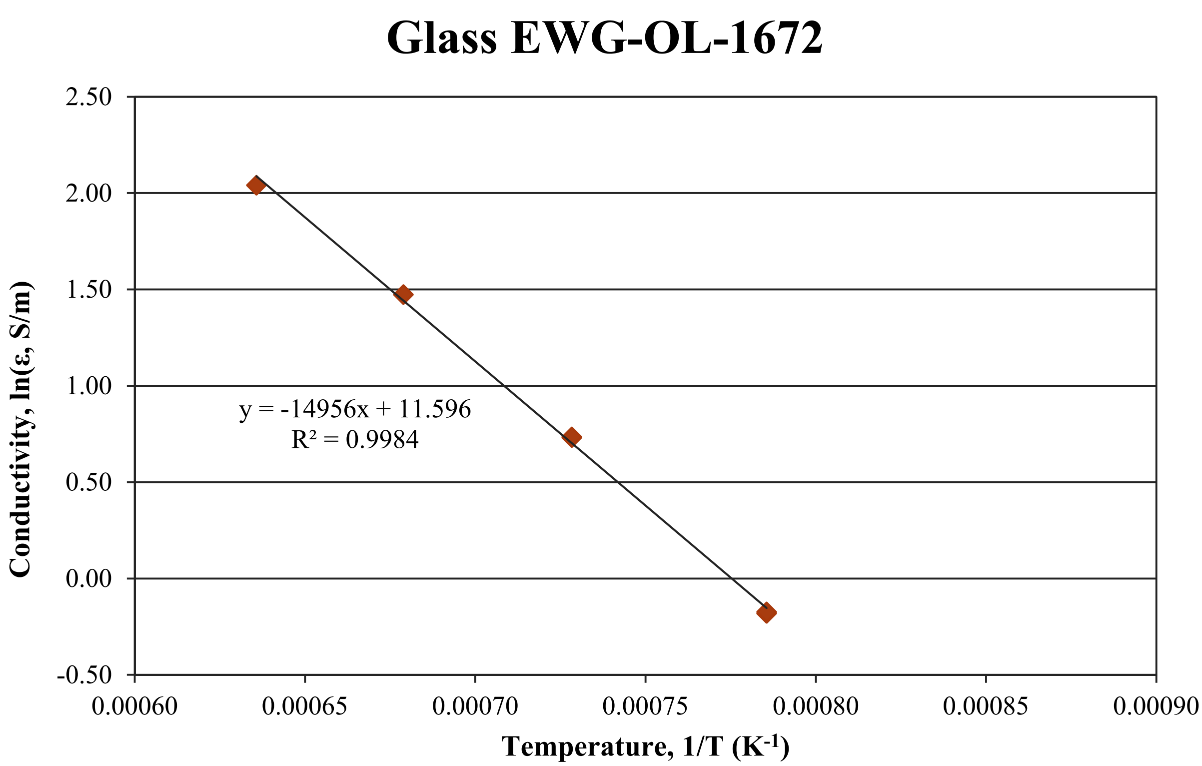

Figure F.6. Electrical Conductivity -Temperature Data and Arrhenius Equation Fit for Glass EWG-OL-1672

F.7 Glass EWG-OL-2463 Electrical Conductivity Data

Table F.7. Electrical Conductivity Data for Glass EWG-OL-2463

Temperature, °C	Conductivity, S/m	1/(T+273.15), K^{-1}	ln(ε, S/m)
900	10.98	0.00085	2.40
900	11.10	0.00085	2.41
1200	41.56	0.00068	3.73
1200	41.32	0.00068	3.72
1100	30.69	0.00073	3.42
1100	30.75	0.00073	3.43
1000	19.77	0.00079	2.98
1000	19.84	0.00079	2.99

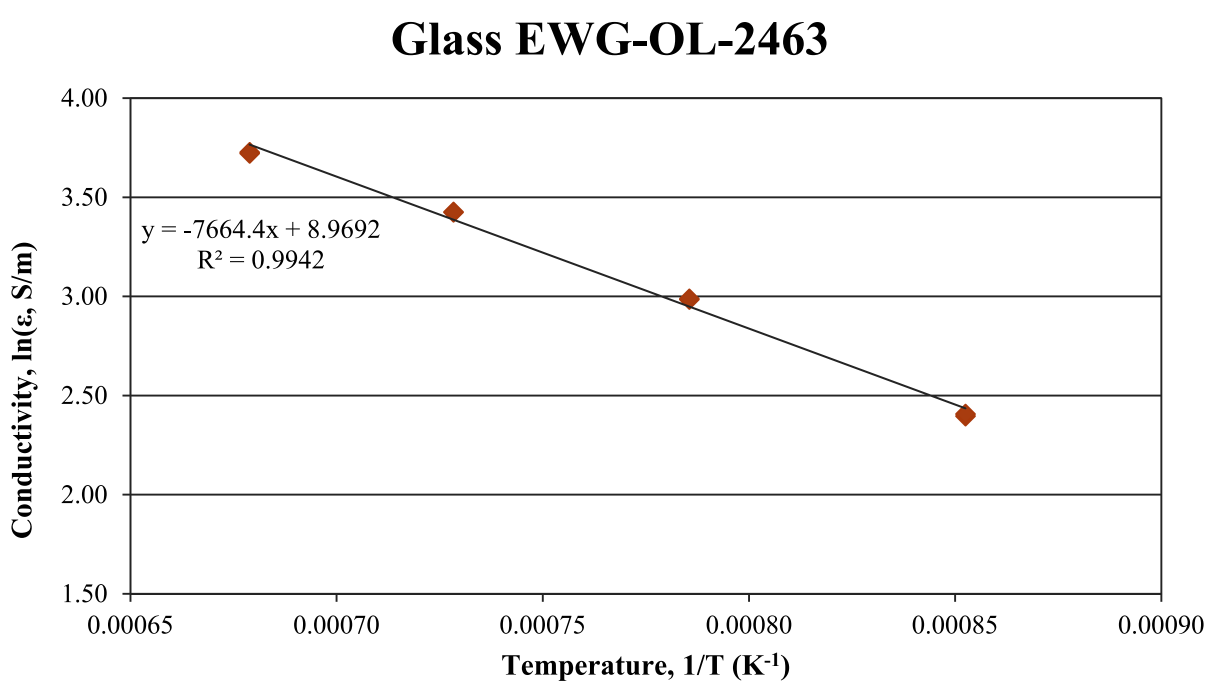

Figure F.7. Electrical Conductivity -Temperature Data and Arrhenius Equation Fit for Glass EWG-OL-2463

F.8 Glass EWG-OL-2619 Electrical Conductivity Data

Table F.8. Electrical Conductivity Data for Glass EWG-OL-2619

Temperature, °C	Conductivity, S/m	1/(T+273.15), K^{-1}	ln(ε, S/m)
1150	5.54	0.00070	1.71
1150	5.58	0.00070	1.72
1250	9.95	0.00066	2.30
1250	9.88	0.00066	2.29
1050	2.55	0.00076	0.94
1050	2.58	0.00076	0.95
950	0.92	0.00082	-0.08
950	0.94	0.00082	-0.06

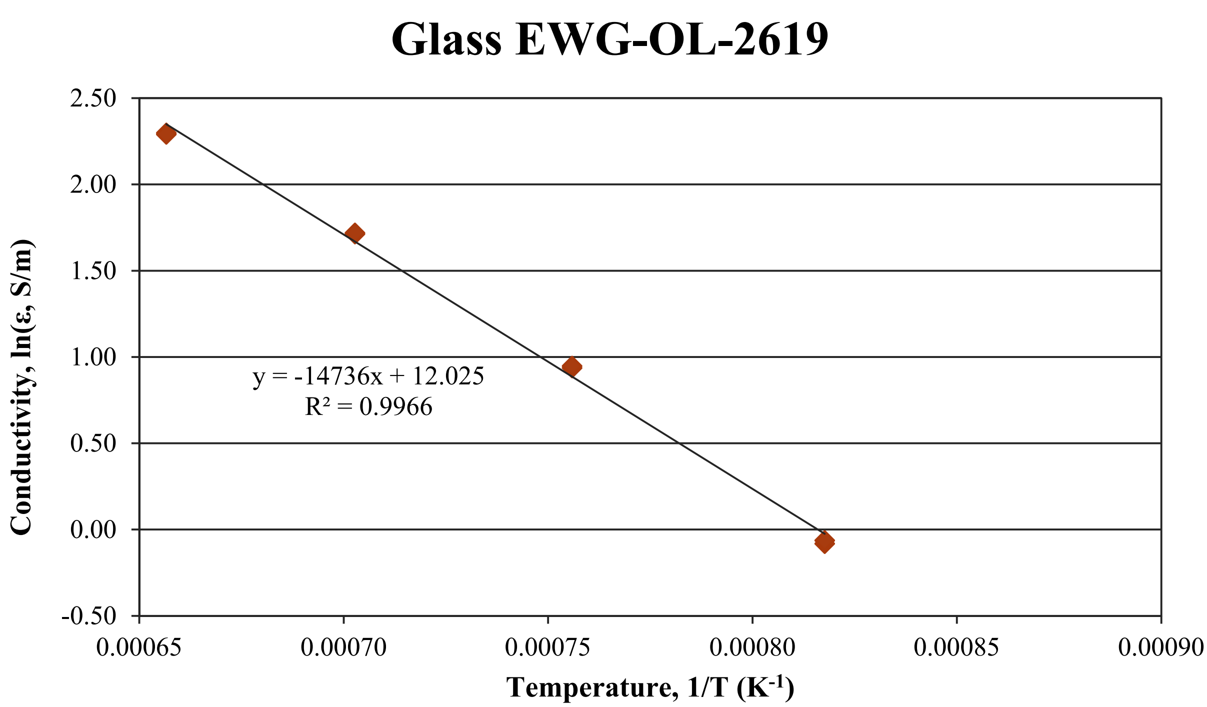

Figure F.8. Electrical Conductivity -Temperature Data and Arrhenius Equation Fit for Glass EWG-OL-2619

F.9 Glass EWG-OL-3122 Electrical Conductivity Data

Table F.9. Electrical Conductivity Data for Glass EWG-OL-3122

Temperature, °C	Conductivity, S/m	1/(T+273.15), K^{-1}	ln(ε, S/m)
1390	55.36	0.00060	4.01
1390	55.31	0.00060	4.01
1300	44.11	0.00064	3.79
1200	32.51	0.00068	3.48
1200	32.60	0.00068	3.48
1100	22.41	0.00073	3.11
1100	22.49	0.00073	3.11

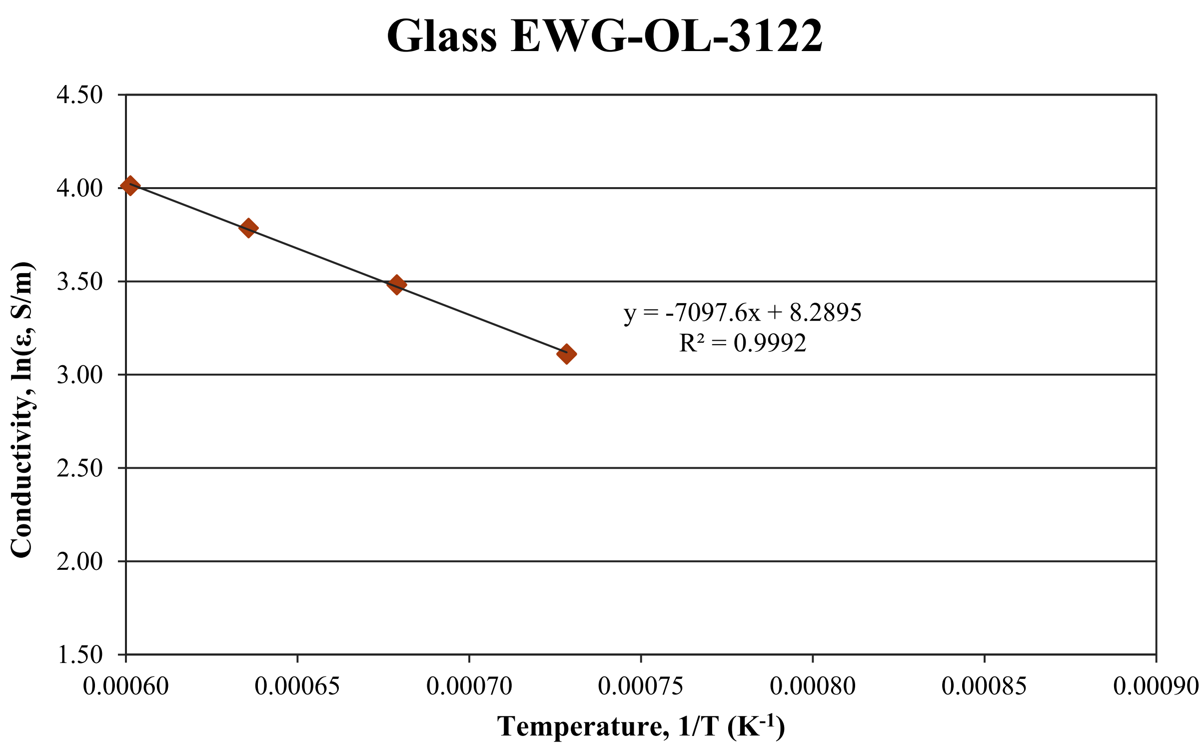

Figure F.9. Electrical Conductivity -Temperature Data and Arrhenius Equation Fit for Glass EWG-OL-3122

F.10 Glass EWG-OL-3208 Electrical Conductivity Data

Table F.10. Electrical Conductivity Data for Glass EWG-OL-3208

Temperature, °C	Conductivity, S/m	$1/(T+273.15)$, K^{-1}	ln(ε, S/m)
800	22.30	0.00093	3.10
800	22.54	0.00093	3.12
1100	64.92	0.00073	4.17
1100	64.47	0.00073	4.17
1000	55.66	0.00079	4.02
1000	55.79	0.00079	4.02
900	38.01	0.00085	3.64
900	38.34	0.00085	3.65

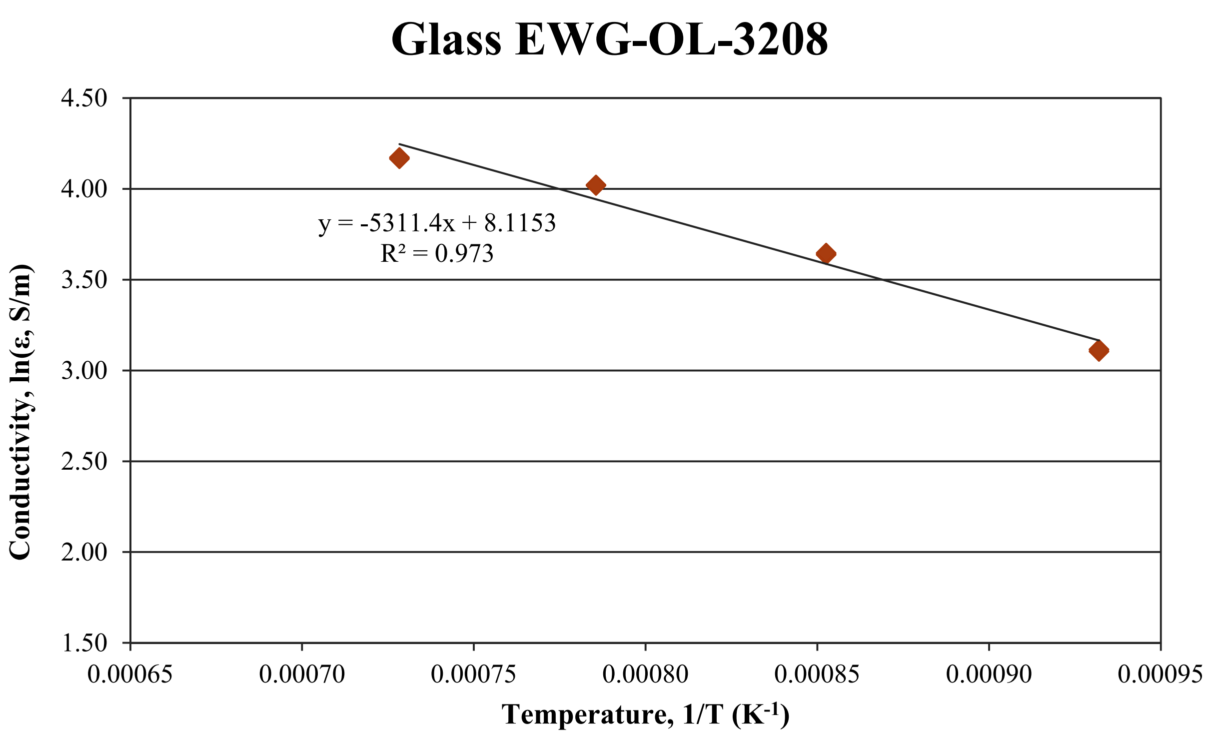

Figure F.10. Electrical Conductivity -Temperature Data and Arrhenius Equation Fit for Glass EWG-OL-3208

F.11 Glass EWG-OL-3231 Electrical Conductivity Data

Table F.11. Electrical Conductivity Data for Glass EWG-OL-3231

Temperature, °C	Conductivity, S/m	1/(T+273.15), K^{-1}	ln(ε, S/m)
800	4.87	0.00093	1.58
800	4.96	0.00093	1.60
1100	32.05	0.00073	3.47
1100	31.86	0.00073	3.46
1000	20.76	0.00079	3.03
1000	20.83	0.00079	3.03
900	11.25	0.00085	2.42
900	11.35	0.00085	2.43

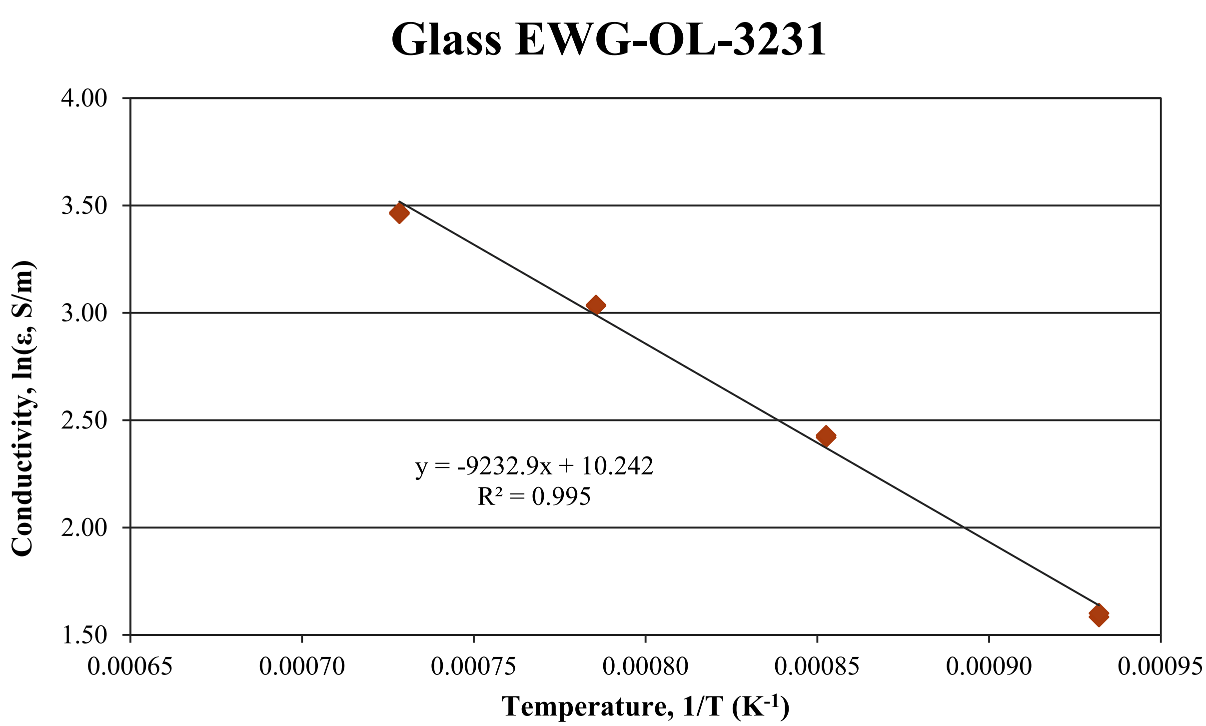

Figure F.11. Electrical Conductivity -Temperature Data and Arrhenius Equation Fit for Glass EWG-OL-3231

F.12 Glass EWG-OL-3388 Electrical Conductivity Data

Table F.12. Electrical Conductivity Data for Glass EWG-OL-3388

Temperature, °C	Conductivity, S/m	1/(T+273.15), K^{-1}	ln(ε, S/m)
875	18.74	0.00087	2.93
875	18.80	0.00087	2.93
1027	35.96	0.00077	3.58
1027	35.74	0.00077	3.58
975	30.13	0.00080	3.41
975	30.16	0.00080	3.41
925	24.23	0.00083	3.19
925	24.28	0.00083	3.19

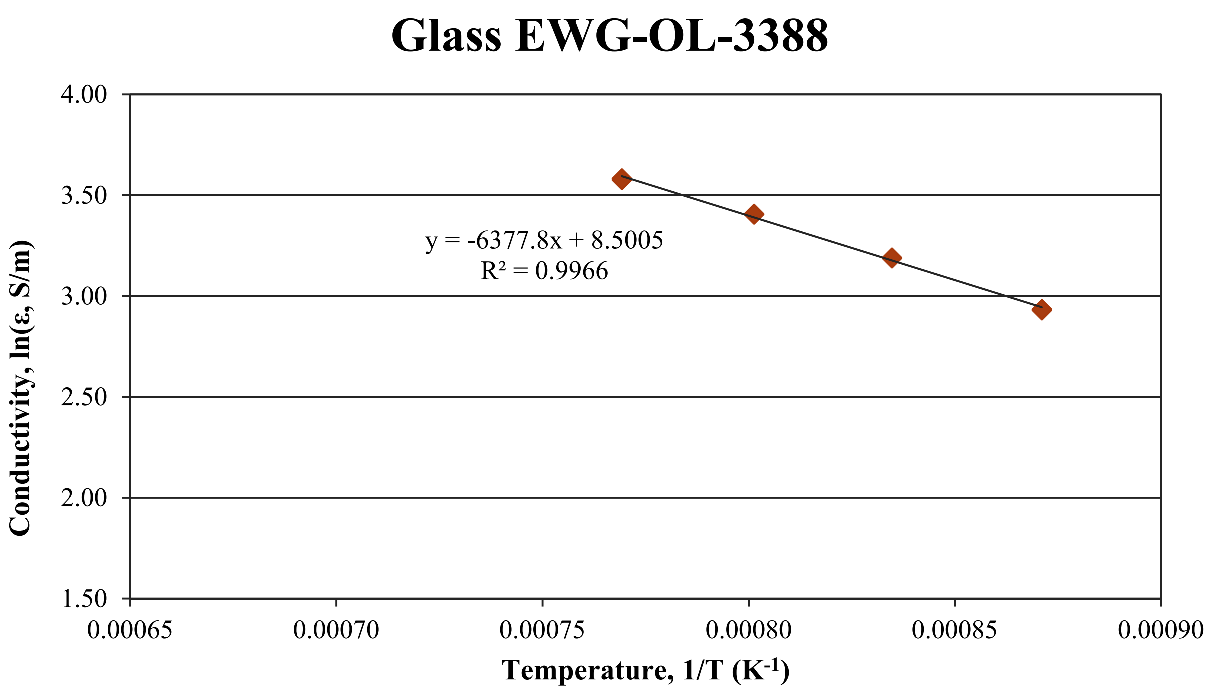

Figure F.12. Electrical Conductivity -Temperature Data and Arrhenius Equation Fit for Glass EWG-OL-3388

F.13 Glass EWG-OL-3872 Electrical Conductivity Data

Table F.13. Electrical Conductivity Data for Glass EWG-OL-3872

Temperature, °C	Conductivity, S/m	1/(T+273.15), K^{-1}	ln(ε, S/m)
850	23.30	0.00089	3.15
850	23.49	0.00089	3.16
1050	59.12	0.00076	4.08
1050	58.65	0.00076	4.07
950	40.86	0.00082	3.71
950	41.29	0.00082	3.72
900	31.51	0.00085	3.45
900	31.70	0.00085	3.46

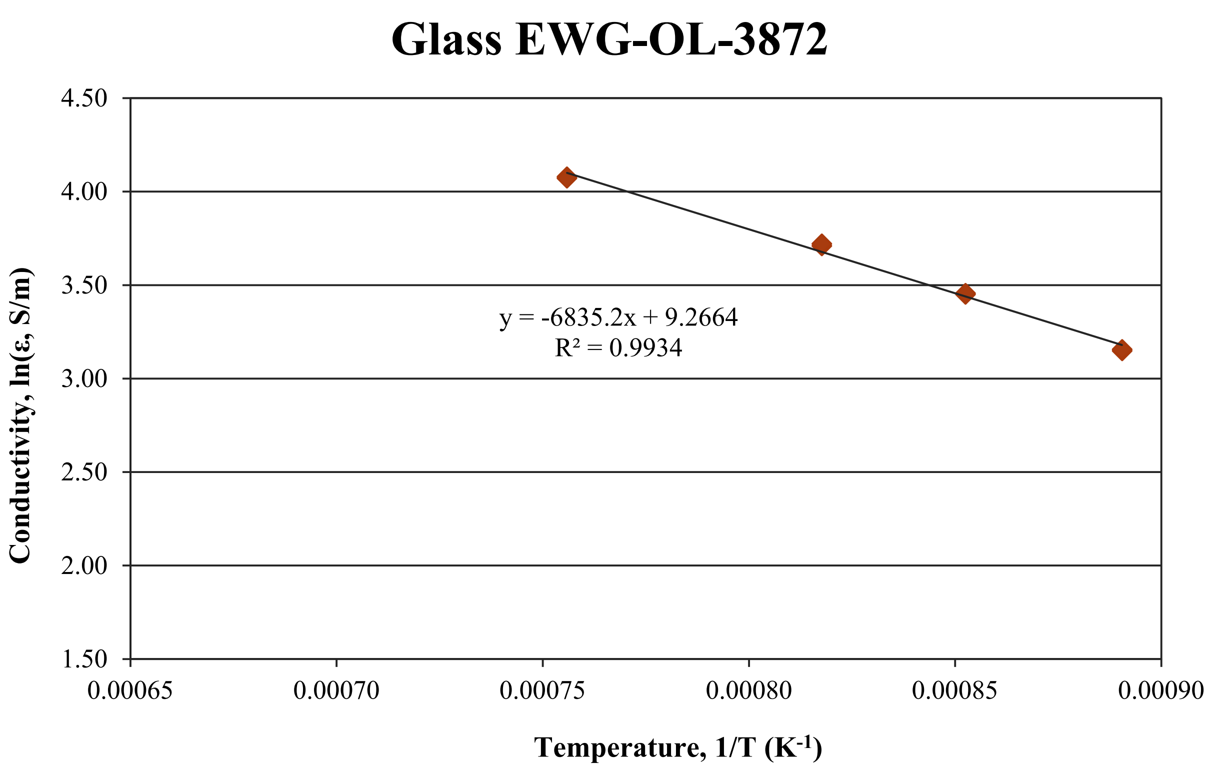

Figure F.13. Electrical Conductivity -Temperature Data and Arrhenius Equation Fit for Glass EWG-OL-3872

F.14 Glass EWG-OL-4099 Electrical Conductivity Data

Table F.14. Electrical Conductivity Data for Glass EWG-OL-4099

Temperature, °C	Conductivity, S/m	1/(T+273.15), K^{-1}	ln(ε, S/m)
850	5.73	0.00089	1.75
850	5.79	0.00089	1.76
1000	16.20	0.00079	2.79
1000	16.13	0.00079	2.78
950	12.30	0.00082	2.51
950	12.38	0.00082	2.52
900	8.67	0.00085	2.16
900	8.75	0.00085	2.17

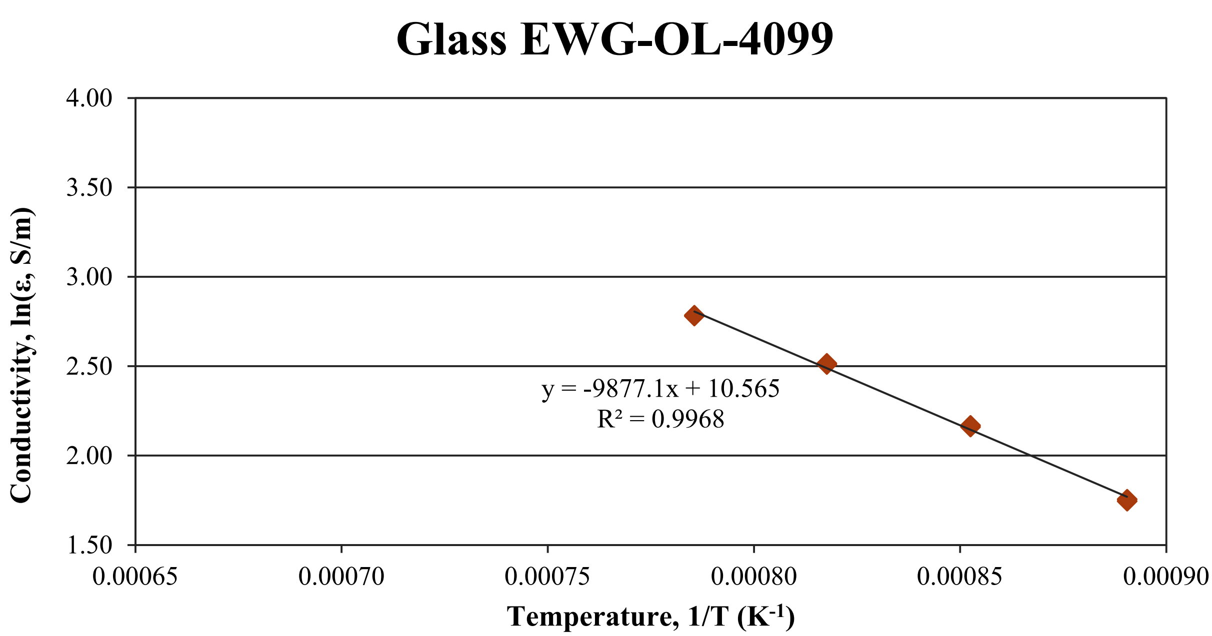

Figure F.14. Electrical Conductivity -Temperature Data and Arrhenius Equation Fit for Glass EWG-OL-4099

F.15 Glass EWG-OL-5155 Electrical Conductivity Data

Table F.15. Electrical Conductivity Data for Glass EWG-OL-5155

Temperature, °C	Conductivity, S/m	1/(T+273.15), K^{-1}	ln(ε, S/m)
850	6.77	0.00089	1.91
850	6.91	0.00089	1.93
1150	34.63	0.00070	3.54
1150	34.42	0.00070	3.54
1050	23.36	0.00076	3.15
1050	23.50	0.00076	3.16
950	13.77	0.00082	2.62
950	13.89	0.00082	2.63

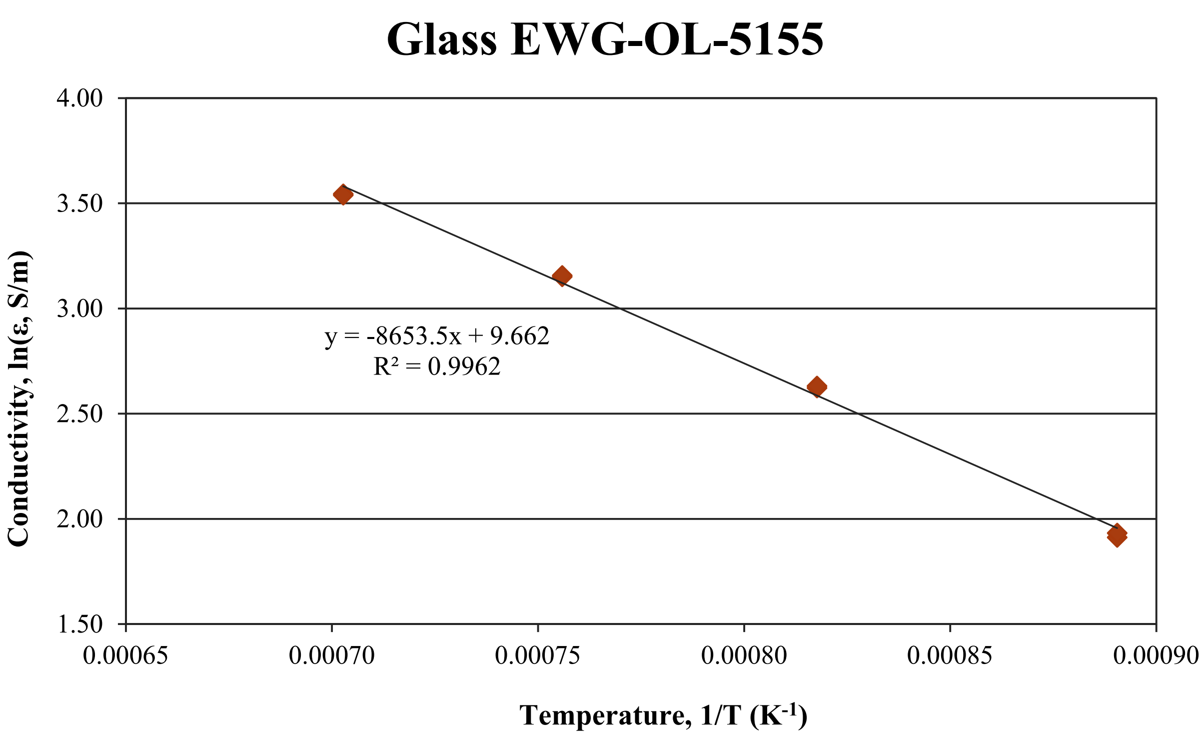

Figure F.15. Electrical Conductivity -Temperature Data and Arrhenius Equation Fit for Glass EWG-OL-5155

F.16 Glass EWG-OL-5549 Electrical Conductivity Data

Table F.16. Electrical Conductivity Data for Glass EWG-OL-5549

Temperature, °C	Conductivity, S/m	1/(T+273.15), K^{-1}	ln(ε, S/m)
850	8.52	0.00089	2.14
850	8.54	0.00089	2.14
1050	27.58	0.00076	3.32
1050	27.54	0.00076	3.32
950	17.04	0.00082	2.84
950	17.11	0.00082	2.84
900	12.35	0.00085	2.51
900	12.38	0.00085	2.52

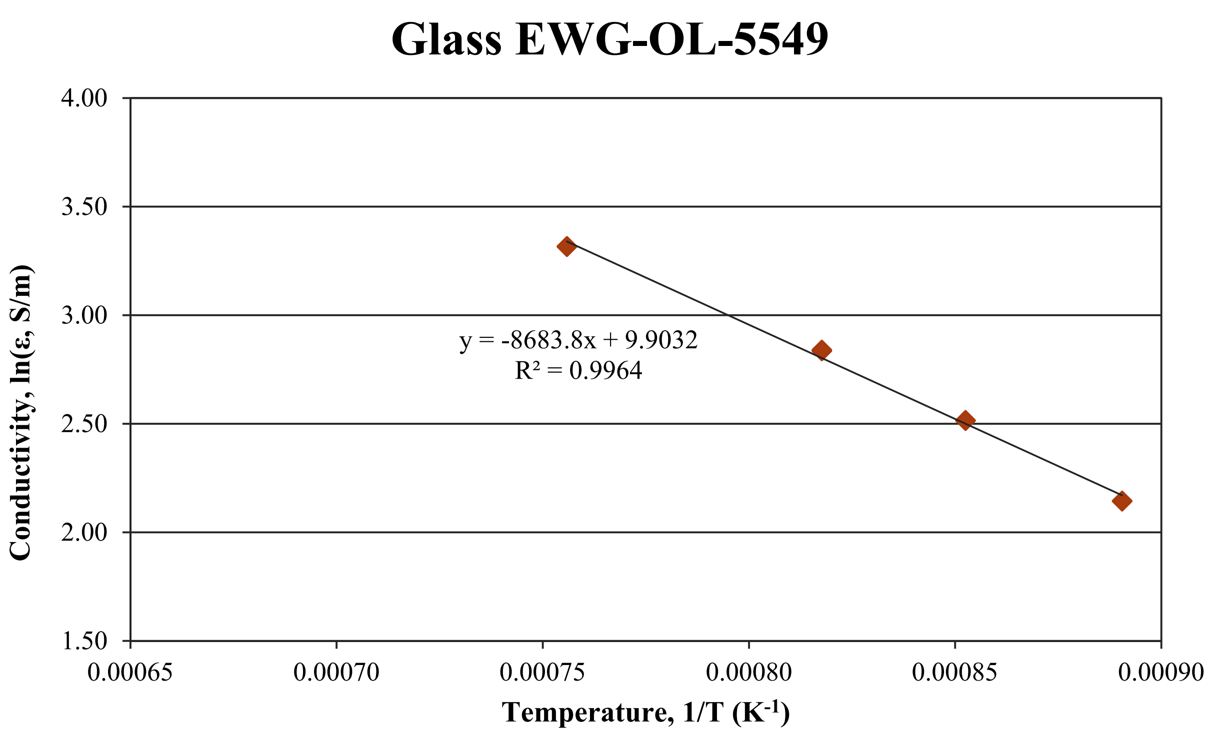

Figure F.16. Electrical Conductivity -Temperature Data and Arrhenius Equation Fit for Glass EWG-OL-5549

F.17 Glass EWG-OL-5801 Electrical Conductivity Data

Table F.17. Electrical Conductivity Data for Glass EWG-OL-5801

Temperature, °C	Conductivity, S/m	1/(T+273.15), K^{-1}	ln(ε, S/m)
1100	26.36	0.00073	3.27
1100	26.27	0.00073	3.27
1000	16.97	0.00079	2.83
1000	17.08	0.00079	2.84
900	9.28	0.00085	2.23
900	9.42	0.00085	2.24
800	4.11	0.00093	1.41
800	4.19	0.00093	1.43

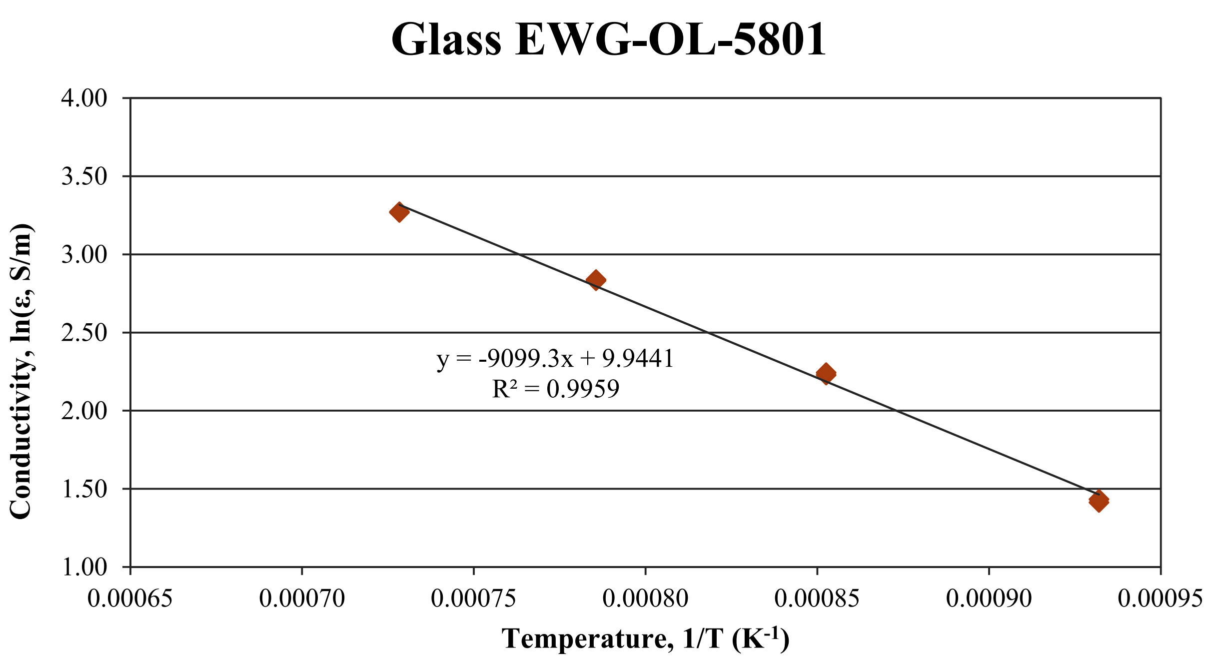

Figure F.17. Electrical Conductivity -Temperature Data and Arrhenius Equation Fit for Glass EWG-OL-5801

F.18 Glass EWG-OL-6080 Electrical Conductivity Data

Table F.18. Electrical Conductivity Data for Glass EWG-OL-6080

Temperature, °C	Conductivity, S/m	1/(T+273.15), K^{-1}	ln(ε, S/m)
1390	12.96	0.00060	2.56
1390	12.91	0.00060	2.56
1300	8.01	0.00064	2.08
1300	8.03	0.00064	2.08
1200	4.14	0.00068	1.42
1200	4.16	0.00068	1.42
1100	1.86	0.00073	0.62
1100	1.88	0.00073	0.63

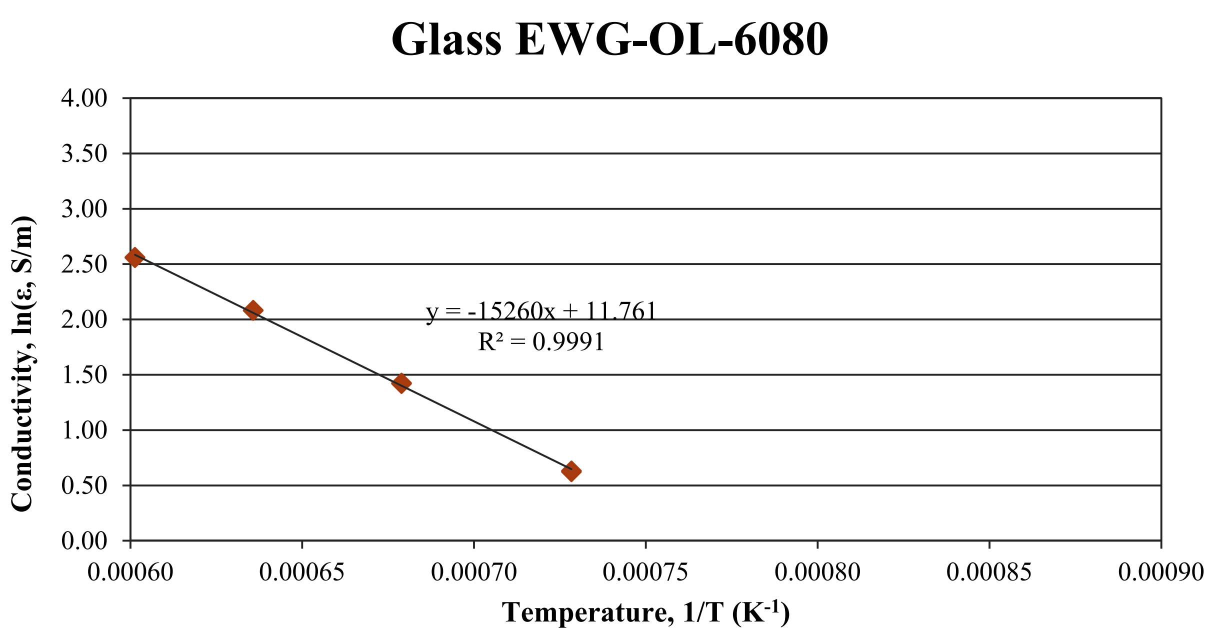

Figure F.18. Electrical Conductivity -Temperature Data and Arrhenius Equation Fit for Glass EWG-OL-6080

F.19 Glass EWG-OL-6198 Electrical Conductivity Data

Table F.19. Electrical Conductivity Data for Glass EWG-OL-6198

Temperature, °C	Conductivity, S/m	1/(T+273.15), K^{-1}	ln(ε, S/m)
1100	32.80	0.00073	3.49
1100	32.69	0.00073	3.49
1000	22.06	0.00079	3.09
1000	22.19	0.00079	3.10
900	12.94	0.00085	2.56
900	13.07	0.00085	2.57
800	6.31	0.00093	1.84
800	6.41	0.00093	1.86

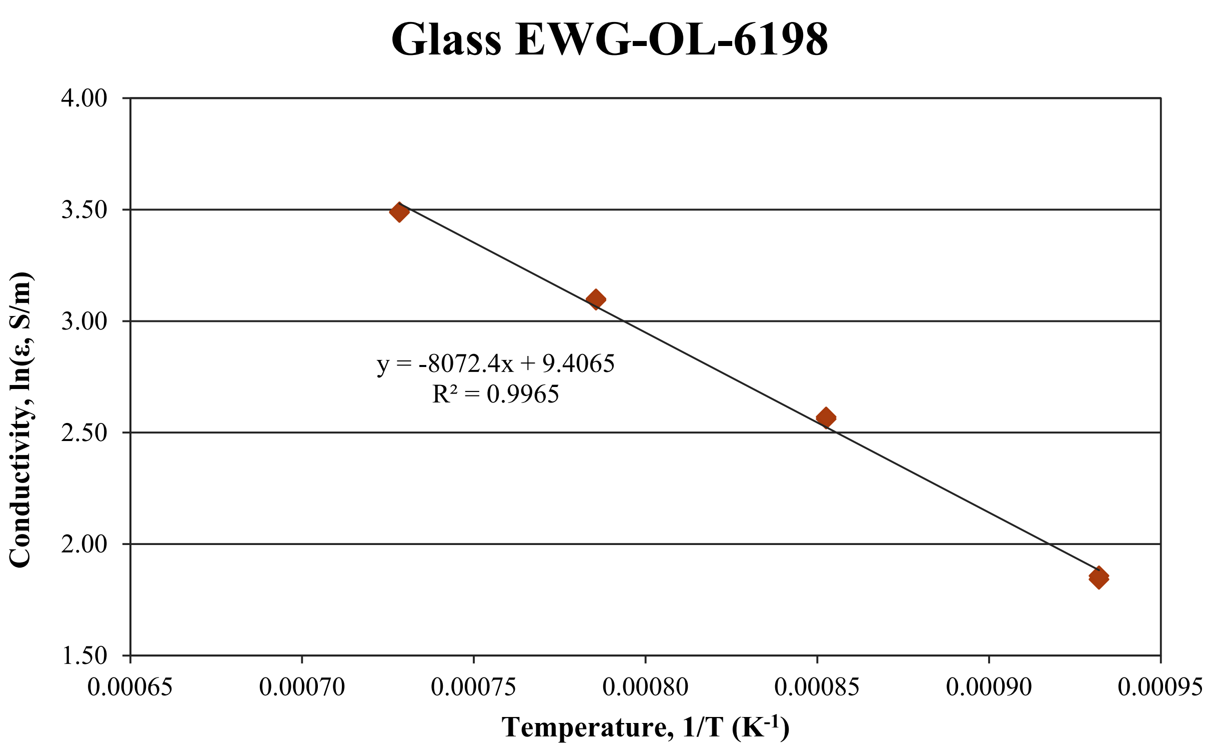

Figure F.19. Electrical Conductivity -Temperature Data and Arrhenius Equation Fit for Glass EWG-OL-6198

F.20 Glass EWG-OL-12707 Electrical Conductivity Data

Table F.20. Electrical Conductivity Data for Glass EWG-OL-12707

Temperature, °C	Conductivity, S/m	1/(T+273.15), K^{-1}	ln(ε, S/m)
850	4.57	0.00089	1.52
850	4.57	0.00089	1.52
1050	15.49	0.00076	2.74
1050	15.40	0.00076	2.73
950	9.36	0.00082	2.24
950	9.41	0.00082	2.24
900	6.64	0.00085	1.89
900	6.66	0.00085	1.90

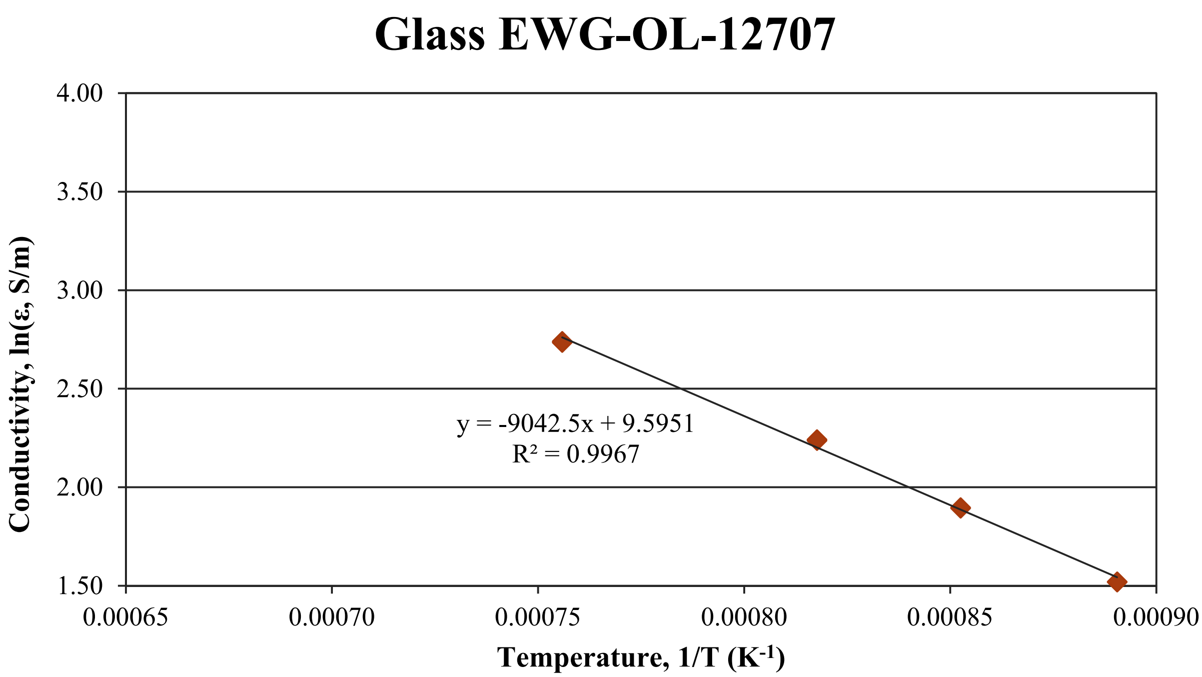

Figure F.20. Electrical Conductivity -Temperature Data and Arrhenius Equation Fit for Glass EWG-OL-12707

F.21 Glass EWG-OL-14827 Electrical Conductivity Data

Table F.21. Electrical Conductivity Data for Glass EWG-OL-14827

Temperature, °C	Conductivity, S/m	1/(T+273.15), K^{-1}	ln(ε, S/m)
850	7.95	0.00089	2.07
850	8.00	0.00089	2.08
980	19.18	0.00080	2.95
980	18.93	0.00080	2.94
950	16.68	0.00082	2.81
950	16.69	0.00082	2.81
900	11.95	0.00085	2.48
900	11.99	0.00085	2.48

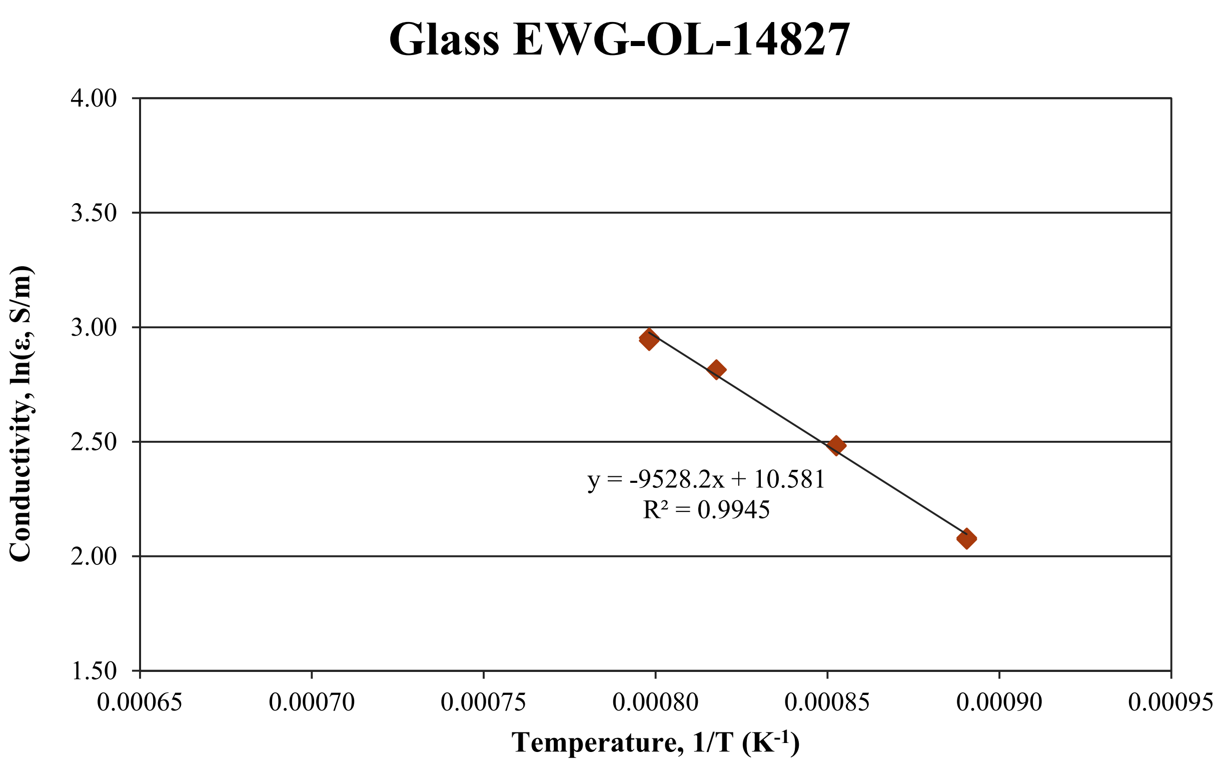

Figure F.21. Electrical Conductivity -Temperature Data and Arrhenius Equation Fit for Glass EWG-OL-14827

F.22 Glass EWG-OL-15968 Electrical Conductivity Data

Table F.22. Electrical Conductivity Data for Glass EWG-OL-15968

Temperature, °C	Conductivity, S/m	1/(T+273.15), K^{-1}	ln(ε, S/m)
850	23.15	0.00089	3.14
850	23.48	0.00089	3.16
1150	71.83	0.00070	4.27
1150	71.45	0.00070	4.27
1050	54.82	0.00076	4.00
1050	54.96	0.00076	4.01
950	38.06	0.00082	3.64
950	38.33	0.00082	3.65

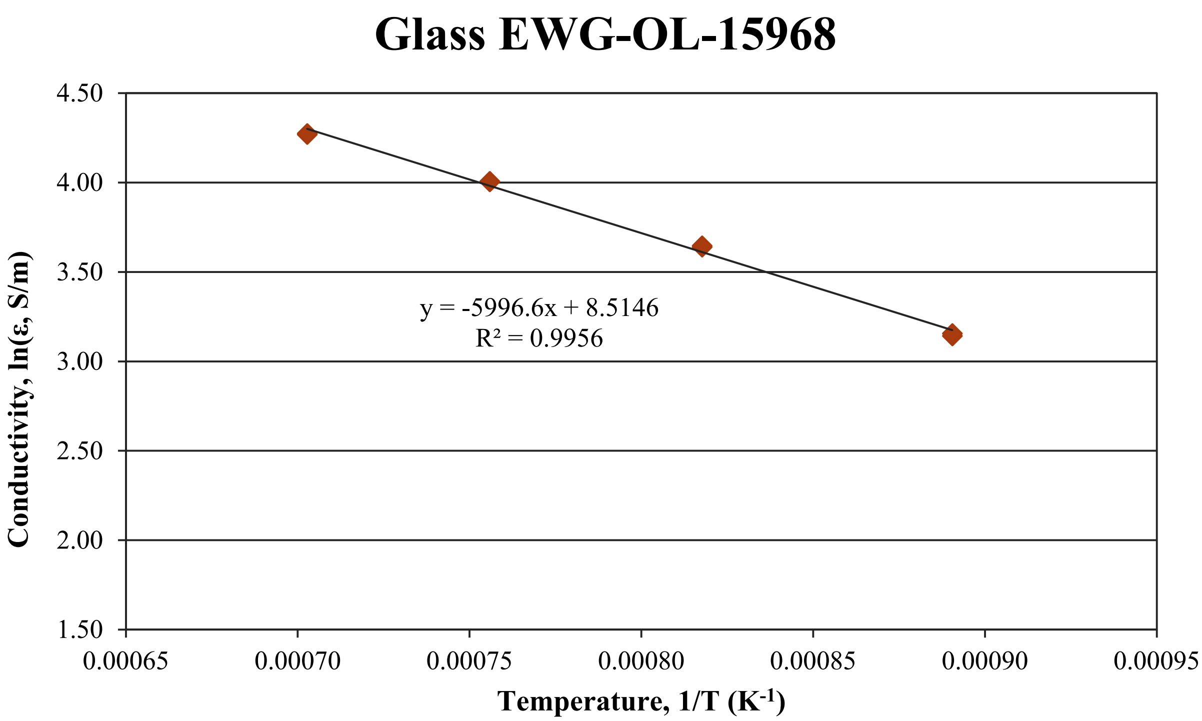

Figure F.22. Electrical Conductivity -Temperature Data and Arrhenius Equation Fit for Glass EWG-OL-15968

F.23 Glass EWG-OL-16450 Electrical Conductivity Data

Table F.23. Electrical Conductivity Data for Glass EWG-OL-16450

Temperature, °C	Conductivity, S/m	1/(T+273.15), K^{-1}	ln(ε, S/m)
950	8.05	0.00082	2.09
950	8.09	0.00082	2.09
1250	17.85	0.00066	2.88
1250	17.56	0.00066	2.87
1150	14.04	0.00070	2.64
1150	14.11	0.00070	2.65
1050	9.98	0.00076	2.30
1050	10.07	0.00076	2.31

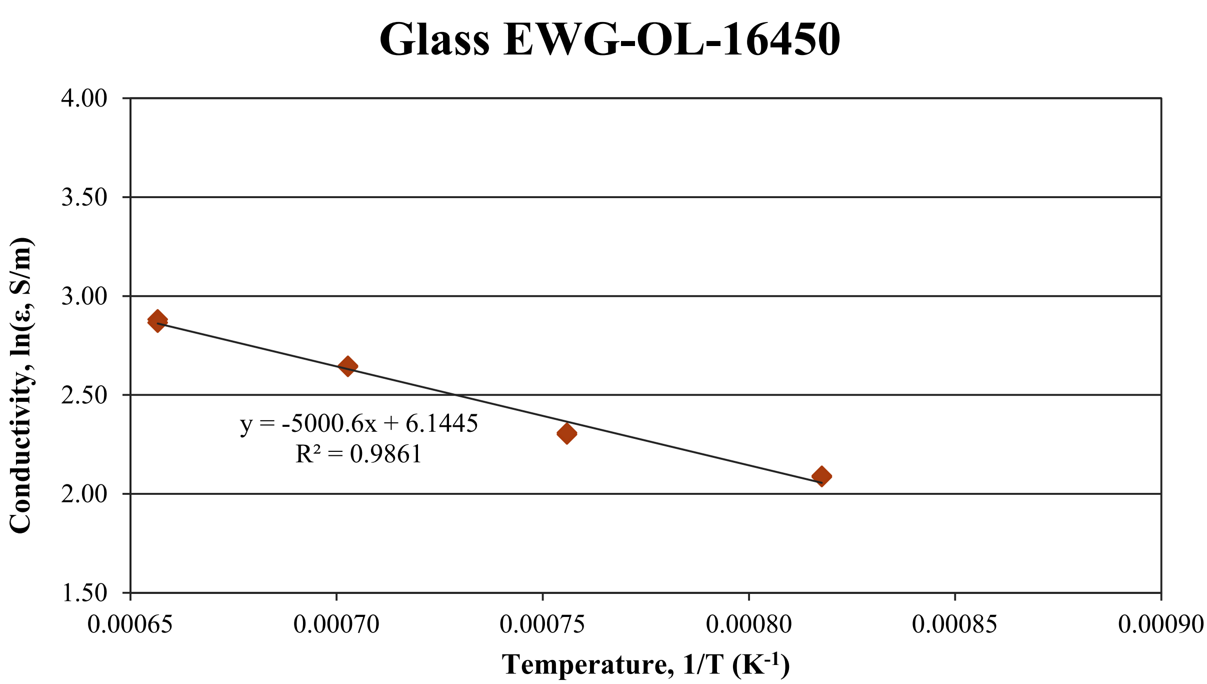

Figure F.23. Electrical Conductivity -Temperature Data and Arrhenius Equation Fit for Glass EWG-OL-16450

F.24 Glass EWG-OL-23401 Electrical Conductivity Data

Table F.24. Electrical Conductivity Data for Glass EWG-OL-23401

Temperature, °C	Conductivity, S/m	1/(T+273.15), K^{-1}	ln(ε, S/m)
1100	21.85	0.00073	3.08
1100	21.91	0.00073	3.09
1390	51.86	0.00060	3.95
1300	41.63	0.00064	3.73
1300	41.63	0.00064	3.73
1200	31.21	0.00068	3.44
1200	31.25	0.00068	3.44

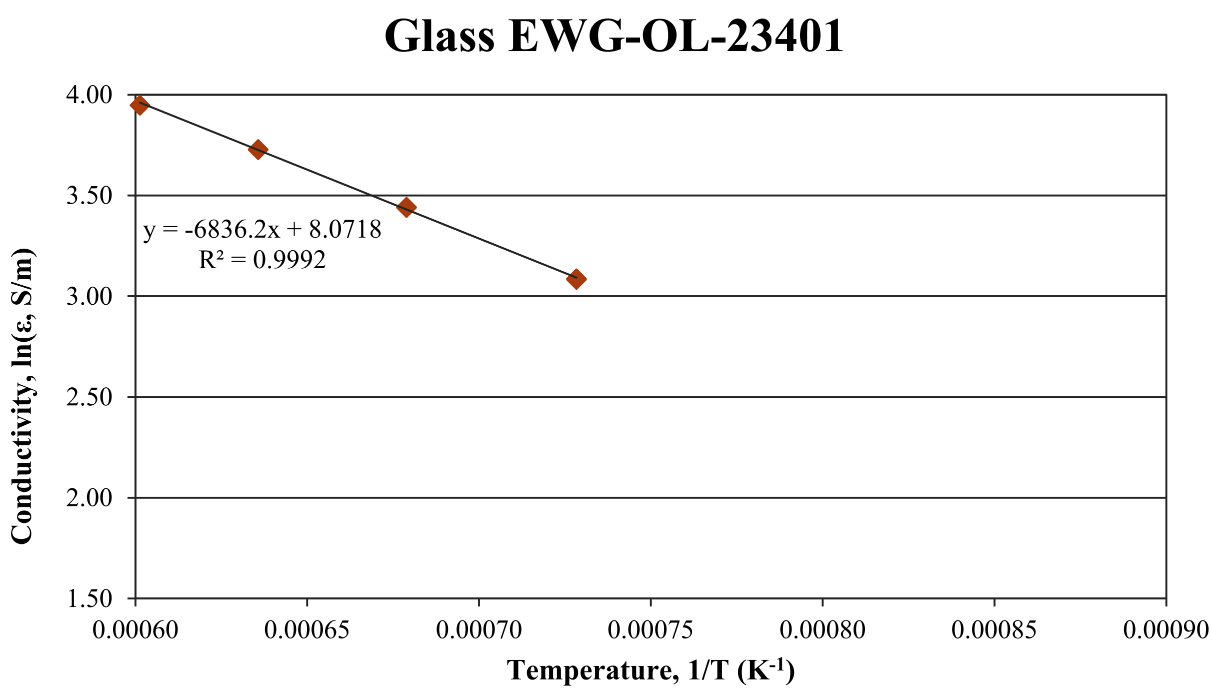

Figure F.24. Electrical Conductivity -Temperature Data and Arrhenius Equation Fit for Glass EWG-OL-23401

F.25 Glass EWG-OL-26012 Electrical Conductivity Data

Table F.25. Electrical Conductivity Data for Glass EWG-OL-26012

Temperature, °C	Conductivity, S/m	1/(T+273.15), K^{-1}	ln(ε, S/m)
950	19.97	0.00082	2.99
950	20.07	0.00082	3.00
1250	47.88	0.00066	3.87
1250	44.17	0.00066	3.79
1150	40.86	0.00070	3.71
1150	40.98	0.00070	3.71
1050	30.05	0.00076	3.40
1050	30.14	0.00076	3.41

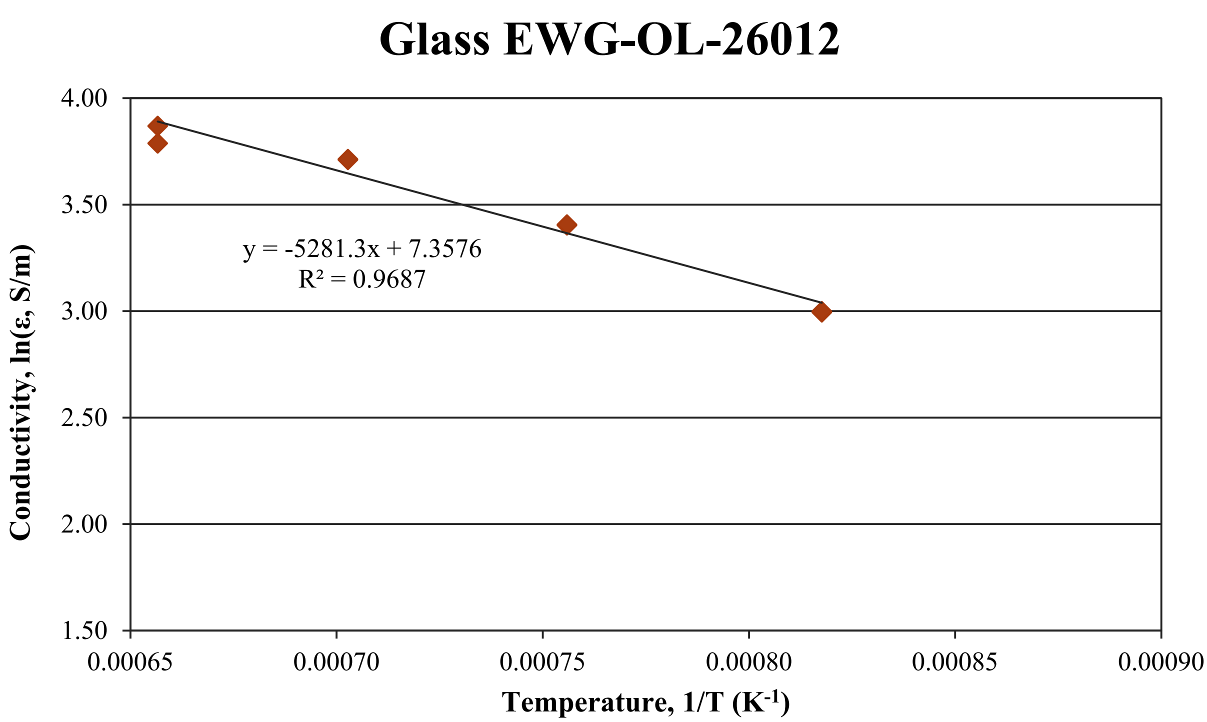

Figure F.25. Electrical Conductivity -Temperature Data and Arrhenius Equation Fit for Glass EWG-OL-26012

F.26 Glass EWG-OL-29285 Electrical Conductivity Data

Table F.26. Electrical Conductivity Data for Glass EWG-OL-29285

Temperature, °C	Conductivity, S/m	1/(T+273.15), K^{-1}	ln(ε, S/m)
1050	1.20	0.00076	0.18
1050	1.21	0.00076	0.19
1350	7.65	0.00062	2.03
1350	7.45	0.00062	2.01
1250	4.63	0.00066	1.53
1250	4.64	0.00066	1.54
1150	2.53	0.00070	0.93

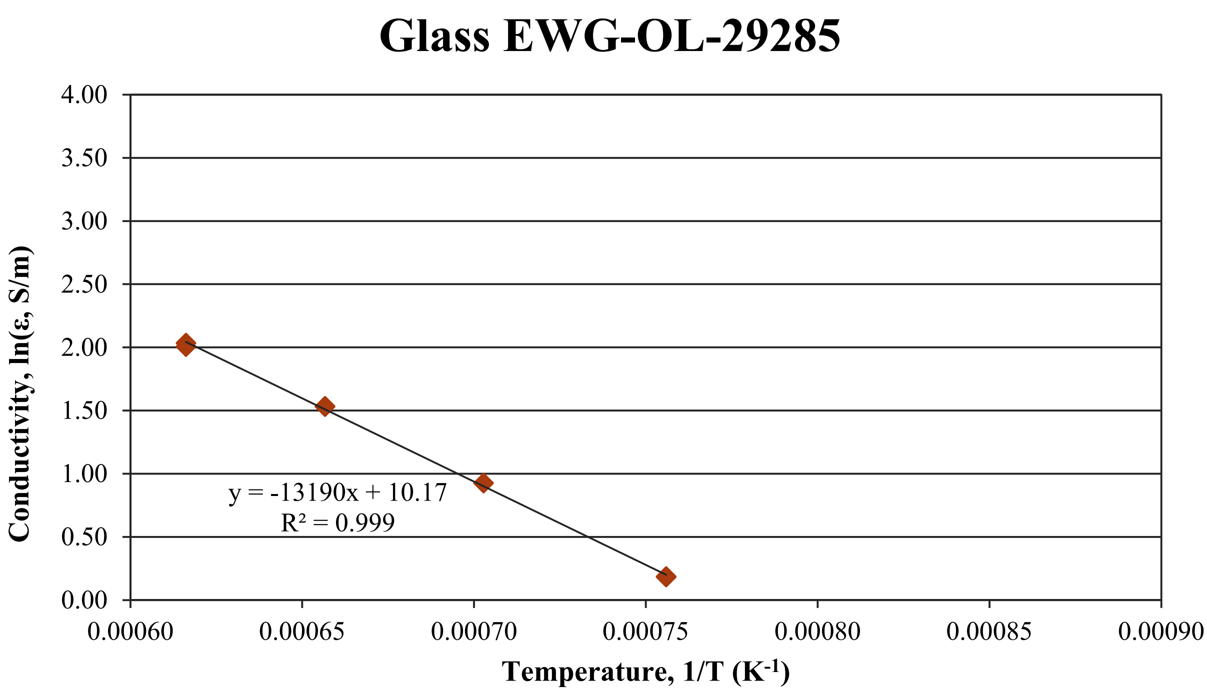

Figure F.26. Electrical Conductivity -Temperature Data and Arrhenius Equation Fit for Glass EWG-OL-29285

F.27 Glass EWG-OL-31644 Electrical Conductivity Data

Table F.27. Electrical Conductivity Data for Glass EWG-OL-31644

Temperature, °C	Conductivity, S/m	1/(T+273.15), K^{-1}	ln(ε, S/m)
1075	5.14	0.00074	1.64
1075	5.14	0.00074	1.64
1375	24.12	0.00061	3.18
1275	15.56	0.00065	2.74
1275	15.60	0.00065	2.75
1175	9.28	0.00069	2.23

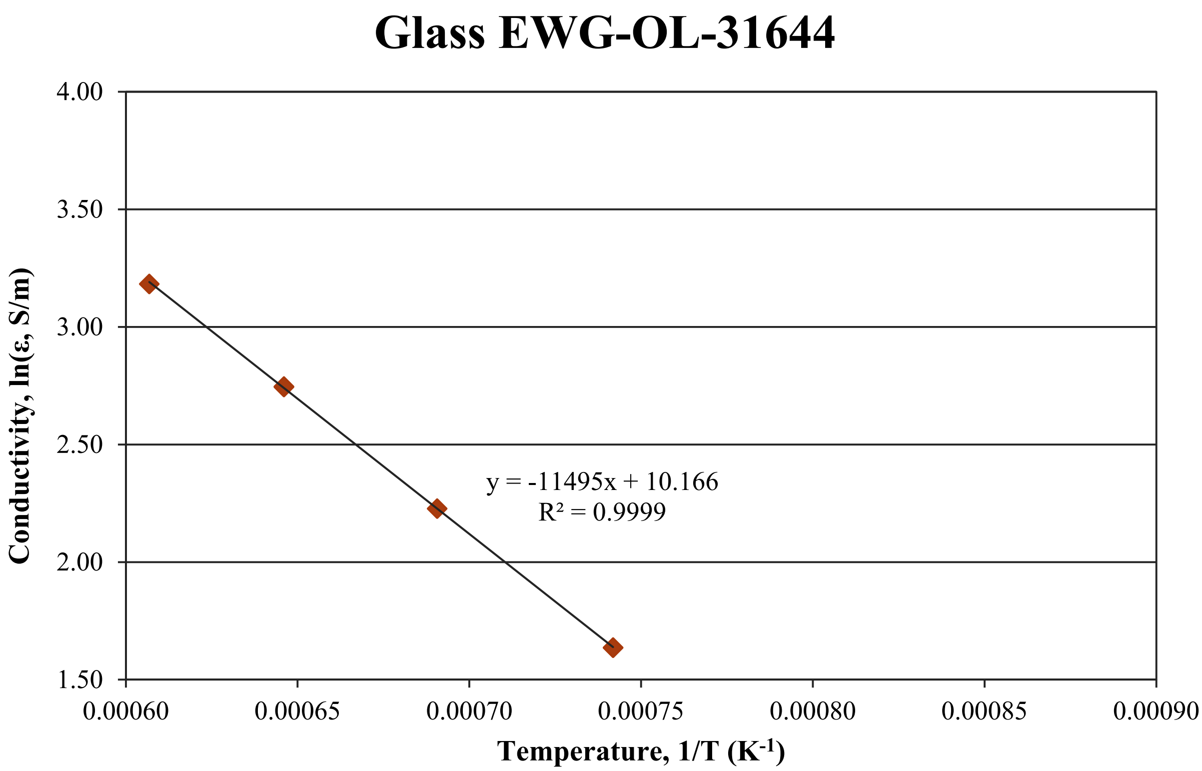

Figure F.27. Electrical Conductivity -Temperature Data and Arrhenius Equation Fit for Glass EWG-OL-31644

F.28 Glass EWG-OL-32706 Electrical Conductivity Data

Table F.28. Electrical Conductivity Data for Glass EWG-OL-32706

Temperature, °C	Conductivity, S/m	1/(T+273.15), K^{-1}	ln(ε, S/m)
1100	6.95	0.00073	1.94
1100	6.96	0.00073	1.94
1390	18.66	0.00060	2.93
1390	18.72	0.00060	2.93
1300	14.25	0.00064	2.66
1200	10.42	0.00068	2.34
1200	10.44	0.00068	2.35

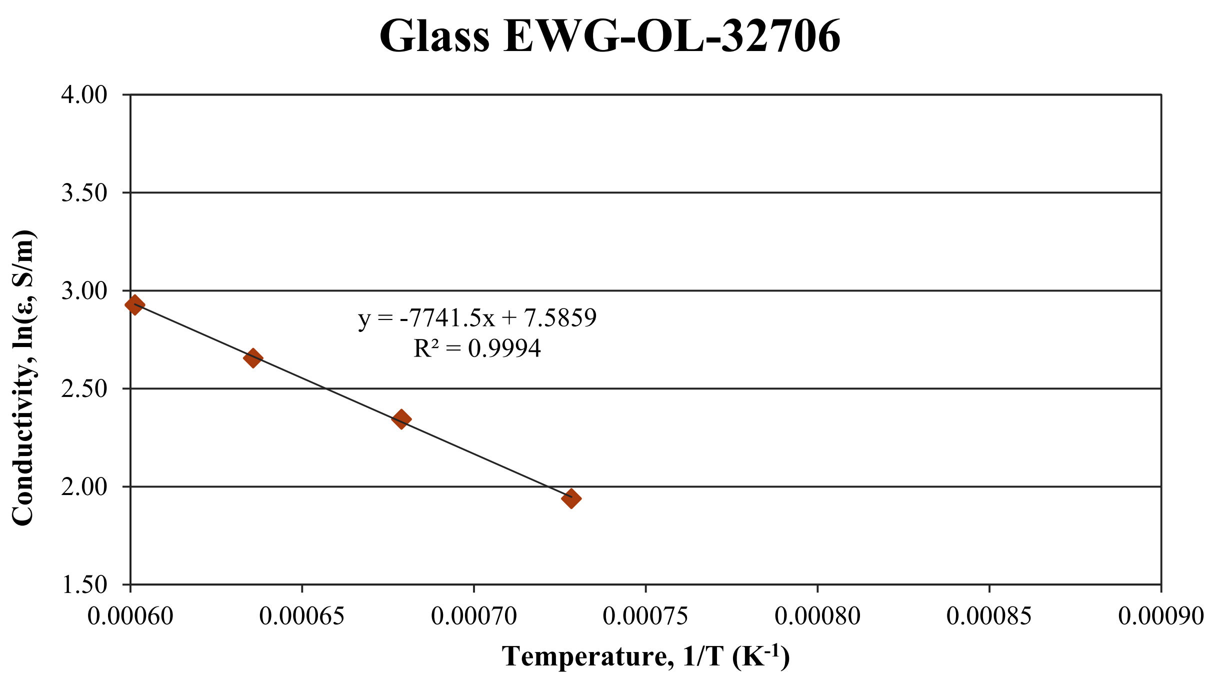

Figure F.28. Electrical Conductivity -Temperature Data and Arrhenius Equation Fit for Glass EWG-OL-32706

F.29 Glass EWG-OL-33115 Electrical Conductivity Data

Table F.29. Electrical Conductivity Data for Glass EWG-OL-33115

Temperature, °C	Conductivity, S/m	1/(T+273.15), K^{-1}	ln(ε, S/m)
1000	1.46	0.00079	0.38
1000	1.47	0.00079	0.39
1300	10.35	0.00064	2.34
1300	10.31	0.00064	2.33
1200	6.11	0.00068	1.81
1100	3.21	0.00073	1.17
1100	3.22	0.00073	1.17

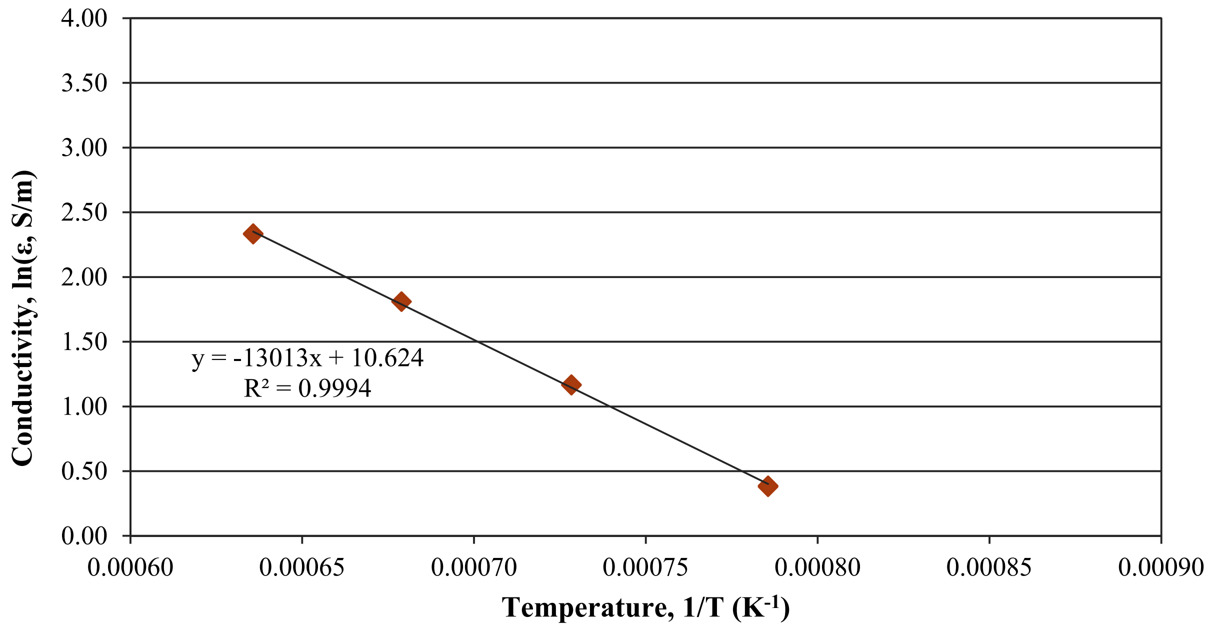

Figure F.29. Electrical Conductivity-Temperature Data and Arrhenius Equation Fit for Glass EWG-OL-33115

F.30 Glass EWG-OL-33558 Electrical Conductivity Data

Table F.30. Electrical Conductivity Data for Glass EWG-OL-33558

Temperature, °C	Conductivity, S/m	1/(T+273.15), K^{-1}	ln(ε, S/m)
1350	13.18	0.00062	2.58
1250	7.94	0.00066	2.07
1250	7.97	0.00066	2.08
1150	4.21	0.00070	1.44
1150	4.22	0.00070	1.44
1050	1.94	0.00076	0.66
1050	1.95	0.00076	0.67

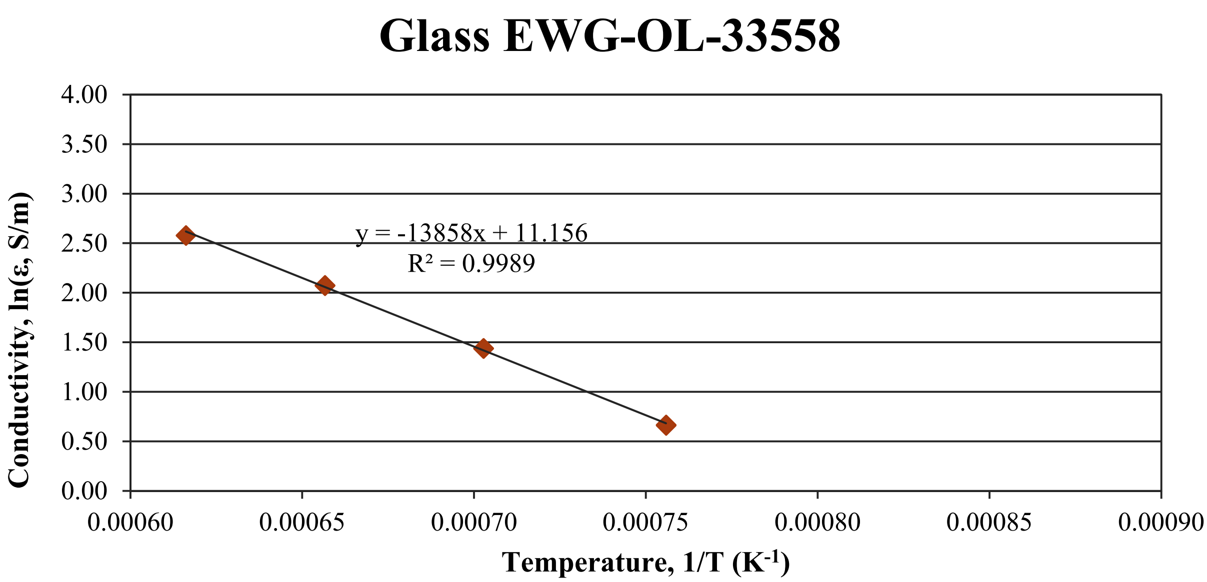

Figure F.30. Electrical Conductivity -Temperature Data and Arrhenius Equation Fit for Glass EWG-OL-33558

F.31 Glass EWG-OL-33694 Electrical Conductivity Data

Table F.31. Electrical Conductivity Data for Glass EWG-OL-33694

Temperature, °C	Conductivity, S/m	1/(T+273.15), K^{-1}	ln(ε, S/m)
1100	3.23	0.00073	1.17
1100	3.23	0.00073	1.17
1390	10.12	0.00060	2.31
1390	10.05	0.00060	2.31
1300	7.55	0.00064	2.02
1300	7.56	0.00064	2.02
1200	5.11	0.00068	1.63

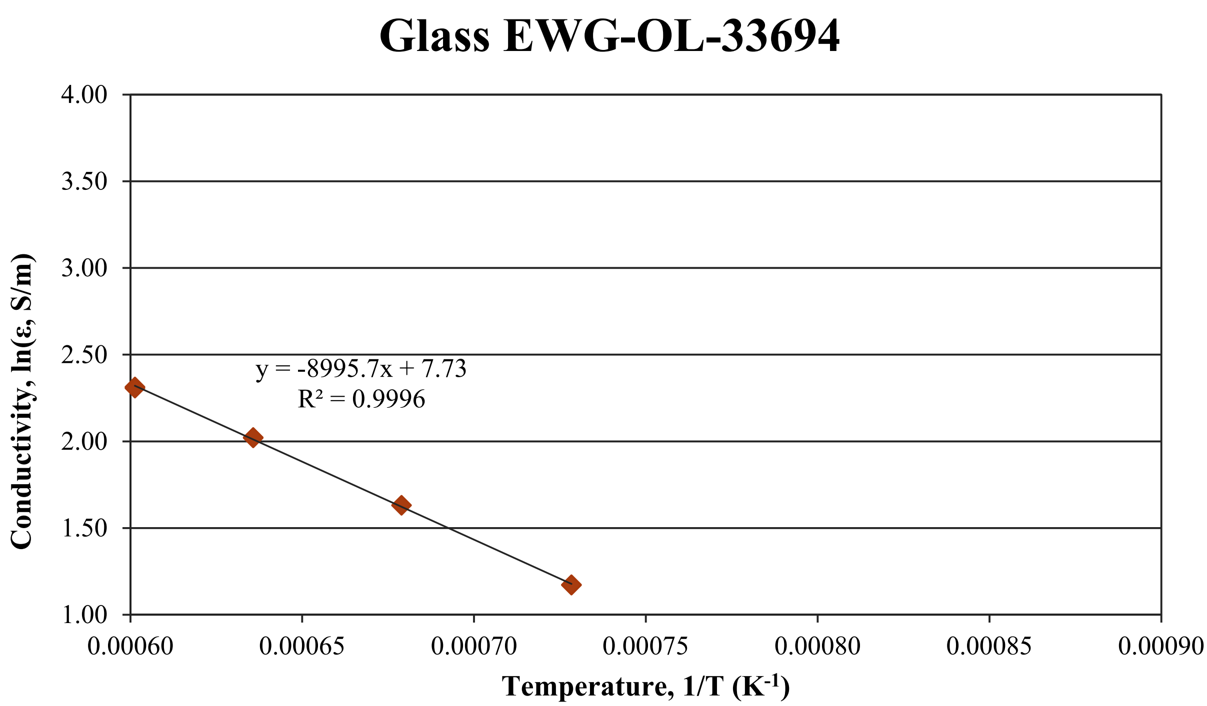

Figure F.31. Electrical Conductivity -Temperature Data and Arrhenius Equation Fit for Glass EWG-OL-33694

F.32 Glass EWG-OL-33858 Electrical Conductivity Data

Table F.32. Electrical Conductivity Data for Glass EWG-OL-33858

Temperature, °C	Conductivity, S/m	1/(T+273.15), K^{-1}	ln(ε, S/m)
1000	14.12	0.00079	2.65
1000	14.18	0.00079	2.65
1300	41.88	0.00064	3.73
1200	31.68	0.00068	3.46
1200	31.72	0.00068	3.46
1100	22.23	0.00073	3.10
1100	22.27	0.00073	3.10

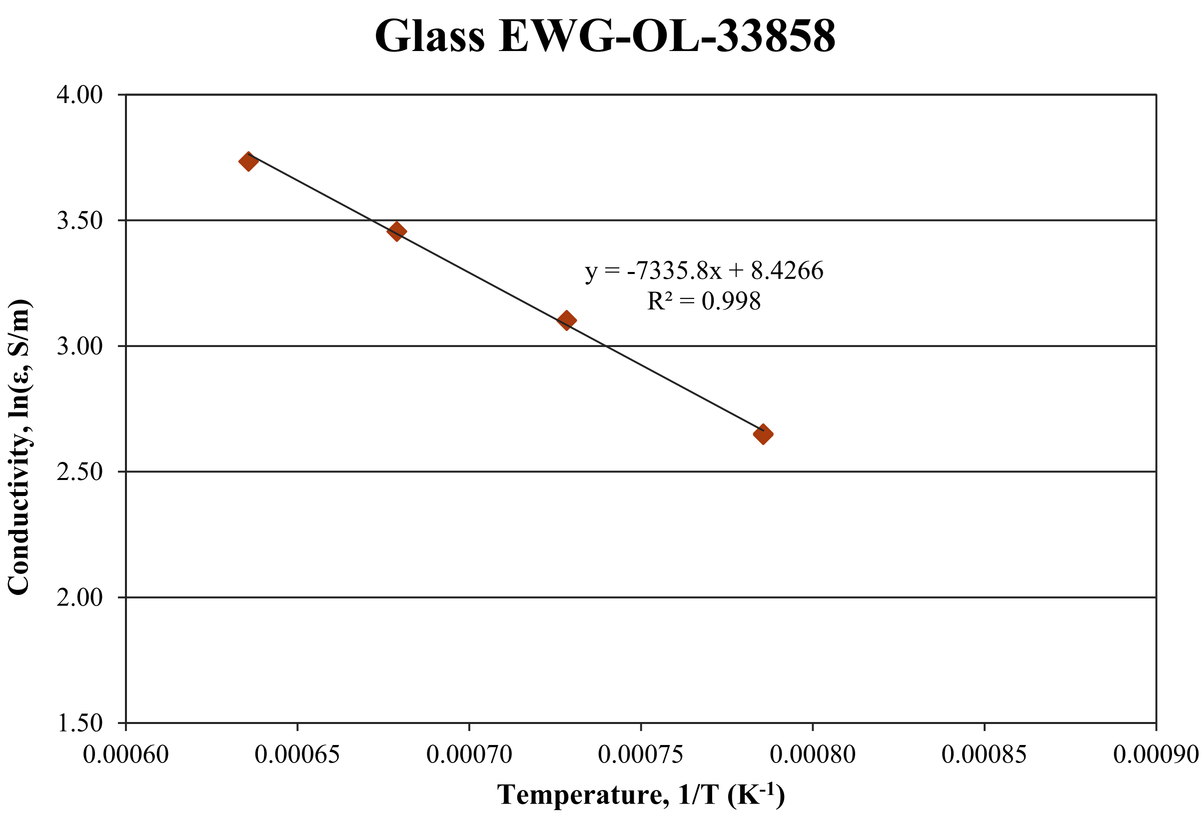

Figure F.32. Electrical Conductivity -Temperature Data and Arrhenius Equation Fit for Glass EWG-OL-33858

F.33 Glass EWG-OL-35387 Electrical Conductivity Data

Table F.33. Electrical Conductivity Data for Glass EWG-OL-35387

Temperature, °C	Conductivity, S/m	1/(T+273.15), K^{-1}	ln(ε, S/m)
1350	48.65	0.00062	3.88
1250	39.40	0.00066	3.67
1150	30.45	0.00070	3.42
1150	30.52	0.00070	3.42
1050	21.96	0.00076	3.09
1050	22.00	0.00076	3.09

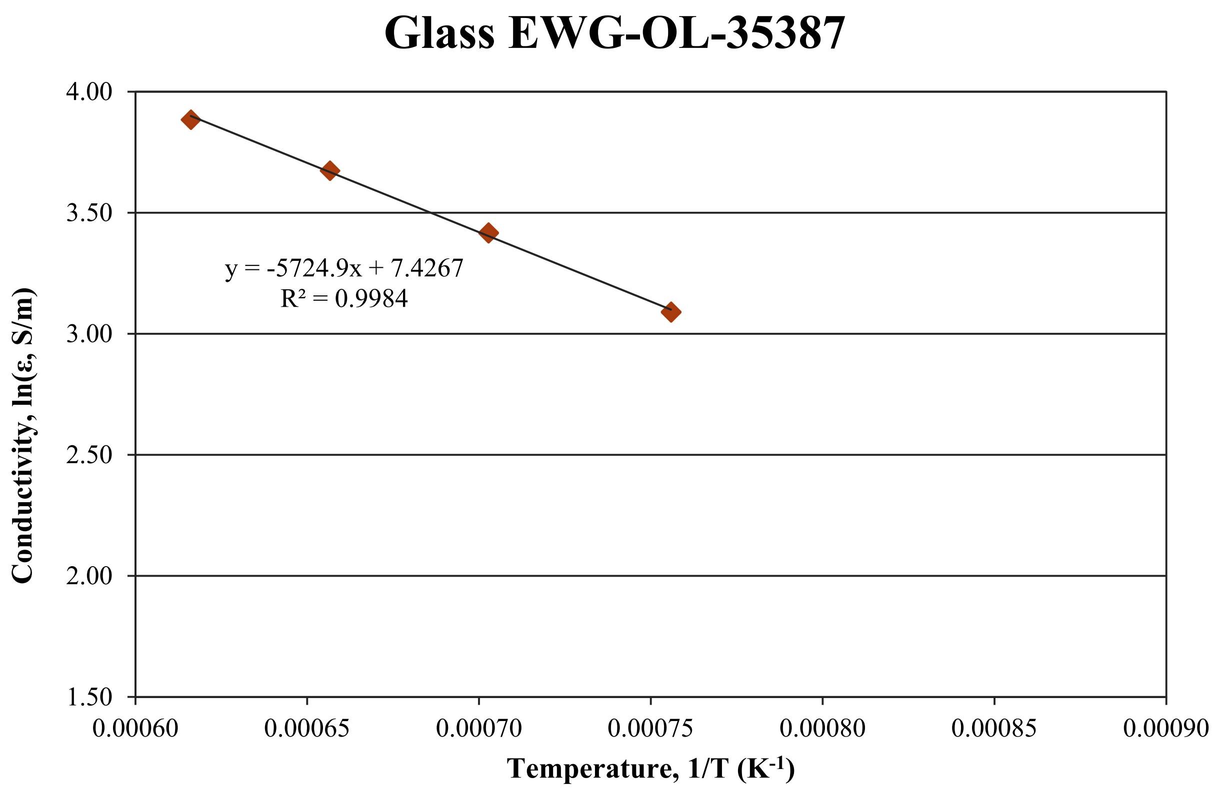

Figure F.33. Electrical Conductivity -Temperature Data and Arrhenius Equation Fit for Glass EWG-OL-35387

F.34 Glass EWG-OL-38081 Electrical Conductivity Data

Table F.34. Electrical Conductivity Data for Glass EWG-OL-38081

Temperature, °C	Conductivity, S/m	1/(T+273.15), K^{-1}	ln(ε, S/m)
1050	23.57	0.00076	3.16
1050	23.59	0.00076	3.16
1350	53.35	0.00062	3.98
1250	43.82	0.00066	3.78
1150	33.40	0.00070	3.51
1150	33.42	0.00070	3.51

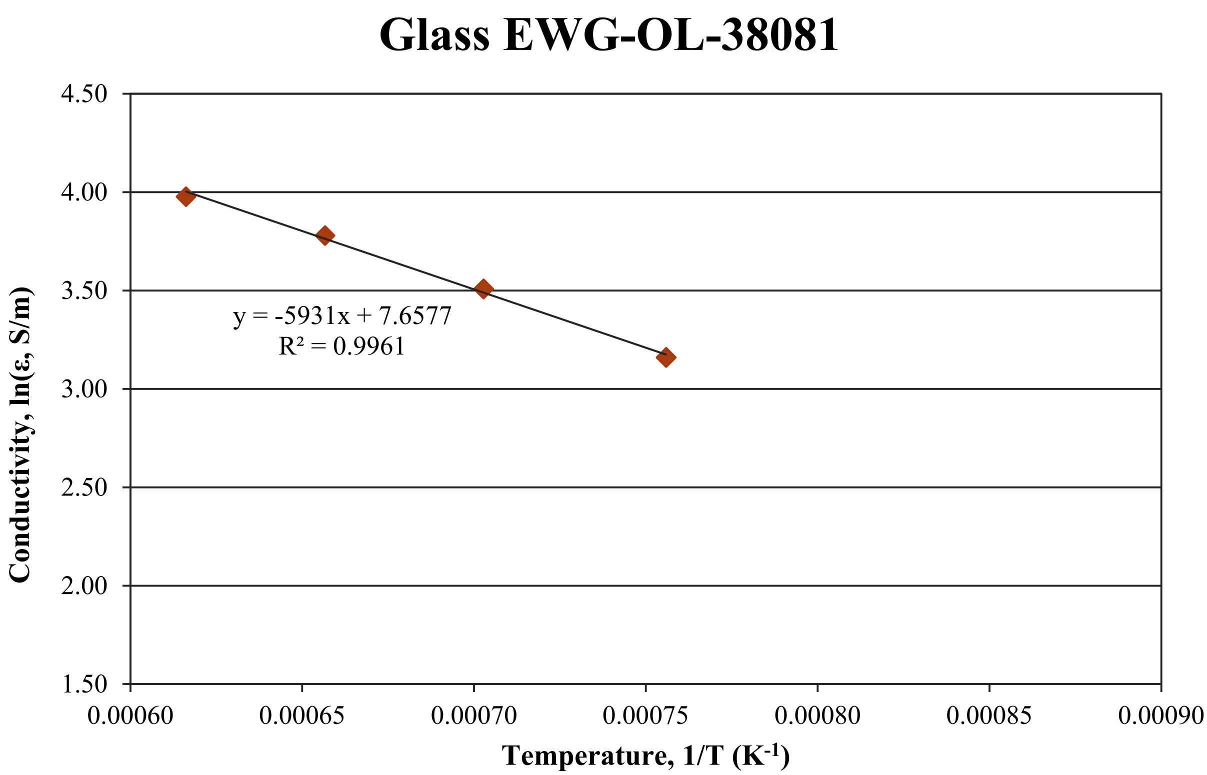

Figure F.34. Electrical Conductivity -Temperature Data and Arrhenius Equation Fit for Glass EWG-OL-38081

F.35 Glass EWG-OL-38552 Electrical Conductivity Data

Table F.35. Electrical Conductivity Data for Glass EWG-OL-38552

Temperature, °C	Conductivity, S/m	1/(T+273.15), K^{-1}	ln(ε, S/m)
1250	45.87	0.00066	3.83
1250	45.71	0.00066	3.82
1150	34.59	0.00070	3.54
1150	34.62	0.00070	3.54
1050	24.10	0.00076	3.18
1050	24.16	0.00076	3.18
950	15.17	0.00082	2.72
950	15.24	0.00082	2.72

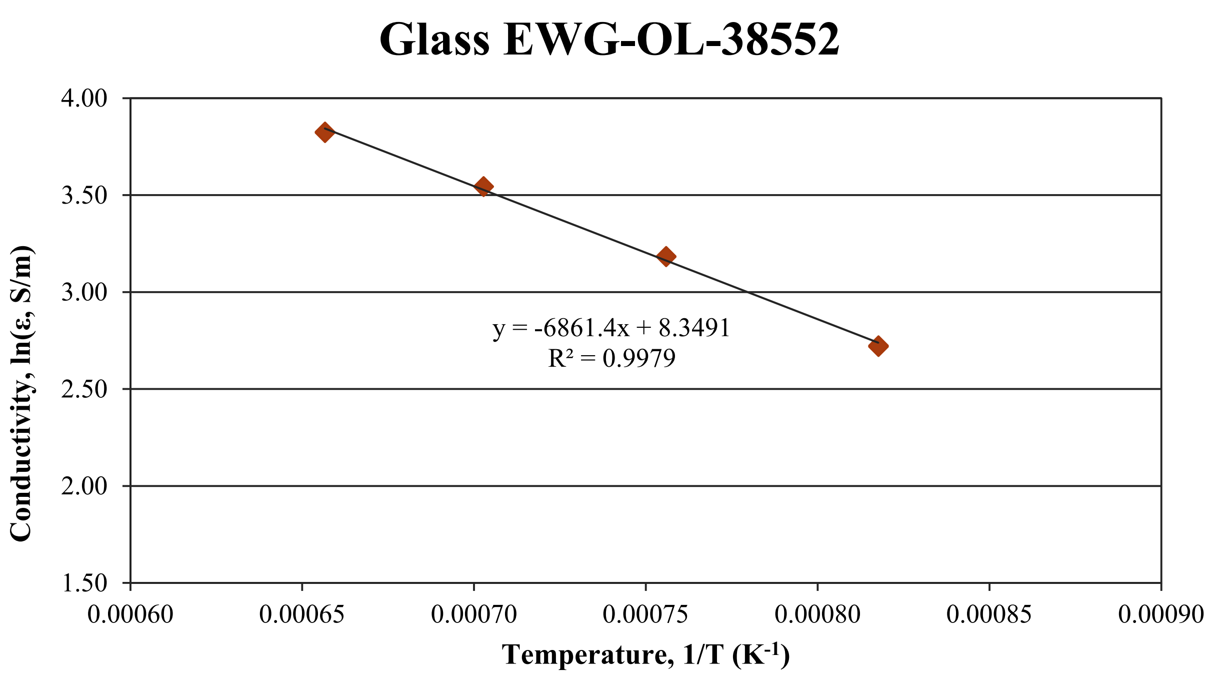

Figure F.35. Electrical Conductivity -Temperature Data and Arrhenius Equation Fit for Glass EWG-OL-38552

F.36 Glass EWG-OL-1755 Mod 8% Fe 10% B Electrical Conductivity Data

Table F.36. Electrical Conductivity Data for Glass EWG-OL-1755 Mod 8% Fe 10% B

Temperature, °C	Conductivity, S/m	1/(T+273.15), K^{-1}	ln(ε, S/m)
1275	44.50	0.00065	3.80
1275	44.37	0.00065	3.79
1150	31.66	0.00070	3.46
1150	31.72	0.00070	3.46
1050	22.21	0.00076	3.10
1050	22.27	0.00076	3.10
950	14.12	0.00082	2.65
950	14.20	0.00082	2.65

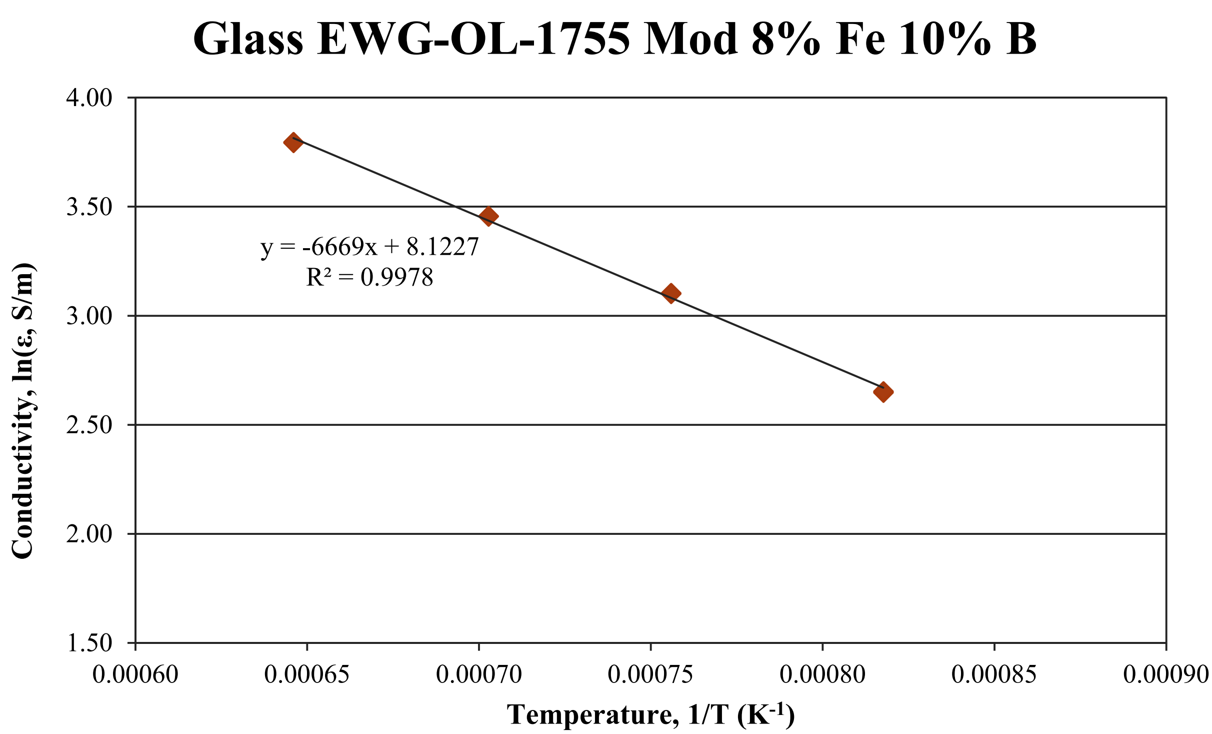

Figure F.36. Electrical Conductivity -Temperature Data and Arrhenius Equation Fit for Glass EWG-OL-1755 Mod 8% Fe 10% B

F.37 Glass EWG-OL-3063 Mod 1% Zr 3% Li Electrical Conductivity Data

Table F.37. Electrical Conductivity Data for Glass EWG-OL-3063 Mod 1% Zr 3% Li

Temperature, °C	Conductivity, S/m	1/(T+273.15), K^{-1}	ln(ε, S/m)
1100	14.95	0.00073	2.70
1100	14.86	0.00073	2.70
1390	35.57	0.00060	3.57
1390	35.64	0.00060	3.57
1300	27.97	0.00064	3.33
1300	28.01	0.00064	3.33
1200	20.64	0.00068	3.03
1200	20.69	0.00068	3.03

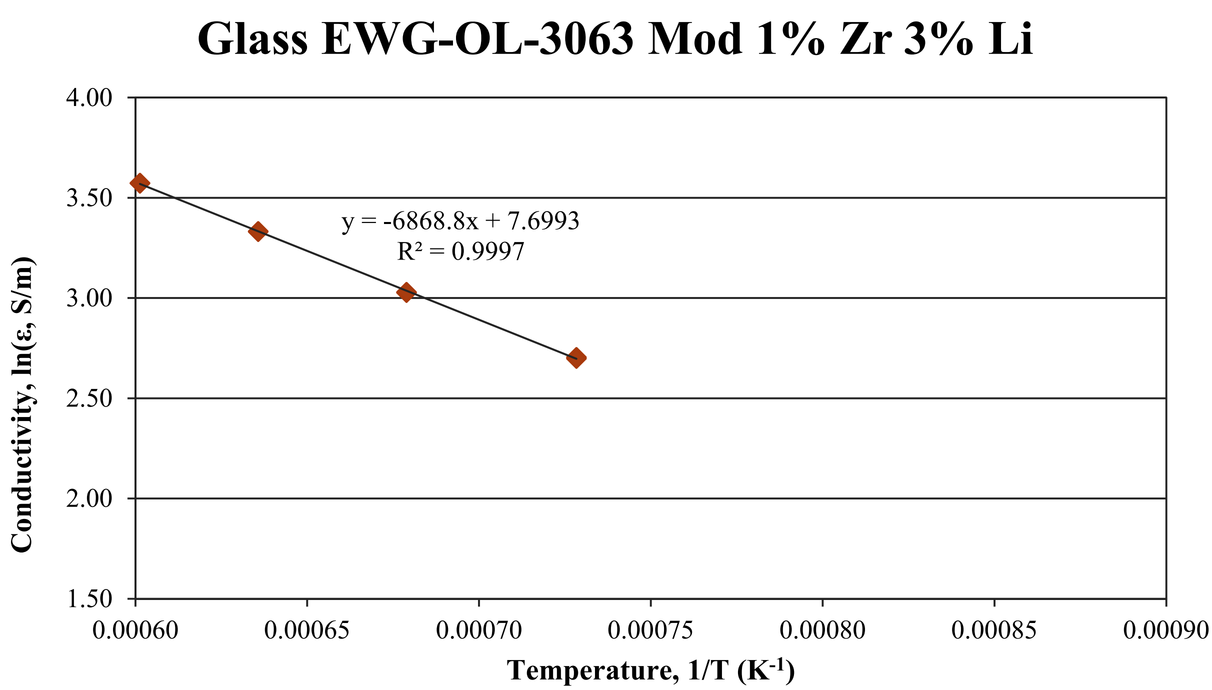

Figure F.37. Electrical Conductivity -Temperature Data and Arrhenius Equation Fit for Glass EWG-OL-3063 Mod 1% Zr 3% Li

F.38 Glass EWG-OL-4744 Mod 7.5% Fe 1% Zr Electrical Conductivity Data

Table F.38. Electrical Conductivity Data for Glass EWG-OL-4744 Mod 7.5% Fe 1% Zr

Temperature, °C	Conductivity, S/m	1/(T+273.15), K^{-1}	ln(ε, S/m)
950	13.90	0.00082	2.63
950	14.59	0.00082	2.68
1250	47.97	0.00066	3.87
1250	47.61	0.00066	3.86
1150	35.13	0.00070	3.56
1150	35.21	0.00070	3.56
1050	23.75	0.00076	3.17
1050	23.88	0.00076	3.17

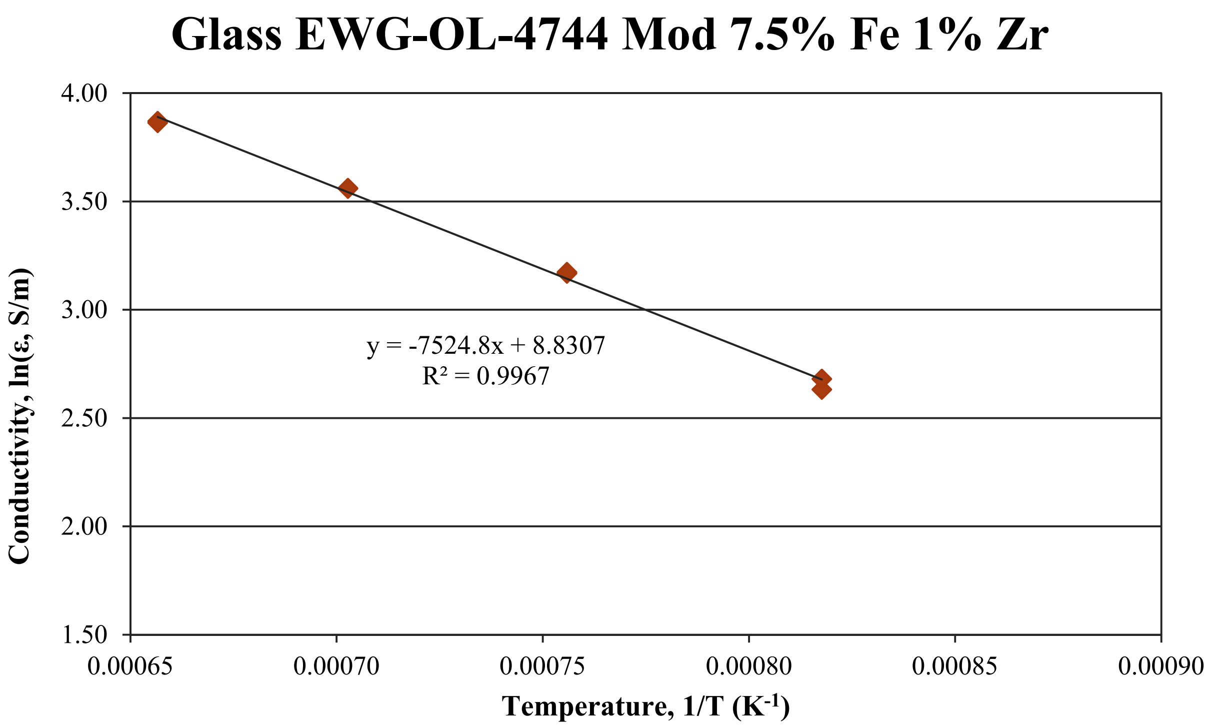

Figure F.38. Electrical Conductivity -Temperature Data and Arrhenius Equation Fit for Glass EWG-OL-4744 Mod 7.5% Fe 1% Zr

F.39 Glass EWG-OL-5385 Mod 12% B 17% Na Electrical Conductivity Data

Table F.39. Electrical Conductivity Data for Glass EWG-OL-5385 Mod 12% B 17% Na

Temperature, °C	Conductivity, S/m	1/(T+273.15), K^{-1}	ln(ε, S/m)
1225	62.18	0.00067	4.13
1125	47.34	0.00072	3.86
1125	47.33	0.00072	3.86
1025	32.58	0.00077	3.48
1025	32.65	0.00077	3.49
925	19.79	0.00083	2.99
925	19.81	0.00083	2.99

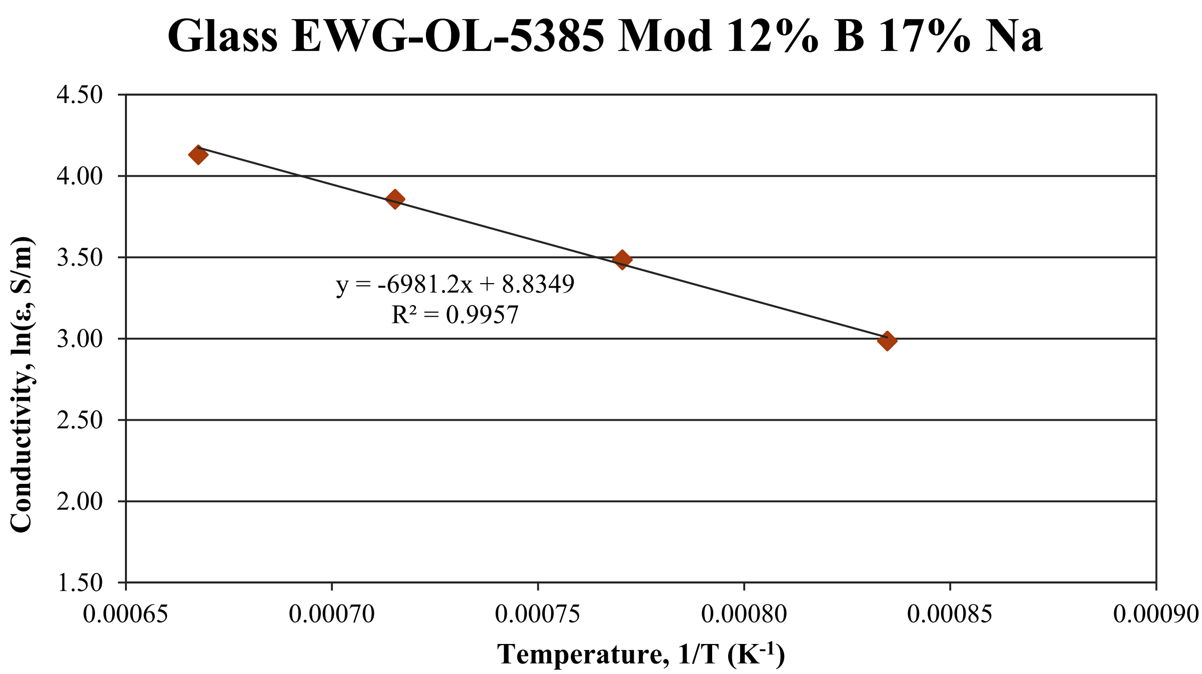

Figure F.39. Electrical Conductivity -Temperature Data and Arrhenius Equation Fit for Glass EWG-OL-5385 Mod 12% B 17% Na

F.40 Glass EWG-OL-6257 Mod 12% B 8% Ca Electrical Conductivity Data

Table F.40. Electrical Conductivity Data for Glass EWG-OL-6257 Mod 12% B 8% Ca

Temperature, °C	Conductivity, S/m	1/(T+273.15), K^{-1}	ln(ε, S/m)
925	8.66	0.00083	2.16
925	8.72	0.00083	2.17
1225	34.06	0.00067	3.53
1225	33.94	0.00067	3.52
1125	24.22	0.00072	3.19
1125	24.28	0.00072	3.19
1025	15.47	0.00077	2.74
1025	15.53	0.00077	2.74

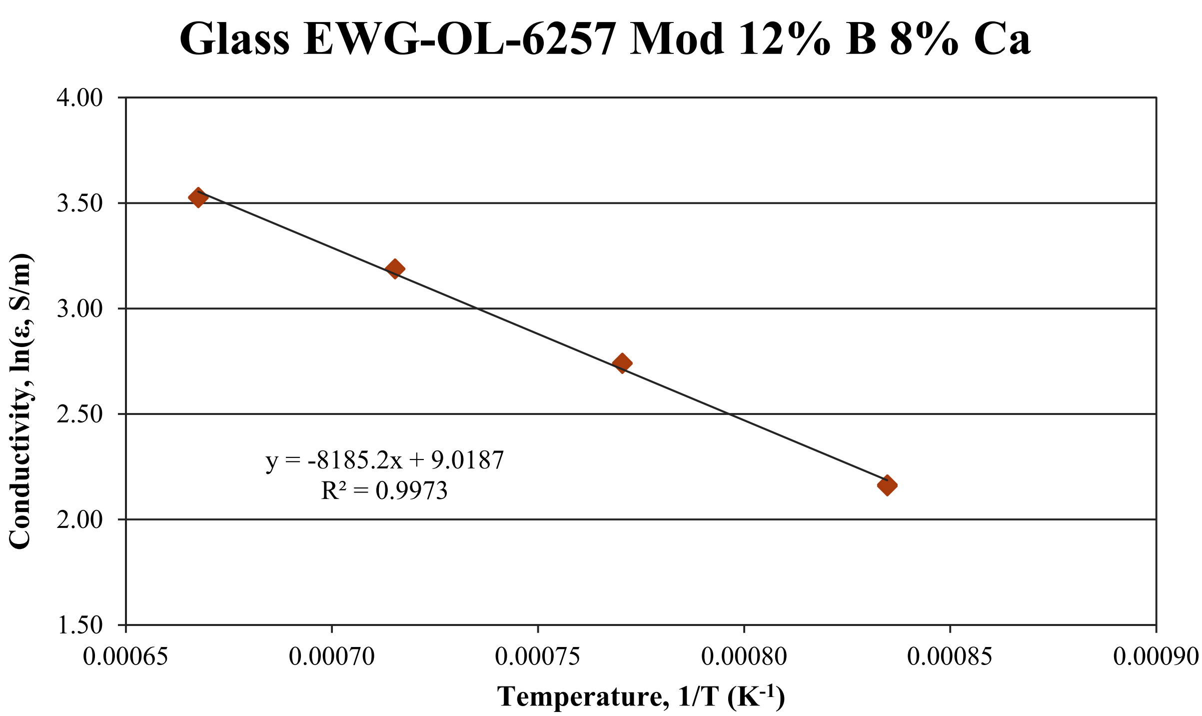

Figure F.40. Electrical Conductivity -Temperature Data and Arrhenius Equation Fit for Glass EWG-OL-6257 Mod 12% B 8% Ca

F.41 Glass EWG-OL-6311 Mod Reduced Na & K Electrical Conductivity Data

Table F.41. Electrical Conductivity Data for Glass EWG-OL-6311 Reduced Na and K

Temperature, °C	Conductivity, S/m	1/(T+273.15), K^{-1}	ln(ε, S/m)
1125	67.32	0.00072	4.21
1125	67.12	0.00072	4.21
1025	48.66	0.00077	3.88
1025	48.99	0.00077	3.89
925	30.53	0.00083	3.42
925	30.77	0.00083	3.43
825	16.39	0.00091	2.80
825	16.68	0.00091	2.81

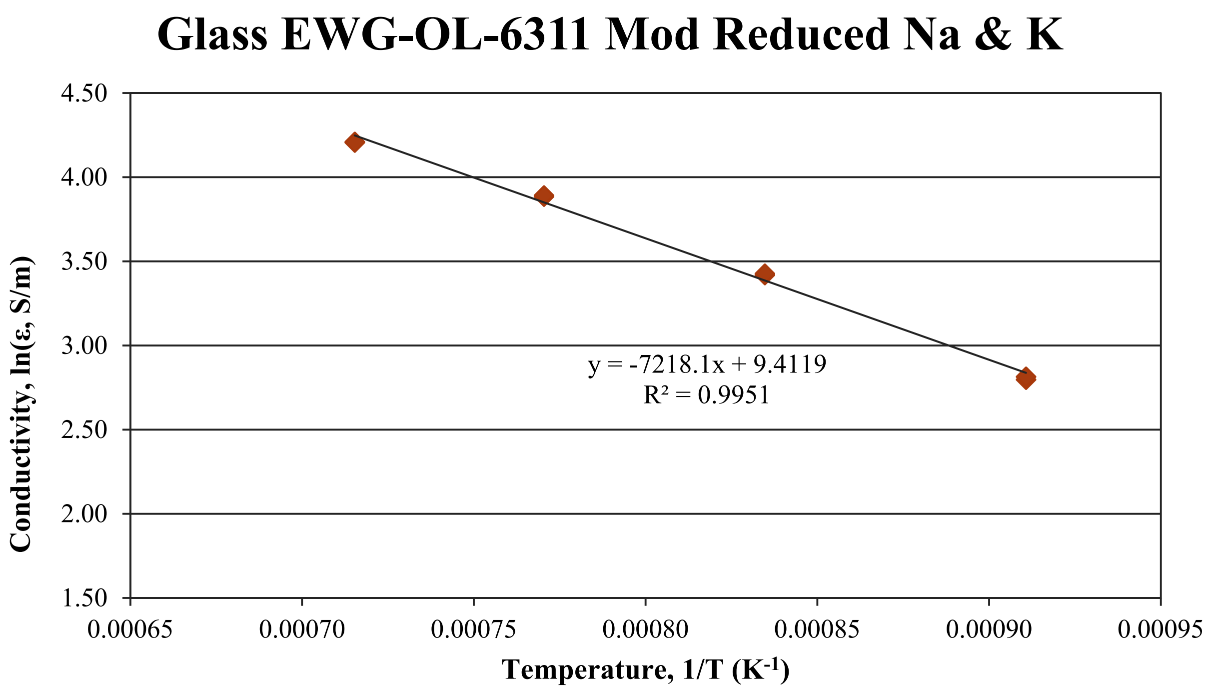

Figure F.41. Electrical Conductivity -Temperature Data and Arrhenius Equation Fit for Glass EWG-OL-6311 Mod Reduced Na and K

F.42 Glass EWG-OL-6489 Mod 11% B 15% Na Electrical Conductivity Data

Table F.42. Electrical Conductivity Data for Glass EWG-OL-1755 Mod 11% B 15% Na

Temperature, °C	Conductivity, S/m	1/(T+273.15), K^{-1}	ln(ε, S/m)
900	21.95	0.00085	3.09
900	22.04	0.00085	3.09
1200	53.30	0.00068	3.98
1200	53.18	0.00068	3.97
1100	49.20	0.00073	3.90
1100	49.53	0.00073	3.90
1000	34.56	0.00079	3.54
1000	35.00	0.00079	3.56

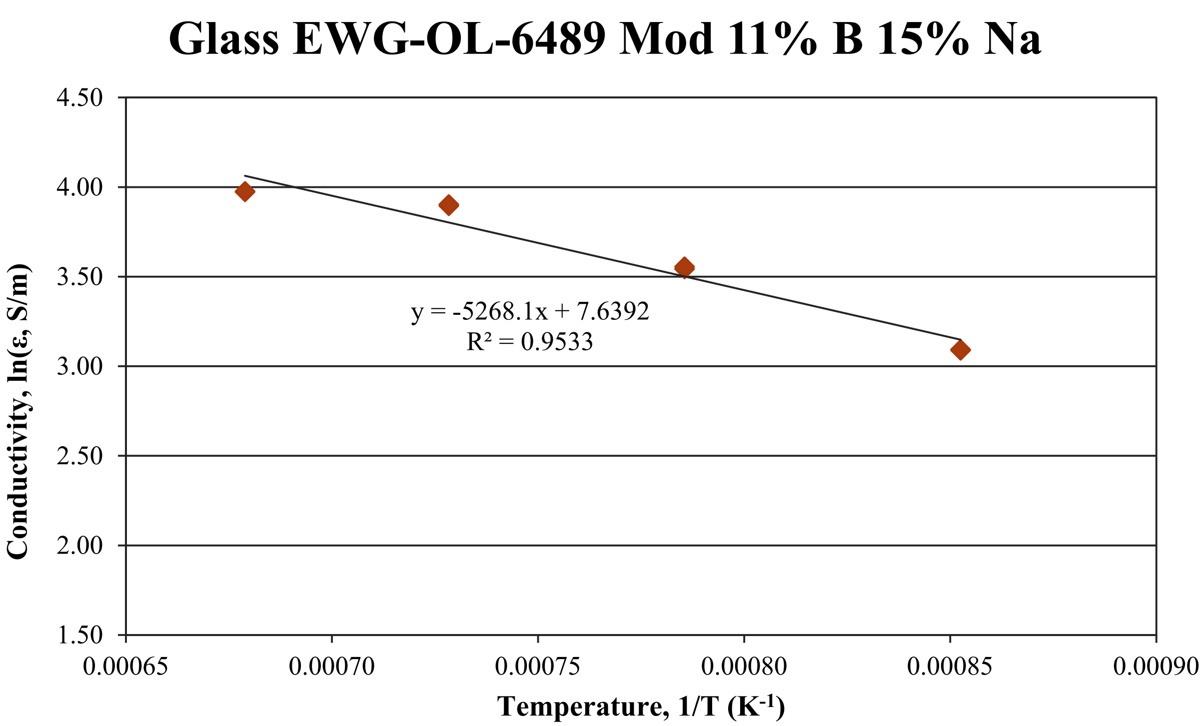

Figure F.42. Electrical Conductivity -Temperature Data and Arrhenius Equation Fit for Glass EWG-OL-6489 Mod 11% B 15% Na

F.43 Glass EWG-OL-8548 Mod 1% Zr Electrical Conductivity Data

Table F.43. Electrical Conductivity Data for Glass EWG-OL-8548 Mod 1% Zr

Temperature, °C	Conductivity, S/m	1/(T+273.15), K^{-1}	ln(ε, S/m)
1300	51.74	0.00064	3.95
1300	51.59	0.00064	3.94
1200	41.34	0.00068	3.72
1200	41.35	0.00068	3.72
1100	31.74	0.00073	3.46
1100	31.79	0.00073	3.46
1000	22.89	0.00079	3.13
1000	22.96	0.00079	3.13

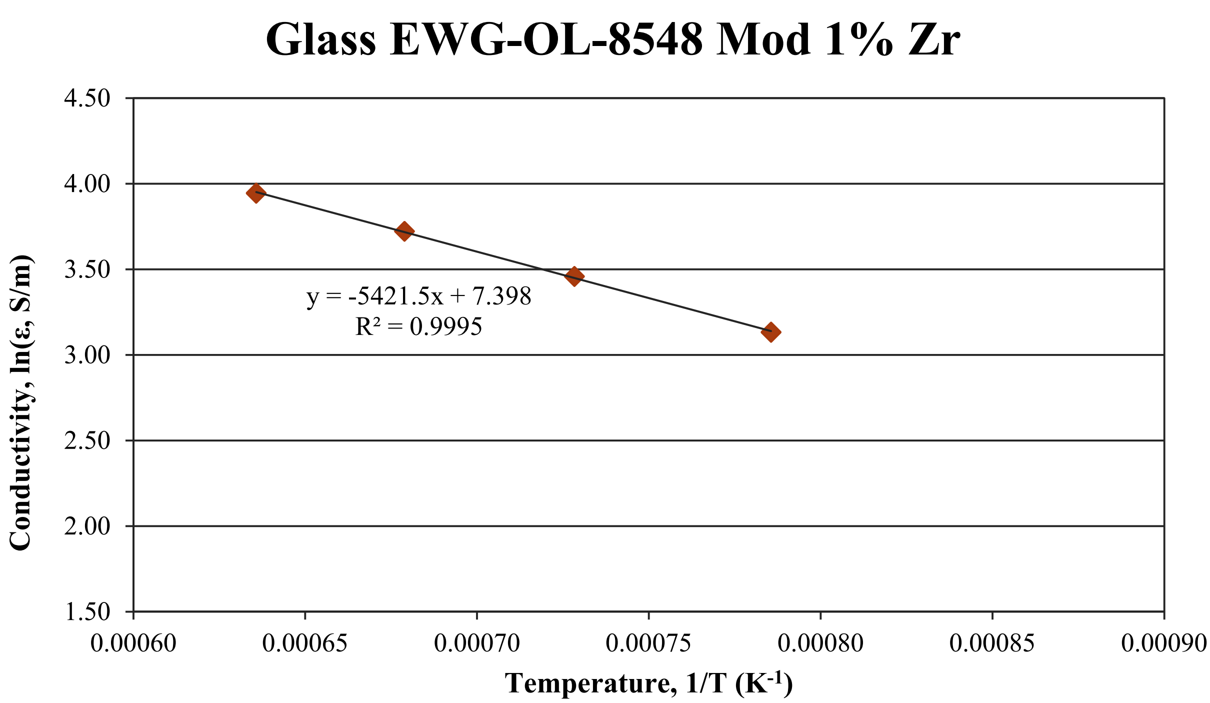

Figure F.43. Electrical Conductivity -Temperature Data and Arrhenius Equation Fit for Glass EWG-OL-8548 Mod 1% Zr

F.44 Glass EWG-OL-10278 Mod 15% B 1% Zr Electrical Conductivity Data

Table F.44. Electrical Conductivity Data for Glass EWG-OL-10278 Mod 15% B 1% Zr

Temperature, °C	Conductivity, S/m	1/(T+273.15), K^{-1}	ln(ε, S/m)
1027	35.79	0.00077	3.58
1027	35.32	0.00077	3.56
975	29.11	0.00080	3.37
975	29.10	0.00080	3.37
925	22.39	0.00083	3.11
925	22.36	0.00083	3.11
875	16.52	0.00087	2.80
875	16.54	0.00087	2.81

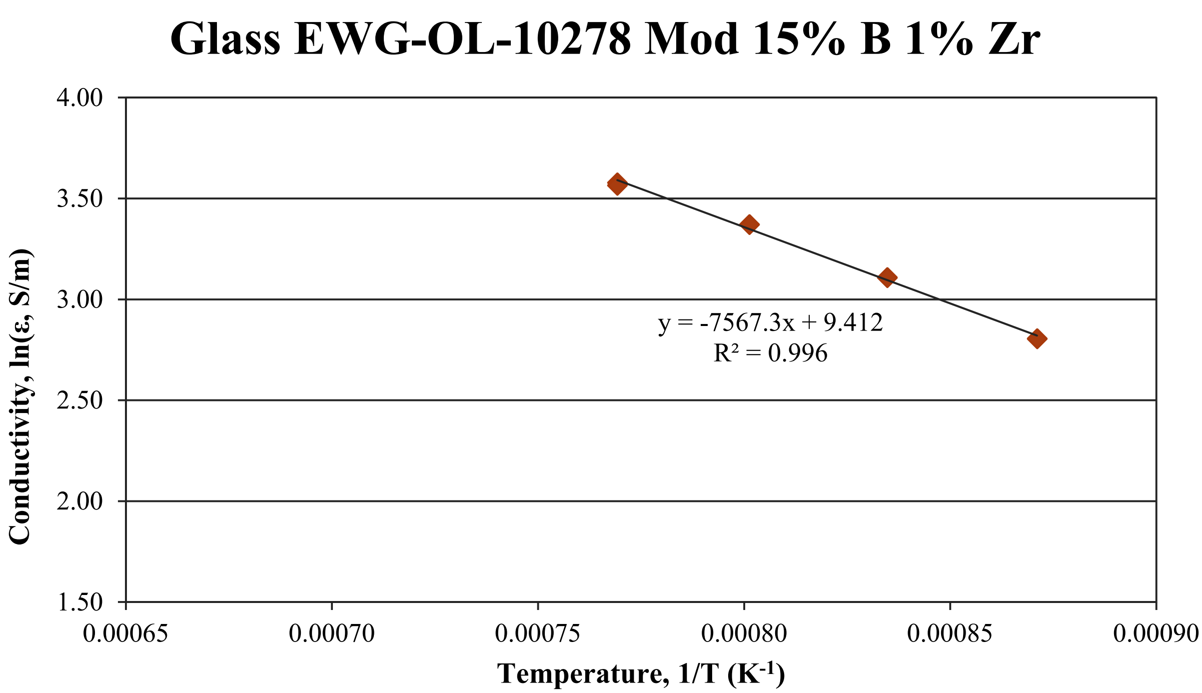

Figure F.44. Electrical Conductivity -Temperature Data and Arrhenius Equation Fit for Glass EWG-OL-10278 Mod 15% B 1% Zr

F.45 Glass EWG-OL-11318 Mod 1% Zr Electrical Conductivity Data

Table F.45. Electrical Conductivity Data for Glass EWG-OL-11318 Mod 1% Zr

Temperature, °C	Conductivity, S/m	1/(T+273.15), K^{-1}	ln(ε, S/m)
1250	41.28	0.00066	3.72
1250	41.16	0.00066	3.72
1150	32.28	0.00070	3.47
1150	32.33	0.00070	3.48
1050	23.39	0.00076	3.15
1050	23.48	0.00076	3.16
950	15.23	0.00082	2.72
950	15.35	0.00082	2.73

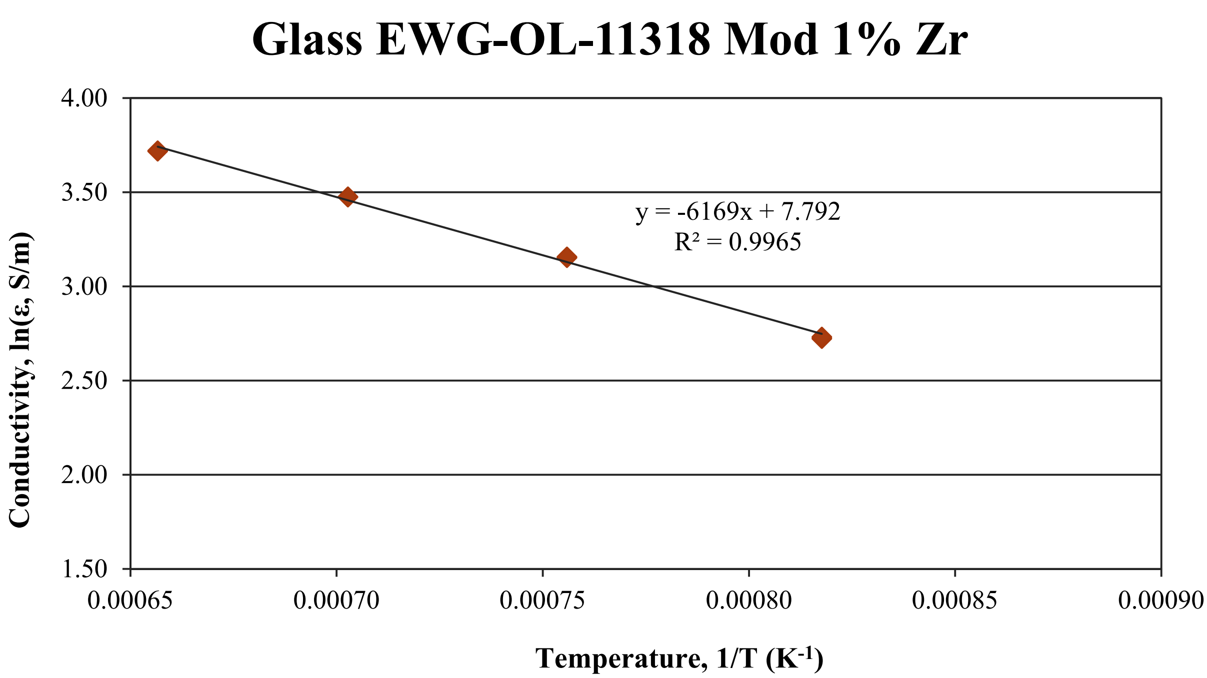

Figure F.45. Electrical Conductivity -Temperature Data and Arrhenius Equation Fit for Glass EWG-OL-11318 Mod 1% Zr

F.46 Glass EWG-OL-14547 Mod Reduced Alkali 1% Zr Electrical Conductivity Data

Table F.46. Electrical Conductivity Data for Glass EWG-OL-14547 Mod Reduced Alkali 1% Zr

Temperature, °C	Conductivity, S/m	1/(T+273.15), K^{-1}	ln(ε, S/m)
1125	50.77	0.00072	3.93
1125	50.37	0.00072	3.92
1025	35.44	0.00077	3.57
1025	35.51	0.00077	3.57
925	21.15	0.00083	3.05
925	21.62	0.00083	3.07
825	9.77	0.00091	2.28
825	10.06	0.00091	2.31

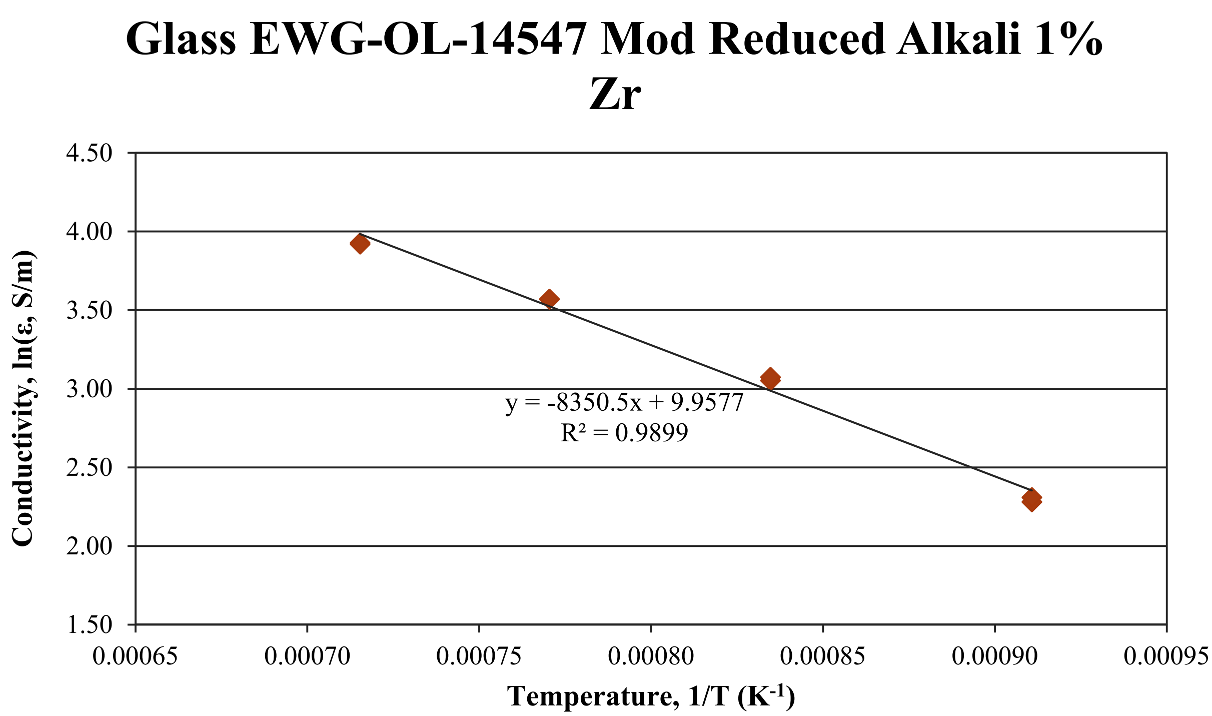

Figure F.46. Electrical Conductivity -Temperature Data and Arrhenius Equation Fit for Glass EWG-OL-14547 Mod Reduced Alkali 1% Zr

F.47 Glass EWG-OL-15698 Mod Low Na Electrical Conductivity Data

Table F.47. Electrical Conductivity Data for Glass EWG-OL-15698 Mod Low Na

Temperature, °C	Conductivity, S/m	1/(T+273.15), K^{-1}	ln(ε, S/m)
1047	34.41	0.00076	3.54
1049	34.77	0.00076	3.55
960	22.98	0.00081	3.13
958	22.88	0.00081	3.13
908	17.20	0.00085	2.85
907	17.09	0.00085	2.84
860	11.60	0.00088	2.45
859	11.50	0.00088	2.44

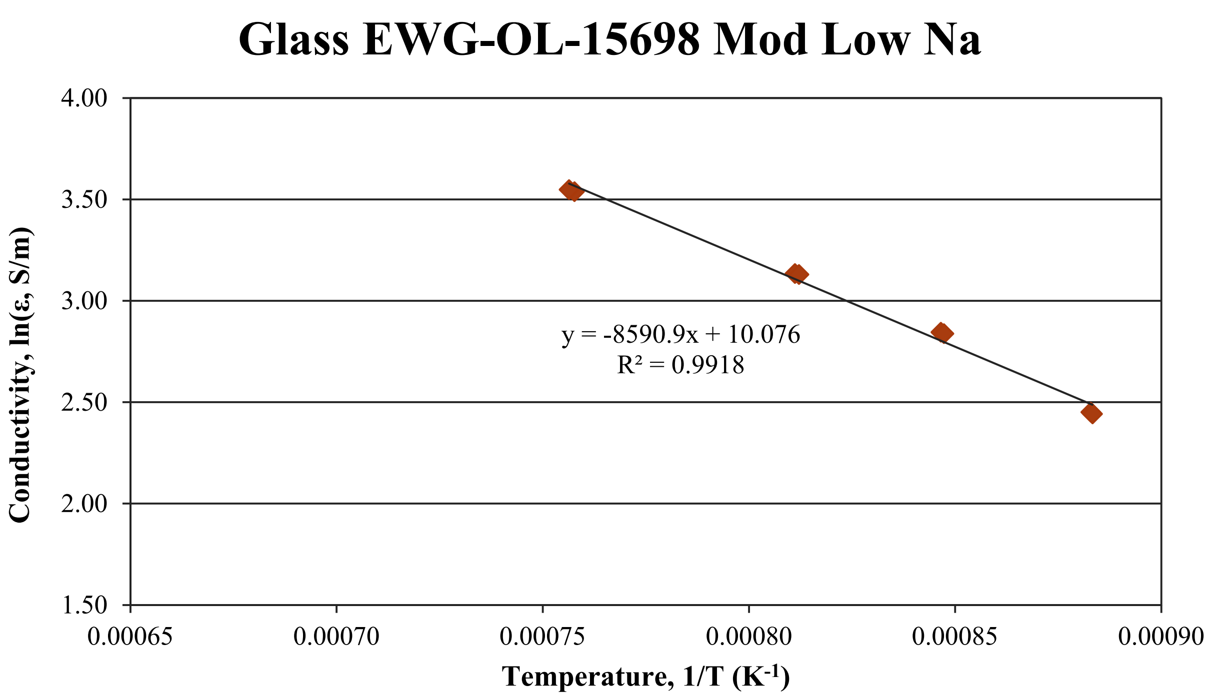

Figure F.47. Electrical Conductivity -Temperature Data and Arrhenius Equation Fit for Glass EWG-OL-15698 Mod Low Na

Appendix G

Crystalline Phase Characterization of Liquidus Temperature

Appendix G

Crystalline Phase Characterization of Liquidus Temperature

This appendix shows the crystalline phase identification and the weight percentages of each identified crystalline phase of the liquidus temperature test at several different temperatures.

Table G.1. Crystal Phase Characterization of HLW Glasses

Glass-ID	Melt Temp (°C)	Wt% Crystallinity	Crystal Phase Identification
EWG-HAI-Centroid-1	950	2.68	$(Li_{0.29}Fe_{1.7})(Li_{0.71}Fe_{1.8}Mn_{1.5})O_8$
	1000	2.48	$(Li_{0.29}Fe_{1.7})(Li_{0.71}Fe_{1.8}Mn_{1.5})O_8$
	1050	1.95	$(Li_{0.29}Fe_{1.7})(Li_{0.71}Fe_{1.8}Mn_{1.5})O_8$
	1201	1.28	$(Li_{0.29}Fe_{1.7})(Li_{0.71}Fe_{1.8}Mn_{1.5})O_8$
EWG-HAI-Centroid-2	950	2.68	$(Li_{0.29}Fe_{1.7})(Li_{0.71}Fe_{1.8}Mn_{1.5})O_8$
	1000	1.72	$(Li_{0.29}Fe_{1.7})(Li_{0.71}Fe_{1.8}Mn_{1.5})O_8$
	1050	1.57	$(Li_{0.29}Fe_{1.7})(Li_{0.71}Fe_{1.8}Mn_{1.5})O_8$
	1100	1.20	$(Li_{0.29}Fe_{1.7})(Li_{0.71}Fe_{1.8}Mn_{1.5})O_8$
	1147	1.28	$(Li_{0.504}Fe_{0.496})(Li_{0.18}Fe_{0.662}Mn_{1.158})O_4$
	1201	1.00	$(Li_{0.504}Fe_{0.496})(Li_{0.18}Fe_{0.662}Mn_{1.158})O_4$
EWG-OL-801	902	0.26	Quartz low
	1000	0.68	Al_2O_3
	1050	0	Amorphous
	1100	0	Amorphous
EWG-OL-1369	999	1.39 0.43 1.51 0.30 0.51	Gehlenite $Na_{15.6}Ca_{3.84}(Si_{12}O_{36})$ Eskolaite Quartz low $Cr_2(SiO_4)$
	1000	0.45 0.41 1.43 2.86 0.49	Gehlenite $Na_{15.6}Ca_{3.84}(Si_{12}O_{36})$ Eskolaite Quartz low $Cr_2(SiO_4)$
	1049	0.55 0.65 1.42 0.19 0.05	Gehlenite $Na_{15.6}Ca_{3.84}(Si_{12}O_{36})$ Eskolaite Quartz low $Cr_2(SiO_4)$
	1050	0.79 1.33 0.15 0.04	$Na_{15.6}Ca_{3.84}(Si_{12}O_{36})$ Eskolaite Quartz low $Cr_2(SiO_4)$
	1099	0.14 0.08 1.28	Gehlenite $Na_{15.6}Ca_{3.84}(Si_{12}O_{36})$ Eskolaite
	1150	1.09	Eskolaite
	1200	0.80	Eskolaite

Glass-ID	Melt Temp (°C)	Wt% Crystallinity	Crystal Phase Identification
EWG-OL-1580	890	2.00	Eskolaite
		0.16	$Ca_2(SiO_4)$
		3.73	Apatite (B-containing)
	1002	1.84	Eskolaite
		0.33	$Mn(CrMn)O_4$
		1.59	Apatite (B-containing)
	1039	1.78	Eskolaite
		0.33	$Mn(CrMn)O_4$
	1089	1.29	Eskolaite
		0.53	$Mn(CrMn)O_4$
	1152	0.84	Eskolaite
		0.29	$Mn(CrMn)O_4$
	1199	0.94	Eskolaite
	1251	1.59	Eskolaite
EWG-OL-1672	950	1.00	Eskolaite
		0.54	Quartz low
		2.80	Akhtenskite
		0.70	$Ca_2(Al_2O_5)$
	1000	0.29	Quartz low
		2.21	Akhtenskite
		1.96	$Ca_2(Al_2O_5)$
		0.56	Eskolaite
	1050	0.36	Quartz low
		2.65	Akhtenskite
		1.52	$Ca_2(Al_2O_5)$
		0.50	Eskolaite
	1100	0.04	Quartz low
		0.32	Akhtenskite
		0.20	$Ca_2(Al_2O_5)$
		1.84	Eskolaite
	1150	2.76	Eskolaite
	1198	1.04	Eskolaite
EWG-OL-2463	989	1.30	Baddeleyite
		15.24	Nepheline ($Na(Al(SiO_4))$)
		4.47	$MnFe_2O_4$
		0.47	Hibonite
		1.00	Almandine
		1.81	Zirconia (nanocrystalline)
		1.93	SiO_2
		4.69	Nepheline ($Na_{15.6}Ca_{3.84}(Si_{12}O_{36})$)
		1.81	Zirconia (nanocrystalline)
	993	1.24	Baddeleyite
		15.89	Nepheline ($Na(Al(SiO_4))$)
		4.36	$MnFe_2O_4$
		0.45	Hibonite
		1.19	Almandine
		1.95	Zirconia (nanocrystalline)
		0.89	SiO_2
		4.10	Nepheline ($Na_{15.6}Ca_{3.84}(Si_{12}O_{36})$)
		0.79	$Ca_2Mn_2O_5$
	1039	1.37	Baddeleyite
		1.16	Nepheline ($Na(Al(SiO_4))$)
		3.43	$MnFe_2O_4$

Glass-ID	Melt Temp (°C)	Wt% Crystallinity	Crystal Phase Identification
		0.54	Hibonite
		1.92	Zirconia (nanocrystalline)
		2.01	$Ca_2Mn_2O_5$
	1089	1.16	Baddeleyite
		2.63	$MnFe_2O_4$
		1.86	Zirconia (nanocrystalline)
		2.07	$Ca_2Mn_2O_5$
	1139	1.45	Baddeleyite
		3.32	$MnFe_2O_4$
		1.82	Zirconia (nanocrystalline)
		1.97	$Ca_2Mn_2O_5$
EWG-OL-2619	950	1.59	Magnetite
		3.23	Hematite
		2.53	Baddeleyite
	1000	2.38	Baddeleyite
		2.46	Hematite
		1.31	Magnetite
	1050	1.88	Baddeleyite
		1.07	Hematite
		1.04	Magnetite
	1100	1.90	Baddeleyite
		1.12	Magnetite
	1148	0.82	Baddeleyite
	1200	0.52	Baddeleyite
	1201	0.63	Baddeleyite
EWG-OL-3122	1039	3.74	Sodalite (permanganate, basic)
		6.18	Nepheline
		0.41	$K_3(MnO_4)(MnO_4)$
		1.94	Magnetite, magnesian
	1047	3.34	Sodalite (permanganate, basic)
		6.28	Nepheline
		1.66	Magnetite, magnesian
	1089	2.89	Sodalite (permanganate, basic)
		1.41	Magnetite, magnesian
	1089	3.17	Sodalite (permanganate, basic)
		1.32	Magnetite, magnesian
	1139	1.82	Sodalite (permanganate, basic)
		1.69	Magnetite, magnesian
		6.55	Nepheline
	1143	1.85	Sodalite (permanganate, basic)
		1.10	Magnetite, magnesian
	1167	0.61	Sodalite (permanganate, basic)
		1.09	Magnetite, magnesian
	1188	0.98	Magnetite, magnesian
	1239	0.58	Magnetite, magnesian
EWG-OL-3208	974	0.73	Manganochromite
	1004	0	Amorphous
	1049	0	Amorphous
	1099	3.59	Potassium Sodium Aluminum Silicate
		1.64	SiO_2
		21.23	$Na_{1.15}(Al_{1.15}Si_{0.85}O_4)$
		3.21	Olympite

Glass-ID	Melt Temp (°C)	Wt% Crystallinity	Crystal Phase Identification
EWG-OL-3231	890	3.27 1.87	Apatite (B-containing) Manganochromite
	939	2.56 1.69	Apatite (B-containing) Manganochromite
	1002	1.67	Manganochromite
	1039	0.93	Manganochromite
	1101	0.83	Manganochromite
	1152	0.42	Eskolaite
EWG-OL-3388	890	3.91	Manganochromite
	938	3.73	Manganochromite
	1002	4.06	Manganochromite
	1038	3.27	Manganochromite
	1101	2.08	Manganochromite
	1152	4.86	Manganochromite
	1200	2.91	Manganochromite
EWG-OL-3872	799	0	Amorphous
	851	11.13 2.01 1.45	Nepheline Lazurite $Na_{7.96}(Al_{10.8}Si_{25.2}O_{72})$
	900	1.56 0.88	Lazurite $Na_{7.96}(Al_{10.8}Si_{25.2}O_{72})$
	949	0	Amorphous
	999	0	Amorphous
EWG-OL-4099	823	3.35	Oxyapatite
	889	1.74	Oxyapatite
	914	1.03	Oxyapatite
	950	0	Amorphous
EWG-OL-5155	1000	9.65 2.42 1.12	Spinel Baddeleyite Chromite
	1050	7.23 1.92 0.81	Spinel Baddeleyite Chromite
	1089	6.79 1.32	Spinel Baddeleyite
	1148	6.00 0.71	Spinel Baddeleyite
	1200	4.37	Spinel
	1251	6.08	Spinel
EWG-OL-5549	823	8.84 0.66 0.79 7.76 0.64	Nepheline $Na_6(AlSiO_4)_6$ SiO_2 $K_{0.25}Na_6Al_{6.24}Si_{9.76}O_{32}$ Akemanite
	849	5.28 0.39 3.80 0.45	Nepheline $Na_6(AlSiO_4)_6$ $K_{0.25}Na_6Al_{6.24}Si_{9.76}O_{32}$ Akemanite
	865	2.88 0.21	$K_{0.25}Na_6Al_{6.24}Si_{9.76}O_{32}$ $Na_6(AlSiO_4)_6$

Glass-ID	Melt Temp (°C)	Wt% Crystallinity	Crystal Phase Identification
	890	0	Amorphous
EWG-OL-5801	1002	6.95 2.16	Spinel ($MgAl_{0.2}Fe_{1.8}O_4$) Baddeleyite
	1050	4.99 1.88	Spinel Baddeleyite
	1100	2.77 1.29	Spinel Baddeleyite
	1150	1.01 0.67	Spinel ($MgAl_{0.2}Fe_{1.8}O_4$) Baddeleyite
	1150	0.89 0.77	Spinel ($MgAl_{0.2}Fe_{1.8}O_4$) Baddeleyite
	1198	2.68	Spinel ($MgAl_{0.2}Fe_{1.8}O_4$)
EWG-OL-6080	950	8.01 0.43 0.34 0.40 0.54 1.72	Spinel Braunite $K_2(Fe_2O_4)$ ZrO_2 $(MgAl_2Si_3O_{10})_{0.6}$ Corundum (Al_2O_3)
	1000	8.33 0.25 0.16 0.14 0.39 1.62	Spinel Braunite $K_2(Fe_2O_4)$ ZrO_2 $(MgAl_2Si_3O_{10})_{0.6}$ Corundum (Al_2O_3)
	1050	8.24	Spinel
	1089	7.31	Spinel
	1148	6.18	Spinel
	1199	5.13	Spinel
	1386	1.12	Spinel
EWG-OL-6198	989	1.19 6.63	Baddeleyite Chromite
	1039	0.76 5.75	Baddeleyite Chromite
	1100	5.18	Chromite
	1139	0.76 5.76	Baddeleyite Chromite
	1152	4.48	Chromite
	1199	4.14	Chromite
EWG-OL-12707	799	1.03 3.25 0.68 9.19 0.84 6.29 2.39 0.83 0.67	Brownmillerite $Ca_2(SiO_4)$ Spodumene beta Malinkoite Al_2O_3 Nepheline (Si-rich) Sodalite (permanganate) SiO_2 Bimessite
	849	0.97 2.31 0.51 8.97 0.27	Brownmillerite $Ca_2(SiO_4)$ Spodumene beta Malinkoite Al_2O_3

Glass-ID	**Melt Temp (°C)**	**Wt% Crystallinity**	**Crystal Phase Identification**
		0.95 1.42 1.12 0.33	Nepheline (Si-rich) Sodalite (permanganate) SiO_2 Bimessite
	900	0.60 1.94 0.23 5.94 0.50	Brownmillerite $Ca_2(SiO_4)$ Spodumene beta Malinkoite Al_2O_3
	949	0.22 3.23 1.78	Brownmillerite $Ca_2(SiO_4)$ Malinkoite
	1000	0	Amorphous
EWG-OL-14827	891	2.12	Manganochromite
	939	1.43	Manganochromite
	988	1.09	Manganochromite
	1013	1.17	Eskolaite
	1089	0.79	Manganochromite
	1152	0.59	Manganochromite
	1199	0.29	$Na_{15.6}Ca_{3.84}(Si_{12}O_{36})$
	1248	0.11	Hausmannite
EWG-OL-15968	849	1.02	Magnesiochromite
	891	1.11	Magnesiochromite
	950	0.89	Magnesiochromite
	973	0.38	Magnetite
	974	0.65	Magnesiochromite
	1000	0.20	Magnesiochromite
	1050	0	Amorphous
EWG-OL-16450	823	11.82 0.63	$Mg_2(B_2O_5)$ $Al_2Si_4O_{10}(OH)_2$
	891	2.21 1.89	Magnesiochromite Sodalite (permanganate, basic)
	939	2.12 0.17	Magnesiochromite Sodalite (permanganate, basic)
	1000	0.78	Magnesiochromite
	1048	0.46	Magnesiochromite
	1101	0.49	Magnesiochromite
	1150	0.55	Magnesiochromite
	1201	0	Amorphous
EWG-OL-23401	900	0.91 8.93 2.50 0.27	Eskolaite SiO_2 Nepheline ($NaAlSiO_4$) $Na_6(AlSiO_4)_6$
	950	1.26 0.213	Eskolaite SiO_2
	1000	1.32 0.27	Eskolaite SiO_2
	1050	1.26	Eskolaite
	1099	0.77	Eskolaite
	1101	0.57	Eskolaite

Glass-ID	Melt Temp (°C)	Wt% Crystallinity	Crystal Phase Identification
	1150	0.35	Eskolaite
	1200	0.09	Eskolaite
		0.09	Parawollastonite
EWG-OL-26012	801	18.74	Nepheline
		2.29	$Na_{7.96}(Al_{10.8}Si_{25.2}O_{72})$
		2.50	Li_5AlO_4
	851	0	Amorphous
	902	0	Amorphous
	951	0	Amorphous
EWG-OL-29285	902	2.17	Baddeleyite
		4.82	Apatite (B-containing)
	902	1.84	Baddeleyite
		4.78	Apatite (B-containing)
	1000	2.11	Baddeleyite
		3.77	Apatite (B-containing)
		0.30	$ZrSi_{0.993}O_4$
	1050	1.04	Baddeleyite
		2.65	Apatite (B-containing)
		1.47	$ZrSi_{0.993}O_4$
	1100	3.14	Baddeleyite
		11.32	Spinel
		0.73	SiO_2
	1102	1.011	Apatite (B-containing)
		2.24	$ZrSi_{0.993}O_4$
	1154	1.47	$ZrSi_{0.993}O_4$
EWG-OL-31644	1101	5.45	Chromite
	1148	4.51	Chromite
	1199	3.42	Chromite
	1251	2.62	Chromite
EWG-OL-32706	1100	1.14	$ZrSi_{0.993}O_4$
		0.87	Baddeleyite
	1147	0.61	$ZrSi_{0.993}O_4$
		1.25	Baddeleyite
	1164	0.58	$ZrSi_{0.993}O_4$
		0.69	Baddeleyite
	1188	0.94	Baddeleyite
	1239	0.51	Baddeleyite
EWG-OL-33115	1000	7.47	Spinel
		4.45	Oxyapatite
	1050	4.61	Spinel
		3.60	Oxyapatite
	1089	2.97	Spinel
		2.32	Oxyapatite
	1100	2.46	Spinel
		2.02	Oxyapatite
	1139	1.27	Spinel
	1152	1.27	Spinel
	1164	0.48	Spinel
EWG-OL-33558	1089	3.12	Magnetite
		0.71	Gehlenite
		1.28	$Na_2Ca_2(Si_2O_7)$

Glass-ID	Melt Temp (°C)	Wt% Crystallinity	Crystal Phase Identification
	1139	1.52	Magnetite
	1164	0.95	Magnetite
	1188	0	Amorphous
EWG-OL-33694	823	1.49 2.77 3.67 2.16 1.58 6.45	Nepheline ($Na_6(AlSiO_4)_6$ Nepheline $MnMg(B_2O_5)$ SiO2 Spinel ($Mg_{0.3125}Mn_{2.0625}Al_{0.625}O_4$) Sodalite (permanganate)
	889	6.36	$MnMg(B_2O_5)$
	938	4.09	$MnMg(B_2O_5)$
	1000	1.02	$MnMg(B_2O_5)$
	1038	0	Amorphous
	1138	0	Amorphous
EWG-OL-33858	1052	6.37	$(Mg_{0.80}Al_{0.18})(Al_{1.86}Mg_{0.14})O_4$
	1091	5.12	$(Mg_{0.80}Al_{0.18})(Al_{1.86}Mg_{0.14})O_4$
	1139	4.24	$(Mg_{0.80}Al_{0.18})(Al_{1.86}Mg_{0.14})O_4$
	1188	2.84	$(Mg_{0.80}Al_{0.18})(Al_{1.86}Mg_{0.14})O_4$
EWG-OL-35387	1002	2.30	$MgMn_{1.75}Al_{0.25}O_4$
	1089	1.85	$MgMn_{1.75}Al_{0.25}O_4$
	1139	1.68	$MgMn_{1.75}Al_{0.25}O_4$
	1164	1.77	$MgMn_{1.75}Al_{0.25}O_4$
	1189	1.68	$MgMn_{1.75}Al_{0.25}O_4$
	1238	1.64	$MgMn_{1.75}Al_{0.25}O_4$
	1386	1.41	$MgMn_{1.75}Al_{0.25}O_4$
EWG-OL-38081	1139	1.93 0.48	Baddeleyite $Na_{1.95}(Al_{1.95}Si_{0.05}O_4)$
	1164	1.71	Baddeleyite
	1189	1.64 0.24	Baddeleyite SiO_2
	1238	1.36	Baddeleyite
EWG-OL-38552	950	8.05 20.72 2.70 0.49 0.37	Hercynite Psuedo-eucryptite Baddeleyite Zirconia SiO_2
	1000	2.93 6.92 2.84 0.17 0.17 5.03	Hercynite Psuedo-eucryptite Baddeleyite Zirconia SiO_2 Spinel
	1050	1.28 2.49 5.61	Hercynite Baddeleyite Spinel
	1100	6.30 2.26 0.09	Spinel Baddeleyite ZrO_2
	1150	4.65 2.17 0.08	Spinel Baddeleyite ZrO_2

Glass-ID	Melt Temp (°C)	Wt% Crystallinity	Crystal Phase Identification
	1200	2.65 1.68 0.06	Spinel Baddeleyite ZrO_2
	1251	1.19	Baddeleyite
EWG-OL-1755 Mod 8% Fe, 10% B	1052	4.14	$(Li_{0.64}Fe_{5.36})O_8$
	1089	3.43	$(Li_{0.64}Fe_{5.36})O_8$
	1139	2.99	$(Li_{0.64}Fe_{5.36})O_8$
	1188	2.28	$(Li_{0.64}Fe_{5.36})O_8$
	1239	2.01	$(Li_{0.64}Fe_{5.36})O_8$
	1337	7.27	$(Li_{0.64}Fe_{5.36})O_8$
EWG-OL-3063 Mod 1% Zr 3% Li	948	3.27 2.45 1.10	$Fe_{21.34}O_{32}$ Hematite Eskolaite
	998	1.92 2.76 0.77	$Fe_{21.34}O_{32}$ Hematite Eskolaite
	1048	1.63 2.43	$Fe_{21.34}O_{32}$ Hematite
	1048	0.99	Eskolaite
	1101	1.37 2.06	$Fe_{21.34}O_{32}$ Hematite
EWG-OL-4744 Mod 7.5% Fe 1% Zr	1052	4.93 2.74	Chromite Haueyne
	1089	4.39 1.59	Chromite Haueyne
	1152	3.26	Chromite
	1152	3.15	Chromite
	1189	2.85	Chromite
	1238	2.48	Chromite
EWG-OL-5385 Mod 12% B 17% Na	820	27.59	Nepheline
	862	18.45	Nepheline
	865	18.45	Nepheline
	889	14.04	Nepheline
	906	9.40	Nepheline
	914	7.19	Nepheline
	939	0	Amorphous
EWG-OL-6257 Mod 12% B 8% Ca	823	13.92 5.50 11.12	Psuedo-eucryptite Spinel Nepheline (Si-rich)
	889	3.31 3.25	Psuedo-eucryptite Spinel
	939	5.43	$(Mg_{0.69}Al_{0.29})(Al_{1.74}Mg_{0.24})O_4$
	989	5.77	$(Mg_{0.69}Al_{0.29})(Al_{1.74}Mg_{0.24})O_4$
	1038	5.96	$(Mg_{0.69}Al_{0.29})(Al_{1.74}Mg_{0.24})O_4$
	1150	4.70	$(Mg_{0.69}Al_{0.29})(Al_{1.74}Mg_{0.24})O_4$
	1200	4.45	$(Mg_{0.69}Al_{0.29})(Al_{1.74}Mg_{0.24})O_4$
EWG-OL-6311 Mod Reduced Na & K	889	9.16 3.70	$MgAl_{0.6}Fe_{1.4}O_4$ Nosean
	939	7.43	$MgAl_{0.6}Fe_{1.4}O_4$
	988	7.27	$MgAl_{0.6}Fe_{1.4}O_4$

Glass-ID	Melt Temp (°C)	Wt% Crystallinity	Crystal Phase Identification
	1038	5.59	$MgAl_{0.6}Fe_{1.4}O_4$
	1101	4.85	$MgAl_{0.6}Fe_{1.4}O_4$
	1198	5.31	$MgAl_{0.6}Fe_{1.4}O_4$
EWG-OL-6489 Mod 11% B 15% Na	1000	12.25 13.04	Spinel Nepheline
	1052	11.76	Spinel
	1101	10.91	Spinel
	1147	10.02	Spinel
	1152	10.24	Spinel
	1238	10.50	Spinel
	1386	11.11	Spinel
EWG-OL-8548 Mod 1% Zr	1052	12.21 0.39 11.62	$MgCr_{0.6}Fe_{1.4}O_4$ $MgCrO_4$ Nepheline
	1089	10.81 0.19	$MgCr_{0.6}Fe_{1.4}O_4$ $MgCrO_4$
	1152	10.20	$MgCr_{0.6}Fe_{1.4}O_4$
	1189	9.39	$MgCr_{0.6}Fe_{1.4}O_4$
	1238	8.79	$MgCr_{0.6}Fe_{1.4}O_4$
EWG-OL-10278 Mod 15% B 1% Zr	820	30.13 1.78 3.34	Nepheline Quartz low $Li_{0.89}Mn_2O_{3.84}$
	823	28.07 1.63 3.52	Nepheline Quartz low $Li_{0.89}Mn_2O_{3.84}$
	857	18.30 1.59 0.73	Nepheline Quartz low $K_3(MnO_4)$
	865	0.63 1.81 16.47	$K_3(MnO_4)$ Quartz low Nepheline
	880	16.34	Nepheline
	889	10.20	Nepheline
	906	5.17	Nepheline
	906	4.96	Nepheline
	914	1.76	Nepheline
	939	0	Amorphous
	1089	0	Amorphous
EWG-OL-11318 Mod 1% Zr	989	2.23 1.49	$MgMn_{1.75}Al_{0.25}O_4$ $Mg_{0.3125}Mn_{2.0625}Al_{0.625}O_4$
	1101	2.97 0.47	$MgMn_{1.75}Al_{0.25}O_4$ $Mg_{0.3125}Mn_{2.0625}Al_{0.625}O_4$
	1139	3.33	$MgMn_{1.75}Al_{0.25}O_4$
	1164	3.14	$MgMn_{1.75}Al_{0.25}O_4$
	1189	3.10	$MgMn_{1.75}Al_{0.25}O_4$
	1238	2.89	$MgMn_{1.75}Al_{0.25}O_4$
EWG-OL-14547 Mod Reduced Alkali 1% Zr	889	9.44 4.57 4.99	$K_{0.25}Na_6Al_{6.24}Si_{9.76}O_{32}$ Sodalite (permanganate, basic) $(Li_2O)(Fe_2O_3)_{3.6}(Cr_2O_3)_{1.4}$
	939	3.26	Sodalite (permanganate, basic)

Glass-ID	Melt Temp (°C)	Wt% Crystallinity	Crystal Phase Identification
		3.54	$(Li_2O)(Fe_2O_3)_{3.6}(Cr_2O_3)_{1.4}$
	988	2.61 2.37	$(Li_2O)(Fe_2O_3)_{3.6}(Cr_2O_3)_{1.4}$ Sodalite (permanganate, basic)
	989	2.46	Sodalite (permanganate, basic)
	1013	1.85	$(Li_2O)(Fe_2O_3)_{3.6}(Cr_2O_3)_{1.4}$
	1024	1.51	$(Li_2O)(Fe_2O_3)_{3.6}(Cr_2O_3)_{1.4}$
	1047	1.39	$(Li_2O)(Fe_2O_3)_{3.6}(Cr_2O_3)_{1.4}$
EWG-OL-15698 Mod Low Na	898	8.05 13.87 1.12 2.25	Magnetite Nepheline SiO_2 Haueyne
	939	6.80 2.20 2.02	Magnetite SiO_2 Haueyne
	988	6.38	Magnetite
	1089	2.10	Magnetite
	1139	0.76	Magnetite

Distribution

No. of
Copies

2 U.S. Department of Energy
Office of River Protection
AA Kruger
B Hamel

1 Savannah River National Laboratory
KM Fox

No. of
Copies

Local Distribution
Pacific Northwest National Laboratory
CB Bonham
SK Cooley
WC Eaton
V Gervasio
T Jin
JB Lang
JM Mayer
BP McCarthy
GF Piepel
RL Russell
MJ Schweiger
BA Stanfill
JD Vienna
Information Release (PDF)

Pacific Northwest
NATIONAL LABORATORY

U.S. DEPARTMENT OF
ENERGY

Proudly Operated by **Battelle** *Since 1965*

902 Battelle Boulevard
P.O. Box 999
Richland, WA 99352
1-888-375-PNNL (7665)